Cardiac Resynchronisation Therapy and Myocardial Metabolism: Acute and Chronic Effects in Heart Failure

Peregrine George Green

Keble College

University of Oxford

A thesis submitted in partial fulfilment of the requirements for the degree of

Doctor of Philosophy in Physiology, Anatomy and Genetics

Michaelmas Term 2021

Declaration

This thesis is entirely my own work unless otherwise indicated. It has not been submitted, either wholly or substantially, for another degree at this university, or for a degree at any other institution. I have acknowledged assistance from colleagues and collaborators where relevant.

The word count, not including references, abstract and front matter is 35,475

Table of Contents

Acknowledgements

The work presented in this thesis would not have been possible without the contribution and support of numerous colleagues, departments and organisations. Thank you first and foremost to my supervisors, Professor Neil Herring and Professor Oliver Rider, for their help and guidance throughout my DPhil, as well as to the British Heart Foundation for funding this work through my Clinical Research Training Fellowship. Particular thanks must go as well to Dr William Watson, who both helped co-recruit some of the participants and with whom I ran the majority of the study protocols.

Thank you to Professor Tim Betts, Professor Ladislav Valkovic, Dr David Holdsworth, Dr Giovanni Luigi De Maria and Miss Cristiana Monteiro for their help with specific aspects of administering the study protocols and data analysis, as well as to all the fellows, radiographers, research nurses and clinical and administrative staff; they are too numerous to mention by name but have without fail willingly offered help and advice with good humour whenever needed.

Above all, thank you to my parents for providing me with an education and with every opportunity which has brought me this far and to my wife Seema, to whom this thesis is dedicated and whose encouragement, love and support has made it possible; this is as much your achievement as it is mine.

Abstract

Since its development in the 1990s, cardiac resynchronisation therapy has evolved to occupy a key position in the management of heart failure with a reduced ejection fraction and broadened QRS duration, inducing both acute haemodynamic improvements as well as chronic reverse remodelling. However, approximately 30% of patients appear to not respond to CRT. Whilst factors such as heart failure aetiology and patient comorbidity, e.g. diabetes mellitus, have been shown to correlate with poor response, the mechanisms responsible for this and strategies to improve response have in large part remained elusive. Meanwhile, changes in myocardial metabolic substrate usage and flux are increasingly thought to play a causative role in heart failure. Given the changes in cardiac efficiency and regional substrate uptake which are induced by CRT, this raises the intriguing possibility that changes in myocardial metabolism may influence reverse remodelling. This thesis aims to therefore further investigate the links between CRT and myocardial metabolism.

In Chapter 3, the effects of substrate manipulation on cardiac function and energetics are assessed in participants with diabetes mellitus, with and without systolic heart failure. While metabolic flexibility appears to be maintained in participants with diabetes mellitus alone, with improved cardiac contractility and efficiency on a free fatty acid infusion, this flexibility is reduced or lost in participants with both diabetes mellitus and systolic heart failure. This loss of flexibility may in part account for the reduced CRT response rates seen in these patients.

In Chapter 4, the acute effects of CRT are assessed invasively. Cardiac contractility and oxygen efficiency are shown to be improved regardless of substrate manipulation. In addition, CRT induces a change in cardiac substrate uptake within 2 minutes of the commencement of pacing, with a more physiological picture of lipid derived metabolism as seen in the healthy heart. This increase correlates with improvements in acute cardiac contractility.

In Chapter 5, the influence on reverse remodelling of both baseline cardiac energetics before CRT implant and the acute changes in substrate uptake discussed in Chapter 4, are assessed. Baseline energetic efficiency, in terms of metabolic flux, and changes in free fatty acid uptake appear to correlate with measures of reverse remodelling at 6 months. In addition, calculation of cardiac volumes and QRS duration in response to CRT both acutely (with a pressure-volume loop catheter) and at follow up (using MR-conditional devices) allows the acute influence of electrical resynchronisation to be distinguished from the long term structural reverse remodelling which occurs.

In Chapter 6, optimal CRT programming during exercise stress is assessed, with CPET and 12 lead ECG monitoring used to assess the effectiveness of fusion pacing. Whilst there is no difference between fusion pacing and standard biventricular pacing on QRS duration or exercise capacity, use of whichever programming gives the narrowest QRS duration at rest results in a narrower QRS duration during exercise and improvement in stroke volume and peak cardiac efficiency. This therefore supports the use of fusion pacing in the 40% of patients where this gives a narrower QRS duration and suggests that optimal QRS narrowing at rest should be the target of CRT optimisation.

Together, these results suggest that CRT and myocardial metabolism have reciprocal influences and that the assessment and manipulation of metabolism may help improve CRT rates of response.

Abbreviations and Definitions

2,3-DPG	2,3-Diphosphoglycerate
6MWT	Six Minute Walk Test
^{31}P	31-Phosphorus
ACC	Acetyl-CoA Carboxylase
ACE(i)	Angiotensin Converting Enzyme (Inhibitor)
ACT	Activated Clotting Time
ADP	Adenosine Diphosphate
AF	Atrial Fibrillation
AMP	Adenosine Monophosphate
AMPK	Adenosine Monophosphate Kinase
APV	Average Peak Velocity
ARB	Angiotensin Receptor Blocker
ARNi	Angiotensin Receptor-Neprilysin Inhibitor
ATP	Adenosine Triphosphate
A-V	Arterio-Venous
AV	Atrioventricular
AVD	Atrioventricular Delay(s)
AVN	Atrioventricular Node
BDH1	β-Hydroxybutyrate Dehydrogenase
BiV	Biventricular
BMI	Body Mass Index

BOHB	β-Hydroxybutyrate
BORG-RPE	BORG Rating of Perceived Exertion
BP	Blood Pressure
BSA	Body Surface Area
CCB	Calcium Channel Blocker
CK	Creatine Kinase
CKD	Chronic Kidney Disease
CMR	Cardiac Magnetic Resonance
CoA	Coenzyme A
CS	Coronary Sinus
CSI	Chemical Shift Imaging
CPET	Cardiopulmonary Exercise Test(ing)
CPT1/2	Carnitine Palmitoyl Transferase 1/2
CRT	Cardiac Resynchronisation Therapy
DANTE	Delays Alternating with Nutation for Tailored Excitation
DCM	Dilated Cardiomyopathy
DM	Diabetes Mellitus
dP/dt_{max}	Maximal Rate of Change of Pressure in the Left Ventricle
DPP-4	Dipeptidyl-Peptidase 4
ECG	Electrocardiogram
EDPVR	End Diastolic Pressure Volume Relationship
EDV	End Diastolic Volume
EF	Ejection Fraction
ESPVR	End Systolic Pressure Volume Relationship

ESV	End Systolic Volume
ETC	Electron Transport Chain
FA	Fatty Acid
FACS	Fatty Acyl-CoA Synthase
FAD	Flavin Adenine Dinucleotide
FAT	Fatty Acid Translocase
FDG	^{18}F-Fluorodeoxyglucose
FFA	Free Fatty Acid(s)
GCS	Global Circumferential Strain
GLUT	Glucose Transporter
GRE	Gradient Recalled Echo
HBP	His Bundle Pacing
HFpEF	Heart Failure with Preserved Ejection Fraction
HFrEF	Heart Failure with Reduced Ejection Fraction
HFmrEF	Heart Failure with Mid-Range Ejection Fraction
HIF1	Hypoxia-Inducible Factor 1
HLA	Horizontal Long Axis
HR	Heart Rate
IEGM	Intracardiac Electrogram(s)
ISMO	Isosorbide Mononitrate
IQR	Inter Quartile Range
k_f	Pseudo-First Order Rate Constant of Creatine Kinase
LAD	Left Anterior Descending
LBBB	Left Bundle Branch Block

LDH	Lactate Dehydrogenase
LGE	Late Gadolinium Enhancement
LMS	Left Main Stem
LPL	Lipoprotein Lipase
LV	Left Ventricle/Ventricular
LVEDP	Left Ventricular End-Diastolic Pressure
LVEDV	Left Ventricular End-Diastolic Volume
LVEF	Left Ventricular Ejection Fraction
LVESV	Left Ventricular End-Systolic Volume
LVSV	Left Ventricular Stroke Volume
MAP	Mean Arterial Pressure
MBF	Myocardial Blood Flow
MPC	Mitochondrial Pyruvate Carrier
MRA	Mineralocorticoid Receptor Antagonist
MRS	Magnetic Resonance Spectroscopy
MRI	Magnetic Resonance Imaging
MVO_2	Myocardial Oxygen Consumption
NAD	Nicotinamide Adenine Dinucleotide
NIDDM	Non-Insulin Dependent Diabetes Mellitus
NYHA	New York Heart Association
$O_2\ Pulse^{PEAK}$	Oxygen Pulse at Peak Exercise
$O_2\ Pulse^{VT1}$	Oxygen Pulse at VT1
$O_2\ Pulse^{VT2}$	Oxygen Pulse at VT2
PCr	Phosphocreatine

PPAR	Peroxisome Proliferator Activated Receptor
PDE	Phosphodiesters
PDH	Pyruvate Dehydrogenase
PET	Positron Emission Tomography
PFK	Phosphofructokinase
PV	Pressure-Volume
QoL	Quality of Life
QRSd	QRS Duration
RAAVD	Rate-Adaptive Atrioventricular Delay(s)
RER	Respiratory Exchange Ratio
RER^{PEAK}	Respiratory Exchange Ratio at Peak Exercise
RPP	Rate Pressure Product
RQ	Respiratory Quotient
RV	Right Ventricle/Ventricular
RVEDV	Right Ventricular End-Diastolic Volume
RVEF	Right Ventricular Ejection Fraction
RVESV	Right Ventricular End-Systolic Volume
RVEF	Right Ventricular Ejection Fraction
SA	Short Axis
SAR	Specific Absorption Rate
SCOT	Succinyl CoA:3-ketoacid CoA
SERCA	Sarco-endoplasmic Reticulum Calcium ATPase
SGLT2(i)	Sodium-Glucose Transport Protein 2 (Inhibitor)
SLR	Septal-to-Lateral Wall Ratio

SSFP	Steady State Free Precession
StreST	Stress Saturation Transfer
SV	Stroke Volume
T	Tesla
T2DM	Type 2 Diabetes Mellitus
TAG	Triacylglycerols
TCA	Tricarboxylic Acid
TE	Echo Time
TR	Repetition Time
TRiST	Triple Repetition Saturation Transfer
UCP	Uncoupling Protein
UTE-CSI	Ultra-Short Echo Time-CSI
VLA	Vertical Long Axis
$\dot{V}O_2$	Oxygen Consumption
$\dot{V}O_2^{PEAK}$	Oxygen Consumption at Peak Exercise
$\dot{V}O_2^{VT1}$	Oxygen Consumption at VT1
$\dot{V}O_2^{VT2}$	Oxygen Consumption at VT2
VT1	First Ventilatory Threshold
VT2	Second Ventilatory Threshold
VV	Ventriculo-Ventricular
VVD	Ventriculo-Ventricular Delay(s)

Chapter 1:
Introduction

1.1 Heart Failure Overview

The term 'heart failure' encompasses a wide range of cardiac pathology, which is united by the same clinical symptoms and signs (e.g. breathlessness, oedema) resulting from a common end-point of elevated intra-cardiac pressures and/or inadequate cardiac output[1]. By convention, it is classified by measures of left ventricular (LV) function and in particular left ventricular ejection fraction (LVEF), with heart failure sub-divided into heart failure with preserved ejection (HFpEF; characterised by LVEF ≥50% with structural and/or functional abnormalities consistent with LV diastolic dysfunction), heart failure with reduced ejection fraction (HFrEF; characterised by LVEF <40%) and heart failure with mildly reduced ejection fraction (HFmrEF; characterised by LVEF 41-49%)[1]. All can result from a variety of aetiologies, with HFrEF and HFmEF causes in particular being divided into ischaemic cardiomyopathy and dilated non-ischaemic cardiomyopathy (DCM). Aetiologies of DCM include genetic, infectious, auto-immune and endocrine causes, as well as drugs or toxins[2].

There have been multiple pharmacological and technological advances in recent years in the treatment of HFrEF, with neurohormonal blockade (β-blockers, angiotensin converting enzyme inhibitors (ACEi), angiotensin receptor antagonists (ARB) and mineralocorticoid receptor antagonists (MRA)), sodium glucose co-transporter 2 (SGLT2) inhibitors and device therapy all having recommendations for use in heart failure guidelines [1]. However, despite this, heart failure constitutes a significant health burden, with a prevalence of 900,000 in the UK and 60,000 new diagnoses each year[3]. Additionally, nearly 75,000 patients were hospitalised with heart failure in the UK in 2018-2019, of which the majority were for HFrEF[4]. Of these, the 1 year mortality after discharge was 29%.

There is therefore need for further understanding of the pathophysiology of heart failure, with the potential for development of new treatments as well as optimisation of existing therapies.

1.2 Cardiac Electrophysiology

Heart failure is often associated with disorders of normal cardiac conduction which can exacerbate (or even cause) the underlying pathophysiology.

1.2.1 Normal Cardiac Conduction

Whilst the intrinsic rhythmic property of the heart, along with impulse generation at the sinus venosus, was first recognised by Walter Gaskell in the 19th century[5], the exact origin of the heart beat in the sino-atrial node in the right atrium was first discovered by Keith and Flack in

1907[6]. This region consists of a specialised group of spontaneously depolarising myocardial cells, which initiates the electrical impulse. From here, depolarisation propagates through the atria to the atrio-ventricular (AV) node (AVN) (discovered the year before in 1906 by Tawara[7]), before passing down the rapidly conducting bundle of His, first described by, and named after, Wilhelm His Jr in 1893[7]. This then splits into the left and right bundle branches, which transmit the wave of depolarisation simultaneously to the apical regions of the left ventricle (LV) and right ventricle (RV) respectively. Finally, these divide into the distal Purkinje fibre networks in the sub-endocardium, which had previously been identified by Jan Evangelista Purkinje in 1839 although he did not recognise their role in electrical conduction at the time[8]. These transmit the depolarisation into the main ventricular myocardium. This process is summarised in Figure 1.1 and ensures rapid and simultaneous activation of the heart, with resultant coordinated and efficient myocardial contraction.

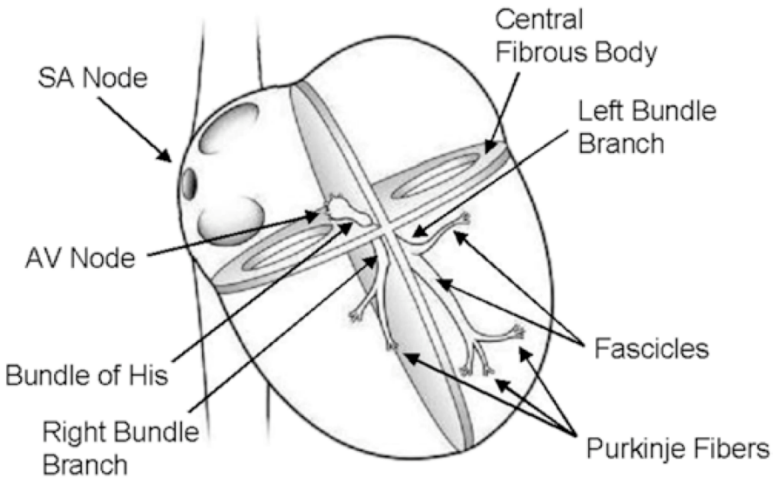

Figure 1.1: *Normal cardiac conduction system (from the Handbook of Cardiac Anatomy, Physiology, and Devices[9])*

1.2.2 Left Bundle Branch Block

Disruption of the normal conduction of the left bundle branch of the conducting system results in a failure to rapidly conduct normal depolarisation and is known as left bundle branch block (LBBB). It can result from degeneration of the conduction system or more specific myocardial pathology or damage, including ischaemia, surgery and aortic valve replacement[10].

The resultant failure of rapid conduction into the LV results in dyssynchronous electrical activation of the heart, with a characteristic pattern and broadening of the QRS in the surface electrocardiogram (ECG)[11]. Left ventricular depolarisation therefore occurs after the RV (which is still rapidly activated by the right bundle branch), with the wave-front generally breaking through the mid-septum into the LV endocardium[10] and then spreading from the septum across the LV through the slow conducting myocardium, with the latest activation being at the lateral base of the heart[12].

1.2.2.1 Haemodynamic Effects of LBBB

The concept that electrical conduction disturbances in the heart have a haemodynamic impact and result in LV systolic dysfunction is not new, having been first discovered by Wiggers in 1925[13] who showed that epicardial stimulation of canine hearts reduced the maximal rate of change of pressure in the LV (dP/dt_{max}). The electrical dyssynchrony and delayed LV activation seen in LBBB results in corresponding inter- and intra-ventricular mechanical dyssynchrony during cardiac systole. In the left ventricle, relative early and late activation of the septum and lateral wall, respectively, results in an inhomogeneous workload

distribution. Septal regions shorten early in systole during isovolumetric contraction, stretching the posterior and lateral walls and so only generating a small amount of constructive work at this point (and to a variable extent later in systole). In mid-systole, septal stretching as a result of lateral wall contraction (known as septal rebound stretch and visualised by echocardiographic strain analysis[14-16]) implies wasted work. Overall therefore, there is a net reduction in septal work, or even negative work[17, 18], during systole with a reduced contribution to LV ejection[19]. Conversely, late-activated regions have increased workload, as demonstrated in pacing models[20]. This dyssynchronous workload leads to adverse remodelling (see section 1.3.4.1). The mechanical dyssynchrony resulting from LBBB is shown in Figure 1.2.

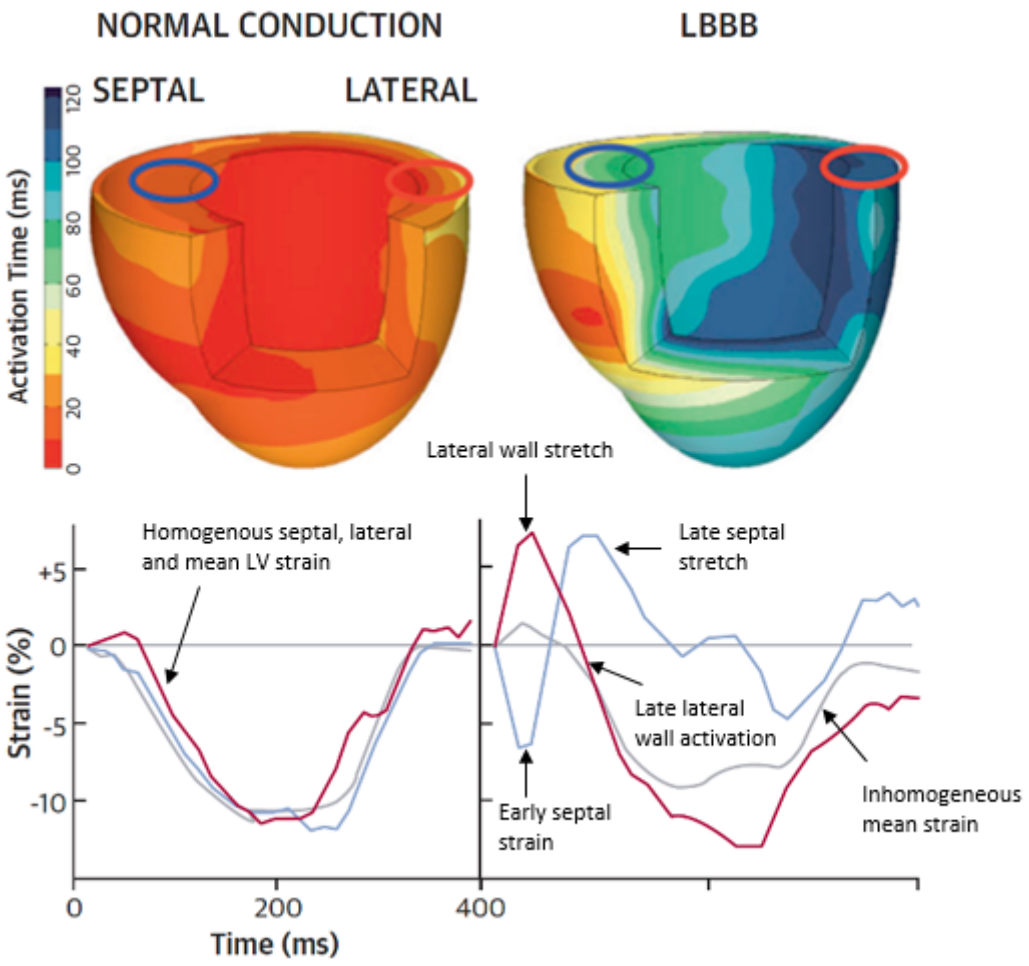

Figure 1.2: *Mechanical dyssynchrony associated with LBBB. In normal conduction (left) synchronous septal (blue circle) and lateral (red circle) activation leads to coordinated LV activation and so strain of the septum (blue trace) and lateral wall (red trace), leading to homogenous mean LV strain (grey trace). In LBBB (right) early septal activation leads to early septal shortening with corresponding lateral wall stretch, with subsequent late lateral wall activation and septal wall stretch later in systole and so overall inhomogeneous mean LV strain (adapted from Leyva et al[21])*

1.2.2.2 Association with Heart Failure

In heart failure, conduction system abnormalities including LBBB can be the result of degeneration or fibrosis of the pathway, direct insult from ischaemia or infarction, or as a result of adverse remodelling and myocardial stretch[10]. Registry analyses have shown that

approximately 20-30% of patients with heart failure have LBBB, with a linear relationship between QRS duration (QRSd) and impairment of LV function[22]. Additionally, the presence of LBBB in heart failure is associated with increased mortality[23-26].

1.3 Cardiac Resynchronisation Therapy

1.3.1 Definition and Overview

Given the association of LBBB with heart failure and the adverse mechanical effect outlined above, it is perhaps not surprising that early studies showed that LBBB was associated with adverse cardiac haemodynamics[27, 28]. Cardiac resynchronisation therapy (CRT) was therefore developed to correct the electrical and mechanical dyssynchrony associated with LBBB (and to a lesser extend with right bundle branch block and other inter-ventricular conduction delay) via biventricular (BiV) pacing of the LV septum and lateral wall. In this way, it aims to restore synchronous biventricular contraction and so improve cardiac haemodynamics and function.

In addition to these effects on dyssynchrony, HFrEF often also coincides with AVN disease. Another key mechanism by which CRT therefore improves haemodynamics is via improvements in AV synchrony[29, 30] (see section 1.3.4.4.3).

1.3.2 History and Trials

The course of CRT development spans a near 30 year period[21]. Whilst BiV pacing with LV epicardial pacing was first described in 1979[31], it was in the 1990s that its benefits in patients with LBBB and heart failure were first realised. Improved haemodynamics with BiV pacing compared to RV pacing were seen in a non-heart failure cohort of patients undergoing coronary artery bypass grafting[32], as well as improved haemodynamics and clinical improvement in a case report of a patient with LBBB[33]. A case series of patients with LBBB and heart failure, starting in 1993, subsequently confirmed improvements in LV function and symptoms[34] and improved haemodynamics in heart failure patients with electrical dyssynchrony was also confirmed in studies in the mid-late 1990s[35-37]. Successful LV pacing via a transvenous approach by placing a pacing lead in the coronary sinus was first reported by Daubert *et al.* in 1998 in 47 patients, a technique which was subsequently aided by the development of over-the-wire pacing leads[38]. This paved the way for BiV pacing (or CRT) to become a therapy in severe heart failure patients with a QRSd, with multiple landmark trials in the 2000s confirming its benefits in terms of both symptoms, morbidity and mortality[39-45]. Cardiac resynchronisation therapy has now become a standard treatment for heart failure with LBBB, included in all major heart failure guidelines[1, 46, 47].

1.3.3 Acute Haemodynamic Effects of CRT

1.3.3.1 Measurement of Cardiac Work

Cardiac systolic function can be assessed by a number of methods, including ejection fraction and dP/dt_{max}[48, 49]. Simultaneous measurement of ventricular pressure and volume by

conductance catheter permits generation of pressure-volume (PV) loops (Figure 1.3), with the area contained within the loop representing external cardiac work and changes in cardiac inotropy reflected in by a relative left or rightward shift in the loop[50] (Figure 1.3). Furthermore, mechanical dyssynchrony is reflected by a change in shape of the loop, with CRT shown to reduce dyssynchrony[51], increase stroke volume (reflected by a wider loop) and increase stroke work (reflected by a greater area of loop)[52, 53] (Figure 1.4).

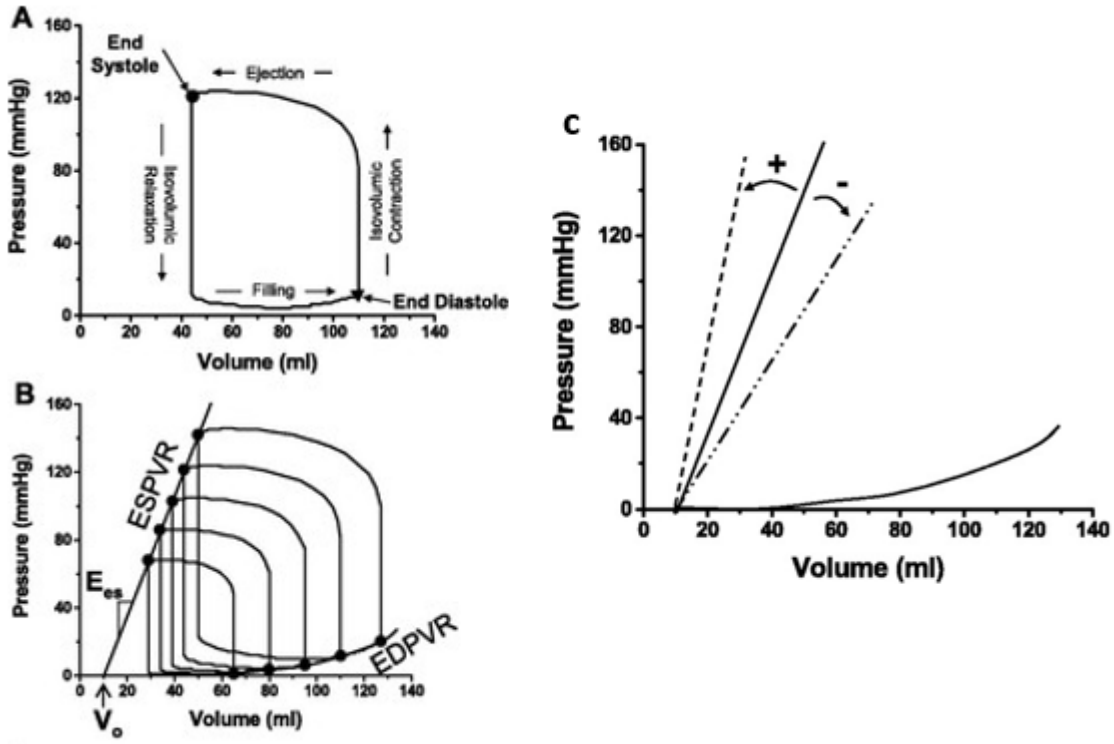

Figure 1.3: *Simultaneous recording of ventricular pressure and volume results in formation of a PV loop (A). Change in preload with a constant contractile state, with subsequent plotting of the end-systolic and end-diastolic pressure-volume points results in generation of the end-systolic pressure-volume relationship (ESPVR) and end-diastolic pressure-volume relationship (EDPVR) (B). An increase in inotropy (+) results in an increase in the slope of the ESPVR, whilst a decrease (-) results in a reduction in slope (C) (from Burkhoff et al.[54])*

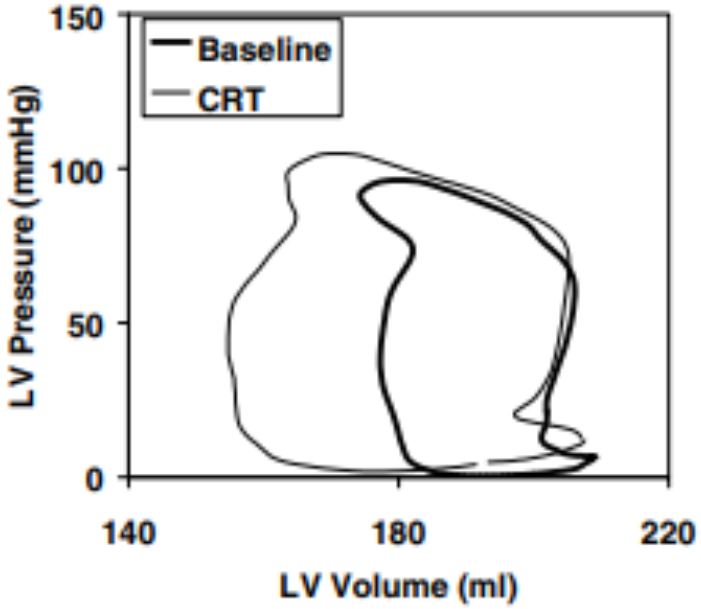

Figure 1.4: *Increased stroke volume and stroke work in response to CRT, as shown by PV loop analysis (from Steendijk et al.[53])*

1.3.3.2 Improvement in Haemodynamics

Multiple studies have therefore demonstrated acutely improved haemodynamics in response to CRT[55-58]. Use of conductance catheters to record PV loops and so assess acute haemodynamic changes during CRT implantation has been shown to aid optimal LV lead placement [58-60], as well as to predict long term response to CRT[57]. Interestingly, whilst both dP/dt_{max} and stroke work are both increased by CRT, it appears that these changes are not related to each other[61], and acute improvement in stroke work has been shown to be more predictive of long term response than dP/dt_{max}[62, 63]. Cardiac resynchronisation therapy therefore reverses the adverse haemodynamics associated with LBBB and indeed the ability of CRT to decrease the amount of wasted septal work[64] and septal rebound stretch[16] predicts response to CRT. Furthermore, computational modelling has suggested that the improvement in septal work is due to increased resistance to septal contraction provided by

the lateral wall, resulting in slower and more effective septal contraction, rather than due to an increase in volume of myocardium recruited in the septum[65].

1.3.4 Chronic Effects of CRT and Reverse Remodelling

1.3.4.1 Remodelling and Reverse Remodelling

Left ventricular remodelling in heart failure describes the changes which occur in the geometry and cellular and extra-cellular composition of the LV in response to changes in mechanical stress and neurohormonal activation[66]. The process of reverse remodelling describes the reversal of this process and the partial or complete recovery of cardiac geometry and systolic function which can occur[67], with multiple variations of measurements of improved LVEF and reduced LV volumes used to define significant reverse remodelling[68]. In addition to changes in chamber volume and a leftward shift in the end-diastolic pressure-volume relationship (EDPVR), reverse remodelling is associated with changes at the cellular, molecular and metabolic level[66, 67]. It can be seen simply when the primary cause of myocardial injury is withdrawn or treated, for example in, alcohol excess[69], thyrotoxicosis, peri-partum cardiomyopathy, or persistent tachycardia[70]. In dilated cardiomyopathies, pharmacological heart failure treatment (in particular neurohormonal blockade) is associated with reverse remodelling and these patients have an improved prognosis, albeit with a morbidity and mortality which is still higher than in the normal population[66, 71, 72]. Aside from medical therapy, both left ventricular assist device and CRT use are associated with reverse remodelling[66, 73].

1.3.4.2 CRT and Reverse Remodelling

Cardiac resynchronisation therapy not only results in acute re-coordination of mechanic synchrony, with improvements in acute cardiac work. Mechanical dyssynchrony and the subsequent inhomogeneous workload, with increased tension and workload in the lateral wall, induces asymmetrical hypertrophy, with thickening of late activated regions and thinning of early activated regions over time as shown in both canine pacing models of dyssynchrony and in patients with LBBB[74, 75]. Overall, this leads to adverse left ventricular remodelling[18, 76, 77]. At the molecular level, canine models of LBBB have shown uniform downregulation of potassium and calcium channel proteins with corresponding reduced ion currents[78], with some reductions demonstrating regionality and being more pronounced in late activated regions[79]. CRT induces long term reversal of these changes and reverse remodelling[80], with chronic improvement in both haemodynamics and cardiac volumes[81-83] which correlate with improved exercise capacity in CRT patients as measured by cardiopulmonary exercise testing (CPET)[84].

The mechanism by which the correction of dyssynchrony by CRT leads to structural and metabolic remodelling is still unclear, although there is some evidence that it results directly from the change in work distribution. A study by Duchenne *et al.* used a pacing-induced model of dyssynchronous heart failure in sheep to compare regional myocardial work (calculated with echocardiography and invasive haemodynamics) and regional glucose metabolism (calculated with ^{18}F-fluorodeoxyglucose (FDG) and positron emission tomography (PET))[85]. They found not only a strong correlation between the two, but that remodelling in response to inhomogeneous loading resulted in subsequent homogenisation of work and glucose metabolism. A clinical proof of concept in four patients undergoing

reverse remodelling in response to CRT showed similar homogenisation of work, giving evidence that reverse remodelling with CRT is triggered by the change in work distribution. The improvement of dyssynchrony and homogenisation of myocardial work induced by CRT therefore seems to start the remodelling process, possibly through changes in neurohormonal activation[18]. Cardiac resynchronisation therapy also partially reverses those molecular changes which are seen in dyssynchrony[78, 79], with an increase in potassium currents, improvements in myocyte contractility, β-adrenergic responsiveness and calcium handling[86, 87] and changes in cellular components of metabolism (see section 1.6.3).

1.3.4.3 Responders and Non-Responders

The degree of reverse remodelling and improvement in cardiac function and symptoms in response to CRT can however be variable and difficult to predict, with 30-50% of patients not experiencing benefit (termed 'non-responders')[88, 89]. The importance of this can be seen by the much better prognosis of responders compared with non-responders at long term follow-up[90, 91]. However, in order to be able to define non-responders, it is first necessary to consider the criteria used to define response to CRT. Whilst this is generally taken to mean an improvement in cardiac function and/or symptoms, the measures used have varied between studies and there is no consensus as to an overall definition. The outcomes used have included clinical measures such as symptom scores and quality of life (QoL) assessments, functional assessments of exercise capacity such as the 6 minute walk test (6MWT), measures of LV reverse remodelling and rates of death or hospitalization from either all-causes, major cardiovascular events or heart failure[39-43, 92] (summarized in Table 1.1). With such a broad

range of criteria, it is therefore important to consider which were used when discussing response rates reported in clinical trials. The importance of this is shown by the study by Fornwalt *et al.*, which found up to 17 different criteria being used in 26 studies, with agreement between these criteria being poor 75% of the time and strong only 4% of the time[93]. Furthermore, non-responder rates tend to be higher when more subjective symptom measurements are used as opposed to 'harder' measures such as LV reverse remodelling or mortality/hospitalisation[94, 95] and one international registry has found that local site-defined non-response tends to underestimate non-responder rates, compared to if the clinical composite score is used[96].

Table 1.1: Measurements of CRT Response

Clinical/Functional	NYHA Class QoL measures (e.g. Minnesota Living with Heart Failure Questionnaire) 6MWT Exercise duration CPET
LV Reverse Remodelling	Acute haemodynamic measurements Increase in LVEF Reduction in LVESV and LVEDV
Outcomes	Reduction in heart failure hospitalization Reduction in cardiac mortality Reduction in all-cause mortality

Another factor to consider along with the measure used to define response, is the range of response. While some patients experience only a modest improvement in a few criteria, some can have an excellent response. Such patients have been termed 'super-responders' and while there is again no consensus as to the definition of super-response, in general it encompasses a marked improvement or even near-normalization in left ventricular volumes and systolic function[97], and is associated with improved clinical outcomes[98]. Although the factors associated with super-response have not been as well characterised as those with non-response, it would appear that, as would be expected, they are often the same factors

but existing at the opposite end of the spectrum[98]. Super-responders may therefore reflect a population who have none of the factors (or the opposite factors) associated with non-responders. In addition, a minority of patients may only respond briefly, with one study finding that 15% of responders (based on reduction in LV end-systolic volume (LVESV)) did not actually have long lasting response at 1-2 years[99]. Whilst all-cause mortality was still better in these patients than in non-responders, it was worse than in long term responders.

Finally, it is important to consider that the term 'response' may be misleading. While some patients may not experience an actual improvement in function or symptoms, CRT may still prevent or slow the rate of any deterioration which would otherwise be expected to occur as part of the HFrEF disease process. These patients have been termed 'non-progressors'[98]. Strictly relying on rates of improvement alone is therefore likely to lead to an over-estimation of non-responder rates. Accordingly, the recent REVERSE study found that patients who were classified as 'stabilised' in response to CRT had a better prognosis than those who worsened[100]. The authors propose that the term 'non-responder' is therefore actually obsolete, and they suggest classifying patients instead as improved, stabilised, or worsened.

1.3.4.4 Factors Affecting and Resulting in Non-Response

Multiple studies, reviews and post-hoc analyses have investigated those factors which are correlated with the degree of response, with the aim of identifying either better patient selection, optimal implant characteristics, optimal post-implant CRT settings or developing novel technology. In general and as would be expected, the degree of resynchronisation as reflected by the extent of QRSd narrowing with BiV pacing is associated with response[101-106], as are other ECG markers of appropriate resynchronisation, such as a dominant S wave in lead

I and large R wave in V1[107, 108]. Those factors in particular which affect responder rates include:

1.3.4.4.1 Patient Selection

Although under-represented in CRT studies[109], multiple studies have indicated that women have better outcomes in response to CRT, with lower all-cause mortality and heart failure hospitalisation[110-112], including in large real world registry data[113], with some evidence in addition that women receive benefit at a shorter pre-implant QRSd[114]. Comorbidity also influences CRT response, with diabetes mellitus (DM), chronic kidney disease (CKD) and chronic obstructive pulmonary disease being associated either with increased all-cause mortality or heart failure admissions[115, 116]. In particular, whilst patients with DM do still receive benefit from CRT[117, 118], a meta-analysis has shown a higher mortality in diabetic patients[119]. This has also been observed in large real world registry studies[115, 120] which have shown that HbA1c, as an expression of poor glycaemic control, is predictive of a worse CRT outcome[121]. Similar studies also suggest a reduction in reverse remodelling following CRT in patients with DM despite similar levels of resynchronisation[65, 122]. In addition, iron deficiency is well recognised as a co-morbidity in the heart failure population, as are the benefits of iron replacement[1] and this appears to extend to the CRT population. A retrospective study of 541 CRT patients showed that iron deficiency was not only correlated with worse symptomatic outcomes, but also with increased all-cause mortality, heart failure admissions and LV reverse remodelling[123], with the latter hypothesized to be related to the role of iron as a co-factor in metabolism[124]. In addition, the recently published results of the IRON-CRT trial have shown

that iron replacement with ferric carboxymaltose in patients with persistently reduced LVEF at least 6 months after CRT and with iron deficiency, results in significantly improved cardiac function compared to standard of care[125].

The aetiology of heart failure is also important, with those with ischaemic cardiomyopathy having worse outcomes[126] and rates of reverse remodelling[127] compared to DCM, presumably due to scar burden which is not able to reverse remodel and recover. Indeed, increased scar burden in ischaemic cardiomyopathy is associated with worse response to CRT[128-130].

True LBBB morphology is also associated with improved response[131], with 2 meta-analyses indicating that CRT only improves clinical outcomes in those with LBBB and not in those with other conduction abnormalities[132, 133]. Finally, QRSd is also key, with those with a broader QRS having a greater response in the RAFT study[134] and in a meta-analysis[135]. Current guidelines therefore recommend CRT in patients with non-LBBB only if the QRSd is > 150 ms. Although those with a very wide QRS >200 ms seem to have worse survival rates after CRT[136] (possibly due to it being a marker of disease severity), there is some evidence that in patients with non-LBBB QRS widening, benefit is only in those with QRS durations >180 ms, even though this may be due to the electrical uncoupling which can be seen in advanced heart failure[137].

Whilst these factors can't normally be modified or altered (if patients are already on optimal medical therapy), their use does allow for potentially better patient selection, reducing the potential number of futile implant procedures and so unnecessary peri-procedural risk.

1.3.4.4.2 Lead Positioning

Given the latent contraction of the lateral LV wall which is associated with LBBB dyssynchrony, it is perhaps not surprising that optimal CRT necessitates placement of the LV lead at this site. Sub-group analyses of the MADIT-CRT[138] and REVERSE[139] trials demonstrated improved outcomes when the LV lead is placed at the lateral wall and also away from the apex of the heart, with a recent retrospective analysis of over 2000 patients confirming a long-term mortality benefit of lateral placement even after adjustment for other variables known to influence response[140]. Furthermore, pacing at site of latest activation as measured by the time from the onset of the surface ECG Q wave to the LV electrogram (Q-LV) has been shown to be associated both with reverse remodelling and QoL[141] and with heart failure hospitalization and mortality[142]. Tying these 2 factors together, if the longest Q-LV is at the lateral wall then it implies that the dyssynchrony is due to a LBBB pattern. Longer interventricular conduction delay (RV-LV conduction time based on intracardiac electrograms (IEGM)) also correlates not only with response as defined by reverse remodelling and QoL[143] but also with heart failure outcome measures[144]. Left ventricular lead placement has been aided further by the advent of quadripolar leads, which allow a more stable distal lead placement with more proximal, basal pacing. This has led to improvements in heart failure hospitalisation rates and mortality[145-147] and may be further aided by active fixation quadripolar leads[148].

Both the TARGET[149] and STARTER[150] trials took the concept of lateral wall lead placement further and suggested that the use of speckle tracking echocardiography to place leads away from myocardial scar or at the latest site of mechanical activation improves response rates.

Identification of scar extent and location as assessed by late-gadolinium enhancement (LGE) on cardiac MRI (CMR) has also shown better response with lead placement away from scarred segments[151]. Furthermore, a meta-analysis of CRT in patients with posterolateral scar showed that there was a 46% lower chance of echocardiographic response and 67% lower chance of clinical response to CRT compared to those with non-significant scar pacing[152], and targeting of LV lead position away from significant scar as identified on LGE-CMR appears a promising technique[153] . Finally, using multi-modality imaging to target lead position closest to the latest mechanically activated non-scarred LV segment appears to reduce the non-responder rate in a randomized controlled trial of 182 patients[154].

However, echocardiographic measures of dyssynchrony alone in the absence of QRS prolongation do not seem to predict response to CRT. The RETHINQ[155], ESTEEM-CRT[156] and then ECHO-CRT[157] studies all showed that echo measures of dyssynchrony in narrow QRS patients did not identify responders, while the PROSPECT[158] study showed that even in patients with a QRSd >130 ms, use of additional echo measures of dyssynchrony did not improve outcomes. It is worth noting, however, that these echo-derived parameters are likely to have been limited by significant intra- and inter-observer variability[159].

In those patients for whom optimal LV lead placement is not possible either due to a lack of suitable target veins, phrenic nerve capture or myocardial scar, newer developments for lead placement have also emerged, including LV endocardial pacing and conduction system pacing (His-bundle pacing (HBP) and left bundle branch area pacing)[160]. Left ventricular endocardial pacing is promising in those with poor CRT response[161], with a recent meta-analysis finding comparable response rates to conventional CRT[162], while the His-SYNC[163] study was the first randomized pilot trial of HBP vs conventional CRT and demonstrated similar primary

outcomes, albeit with the caveat of a high cross-over rate. Left bundle branch area pacing, first described by Huang *et al.*[164], may also be promising, with a recent non-randomized study showing similar response rates in terms of symptoms and LV function compared to both conventional BiV pacing and HBP[165], and a meta-analysis of 4 non-randomized studies even potentially demonstrating better echocardiographic response and symptom improvement compared to BiV pacing[166]. Left bundle branch area pacing may be useful if there is area of block higher in the His system, but in that scenario will not excite the right bundle branch physiologically to produce physiological RV activation. Both HBP and left bundle branch area pacing also suffer from the need for higher pacing outputs, increased thresholds over time and potentially higher lead displacement rates[167, 168]. Finally, leadless LV endocardial pacing using the WiSE-CRT system (EBR systems, Sunnyvale, CA) has also shown promise in non-responders to conventional CRT, with improvement in patient symptoms and LV reverse remodelling[169].

1.3.4.4.3 Programming

The importance of optimising both AV delay (AVD) and ventriculo-ventricular (VV) delay (VVD) in order to maximise CRT effectiveness is well recognised[170]. Indeed, the importance of frequent AVD and VVD optimisation at follow-up and not just at implant has been suggested[171]. Multiple methods have been described to assess AVD optimisation, including echocardiographic measurement of the mitral valve inflow pattern and device algorithms utilising analysis of the IEGM. In addition, the physiological changing of intrinsic AV conduction with exercise[172] has led to methods which allow for adjustment of AVD. Rate-

adaptive AVD (RAAVD) algorithms adjust delays as heart rate changes, with their use shown to increase exercise capacity[173]. The SonR lead (Sorin CRM SAS, Clamart, France) has a peak endocardial acceleration sensor embedded in its tip. As peak endocardial acceleration correlates with LV contractility, this can be assessed at a range of AV and VV delays in order to find the optimal settings at repeated intervals including during exercise[174]. The RESPOND-CRT trial has demonstrated non-inferiority in responder rates with the use of the SonR sensor compared to echo-optimisation[175]. More recently, adaptive AVD optimisation has also become important to allow fusion between intrinsic conduction and LV pacing +/- RV pacing wave fronts (so-called 'fusion pacing')[176]. This is discussed in more detail in section 1.4.

Finally, the advent of multipoint (MPP, Abbott Medical, Chicago, IL, USA) or multisite (Boston Scientific, Marlborough, MA, USA) pacing may also help response[177] and reduce mortality[145]. By pacing at multiple sites in the LV using a quadripolar lead, there is more rapid and uniform activation and additionally it may help overcome local areas of conduction block in the presence of myocardial scar[178]. There is also evidence that combining multisite pacing with optimised LV lead positioning further enhances reverse remodelling and outcomes[179, 180].

1.3.4.4.4 Arrhythmia

Patients with atrial fibrillation (AF) and CRT have worse prognosis, in part due to the loss of AV synchrony and high ventricular rates[181]. In addition, the atrial arrhythmia burden and inhibition of pacing can result in lower BiV pacing percentages. The degree of BiV pacing achieved with CRT has been shown to be key to response, with even a small reduction in percentage adversely affecting outcomes, and better survival rates are seen with BiV pacing >98%[182-184]; those with persistent or permanent AF have lower BiV pacing percentages and

increased mortality[185]. Using device counters as a marker of BiV pacing percentage can be misleading, with overestimation caused by fusion and pseudo-fusion beats meaning that perhaps less than half of patients actually receive >90% effective BiV pacing when assessed by Holter monitoring[186]. To this end, effective rate control of atrial arrhythmia should be aggressively pursued, using either medical therapy or AVN ablation[187], Indeed, the CERTIFY study found that use of AVN ablation in these patients led to lower mortality rates which were similar to patients in sinus rhythm, and higher than those treated with rate-limiting medication alone[188]. Similarly, high rates of ventricular extra-systoles can inhibit effective CRT[189], with evidence that reducing the burden with radiofrequency ablation in non-responders improves the degree of reverse remodelling[190].

1.4 CRT Algorithms and Fusion Pacing

1.4.1 CRT Pacing Intervals

As already discussed, in order to enable optimised CRT and maximise response, pacing intervals can be adjusted to give the best AV synchrony and narrowest QRSd possible. Optimised VVD allows for coordinated and homogenous biventricular activation, taking into account individual differences in interventricular conduction[170]. In addition, AVD optimisation allows maximal passive and active LV filling. If delays are too short then there is truncation of the A wave and so incomplete diastolic LV filling, while if they are too long then there will be fusion of E and A waves, reduced LV filling and diastolic mitral regurgitation[191]. Multiple methods have been described to assess AV optimisation, including

echocardiographic measurement of the mitral valve inflow pattern, and invasive and non-invasive haemodynamic measurements[170, 191]. However, echo based methods are labour intensive, and their value is uncertain[192]. Device algorithms utilising analysis of the IEGM have become an attractive alternative due to their rapid and automated nature[193], although evidence suggests that they may not have clinical benefit over using fixed AVD[194].

1.4.1.1 Changes in Intrinsic Conduction with Exercise

In addition to this baseline optimisation, the importance of dynamic adjustment of AVD with exercise has been increasingly recognised. Intrinsic AV conduction is known to alter with exercise[172], normally becoming shorter as heart rate increases, and so ideally AVD also has to adjust in the same way. Both bradycardia and CRT device algorithms can therefore allow dynamic adjustment of AV delays as they change with exercise and heart rate via RAAVD. Indeed, optimisation of AVD in CRT on exercise has been shown to improve cardiac output[195] and increase exercise capacity[173].

1.4.2 Fusion Pacing

Univentricular pacing of the left ventricle alone (LV-only pacing) has been shown to potentially have improved haemodynamic benefits over conventional BiV pacing, with improved RV haemodynamics[196] and prolonged battery life due to reduced current drain[197]. Subsequent randomised trials generally showed equivalence with BiV pacing[198-204].

However, increasingly LV-only pacing is used in fusion pacing, allowing fusion of the LV pacing wave front with intrinsic conduction[176, 205], as patients with heart failure and LBBB often have normal intrinsic RV activation through the right bundle[206]. In addition, 'triple fusion' can be achieved by fusing intrinsic activation with BiV pacing. Fusion allows for homogenous activation of the LV, shortening LV activation time[207], with studies showing that use of fusion-optimised intervals[193] results in narrower QRSd with improved haemodynamic response[208, 209] and greater LV reverse remodelling[210]. Importantly, as pointed out by Burri *et al.*[176], the original studies of LV univentricular pacing described above did not specifically aim to achieve fusion and better results may have been seen if fusion optimisation had been performed.

In order for fusion pacing to work, it requires relatively preserved intrinsic AV conduction as well as correct timing of LV pacing to RV activation. Indeed, AVD optimisation is key, as if it is too long then LV capture will be predominantly from intrinsic conduction and if it is too short predominantly from LV pacing alone, as shown in Figure 1.5. Therefore device specific algorithms allow dynamic reassessment of intrinsic conduction and so adjustment of the optimal paced/sensed AVD. They can therefore compensate for changes in the intrinsic AVD on exercising, and so maintain adequate fusion pacing and CRT optimisation.

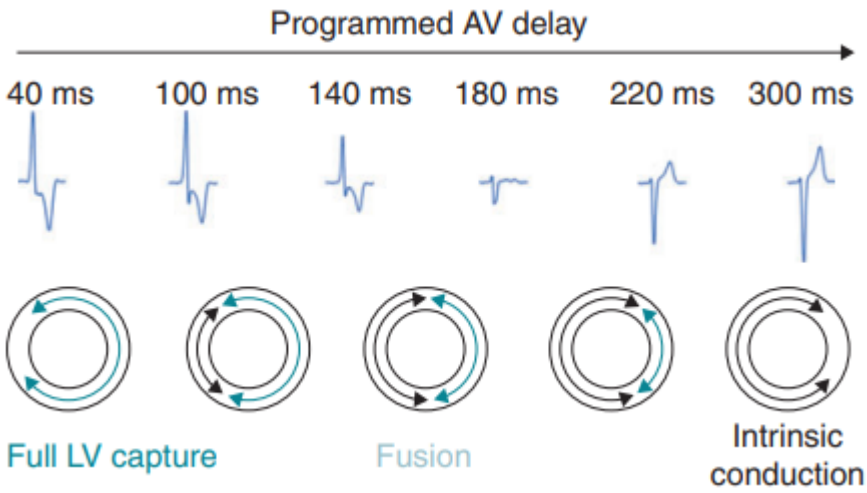

Figure 1.5: *The importance of optimised AVD to allow fusion capture of the LV, with capture from LV pacing alone if delays are too short and from intrinsic conduction alone if delays are too long (from Burri et al.[211])*

1.4.2.1 Existing algorithms

Three main manufacturer algorithms exist. SmartDelay™ from Boston Scientific allows for automatic AVD optimisation and LV-only pacing but does not dynamically reassess intrinsic conduction and can only be optimised during follow-up visits. Its use in the SMART-AV study showed no difference in outcomes compared to either echo-optimised AVD or nominal AVD at 120ms[194].

AdaptivCRT™ from Medtronic (Minneapolis, MN, USA) measures intrinsic conduction every minute and aims to pace at approximately 70% of intrinsic AV conduction. In addition, it allows for switching between LV-only pacing (if normal intrinsic AV conduction and heart rate (HR) <100 bpm) or conventional BiV pacing. Its use in the AdaptivCRT™ trial was overall non-inferior to echo-optimised BiV pacing. However, it included all QRSd >120 ms, not only LBBB, and in the subset with LBBB there were improved outcomes[212]. Additionally RV pacing was

reduced. The ongoing AdaptResponse trial[213] will hopefully give more evidence regarding its effectiveness.

Finally, SyncAV™ from Abbott assesses intrinsic AV conduction every 256 beats on a continuous search cycle, by allowing 3 intrinsic beats and measuring intrinsic AV conduction on the third beat. It then sets a shorter programmed AVD by subtracting a set period (known as the "delta" – adjustable but nominally set to -50 ms) from the intrinsic time. It has been shown to result in shorter QRSd compared to nominal settings or settings as programmed by the QuickOpt™ programme (Abbott)[214-216] as well as improved haemodynamics[217], with patient-optimised deltas generally being preferable to set deltas of -50 ms. There is also evidence that it reduces heart failure hospitalisations and improves LV reverse remodelling[218-220]. The ongoing SyncAV™ Post-Market trial (NCT04100148) is a prospective trial recruiting 1400 patients, randomised to either fixed AVD or SyncAV™, and assessing the impact on long term response, with the primary outcome being reduction in LVESV at 12 months.

1.4.2.2 Fusion Pacing on Exercise

Given the importance of optimised AVD for fusion pacing and the change in AV conduction which occurs physiologically on exercise, one potential limitation of fusion pacing is the ability of these algorithms to maintain fusion on exercise. If there are rapid or non-linear changes in intrinsic AV conduction then this could potentially result in loss of effective resynchronisation. This may especially be an issue with SyncAV™, as AdaptivCRT™ automatically switches to BiV pacing at HR greater than 100 bpm. Firstly, the re-analysis and adjustment intervals of the algorithms may be insufficient to allow effective fusion

throughout exercise if there are rapid changes in intrinsic conduction, resulting in lengthy periods of time during exercise without effective CRT. Secondly, there is evidence that in patients with heart failure AV conduction does not alter with changing HR in a similar way to healthy individuals. One study found that the degree of change is greater on exercise[195] whilst one demonstrated that in a CRT population only a third of patients had a shorter optimal AVD on exercise, with a third being unchanged and a third longer[221], although this was in a population with underlying 1st degree heart block. The use of a fixed delta in SyncAV™ may therefore result in insufficient adjustment of the AVD as intrinsic conduction changes, with its effectiveness therefore depending on how intrinsic conduction changes. The new SyncAV Plus™ (Abbott) algorithm, which is present in Abbott's Gallant™ series of CRT generators is designed to some extent to overcome this issue, as rather than the programmable delta which is subtracted from intrinsic conduction being a fixed value, it is instead a percentage of intrinsic conduction. It may therefore be more able to adjust to non-linear changes in conduction on exercise as it allows for a relative, rather than absolute, shortening.

1.5 Myocardial Metabolism and Metabolic Flexibility

1.5.1 Myocardial Metabolism in the Healthy Heart

The heart is the most metabolically active organ in the body, turning over twenty times its own weight in adenosine triphosphate (ATP) per day[222]. Approximately 60-70% of this ATP hydrolysis is used for contractile shortening and mechanical work, with the remainder used for powering ion pumps, in particular the sarco-endoplasmic reticulum Ca^{2+}-ATPase

(SERCA)[223]. It is also metabolically flexible, being a metabolic 'omnivore' and able to utilise glucose, fatty acids (FA), lactate or ketones to generate ATP and to vary the proportions of these which it uses to match supply availability, e.g. in times of fasting or in response to stress[224]. One theory is that this may stem from an evolutionary requirement to be able to maintain function at all times, regardless of varying substrate availability[225]. At rest, approximately 60-90% of cardiac ATP generation is from β-oxidation of FA[222], with the remainder predominantly being supplied by glucose oxidation, with small contributions from lactate, ketone and amino acid metabolism. At increased workloads, this shifts towards glucose metabolism, partly due to the increased efficiency (ATP generation per ml of myocardial oxygen consumption) of glucose oxidative phosphorylation[223, 226], as described below. The cardiac metabolism of each of the major metabolic substrates will be briefly considered in turn, with a simplified overview given in Figure 1.6.

1.5.1.1 Glucose

Glucose is taken up into cardiomyocytes primarily via the insulin-sensitive GLUT-4 transporter, which is held in cytosolic vesicles which are translocated to the cell membrane in response to insulin, ischaemia and increased workload[227], as well as via the insulin-insensitive GLUT-1 transporter. A small amount can also come from endogenous cardiac glycogen stores[228]. It first undergoes glycolysis to pyruvate, with the first irreversible step (conversion of fructose 6-phosphate to fructose 1,6-bisphosphate) being catalysed by phosphofructokinase (PFK)-1, which is therefore a key regulatory enzyme in the glycolytic pathway. Glycolysis yields a net of 2 ATP molecules per molecule of glucose, as well as generating reduced nicotinamide adenine dinucleotide (NADH). In the presence of sufficient

oxygen, pyruvate enters mitochondria via the mitochondrial pyruvate carrier (MPC) where it is then irreversibly oxidised to acetyl-Co-enzyme A (CoA) by pyruvate dehydrogenase (PDH), which therefore represents the rate-limiting step of glucose oxidation. Acetyl-CoA in turn can enter the tricarboxylic acid (TCA) cycle (also known as Kreb's cycle) to undergo oxidative phosphorylation (see section 1.5.1.4), with Hans Krebs and Fritz Lipmann sharing the Nobel Prize in Physiology or Medicine in 1953 for their work in this discovery. If oxygen is limited, pyruvate is instead converted to lactate in order to regenerate NAD+.

1.5.1.2 Lactate

The healthy heart is a net consumer of lactate even at high workloads[229], except during ischaemia or in diabetes[230], with uptake being facilitated by the monocarboxylate transporter (MCT). Use of radio-labelled isotopes has demonstrated that 80-90% is rapidly converted into pyruvate by lactate dehydrogenase (LDH) and then oxidised to acetyl-CoA to enter the TCA cycle[231, 232]. Indeed, circulating lactate may actually provide the dominant source of pyruvate in the heart[233].

1.5.1.3 Fatty Acids

1.5.1.3.1 Delivery and Uptake

Free fatty acids (FFA) are derived from lipolysis of triacylglycerols (TAG) in adipose tissue and then transported in the plasma bound to albumin. In addition, circulating esterified fatty acids in the form of endogenously synthesised TAG in very-low-density lipoproteins and dietary

TAG in chylomicrons are hydrolysed to FA by lipoprotein lipase (LPL) bound to capillary endothelial cells as well as cardiomyocytes[223]. Fatty acids are then taken up into cardiomyocytes via passive diffusion or by protein-mediated transport via the fatty acid translocase (FAT) CD36[234].

1.5.1.3.2 Metabolism

In the cytoplasm, FA undergo acetylation to CoA via fatty acyl-CoA synthase (FACS) to form long chain fatty acyl-CoA. Use of radio-labelled FA has demonstrated that a small amount (10-30%) are converted into TAG stores, with the majority immediately undergoing oxidation[235]. In order for the fatty acyl-CoA to enter mitochondria and undergo oxidation, it is linked to carnitine by carnitine palmitoyl transferase-1 (CPT1) to form acyl-carnitine and transported into mitochondria via carnitine-acylcarnitine translocase (CAT) as part of the carnitine shuttle. It is then regenerated by carnitine palmitoyl transferase-2 (CPT2), before undergoing repeated cycles of β-oxidation, each of which shortens the acyl-CoA by 2 carbons and releases a molecule of acetyl-CoA[228] which enters into the TCA cycle. β-oxidation also produces NADH and reduced flavin adenine dinucleotide ($FADH_2$), which pass to the electron transport chain (ETC)[234] (see section 1.5.1.6). Carnitine palmitoyl transferase-1 is inhibited by malonyl-CoA, which is formed by carboxylation of acetyl CoA by acetyl-CoA carboxylase (ACC). It therefore is a marker of excess acetyl-CoA and acts as a negative feedback mechanism and potent inhibitor of FA metabolism[236].

1.5.1.4 Ketone Metabolism

Ketone bodies (β-hydroxybutyrate (BOHB) and acetoacetate) are synthesised in the liver in states of high FA availability and are taken up into cardiomyocytes in a concentration-dependent manner via passive diffusion or MCT1. Whilst their contribution to myocardial metabolism is therefore normally relatively small, this increases greatly when plasma concentrations are elevated, e.g. during starvation or poorly controlled diabetes[223]. Once taken up, BOHB is converted to acetoacetate via β-hydroxybutyrate dehydrogenase (BDH1) and acetoacetate is then esterified to CoA by succinyl CoA:3-ketoacid CoA (SCOT). This then generates 2 molecules of acetyl-CoA, which again enters the TCA cycle.

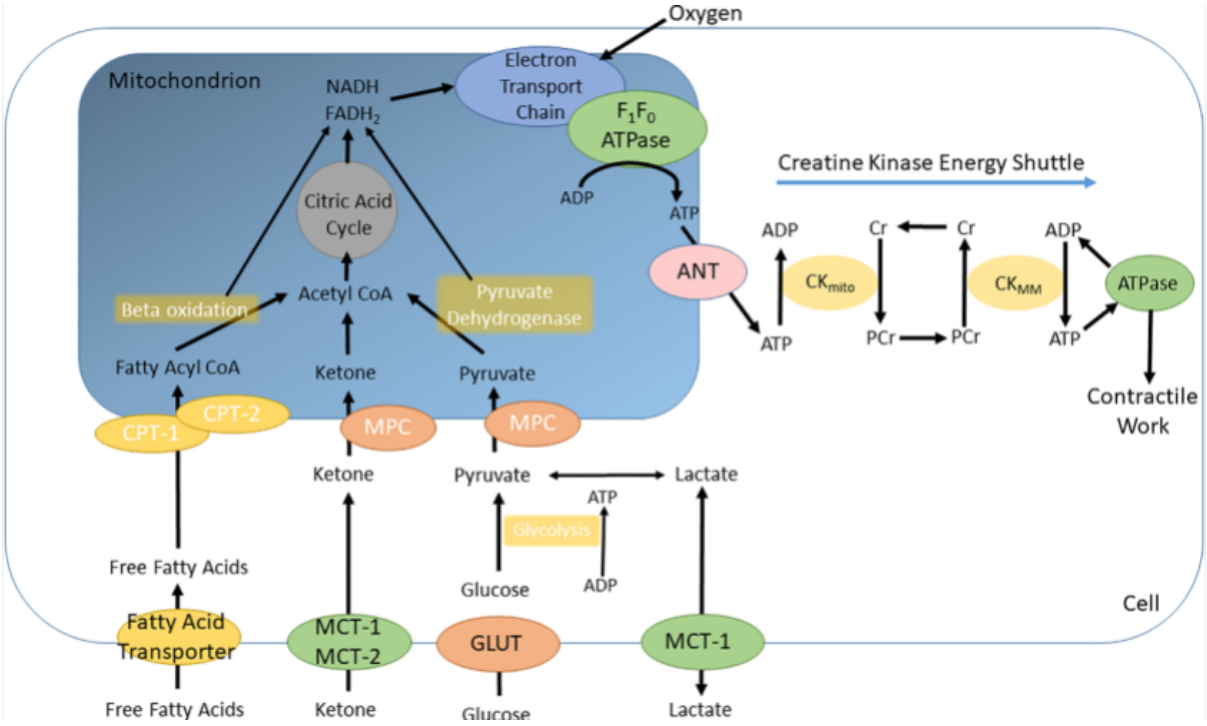

Figure 1.6: *Simplified schematic of myocardial substrate metabolism (from Watson et al.[237])*

1.5.1.5 Oxidative Phosphorylation

Once acetyl-CoA enters the TCA cycle, it undergoes progressive oxidation, generating the reducing agents NADH and $FADH_2$. These NADH and $FADH_2$, along with those produced by FA β-oxidation and NADH produced by glycolysis, then donate electrons to the ETC to generate ATP via oxidative phosphorylation (Figure 1.7). Electrons are donated by NADH at complex I and by $FADH_2$ at complex II, eventually being transferred to oxygen. The transfer of these electrons across the chain drives protons into the intermembrane space, generating an electrochemical proton gradient across the inner mitochondrial membrane. This gradient, and the subsequent passage of protons back into the mitochondrial matrix via complex V (the F_OF_1 ATP synthase), is used to generate ATP from adenosine diphosphate (ADP), with the larger the gradient the greater the energy of synthesis of ATP[238]. Under non-ischaemic conditions, the great majority (at least 95%) of cardiac ATP generation is derived from oxidative phosphorylation[223].

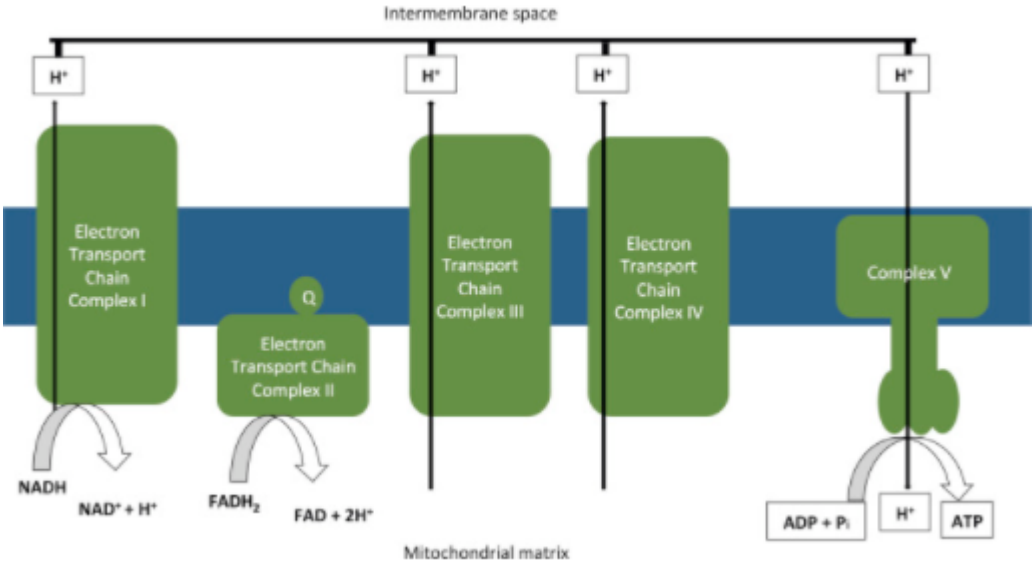

Figure 1.7: *Overview of the ETC (from Wesselink et al.[239]). Q = Ubiquinone*

1.5.1.6 Regulation of Oxidation

Short term control of oxidative pathways occurs through post-translational modifications, interaction with regulatory proteins or allosteric effectors[240]. Fatty acid oxidation and glucose utilisation have an inverse relationship (the 'glucose-fatty acid cycle', first described by Randle *et al.* and so termed the Randle cycle[241]). High rates of FA oxidation inhibit both PDH activity via PDH phosphorylation and PFK1, so decreasing glucose oxidation and glycolysis respectively[242]. Conversely, high rates of glucose oxidation inhibit FA oxidation via increased ACC activity and so increased malonyl-CoA. In addition to the Randle cycle, 5'-adenosine monophosphate (AMP)-activate protein kinase (AMPK) is a key regulator of oxidative metabolism. High levels of AMP in conditions of cellular energy starvation activate AMPK, which in turn both increases glucose and FA oxidation and inhibits ATP-consuming processes, leading to AMPK being described as a cellular 'fuel gauge'[243]. Long term changes in

metabolism occur through the activation of transcription factors and so alterations in the number of enzyme molecules available. One of the largest families of these are the peroxisome proliferator-activated receptors (PPARs), PPARα in particular having a key role in upregulating genes involved in FA uptake and oxidation[240].

1.5.1.7 Phosphocreatine Shuttle

Once ATP is generated at the mitochondria, it needs to be transferred to sites of hydrolysis and so usage at the myofibrils. In order for this to occur, the gamma phosphate group is transferred to creatine in the cytosol to generate phosphocreatine (PCr), catalysed by creatine kinase (CK) in the equation:

$$PCr^{2-} + MgADP^{-} + H+ \rightleftharpoons Cr + MgATP^{2-}$$

This PCr then diffuses (or, in more recent modelling, is transferred via a series of coupled reactions in near equilibrium in a process known as direct channelling[244]) to sites of ATP usage, where CK then regenerates ATP from ADP. In addition, PCr forms a pool which is able to rapidly regenerate ATP at times of high demand. In this way it therefore acts as both a spatial and temporal buffer.

Whilst CK and PCr are responsible for the great majority of phosphotransfer, adenylate kinase (which catalyses: $2ADP \rightleftharpoons ATP + AMP$) is responsible for between 10-20%, with glycolysis also contributing a minor amount[245, 246].

1.5.2 Metabolic Substrate Efficiency

When discussing 'efficiency' of metabolic substrates, it is key to define what parameter is being assessed. In terms of energy storage, FA metabolism is beneficial, with 3-4 times more ATP generated per mole of substrate compared to glucose[247], as well as more energy released by oxidation of each 2 carbon moiety[248]. However, in general efficiency refers to the amount of oxygen required to generate ATP, with the substrate used greatly influencing the efficiency. Fatty acid oxidation is less efficient than glucose oxidation. Metabolism of 1 molecule of glucose via glycolysis and glucose oxidation yields 31 ATP and requires 6 molecules of oxygen. However, metabolism of 1 molecule of palmitate produces 105 molecules of ATP for 23 molecules of oxygen[226], and the phosphate: oxygen (P:O) ratio of glucose oxidation is therefore 2.58 compared to 2.33 for FA oxidation[234, 249], with esterification of FA to fatty acyl-CoA also using 2 ATP molecules[249]. This inefficiency is due to FA being in a relatively reduced state and is also due to β-oxidation of FA generating relatively more $FADH_2$ than NADH compared to glucose and ketone oxidation (1:2 vs 1:4 respectively). As $FADH_2$ donates its electrons to the ETC at complex II, which is at a lower energy level than complex I, where NADH electrons are donated, it therefore generates a smaller proton electrochemical gradient and so energy of ATP synthesis.

However this is not the whole story as to why FA oxidation is less efficient. The differences outlined above would theoretically be expected to give FA oxidation an efficiency of 10-12% less than glucose[223]. However, experimental models utilising invasive measurements of cardiac work and MVO_2 whilst on glucose vs FA substrate infusions to calculate efficiency in both mouse [250] and pig[251] hearts, have demonstrated reduced efficiency of between 27-48%, suggesting that other factors must be responsible. In addition, increased cardiac FFA uptake

in humans without HFrEF has also been shown to increase MVO_2[252]. Multiple mechanisms for this have been suggested. The first involves mitochondrial uncoupling. Uncoupling proteins (UCP) 2 and 3 are present in the inner mitochondrial membrane and dissipate the electrochemical protein gradient, allowing proton leak back from the intermembrane space without passing through the F_OF_1 ATP synthase and so without generating ATP. Levels of these have been shown to correlate with circulating FA levels in human hearts[253], and are postulated to mediate FA uncoupling of oxidative phosphorylation[254]. Secondly, UCP3 exports FA anions from the mitochondrial matrix, which is then required to be esterified to an acyl-CoA for re-entry to the mitochondrion, utilising 2 ATP molecules[234, 255]. This futile cycling also occurs between the inter-conversion of fatty acyl-CoA and storage of FA in intracellular TAG pools[234, 255]. Thirdly, long chain FA activate Ca^{2+} channels in the sarcolemma, resulting in more ATP hydrolysis being required to maintain normal cytosolic Ca^{2+} concentrations[226, 234]. Finally, relative uncoupling of glycolysis and glucose oxidation, with the latter being more inhibited by the Randle cycle, can lead to intracellular acidosis and an increase in ion pump activity to maintain homeostasis[226].

In addition to these differences between FA and glucose efficiency, ketone oxidation has also attracted much interest, with research demonstrating a greater cardiac efficiency than FA oxidation[256]. This results in part from keeping ubiquitone oxidised, increasing the redox potential between complexes I and III in the ETC and so increasing the free energy of ATP hydrolysis[256, 257], as well as proportionally more reducing equivalents reaching the ETC compared to with FA oxidation[258]. The improvement in efficiency seen with glucose perfused hearts following addition of insulin was matched by perfusion with ketone[259]. Finally, ketones, glucose and FA compete as a source of acetyl-CoA to enter the TCA cycle and so one

theory is that increased ketone metabolism may limit FA oxidation and so limit FA oxidation–mediated deleterious effects such as increased reactive oxygen species and UCPs[260].

1.5.3 Assessing Myocardial Energetics Using MR Spectroscopy

Magnetic resonance imaging has revolutionised diagnostic imaging and the ability to assess anatomical structure *in vivo*, leading to the Nobel Prize in Physiology or Medicine being awarded to Peter Mansfield and Paul Lauterbur in 2003. Over recent decades, cardiac MR spectroscopy (MRS) has emerged as a key tool enabling non-invasive assessment of cardiac metabolism[237, 261]. In particular, phosphorus (^{31}P) spectroscopy enables measurement of the phosphorus containing molecules involved in phosphotransfer (i.e. ATP and PCr). Assessment of the relative proportions of these generates a PCr/ATP ratio. Whilst this normally has a value of ~2, it has been shown to be reduced in heart failure (see section 1.5.4) and other pathologies. This is as a result of insufficient rates of oxidative phosphorylation and ATP generation to maintain and replenish the PCr pool, which therefore depletes in order to maintain ATP supply at sites of usage[262]. As ATP concentration is maintained until late in the heart failure process[262], the PCr/ATP ratio is an important marker of metabolic status.

However, a key limitation of the PCr/ATP ratio stems from the fact that it only reflects their relative proportions rather than absolute quantity. Whilst measurement of absolute quantity is possible, it is technically challenging[237, 263] and so not routinely assessed. In addition, the heart has a remarkable ability to match ATP generation and supply to demand, meaning that even under moderate stress the PCr/ATP ratio does not change in healthy hearts[264-266] and so limiting its usefulness to detect changes in metabolism in these settings. Finally, as described above, the PCr/ATP ratio essentially depends on an assumption that ATP concentration is

maintained and constant. However, late in disease processes ATP levels may also start to fall as PCr is unable to keep them fully replenished[262, 267], leading to pseudo-normalisation of the ratio.

A more accurate way of assessing changes in metabolism is therefore to calculate changes in ATP generation from PCr via CK (CK flux)[267]. This in turn is made possible by calculation of the forward pseudo-first order rate constant of the CK reaction (k_f) via a saturation transfer method. In brief, this entails using selective radiofrequency pulses to saturate the y-phosphorus group of ATP and eliminate its signal, essentially rendering it invisible in the phosphorus spectrum[268, 269]. Given the rapid exchange of this group between PCr and ATP in equilibrium, this saturation is transferred to PCr, and the reduction in height of the PCr peak is proportion to the rate of exchange. If PCr concentration is known (calculated from the PCr/ATP and literature values of ATP concentration), then CK flux can be calculated as k_f x [PCr]. Saturation transfer is explained in more detail in Chapter 2.

1.5.4 Myocardial Metabolism in Heart Failure and Metabolic Remodelling

The concept that heart failure and impaired myocardial metabolism are related has been recognised for decades[270, 271], with the heart estimated to contain up to 30% less ATP in end stage heart failure[272]. Multiple studies have demonstrated that PCr/ATP is reduced in HFrEF[273-276], as well as in a range of other pathologies including hypertrophic cardiomyopathy, severe valvular heart disease, obesity and diabetes[268]. Furthermore, reduced PCr/ATP in HFrEF predicts prognosis[277] and may improve with heart failure treatment[274]. Creatine kinase flux is also reduced in HFrEF by up to 50%[278], with this reduction again predicting HF events

and mortality[267, 279] correlating with reduced (non-invasively measured) cardiac work and cardiac efficiency[280]. These findings, amongst others, have led to the theory that the heart is ATP-starved in heart failure[262] and likened to an engine out of fuel[281], although there is still debate as to whether these metabolic changes are causative in HF or not[240]. As well as these changes, it is worth noting that HFrEF is also accompanied by other cellular changes which reduce the efficiency of excitation-contraction coupling, e.g. changes in calcium handling proteins such as SERCA and changes in β receptors and subtypes[282, 283].

1.5.4.1 Changes in Substrate Metabolism

Changes in substrate metabolism with worsening impairment of LV systolic function and heart failure are complex. Overall, there is a reduction in both FA oxidation and glucose oxidation[223, 226, 237, 281], although with a greater reduction in FA oxidation and so a relative shift towards glucose oxidation[240, 284, 285]. However, glucose uptake and glycolysis are increased in heart failure, becoming decoupled from glucose oxidation[249, 286]. These changes are thought to possibly be adaptive, due to the better oxygen efficiency associated with glucose metabolism, although the lactate generation and acidosis associated with the decoupled glycolysis may negatively impact cardiac contractility[249]. It should be noted that while a decrease in FA metabolism as above has generally been accepted with progressive heart failure, some human studies utilising paired arterio-venous (A-V) blood sampling in HFrEF populations have actually shown no change or even an increase in FFA uptake[287, 288]. It has been hypothesised that these divergent results may be due to differences in heart failure severity as well as the presence of co-morbidities such as obesity[272].

In addition to these changes, there is also evidence of increased cardiac ketone uptake[288] and oxidation in heart failure[223, 240, 289, 290], which has been postulated to reflect its beneficial oxygen efficiency compared to FA oxidation, and increased lactate usage[291]. Indeed, infusion of ketone in patients with heart failure has been shown to improve cardiac output and LVEF[292].

Overall, these changes appear to be mediated by down-regulation of PPAR-α, changes in the cellular energetic state with decreased NADH/NAD^+ and acetyl-CoA/free CoA ratios and increased hypoxia-inducible factor-1 (HIF1) signalling[248]. Together, these changes are thought to represent a loss in the normal metabolic flexibility which the healthy heart exhibits. It should be noted that in addition heart failure is associated with insulin resistance[272]. A proposed mechanism for this is that the hyper-adrenergic state and activation of the renin-angiotensin system which is associated with heart failure leads to increased plasma FFA, which in turn decreases glucose uptake and metabolism and causes pancreatic damage[293].

1.5.5 Myocardial Metabolism at Stress

A key component of the modulation of metabolic flux in response to stress and increased ATP demands is the mitochondrial acetyl-CoA/CoA ratio[294]. With increasing work rate, feedback through the PCr shuttle results in increased TCA cycle flux and so a decrease in the acetyl-CoA/CoA ratio. This in turn leads to reduced inhibition of PDH, 3-ketoacyl-CoA thiolase and mThiolase, increasing oxidation rates of glucose, FA and ketones respectively[294]. In addition, levels of malonyl-CoA decrease, removing inhibition of CPT1 and so increasing β-oxidation of FA, while HIF1 stimulates glycolysis at the same time as inhibiting PDH via PDK1, thus

inhibiting pyruvate oxidation and so reducing oxygen demand[295]. In addition to these changes, β-adrenergic stimulation increases PDH activity and glucose oxidation[296, 297], as well as stimulating lipolysis at adipocytes[298], with circulating FFA levels increasing on exercise[234]. Finally, studies with exercise show increased circulating lactate levels lead to a correlating increase in myocardial lactate uptake, as well as increased glucose uptake[231], with similar results with atrial pacing[229]. Overall, the relative increase in myocardial substrate uptake with exercise in humans appears to be greater for carbohydrates than for FA[234].

Whilst there have been few studies assessing changes in metabolism with stress in HFrEF, a study using pacing stress and paired A-V blood sampling in humans with both DCM and healthy controls showed that glucose uptake (which was already higher in the DCM cohort) was unable to increase further in response to stress, unlike in control participants, with no significant changes in FA uptake in either group[285]. A similar limitation of glucose uptake in DCM in response to stress was shown in a further study, which in addition showed that in participants who also had impaired glucose tolerance glucose uptake did not increase at all and instead there was a greater increase in FA oxidation to meet the requirements of the increased workload[299]. Overall, these studies suggest impaired metabolic flexibility in response to stress in the heart failure population.

1.5.6 Diabetes Mellitus and Heart Failure

Diabetes mellitus and heart failure are closely linked. Patients with diabetes have up to a 74% increased risk of developing heart failure and almost one third have undiagnosed LV dysfunction[300], while conversely one third of patients admitted with HFrEF have DM[4]. Whilst a proportion of this relates to the increased rates of atherosclerosis associated with DM and

so corresponding increased ischaemia, a series of population-based studies, starting with the Framingham Heart Study, have demonstrated that DM confers increased risk of heart failure independently of the increased atherosclerotic risk and other risk factors[301-303]. It has therefore been identified as an independent risk factor, with the identification of a separate disease entity, diabetic cardiomyopathy, which can be defined as "myocardial disease in patients with diabetes, not attributable to hypertension, coronary artery disease or other cardiac disease"[300]. It includes both HFpEF and HFrEF and as 90% of DM is type 2 diabetes mellitus (T2DM)[300], it is this which is generally considered. Energetic changes induced by DM are key to this process and indeed changes in metabolic substrate usage in mouse models seem to precede the development of cardiac dysfunction[304], although other aspects of DM may also contribute to the diabetic cardiomyopathy, including coronary microvascular dysfunction and autonomic neuropathy[305].

1.5.6.1 Energetic and Metabolic Changes

The impact of T2DM on myocardial metabolism can be seen by the decreased PCr/ATP ratio which is seen at rest[306, 307] and which is further worsened with increasing workload[307]. Interestingly, in a rat model, whilst PCr/ATP was lower in diabetic animals, CK flux was unchanged due to a compensatory increase in k_f[308] and similar findings have been in found in human participants with obesity[309].

At the metabolic level, the insulin resistant state associated with T2DM results in high circulating levels of FFA, with increased myocardial FA uptake[310]. Glucose uptake and oxidation is reduced[311] and at the same time FA oxidation is increased[312], as shown in both

mouse models[304, 313] and human studies[314]. Overall therefore, there is a shift towards almost exclusive FA metabolism and a loss of metabolic flexibility. This has implications for metabolic efficiency, as discussed above. However, in addition the increase in FA uptake is greater than the increase in oxidation[311], leading to a greater formation of intracellular TAG stores and myocardial steatosis[315, 316]. Steatosis has been shown to correlate with LV contractile dysfunction[317] and is associated with cardiac lipotoxicity.

1.5.6.2 Lipotoxicity

The accumulation of intracellular lipid has been found to negatively impact myocardial metabolism and function through an accumulation of intermediates in lipid metabolism. For example, long-chain acylcarnitines accumulate within mitochondria, inhibiting pyruvate and lactate metabolism[318] as well as oxidative phosphorylation[319]. There is also an accumulation long-chain acyl-CoA which is then diverted to non-oxidative processes with production of diacylglycerols and ceramides[320]. These in turn inhibit intracellular insulin signalling and so further reduce glucose uptake and oxidation[311], as well as affecting ATP production and apoptosis[320]. As well as this, generation of reactive oxygen species, FA-induced uncoupling of oxidative phosphorylation and accumulation of acetyl-CoA can lead to mitochondrial oxidative stress and damage[321]. Furthermore, hyper-acetylation of mitochondrial proteins in a rat model of T2DM has recently been shown to drive energetic dysfunction, a process which can be partially reversed using the Sirtuin 3 (an NAD+ dependent deacetylase) activator honokiol[322].

1.6 Effects of CRT on Myocardial Metabolism

Combining the fields of CRT and myocardial metabolism, there is an increasing body of evidence that each may influence the other[323-325]. This gives rise to the possibility that CRT response may therefore be, at least to an extent, dictated or influenced by both baseline (i.e. pre-implant) myocardial metabolism and flexibility, as well as the changes in these which CRT is able to induce. For example, it may help explain the reason for worse responder rates which are seen in patients with DM[65, 122], as previously discussed.

1.6.1 Myocardial Metabolism in Cardiac Dyssynchrony due to LBBB

Pacing models of dyssynchrony have shown reduced cardiac efficiency (i.e. cardiac work / MVO_2) [326], while large animal models have shown that LBBB is associated with decreased septal myocardial blood flow (MBF) and subsequent LV remodelling with lateral wall hypertrophy[77]. Myocardial glucose uptake has been studied in mechanical dyssynchrony using the radiolabelled glucose analogue FDG-PET. This has shown that in patients with LBBB and no coronary artery disease, there is decreased septal FDG uptake compared to controls without LBBB [327], with similar findings in a canine pacing model of LBBB[328]. This decrease in septal FDG uptake has also been shown to correlate with mechanical dyssynchrony as assessed by echocardiography[329], and with decreased septal work as assessed by feature-tracking CMR[330] . The decreased glucose uptake in the septum in LBBB therefore appears to reflect its lack of contribution to LV contraction, and possible waste of energy due to systolic stretching, with FDG uptake correlating with myocardial work in a sheep model[85]. However,

changes in cardiac perfusion also have to be taken into account. Changes in glucose uptake may result from alterations in blood flow and so glucose delivery, as opposed to true changes in substrate utilisation, although delineating in this way is difficult as substrate utilisation and blood flow are likely to be linked with changes in myocardial work likely to affect both together.

^{13}N-ammonia (^{13}N-NH_3)-PET imaging has therefore been used in combination with FDG-PET to try to separate changes in perfusion from metabolic changes in glucose uptake. Initial studies demonstrated that decreased glucose uptake occurred without changes in perfusion[327, 331]. However, a more recent study showed that when absolute MBF is calculated there is decreased septal FDG uptake along with decreased MBF, although the septal-to-lateral wall ratio (SLR) was lower for FDG than it was for MBF[332]. Late ^{13}N-NH_3 uptake did not show any regional differences however, with the authors concluding that it reflected a composite measure of altered regional MBF and metabolism and is therefore a poor parameter for MBF alone. This may explain the discordant earlier findings.

Overall, it appears that LBBB is associated with heterogeneous myocardial perfusion, although whether this is caused by septal hypoperfusion or lateral wall hyperperfusion is still unclear[333]. However, septal glucose uptake is reduced more relative to perfusion, in a phenomenon that has been termed reverse-mismatch[333, 334]. In addition, the SLR of FDG appears to correlate with measures of dyssynchrony whilst MBF SLR does not[329].

A more accurate method to assess myocardial metabolism is through the use of radiolabelled ^{11}C-Acetate PET to measure myocardial oxidative metabolism and so non-invasively assess MVO_2[17, 335]. In patients with LBBB, this has confirmed not only lower global MVO_2 across the myocardium, but again a heterogeneous distribution, with regional variations and highest MVO_2 (and MBF) in the lateral wall, as would be expected[336].

1.6.1 Effects of CRT on Myocardial Metabolism Assessed by PET

Given that mechanical dyssynchrony appears to therefore be associated with decreased and heterogeneous myocardial metabolism, this could be expected to improve in response to correction of the dyssynchrony. Cardiac resynchronisation therapy has indeed been shown to improve septal myocardial glucose uptake, homogenising its uptake across the LV[337, 338]. Importantly, the degree of pre-existing septal reverse mismatch prior to CRT has been shown to predict response at 3 months in a study of 49 patients, with higher mismatch in responders possibly reflecting a greater potential for reversibility[334], with similar findings when FDG SLR correlated with dyssynchrony[329]. However, in ischaemic populations, one study has demonstrated that FDG uptake correlates with the amount of viable myocardium, which could explain the correlations with response in this cohort[339]. ^{11}C-Acetate PET has also been used in a number of studies in CRT patients to show that stroke volume increases in response to CRT without a change in global LV oxidative metabolism[340-343]. Furthermore, whilst global metabolism may be unchanged, septal oxidative metabolism does appear to increase relative to the lateral wall, in keeping with increased septal work[340, 344]. Interestingly, there is also evidence that this homogenisation is more effective in non-ischaemic as opposed to ischaemic cardiomyopathies[344]. These changes occur without associated changes in oxygen consumption, although the effect on changes in perfusion or MBF are mixed[337, 341, 344]. Finally, uptake of ^{99m}Technicium-sestamibi scans, which indicates cellular perfusion and mitochondrial function, has been found to improve with CRT even in some patients with no change in LVEF, which has been postulated to account for the improvement in symptoms in some patients even without objective improvements in cardiac function[325, 345].

1.6.1 Effects of CRT on Myocardial Metabolism Assessed Invasively

Alterations in cardiac metabolism in response to CRT has not only been shown using PET studies however. Pioneering work by Nelson *et al.*[346] used invasive measurement of myocardial work with a PV catheter along with paired A-V blood sampling across to the heart to assess MVO_2 in 10 patients with non-ischaemic cardiomyopathy. This demonstrated that CRT improved cardiac work but again that MVO_2 did not increase in line with this. It should be noted however that it was only possible to actually analyse PV loops in 3 of the patients due to poor quality recordings and so dP/dt_{max} was the main assessment of cardiac function which was used. A similar approach was taken by Kyriacou *et al.*[347], who showed conversely that while cardiac work increased, MVO_2 also increased, although the improvement in work was 80% greater and so cardiac efficiency was still improved.

As previously discussed, the linkage between myocardial substrate metabolism and myocardial work and efficiency is well recognised. In CRT patients, substrate usage may therefore affect the heart's ability to respond to CRT and reverse remodel. In a study in which 22 patients with non-ischaemic cardiomyopathy undergoing CRT had paired A-V blood sampling across the heart for metabolite analysis, patients with a higher cardiac FFA extraction were more likely to be non-responders[348]. The authors therefore suggest that FFA uptake may serve as a biomarker to identify non-responders. This implies that the effectiveness of CRT may be limited on an individual basis by the pre-existing cardiac metabolic usage, but what is less understood is the extent to which CRT may influence substrate usage itself and whether this may be partly responsible for the metabolic changes seen in response to CRT. In addition, whilst the authors calculated substrate fluxes based on the ratio of A-V substrate differences to A-V O_2 differences, they did not calculate MBF and so could not quantify absolute substrate uptake.

Intriguingly, a recent study conducted by Martens *et al.* has analysed coronary sinus (CS) and peripheral venous blood samples at time of CRT implant and peripheral samples at 6 months post-CRT to assess the impact of CRT on global and cardiac metabolism[349]. In conjunction with ^{99m}Technicium-sestamibi myocardial wash-out scans to assess mitochondrial membrane potential, they showed that CRT induces a shift towards FA metabolism, which is associated with an improvement in mitochondrial function. Importantly however, arterial blood samples and coronary flow rates were not obtained and so cardiac extraction and uptake could not be calculated.

To our knowledge, the influence of CRT on absolute cardiac substrate uptake has not yet been assessed.

1.6.2 CRT and Cardiac Efficiency

The PET and invasive studies above together demonstrate a key characteristic of CRT, namely that cardiac work is increased without a corresponding increase in MVO_2. This means that cardiac efficiency (if defined as cardiac work / oxygen consumption) is improved. This improvement seems to persist in the long-term with responders having similar efficiency to mild heart failure patients without LBBB[341, 350]. In addition, this improvement in efficiency also appears to predict outcomes following CRT[342].

1.6.3 Molecular Changes in Response to CRT

In addition to evidence that CRT improves glucose uptake and oxidative metabolism as a whole, it appears that this is reflected in changes in the metabolic machinery at the molecular

level. Analysis of mitochondrial proteins in a canine model of dyssynchronous or synchronous heart failure suggested that CRT altered the expression and post-translational status of mitochondrial enzymes, leading to improved mitochondrial function[351], and all subunits of the ETC (with the exception of complex IV) appear to be upregulated[323]. Increased ATPase activity was also shown in the myocardium of canines which had undergone CRT, in a dyssynchronous heart failure model[352]. In a human study, 24 patients undergoing CRT underwent metabolomic profiling at baseline and then again 3 months post-CRT, with responders demonstrating an improvement in markers of oxidative and glycolytic metabolism compared to non-responders[353]. Other studies have also confirmed these metabolomic differences between responders and non-responders[354, 355]. These studies tie into the wider search for biomarkers (both metabolic and non-metabolic) which may help to predict response to CRT[356].

The majority of ATP consumption in myocardial cells is accounted for by excitation-contraction coupling via the myosin ATPase, the SERCA and the NA+/K+ ATPase[240], with approximately 60-70% actually used for contractile shortening and 30-40% used by SERCA and other ion pumps[223]. Changes in calcium handling have been seen in response to CRT. In a pacing induced model, a reduction in the L-type calcium channel current and abnormal calcium homeostasis was partially restored by CRT[78]. In addition, the lower SERCA and phospholamban expression in heart failure is partially reversed by CRT[357, 358], with this only seeming to occur in responders as opposed to non-responders[359]. However, in addition to these (and other) changes in calcium handling, findings include upregulation of the sodium-calcium exchanger, reversal of T-tubular system regression, recovery of β-adrenergic responsiveness with upregulation of β1 receptors, reversal of the reduction in myosin heavy chain alpha and restored calcium sensitivity of myofilaments[18]. Changes in the cytoskeleton

are hypothesised to provide the link between the mechanical effects of CRT and these molecular changes[323]. Improved cellular bioenergetics may therefore underpin the macroscopic changes in metabolism seen in CRT.

1.7 Aims of the Thesis

The aims of this thesis are therefore to examine the links and interplay between CRT and cardiac metabolism at rest and during stress, both acutely and over the course of longer term reverse remodelling. Specifically:

In Chapter 3, multi-parametric CMR is used to examine the effect of substrate manipulation on cardiac function and energetics in participants with DM and both normal cardiac function and HFrEF.

In Chapter 4, invasive measurements at the time of CRT implant are used to examine the acute effects of CRT on cardiac efficiency and metabolic substrate uptake.

In Chapter 5, baseline MRS measurements and invasive CRT measurements are correlated to measures of CRT response at 6 months.

In Chapter 6, CPET is used to assess the effectiveness and efficiency of a dynamic AVD algorithm enabling fusion pacing, in participants who have already responded to CRT.

Chapter 2:
Methods

2.1 Ethical Approval

All research was carried out in accordance with the Declaration of Helsinki and was approved by the National Research Ethics Service (Altering Substrate Selection as a Potential Therapeutic Target in Heart Failure, REC reference 18/SC/0170; Assessing the Effect of the SyncAV^{TM} Algorithm in Cardiac Resynchronisation Therapy on Exercise Capacity and QRS Duration on Exercise, REC reference 18/SC/0611).

2.2 Randomisation

All randomisations were performed using a tool available on www.randomizer.org.

2.3 Basic Measurements and Investigations

2.3.1 Anthropomorphic Measurements

Participant height and weights were measured using a digital weighing scale with an integrated attached measure (Marsden, UK). These were used to calculate Body Mass Index (BMI) and Body Surface Area (BSA). Hip/waist ratios were measured using a standard tape measure.

2.3.2 Blood Pressure

Blood Pressure (BP) was recorded as the best of 3 measurements taken after 5 minutes of sitting at rest, using an automated cuff (Carescape Dinamap^{TM} V100, GE, USA).

2.3.3 Electrocardiogram

Standard 12 lead ECG recordings were performed using an electrocardiograph (Marquette Mac 3500^{TM}, GE, USA). ECG interval measurements were taken from the automated ECG analysis.

2.3.4 Six Minute Walk Test

Standardised six minute walk tests (6MWT) were performed[360], with participants instructed to walk at a brisk but comfortable pace back and forth along a 20 metre corridor for 6 minutes,

with standardised instruction and encouragement. Total distance achieved was recorded. Participants with exercise tolerance acutely limited for a non-cardiac reason (e.g. acute arthritis or intercurrent illness) were excluded.

2.3.5 EQ-5D-3L Questionnaire

Participants were requested to complete a EQ-5D-3L health questionnaire (see Appendix) as per standard instructions[361]. Approval for usage was obtained following registration with EuroQol (Registration ID 31167).

2.4 Intravenous Infusions

2.4.1 Intralipid™

20% Intralipid™ (Fresenius Kabi, UK) was infused intravenously at a fixed rate of 60 ml/hr. In CMR experiments, unfractionated heparin (Monoparin™, CP Pharmaceuticals, UK) was concomitantly infused at 0.4 U/kg/hr. In invasive experiments, heparin was administered intra-arterially as a bolus (100 U/kg) with an activated clotting time (ACT) subsequently checked approximately every 15-20 minutes and further boluses given as required to maintain an ACT ≥250 seconds.

2.4.2 Insulin/Dextrose

A hyperinsulinaemic euglycaemic insulin clamp technique was used[362]. A cannula was placed into a large vein in each arm, with one used for blood sampling via a three-way tap and one used for co-infusion of insulin and glucose. Blood sugar was measured from venous samples using a point of care testing device (Freestyle Optimum Neo™, Abbott Diabetes, UK). A baseline sample was taken prior to commencing the infusion, with this level taken as the target blood sugar level. Insulin (Actrapid™, Novo, Denmark) was infused at a constant rate of 20 mU/m^2/min (participants without DM) or 40mU/m^2/min (participants with DM) following a 10 minute loading regime (63.8 mU/m^2/min for 1 minute, 56.8 mU/m^2/min for 1 minute, 50.6 mU/m^2/min for 1 minute, 45.1 mU/m^2/min for 1 minute, 40.1 mU/m^2/min for 1 minute, 35.7 mU/m^2/min for 1 minute, 31.8 mU/m^2/min for 1 minute, 28.4 mU/m^2/min for 1 minute, 25.2 mU/m^2/min for 1 minute, 22.5 mU/m^2/min for 1 minute in participants without DM; rates were doubled in participants with DM). At 10 minutes, the venous blood sugar level was checked and then thereafter every 5 minutes during the first hour. Subsequent blood sugar levels were checked at opportune moments during the research protocols. An infusion of 20% dextrose was started at minute 4 at a rate of 2 mg/kg/min, then from minute 15 the rate was titrated based on the difference between the measured and baseline blood sugar readings. This calculation was aided via the use of an in-house Microsoft Excel™ (Microsoft, Washington, USA) spreadsheet which was kindly provided by the department of Diabetes and Endocrinology, Oxford University Hospitals NHS Foundation Trust.

2.4.3 Dobutamine

Following baseline heart rate and blood pressure recording, dobutamine (Hameln pharma, UK) was infused at a starting rate of 5 mcg/kg/min and then titrated as necessary at 2 minute intervals (up to a maximum of 40 mcg/kg/min) to reach a target of 65% of the predicted maximum heart rate for age (220 minus age in years). Participants were monitored non-invasively with heart rate, non-invasive blood pressure and pulse oximetry measured via an Expression™ MR200 MRI safe monitoring system (MR Devices, UK). Blood pressure was recorded every 4 minutes.

2.5 Echocardiograms

All echocardiograms were performed on an EPIQ™ 7c ultrasound system (Philips, NL), with left ventricular volumes and ejection fraction calculated via the Simpson's biplane method.

2.6 Magnetic Resonance Scans

2.6.1 Cardiac Volumes and Function

All scans were performed in a Tim Trio™ 3 Tesla (3T) scanner (Siemens, Erlangen, Germany), with the exception of post-CRT implantation follow up scans, which were performed in a Magnetom Avanto™ 1.5 Tesla (1.5T) scanner (Siemens, Erlangen, Germany). Participants lay

supine and a 24 channel spine matrix and 6 channel body matrix were used (except for during dobutamine stress, when scans were performed using the integrated body coil).

For imaging on the 3T Trio™, steady state free precession (SSFP) imaging was used, with typical scan parameters of: slice thickness 8 mm, gap 2 mm, echo time (TE) 1.5 ms, repetition time (TR) 46 ms, flip-angle 50°, field-of-view (FOV) 400 mm. For imaging on the 1.5T Avanto™ system, gradient recalled echo (GRE) imaging was used in order to minimise the artefact from implanted CRT devices[363], with typical scan parameters of: slice thickness 7 mm, gap 3 mm, TE 2.0 ms, TR 28 ms, flip-angle 15°, FOV 380 mm. Prior all post-CRT scans, CRT devices were programmed to MRI-conditional mode as per Section 2.8.2 and ECG and pulse oximetry monitoring was used during the scan as per our institutionally agreed operating procedure. All scans were acquired in end-expiration breath-hold using retrospective ECG-gating, except in the case of significant arrhythmia when prospective triggering was employed. Following acquisition of standard pilot images, horizontal long axis (HLA), vertical long axis (VLA) and short axis (SA) cine scans were obtained.

Scans were analysed off-line, using CVI 42™ version 5.10.1 (Circle Cardiovascular Imaging Inc, Calgary, Alberta, Canada). Manual contouring of the LV and RV at end-systole and end-diastole was performed, as shown in Figure 2.1. For stress assessment, biplane measurements using HLA and VLA cines alone were used. All contouring was carried out blinded to randomisation.

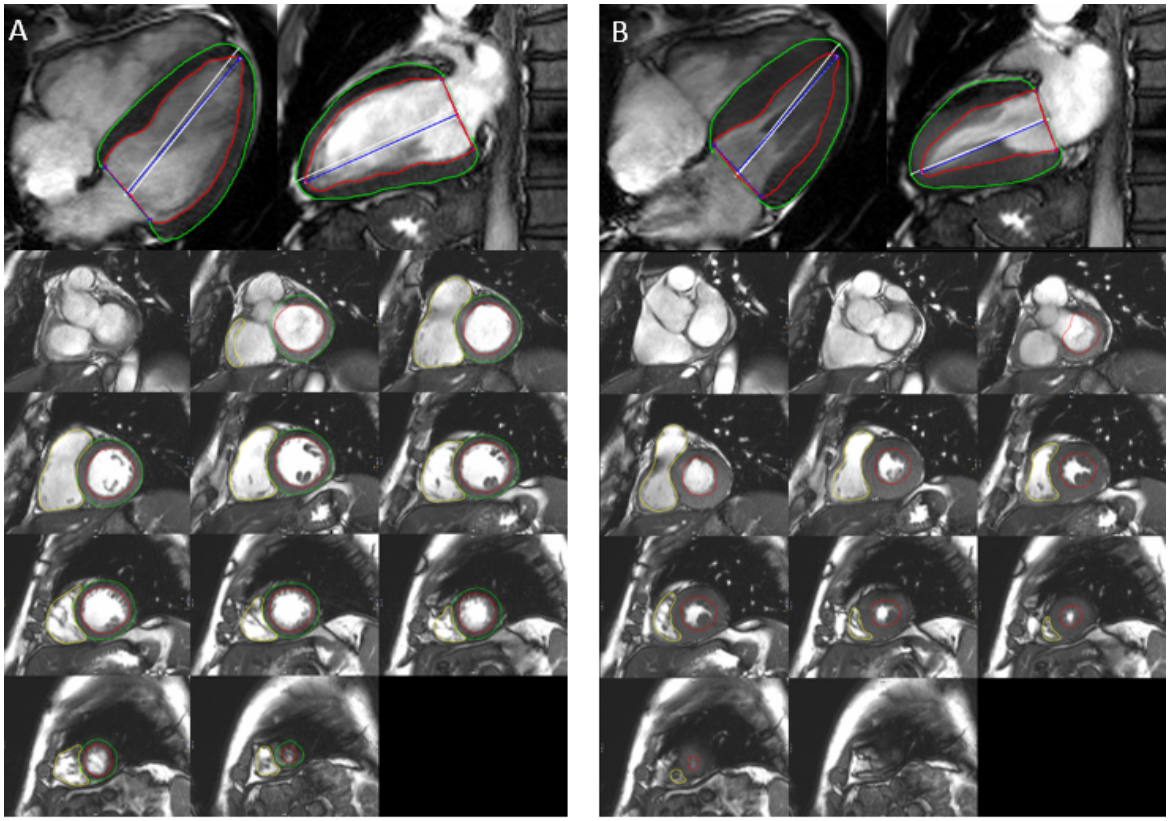

***Figure 2.1**: HLA, VLA and SA ventricular contours, respectively, at end-diastole (A) and end-systole (B). Green contour = epicardial LV, red contour = endocardial LV, yellow contour = endocardial RV. Analysis performed using Circle CVI 42™. Images obtained from a participant at 3T*

2.6.2 CMR Derived Measures of Cardiac Work

Resting HR and arterial BP were measured in the scanner immediately prior to starting Dobutamine. Average stress HR and mean arterial pressure (MAP) were taken as the measurements closest in time to when target heart rate (or maximum heart rate if this was not achieved) were reached.

MAP (mmHg) was calculated as:

((2 x diastolic BP) + systolic BP) / 3

Rate pressure product (RPP, mmHg.bpm) was calculated as:

HR x systolic BP

Stroke work (ml.mmHg) was calculated as:

Stroke volume x MAP

Cardiac work (L.mmHg/min) was calculated as:

Stroke volume x heart rate x MAP

2.6.3 Left Ventricular Strain Analysis

Automated 3D Global Circumferential Strain (GCS) was calculated using tissue tracking technology on Circle CVI 42^{TM}, using 4 mid-ventricular SA slices (Figure 2.2)

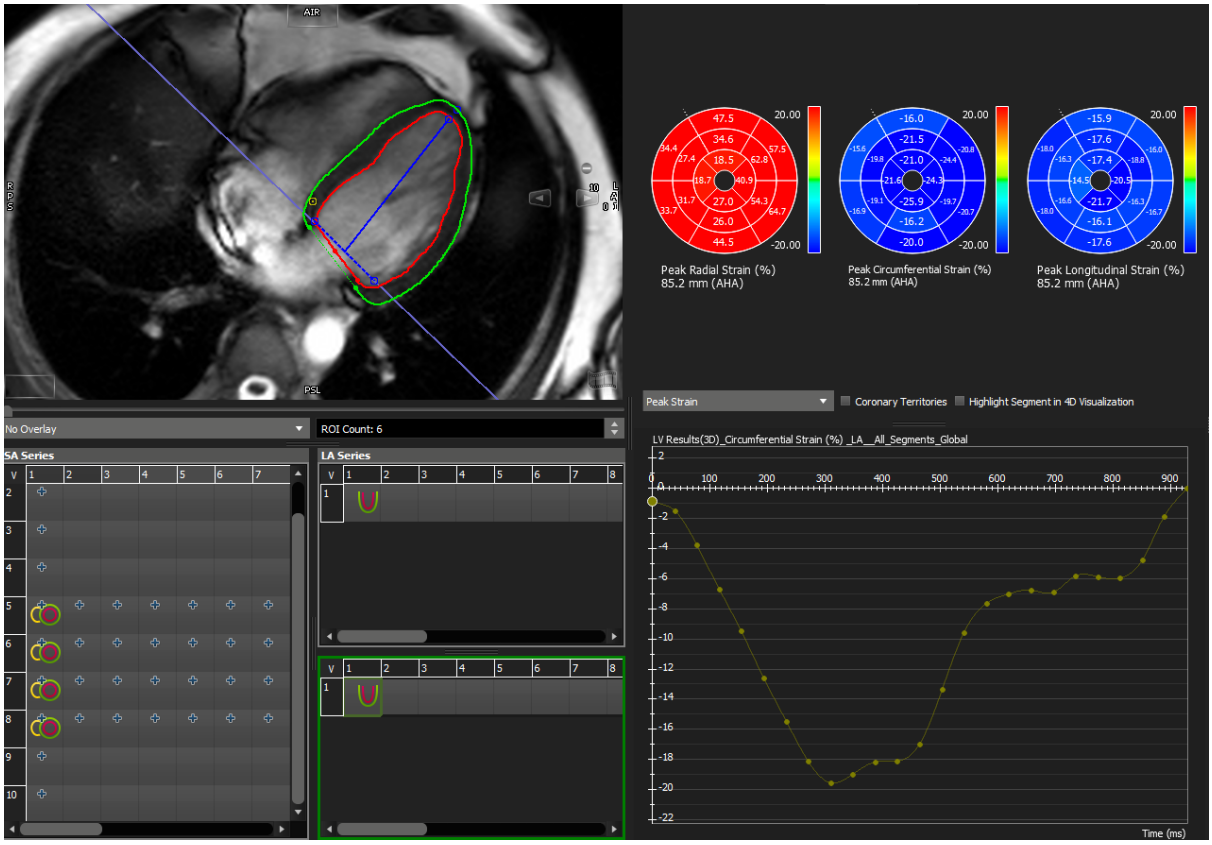

***Figure 2.2**: Example of automated GCS analysis, performed using Circle CVI 42™. Images obtained from a participant at 3T*

2.6.4 ^{31}P 3D Chemical Shift Imaging for Phosphorus Spectroscopy

All scans were performed on a Tim Trio™ 3T system (Siemens, Erlangen, Germany), using a modified 1.5T Heart/Liver ^{31}P coil (Siemens, Erlangen, Germany), consisting of a large ^{1}H transmit-receive and ^{31}P transmit outer element (26 x 28 cm) and a smaller ^{31}P receive loop/butterfly pair (12 x 15 cm loop and 23 x 12 cm butterfly).

Participants were scanned prone with their left ventricle positioned over the centre of the coil, at the magnet iso-center, with proton localisers used to enable correct positioning. Ten

free induction decay inversion recovery curves (utilising 1 ms hard inversion pulses and with increasing inversion delay from 100 – 3000 ms) were acquired, along with the locations of phenylphosphonic acid fiducial and cod liver oil phantoms.

3D acquisition-weighted chemical shift imaging (CSI) was used (acquisition matrix size 16 x 8 x 8, FOV 240 x 240 x 200 mm, voxel size 11.25 ml). Pilot images in VLA, HLA and SA axis planes were taken to enable positioning of the CSI matrix, with the grid oriented to place voxels along the interventricular septum. Three saturation bands were placed over skeletal muscle in the chest wall and the liver in order to minimise signal contamination (Figure 2.3).

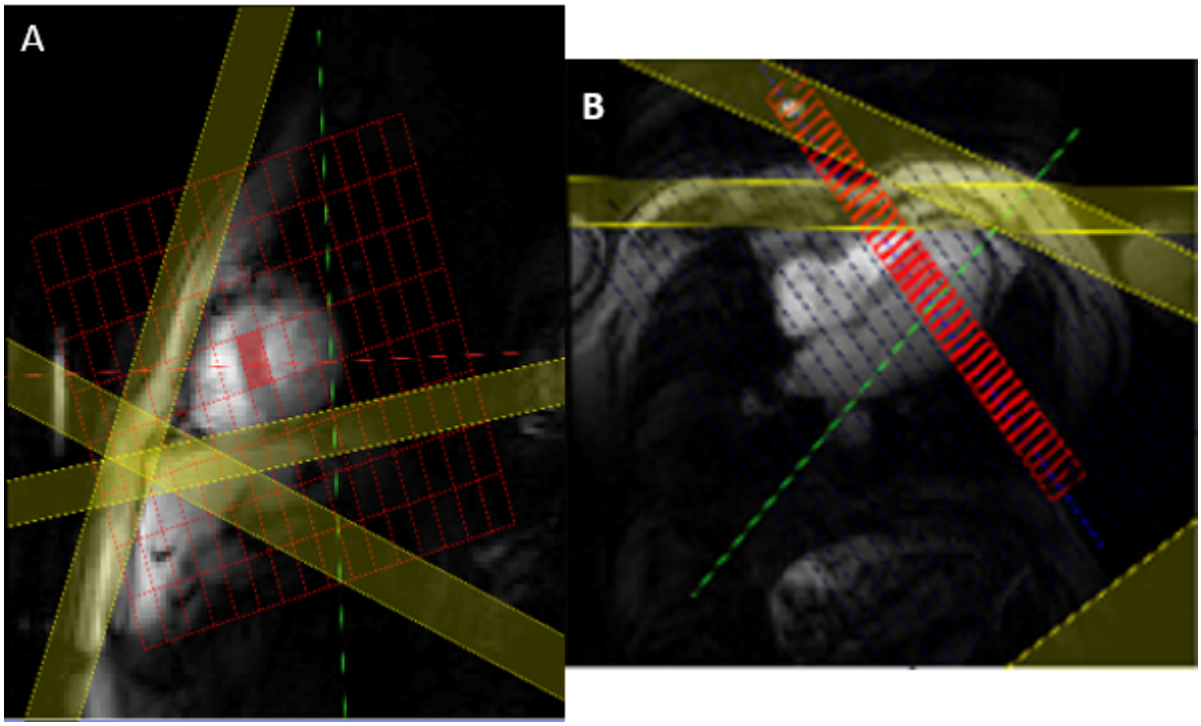

***Figure 2.3**: CSI grid (in red) positioned with a voxel of interest over the mid-ventricular septum in short axis (A) and HLA (right) views. Saturation bands (yellow cross-hatched areas) are positioned over skeletal muscle and liver. Images obtained from a participant at 3T*

The radio frequency pulse was centred between γ and α-ATP peaks by subtracting 250 Hz from the observed PCr frequency to ensure uniform excitation of the spectral peaks[364]. The acquisition was non-gated with TR around 910-1010 ms depending upon specific absorption rate (SAR) and TE reduced to a minimum using the ultra-short echo time (UTE-CSI) technique[365] . Nuclear Overhauser enhancement was used to increase signal-to-noise ratio in acquired spectra. Total acquisition time was approximately 11 minutes.

2.6.4.1 Analysis

In participants with DM, a basal-mid septal voxel and the adjacent voxel by half-voxel shift were selected for analysis, with results averaged. In participants without DM, the most basal septal voxel was used. All efforts were to ensure voxels selected were matched for each participant's paired scans on separate substrate. The flip angle for the selected voxel was determined by an in-house Matlab™ (Mathworks, MA, USA) program, which co-registered the SA images with the spectral data. Variation in flip angle due to coil loading effects was calculated by the use of acquired inversion recovery data and the localizer containing the fixed locations of the cod liver oil capsules and the fiducial, which were manually identified (Figure 2.4).

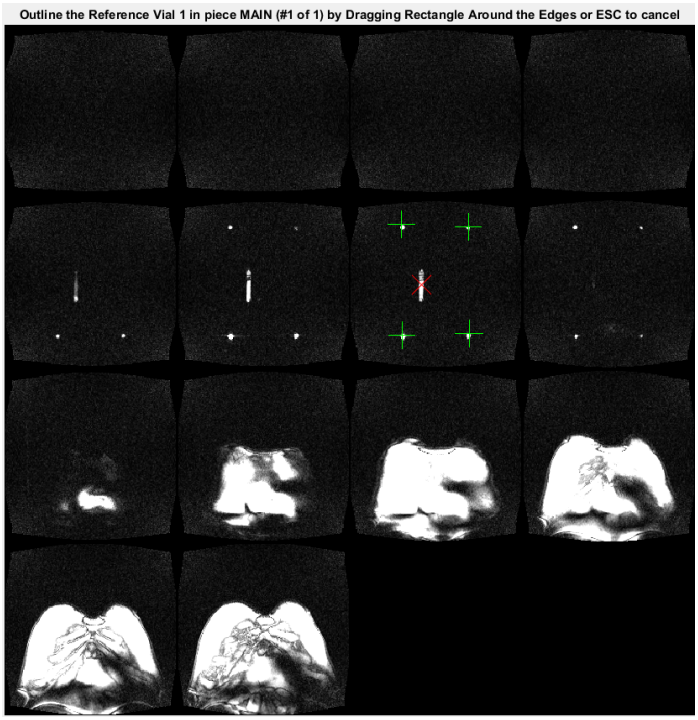

Figure 2.4: *Example of manual cod liver oil capsule (green crosses) and fiducial (red cross) identification. Images obtained from a participant at 3T*

Spectral peaks for PCr, α, β and γ-ATP, 2,3-diphosphoglycerate (2,3-DPG) and phosphodiesters (PDE) were fitted using the AMARES (advanced method of accurate, robust and efficient spectroscopic fitting) method[366] (Figure 2.5). Automated analysis involved correcting peak areas for radio frequency partial saturation effects and spectral overlap with the NADH peak. The value of the ATP peak was corrected for blood contamination by subtracting 11% of the DPG peak area[364].

PCr/ATP ratio was calculated using the average of the three ATP peaks. The quality of spectral fit was assessed using the coefficient of variation in the measured PCr/ATP ratio, based on Cramer-Rao lower bounds (an indicator of signal to noise ratio in the sample). In general,

spectra with a coefficient of variation greater than 20% were excluded, unless spectra were manually judged to be of sufficient quality for inclusion by a second assessor. In addition, PCr/ATP ratios ≥3 were excluded as non-physiological.

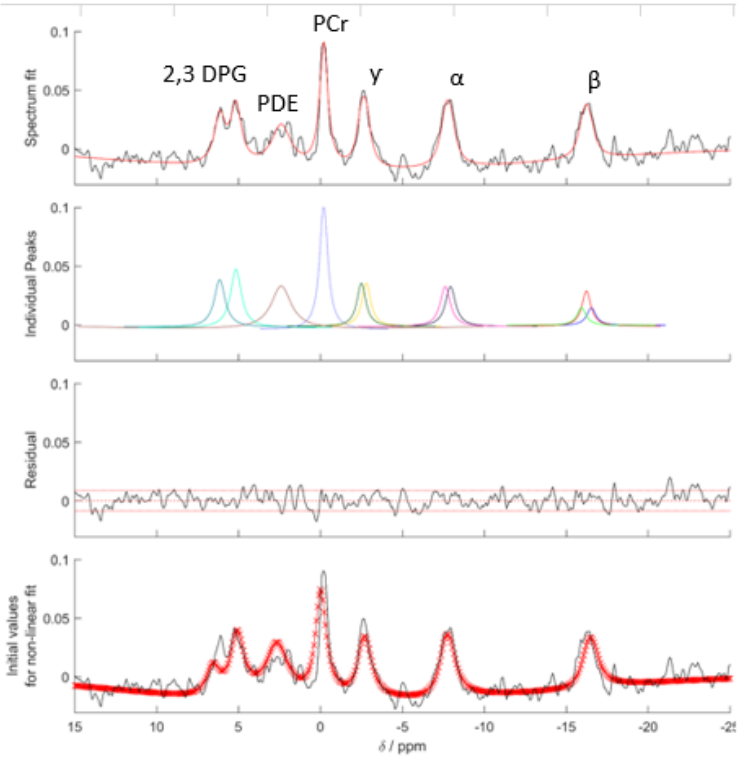

Figure 2.5: *Example of a spectral fit using the in-house Matlab™ analysis package, with spectral peaks labelled. Spectra obtained from a participant at 3T*

2.6.5 Triple Repetition Saturation Transfer and Stress Saturation Transfer

2.6.5.1 Theory

The CK equilibrium reaction can be simplified as:

$$PCr \underset{kr}{\overset{kf}{\leftrightharpoons}} \gamma\text{-ATP}$$

where k_f and k_r are the unidirectional forward (ATP producing) and reverse (PCr producing) pseudo first-order rate constants, respectively. Saturation transfer allows calculation of k_f, by selectively saturating the γ-ATP peak using a radio frequency pulse, rendering it effectively invisible in the phosphorus spectrum. As the saturated phosphate from γ-ATP is transferred to creatine to form PCr, this saturation is also transferred to the PCr peak. The degree of saturation (and so decrease in height) of the PCr peak is then proportional to the forward rate of the reaction (Figure 2.6).

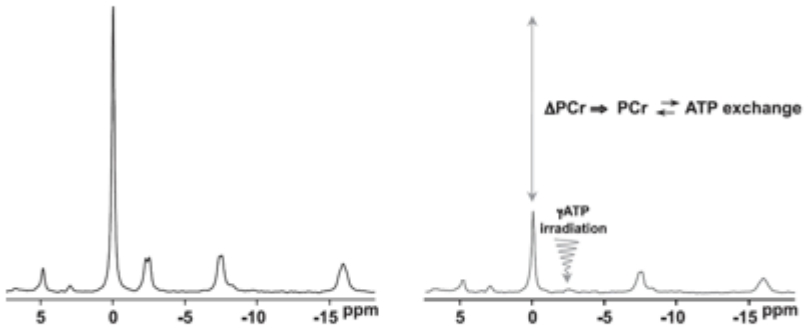

***Figure 2.6**: Saturation transfer results in a fall in the height of the PCr peak, proportional to the rate of k_f (adapted from Befroy and Shulman[367])*

In order to calculate k_f, it is necessary to calculate each parameter in the following equation:

$$kf = \frac{1}{T'1, PCr} \cdot \left(\frac{M'0, PCr}{M0, PCr} \right)$$

Where $M'_{0,PCr}$ is the magnetization of PCr during γ-ATP saturation, $M_{0,PCr}$ is the magnetization of PCr without γ-ATP saturation and $T'_{1,PCr}$ is the apparent T1 of PCr during γ-ATP saturation.

In order to achieve this, the triple repetition time saturation transfer (TRiST) method was used[368, 369], consisting of four acquisitions; a short TR sequence with no γ-ATP saturation, a short TR sequence with γ-ATP saturation, a long TR sequence with γ-ATP saturation and a short TR sequence with a 'control' saturation pulse falling down field of PCr. This takes approximately 1 hour in total. An extension (stress saturation transfer or StreST) allows an additional measurement of k_f to be made during stress, taking only 18 minutes (described below)[368].

2.6.5.2 Method

All scans were performed in a Tim Trio™ 3T scanner (Siemens, Erlangen, Germany). Participants were scanned supine, with either a 10 cm loop transmit-receive ^{31}P surface coil (Pulse Teq, Chobham, UK) or a 17 cm loop transmit and 11 cm loop receive ^{31}P surface coil (Pulse Teq, Chobham, UK) positioned over the left ventricle, at the iso-centre of the scanner. Axial and sagittal proton localisers were used to confirm coil position over the LV, aided by a phantom positioned in the centre of the coil.

The centre frequency and γ-ATP and control saturation offsets were calculated using a 1D-CSI sequence run prior to the main TRiST acquisition (TR 330 ms, TE 2.3 ms, flip angle 35°, 125 averages).

The 1D-CSI matrix (200 x 200 x 160 mm) was oriented with voxels parallel to the chest wall, fully covering the heart and centred on the centre point of the receive coil as per Figure 2.7, with a saturation band across skeletal muscle. The most apical cardiac voxel was chosen as the voxel of interest. Results from other voxels could subsequently be used if necessary if

judged to be of sufficient quality by a second experienced and blinded operator. All efforts were to ensure voxels selected were matched for each participant's paired scans on separate substrate.

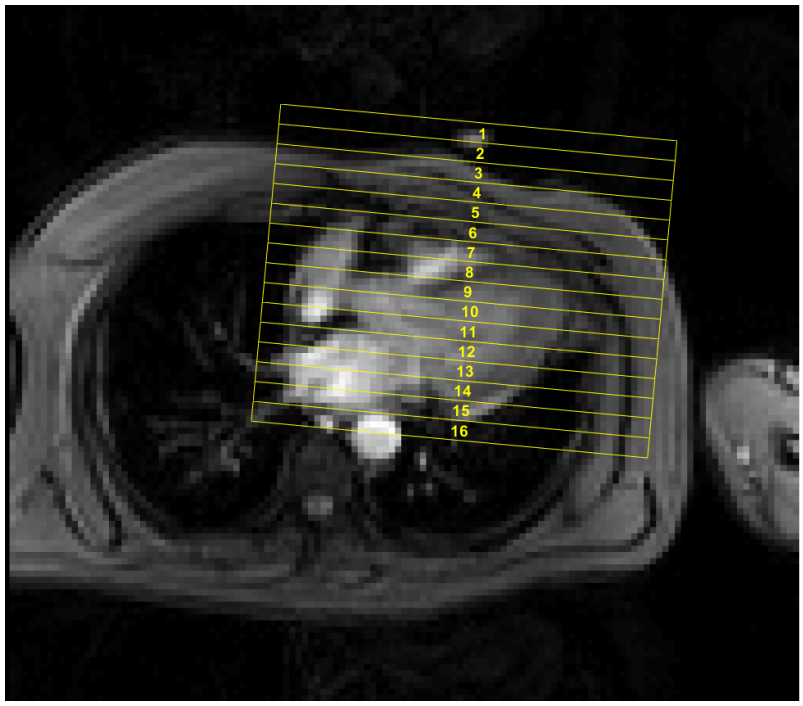

***Figure 2.7**: Positioning of the 1-D CSI grid (yellow), with voxels oriented parallel to the coil and chest wall. For the initial CSI sequence to calculate offsets prior to the main TRiST acquisition, a saturation band was also placed across skeletal muscle (not shown). Image obtained from a participant at 3T.*

The centre frequency was initially set by subtracting 70Hz from the PCr peak, to position it halfway between the PCr and γ-ATP peaks.

This acquisition was then analysed in a dedicated Matlab™ tool to generate the centre and offset frequencies (Figure 2.8), after identifying the PCr peak in the voxel of interest. For each voxel, the γ-ATP saturation offset is given as the offset required from the centre frequency to

saturate γ-ATP and the control offset is given as the offset required to saturate on the contralateral side of the PCr peak, the same distance away from it as the γ-ATP saturation. The fourth step of the TRiST sequence utilising this control saturation pulse allows for adjustment to account for any unintended partial saturation of the PCr peak by the γ-ATP saturation pulse.

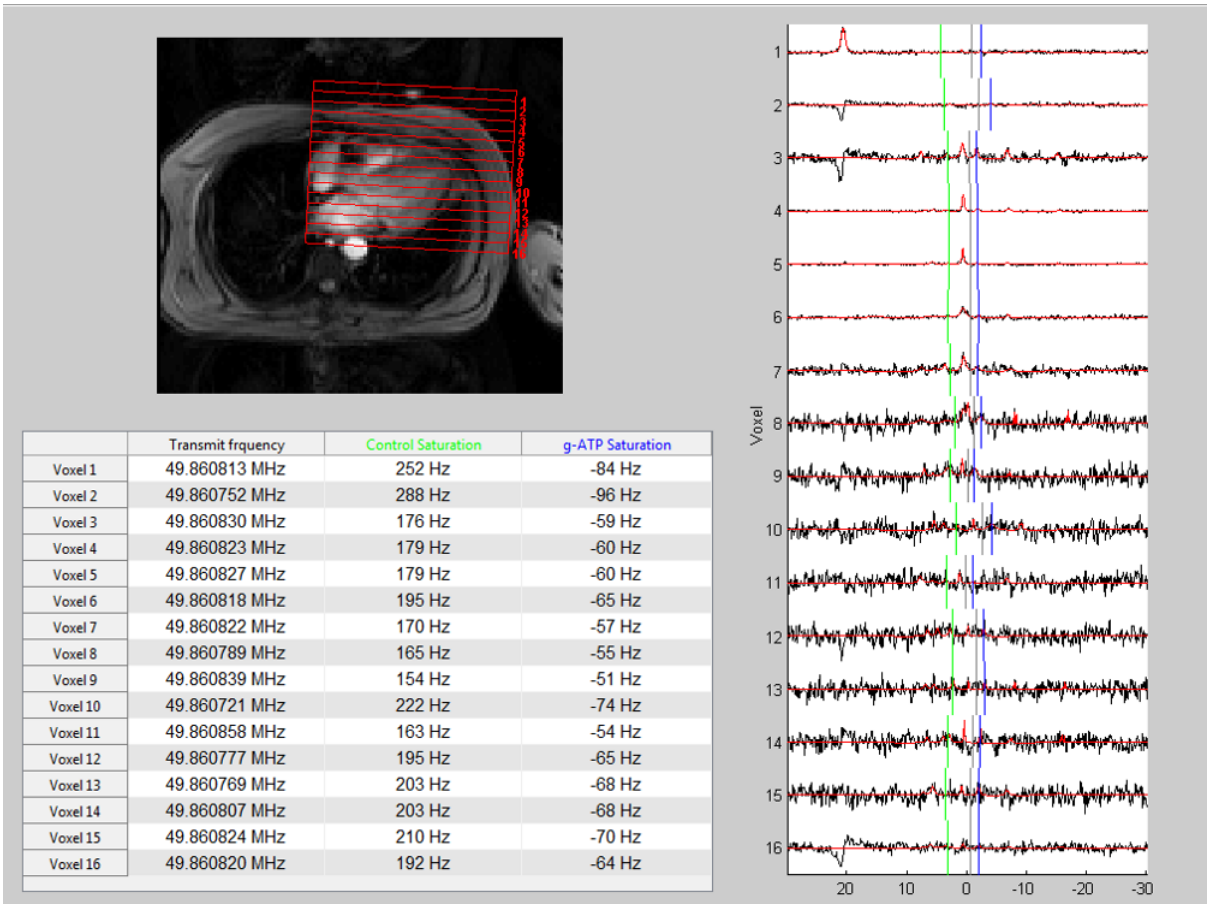

	Transmit frquency	Control Saturation	g-ATP Saturation
Voxel 1	49.860813 MHz	252 Hz	-84 Hz
Voxel 2	49.860752 MHz	288 Hz	-96 Hz
Voxel 3	49.860830 MHz	176 Hz	-59 Hz
Voxel 4	49.860823 MHz	179 Hz	-60 Hz
Voxel 5	49.860827 MHz	179 Hz	-60 Hz
Voxel 6	49.860818 MHz	195 Hz	-65 Hz
Voxel 7	49.860822 MHz	170 Hz	-57 Hz
Voxel 8	49.860789 MHz	165 Hz	-55 Hz
Voxel 9	49.860839 MHz	154 Hz	-51 Hz
Voxel 10	49.860721 MHz	222 Hz	-74 Hz
Voxel 11	49.860858 MHz	163 Hz	-54 Hz
Voxel 12	49.860777 MHz	195 Hz	-65 Hz
Voxel 13	49.860769 MHz	203 Hz	-68 Hz
Voxel 14	49.860807 MHz	203 Hz	-68 Hz
Voxel 15	49.860824 MHz	210 Hz	-70 Hz
Voxel 16	49.860820 MHz	192 Hz	-64 Hz

***Figure 2.8**: Example of the calculation of centre and offset frequencies using Matlab™ analysis. After selecting the PCr peak in the chosen voxel, automated analysis calculates the appropriate centre frequency, γ-ATP saturation offset and control saturation offset. The blue line shows the position of γ-ATP, the grey line the centre frequency (halfway between PCr and γ-ATP) and the green line the position for the control saturation. Spectra obtained from a participant at 3T*

Using these calculated offsets, the TRiST and StreST sequences were run (acquisition parameters in Table 2.1).

Table 2.1: TRiST and StreST acquisition parameters

Sequence	**TR** *(s)*	**Selective saturation**	**Averages**	**Duration** *(min)*	**Measured parameters**
1	15	None	2	9	$M_{0,PCr}$
2	1.5	$^{\gamma}$ATP	18	11	$M'_{1.5s,PCr}$
3	9.5	$^{\gamma}$ATP	8	21	$M'_{9.5s,PCr}$
4	15	Control	2	9	M^{Ctrl}_{PCr}
StreST 1	15	Control	2	9	M^{Ctrl}_{PCr}
StreST 2	15	$^{\gamma}$ATP	2	9	$M'_{15s,PCr}$

Adiabatic half-passage pulses were used in order to achieve 90° excitation irrespective of distance from the coil and so B_1 transmit strength. In general, voltages of 210-220 V were used. Saturation was achieved with a modified Delays Alternating with Nutation for Tailored Excitation (DANTE) pulse train (duration 0.1 ms, inter-pulse delay 0.25 ms) with the maximum possible allowed voltage within SAR limits to achieve saturation (~30-40 V). Examples of the 6 spectra obtained by TRiST and StreST are shown in Figure 2.9.

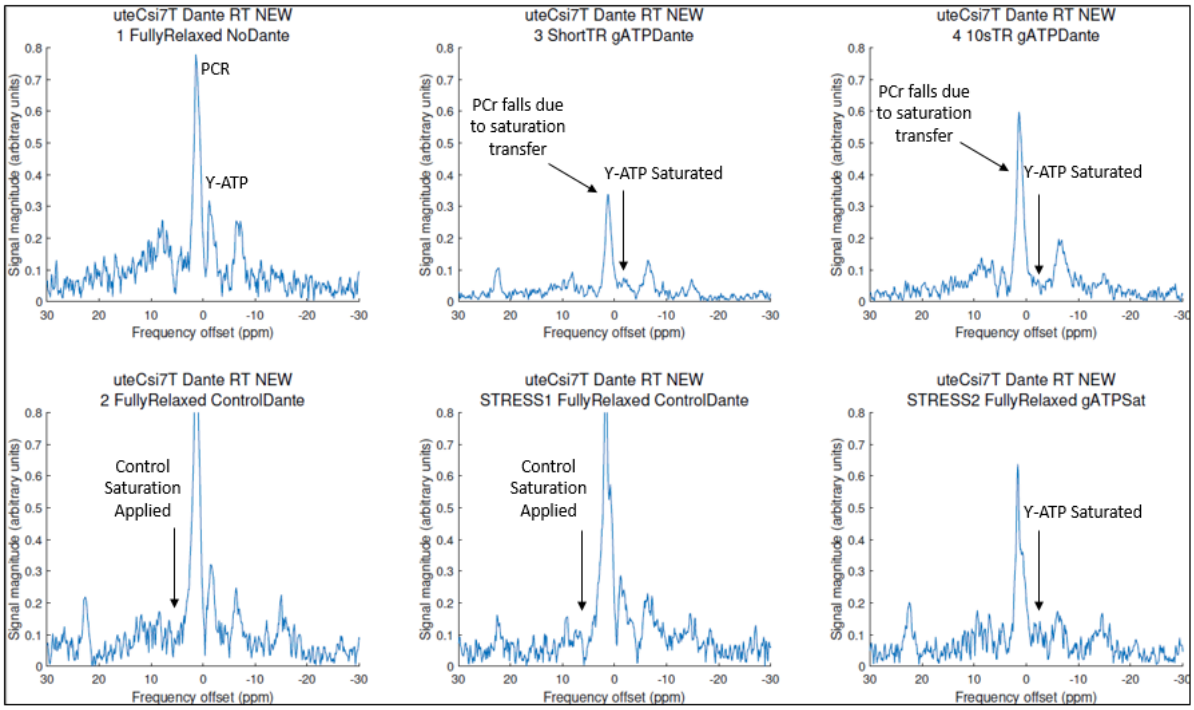

***Figure 2.9**: The six spectra generated as part of the TRiST and StreST acquisitions. When y-ATP is saturated by the DANTE pulse, PCr falls due to saturation transfer. Spectra obtained from a participant at 3T*

These acquisitions then allow calculation of the necessary parameters for calculation of k_f. $T'_{1,PCr}$ is calculated from the long and short y-ATP saturation acquisitions using a two-TR partial saturation method[369]. $M^{Ctrl}{}_{PCr}$ is substituted for $M_{0,PCr}$.

$M'_{0,PCr}$ is then calculated as:

$$M'0, PCr = \frac{M'1.5s, PCr}{1 - e^{-1.5s}/T'1}$$

And then k_f is calculated as:

$$kf = \frac{1}{T'1PCr} \cdot (\frac{M'0, PCr}{MCtrl\ 0, PCr})$$

For calculation of k_f at stress, it is assumed that T1 remains constant and new values from the additional two StreST sequences are substituted in.

Obtained k_f values were multiplied by 1.333 to correct for underestimation due to supine scanning and improve comparability with previous prone measurements[368]. Values with a standard deviation >1.0 were generally excluded, unless judged to be of sufficient quality by a second blinded and experienced operator.

Forward CK flux was calculated as [PCr] x k_f, where [PCr] is calculated by multiplying PCr/ATP by literature values for [ATP] (normal hearts: 5.7 µmol/g wet weight; heart failure: 5.2 µmol/g wet weight)[278]. For flux at stress, PCr/ATP was taken as the PCr/γ-ATP obtained from the fully relaxed control saturation spectrum obtained during StreST. Non-invasive assessment of CK activity by MR spectroscopy in this way has previously been validated by our group against biopsy measurements[370].

2.7 Invasive Arteriovenous and Haemodynamic Measurements

All measurements were taken during a CRT pacemaker or defibrillator implantation. Following placement of the pacing leads, the catheter to the CS (typically a Worley™ CS guide catheter, Merit Medical, UK) was left *in situ* and used for aspiration of venous blood samples from the CS ostium. Arterial access was established radially (6Fr) and femorally (8Fr). An appropriate guide catheter (typically Launcher™ Extra Back-Up (EBU), Medtronic, Minneapolis, USA) was passed to the left main stem (LMS) coronary artery from the radial route and an angiogram undertaken to enable measurement of the diameter of the LMS.

A doppler guidewire (Volcano Flowire™, Phillips, NL) was then positioned via the guide catheter in the LMS (or if this was not possible, the left anterior descending (LAD) artery) and used to record flow velocity, with data recorded on a Volcano Combomap™ system (Philips, NL). An Inca™ conductance (or PV) catheter (CD Leycom, NL) was passed via the femoral route to the left ventricular apex. This catheter is described in more detail below. Data was recorded via an Inca™ analysis station (CD Leycom, NL). A representative fluorogram showing the positioning of all leads and catheters is shown in Figure 2.10.

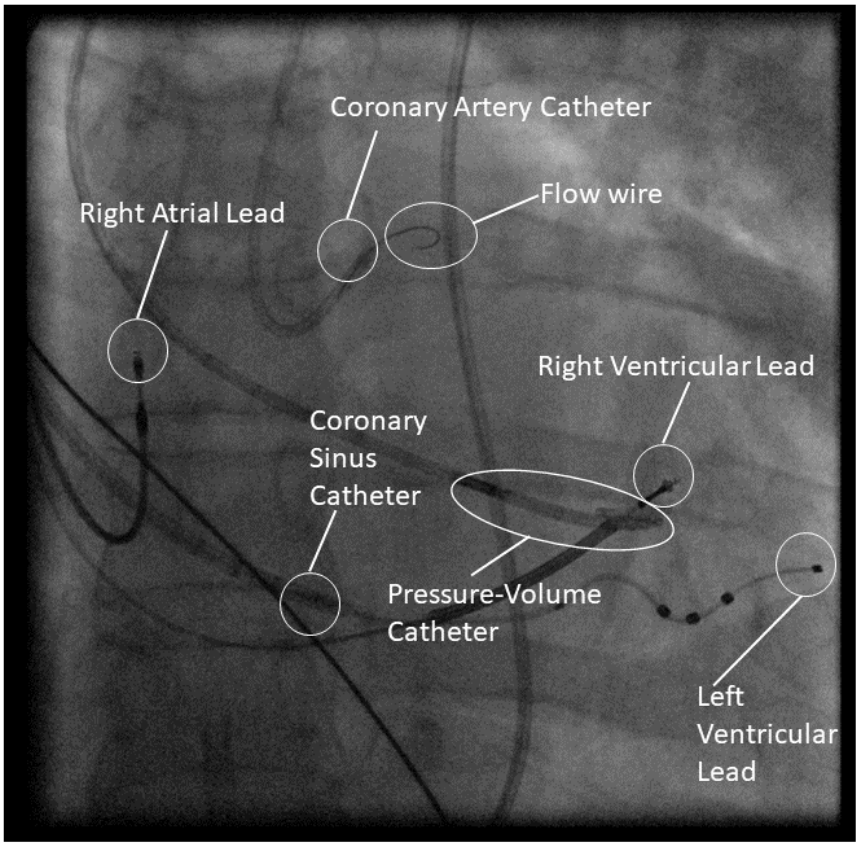

***Figure 2.10**: Example positioning of catheters, wires and pacing leads during invasive measurements (anteroposterior projection)*

After at least one minute of being established on each pacing setting, measurements were recorded from the Volcano Flowire™ and the Inca™ conductance catheter for one minute. At the end of this minute, serum, plasma and blood gas samples were drawn simultaneously from the coronary artery and CS catheters and placed on ice until they were processed. In 2 cases, it was not possible to place a catheter in the LMS and so arterial samples were taken from the femoral artery sheath instead.

2.7.1 Inca™ Conductance Catheter

The Inca™ conductance catheter consists of 12 electrodes. In brief, two electrical fields are generated between the 2 proximal and the 2 distal electrodes, with electrical homogeneity improved by this dual field (dual excitation) method[371]. The remaining electrodes measure segmental electrical conductances, which are used to calculate real time LV segmental volumes, either calibrated using prior imaging assessment of LV volumes or via a combination of hypertonic saline infusion (to calculate parallel conductance of extra-cardiac tissue) and thermodilution[52]. Total LV volume is then calculated from the sum of the segments inside the LV cavity. Simultaneous pressure recordings are recorded by a solid-state pressure sensor in the middle of the catheter. A diagram of the catheter is shown in Figure 2.11.

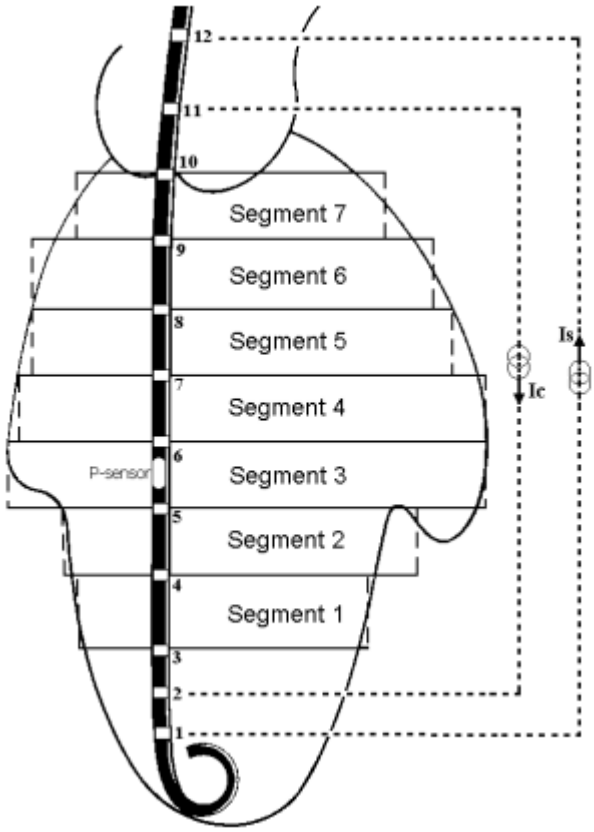

Figure 2.11: *Overview of the Inca™ conductance catheter. Dual electrical fields are generated between proximal and distal electrodes, with electrical conductance measured by remaining electrodes in 7 segments used to calculate LV segmental volumes. Pressure is measured by a sensor (P-sensor) in the middle of the catheter.*

2.7.2 Analysis

Conductance catheter data was analysed using commercial software provided by the manufacturer (Conduct NT™, version 3.18.1, CD Leycom, NL), see Figure 2.12. A 10 Hz filter was applied to recordings and volumes were calibrated using baseline CMR data as calculated in Section 2.5.1 (or using Simpson's biplane LV measurement on an echocardiogram if CMR was unavailable. Clinical CMR or echocardiogram data was used if a research scan had not been performed). Pressure was adjusted to correct for any offset recorded at the time of

catheter withdrawal from the femoral artery. Any catheter segments not in the LV were discarded from the final calculations and auto systolic and diastolic markers were manually checked for accuracy and adjusted if necessary. Final measurements were averaged from 30 representative consecutive beats in each recording. In the case of ectopy, the ectopic beat and the preceding and following beats were discarded from the recording. Mechanical dyssynchrony during systole was calculated automatically by the software. A segmental volume was defined as dyssynchronous if its change was opposite to the simultaneous change in the total LV volume[51]. This was then quantified as the percentage of time within the cardiac cycle that the segment was dyssynchronous to the total volume, with total dyssynchrony given as the mean of all segmental dyssynchrony.

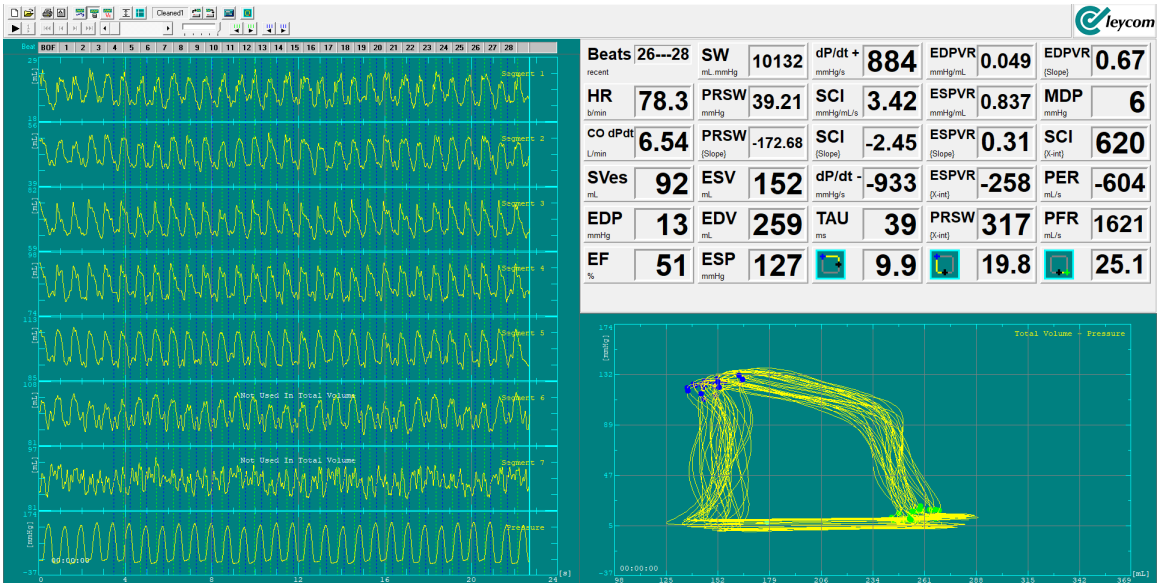

***Figure 2.12**: Example of a conductance catheter recording from the CD Leycom analysis software. Segmental volumes and pressure tracings over time (left), derived indices (upper right) and pressure-volume loops (lower right) are shown. Note the bottom 2 volume recordings were from segments not reliably in the LV and so were excluded from analysis*

Flowire™ data was analysed using commercial software provided by the manufacturer (Combomap™ Version 1.9, Philips, NL), see Figure 2.13. The doppler recording of velocity was auto-contoured by the software to provide an average peak velocity (APV – cm/s) for each heartbeat. This was then averaged over 10 representative beats, again with ectopics and their succeeding and preceding beats excluded.

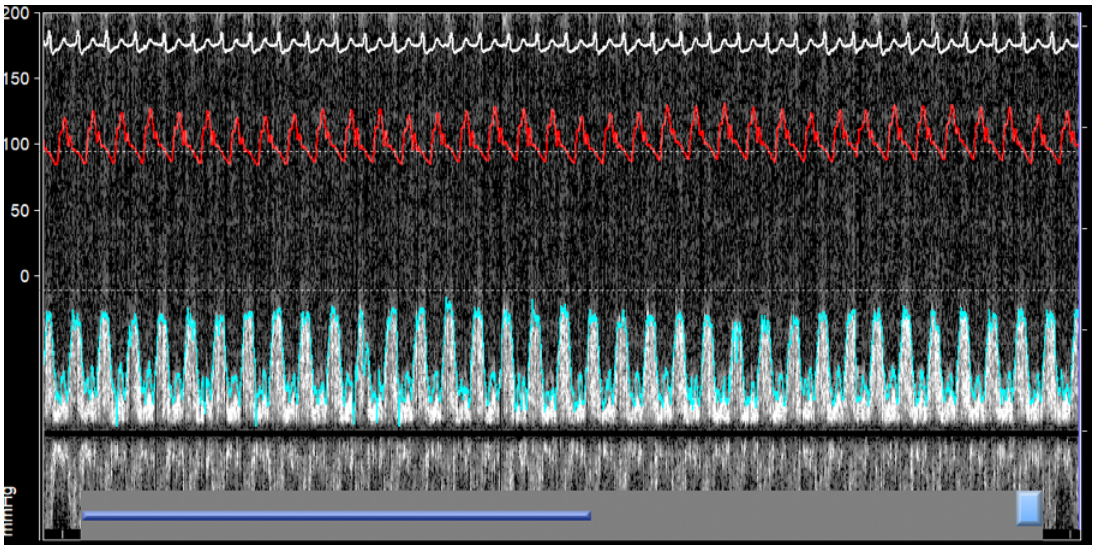

Figure 2.13*: Example of a Volcano doppler flow wire recording. Upper trace: ECG. Middle trace: aortic pressure. Bottom trace: coronary flow (with blue tracing showing auto-contouring around the flow integral)*

Flow volume was then calculated as APV multiplied by cross-sectional area of the LMS/LAD (calculated from the average of 2 orthogonal diameters measured on angiogram, see Figure 2.14). Coronary diameter has previously been demonstrated to be unchanged during LV pacing[346] and so baseline measurements only were taken. In 3 cases the LMS catheter could not be placed or the recording was of insufficient quality and so the average LMS flow from the other participants at each pacing setting was used.

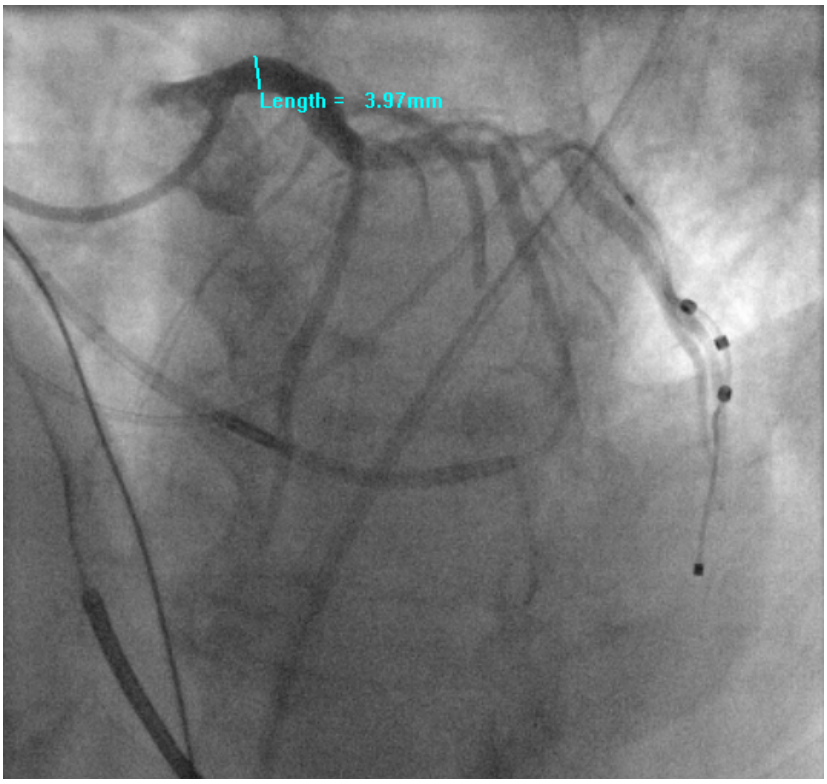

***Figure 2.14**: Example of coronary angiogram demonstrating measurement of the LMS diameter (left anterior-oblique cranial view)*

Oxygen content of blood was calculated as:

1.36 x Haemoglobin x (Oxygen Saturation / 100) + 0.0031 x Partial Pressure of Oxygen

Where haemoglobin is in grams per decilitre, oxygen saturation in percentage and pressure of oxygen in mmHg (kPa multiplied by a conversion factor of 7.5).

Absolute oxygen and metabolic substrate uptake was then calculated by multiplying A-V differences by LMS flow.

2.8 Cardiopulmonary Exercise Testing

All tests were performed using a static bicycle ergometer (Ergoselect™, Ergoline, Germany) and a spiroergometry system (Metalyzer™ 3B, Cortex Medical, Germany), in conjunction with an oro-nasal V2 reusable facemask (Hans Rudolph, KS, USA). The system was calibrated to atmospheric pressure and with a calibration gas of fixed oxygen and carbon dioxide concentration prior to each test. A 15 watt step protocol was used, with 3 minute stages and a 15 minute recovery period, and the researcher administering the test was blinded to CRT programming. Data was recorded using commercial software (MetaSoft™ Studio Version 5.13.0, Cortex Medical) (see Figure 2.15) and simultaneous 12 lead ECG recordings were obtained using separate commercial software (Custo Med, Germany).

A cannula was placed in a large vein in the arm prior to testing, with subsequent blood samples withdrawn via a three-way tap. At the end of each stage, blood pressure was measured using a manual sphygmomanometer (Accoson Freestyle™, Accoson, UK) and participants were asked to indicate their level of perceived exertion on a standardised BORG-RPE scale[372, 373] (see Appendix). Tests were terminated when participants were unable to maintain increasing workload.

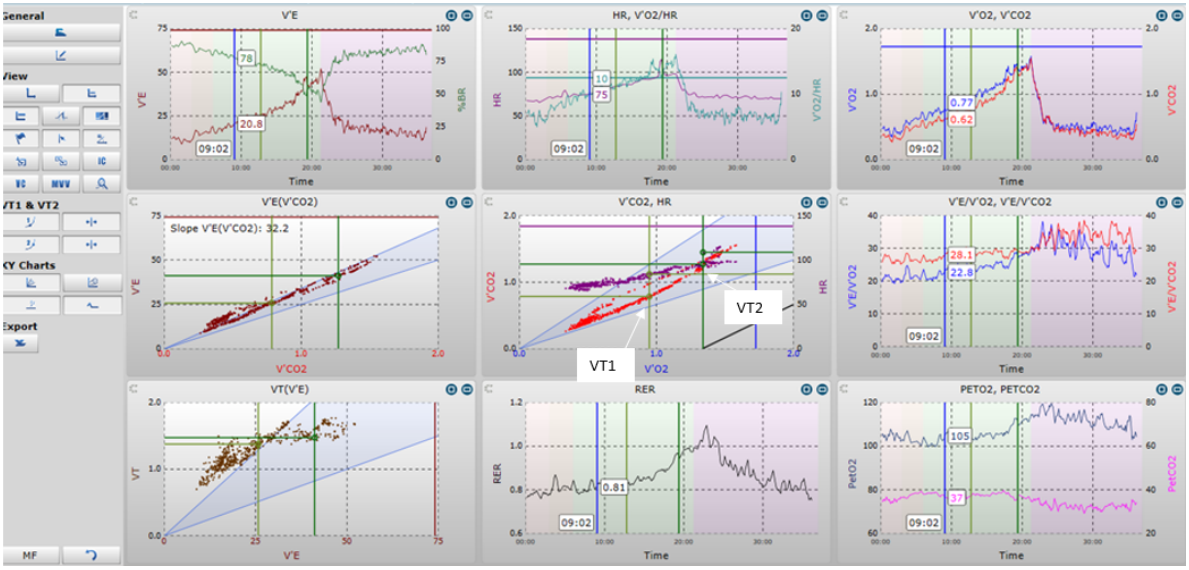

Figure 2.15: *Example CPET recording, showing a standard 9-panel plot. VT1 (light green line) and VT2 (dark green line) are indicated on the central panel.*

2.8.1 Analysis

Manual assessment of the Ventilatory Threshold (VT) 1 and 2 points (shown in Figure 2.15) was checked by a second experienced operator, blinded to randomisation. Assessment of ECG intervals was performed automatically by the recording software (Custo-Med). In brief, the software analyses the last 10 seconds of recording at the end of each stage and automatically selects those complete beats which are suitable for analysis. Average QRSd is calculated from the earliest and latest markers on any lead (Figure 2.16). For analysis of intervals immediately before and after SyncAV^{TM} adjustments, the 10 seconds prior to and after the adjustment were manually selected. In all cases, the analysed periods were manually checked to ensure that ectopic or intrinsic beats had not been included for analysis. Additionally, the placement of the automatic ECG interval markers for each lead was also manually checked for accuracy

and in the case of significant error markers were manually adjusted. All ECG markers where finally checked by a second experienced clinician, blinded to randomisation.

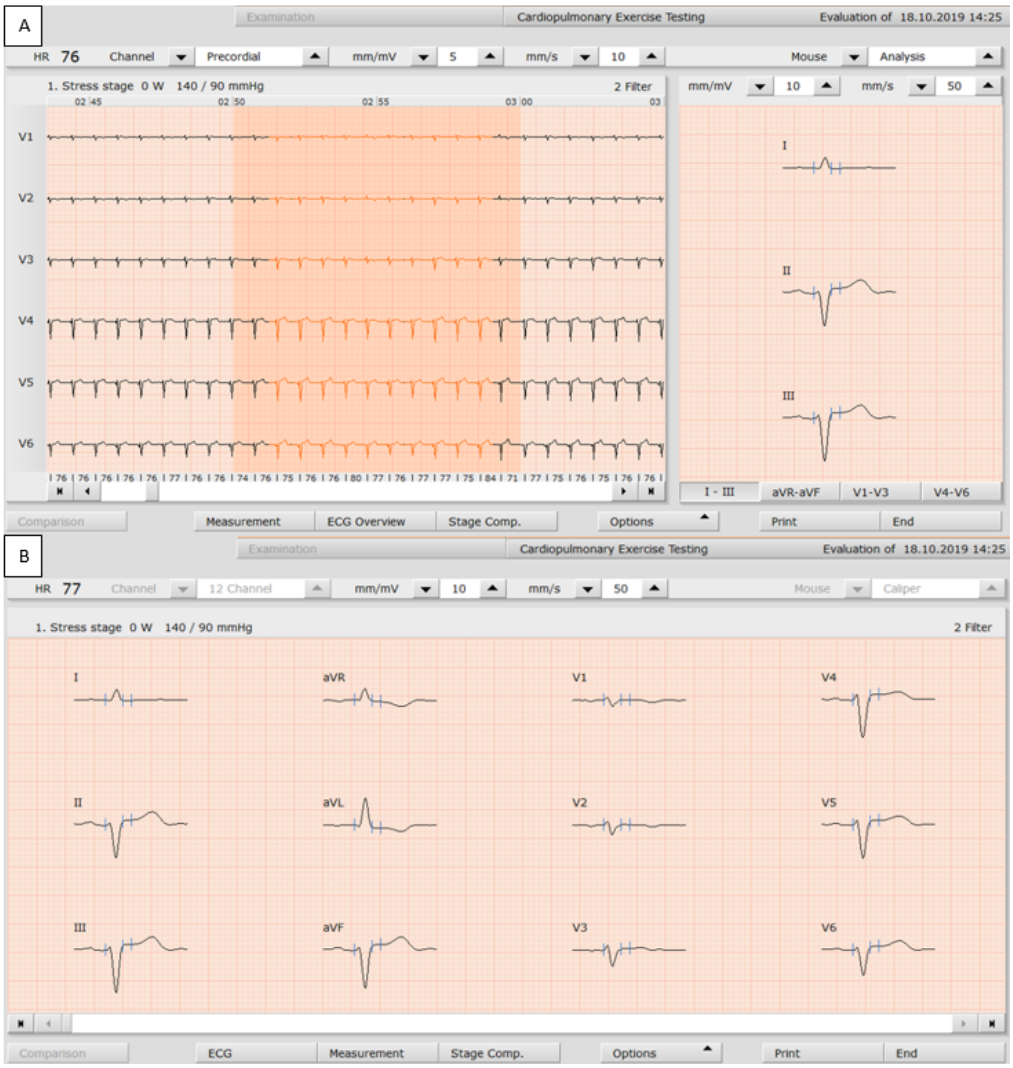

Figure 2.16: *Example of an ECG recording using the Custo Med software. A: Complexes meeting the program's criteria for evaluation within a 10 second period (shading) are automatically selected (highlighted in orange). B: Automatic placement of interval markers (light blue lines, first 2 marking QRS duration for each lead).*

2.9 CRT Device Interrogation

2.9.1 Pre- and Post-CPET

All CRT devices were interrogated and programmed using a Merlin™ programming system (Abbott, Illinois, USA).

2.9.2 Pre- and Post-MRI

All CRT devices were interrogated and programmed using a Zoom Latitude™ programming system (Boston Scientific, Massachusetts, USA). Devices were set into an MRI safe mode as per the manufacturer's instructions, with asynchronous pacing set 10 bpm above the participant's intrinsic heart rate, to prevent competitive pacing. Lead and device parameters were re-checked when MRI safe mode was exited.

2.10 Blood Sample Collection and Processing

Blood samples were withdrawn from cannulae via a vacutainer system or, for invasive samples at taken at CRT implant, aspirated via a syringe and then placed in vacutainer tubes. Blood samples were either sent directly to laboratories in Oxford University Hospitals NHS Foundation Trust for analysis (full blood count, HBA1c and renal function) or alternatively serum and plasma samples were centrifuged for 10 minutes at 3000 rpm and 6°C. The supernatant was pipetted into individual sample vials and stored at -80°C in departmental

freezers prior to transport to laboratories in Oxford University Hospitals NHS Foundation Trust for further analysis. Blood gas samples were analysed at point of care on a clinical blood gas analyser (Seca, USA).

2.11 Statistical Methods

Statistical analysis and graph production was performed with SPSS statistics Version 26.0 (IBM Corp, NY, USA) or Graphpad^{TM} Prism Version 9 (Graphpad Holdings, CA, USA). Due to the small sample sizes, and unless otherwise specified, two-tailed non-parametric tests were used, with Wilcoxon signed rank tests for paired data, Mann-Whitney tests for unpaired data, Friedman tests or mixed effect models for more than 2 groups and Spearman r tests for correlations. Where parametric tests were used, groups underwent normality testing using a one sample Kolmogorov-Smirnov test. Categorical data was assessed using Fisher's Exact test. Where single outliers were visually appreciated, they were excluded if identified as an outlier with Grubbs' Test. Statistical significance was taken at a p value of ≤0.05. Continuous data is presented as median [Inter Quartile Range (IQR)] and discrete data as 'n' or %.

Chapter 3:

Cardiac Function and Energetics in Response to Substrate Manipulation in Diabetic Participants with and without Systolic Heart Failure

---

3.1 Introduction

The finding of an energetic deficit in HFrEF is well established, with both PCr/ATP ratio[273-276] and CK flux[278] found to be reduced and this reduction correlating with outcomes and mortality[277, 279]. In addition, cardiac substrate uptake and metabolism is also altered, with a decrease in FA oxidation[240, 249, 284]. Glucose metabolism becomes uncoupled, with an increase in glycolysis and glucose uptake but unchanged or even decreased glucose oxidation[240, 249, 285, 286, 374] and overall there is therefore a relative shift towards glucose metabolism. These energetic changes are thought to potentially have a causal role in heart failure[281]. In addition, HFrEF represents an insulin-resistant state[293]. Insulin resistance is also the hallmark of T2DM, which is also associated with impaired energetics as shown by a lower PCr/ATP ratio[306, 307].

Furthermore, in recent years it has become recognised that DM alone can be associated with HFrEF independently of atherosclerotic disease, in a pathology termed diabetic cardiomyopathy[300]. Regardless of the cause, the energetic theory of heart failure suggests that a mismatch between ATP supply and demand can cause contractile dysfunction.

Both HFrEF and T2DM are therefore thought to represent metabolically inflexible states, with the heart becoming more reliant on either glucose or FA metabolism respectively. As ATP production is inherently linked to the substrate oxidised, it is unsurprising that reduced quantity of, and/or flexibility to switch, substrate use when needed is related to contractile dysfunction. What is less appreciated is to what extent this flexibility can be altered by substrate manipulation and how this influences cardiac function and energetics. Recent work by our group (unpublished) has demonstrated preserved substrate flexibility in participants with non-ischaemic cardiomyopathy without DM, with FFA infusion resulting in increased LVEF and cardiac work and a higher PCr/ATP than on an insulin-dextrose infusion, but no change in k_f. In contrast, in a healthy control group k_f and CK flux were higher than on insulin/dextrose but PCr/ATP was unchanged. Furthermore, resting PCr/ATP correlated with measures of cardiac contractility in the heart failure group but this was not the case in the control group. This led us to conclude that in non-diabetic, non-ischaemic HFrEF, a FFA infusion is able to increase the ATP delivery rate and improve the energetic state of the heart and LV contractility, as the improved ATP supply removes the limitation this places on contractility.

However, it is not known to what extent these findings may apply in T2DM alone or when T2DM is combined with HFrEF. We hypothesised that while participants with T2DM may

retain a degree of metabolic flexibility, the combination of T2DM with HFrEF would represent an inflexible state which could not be influenced by substrate manipulation. We therefore aimed to assess substrate flexibility, cardiac function and cardiac energetics using multi-parametric CMR, in participants with non-insulin dependent diabetes mellitus (NIDDM) with both preserved cardiac function and with non-ischaemic HFrEF.

3.2 Methods

3.2.1 Recruitment

Participants were recruited from those who had previously taken part in research studies and agreed to be contacted to take part in further studies, as well as poster adverts displayed at the John Radcliffe Hospital and an approved Tweet on Twitter. In addition, those with heart failure were recruited from cardiology services of the Oxford University Hospitals NHS Foundation Trust.

3.2.1.1 Inclusion Criteria

- Participant willing and able to give informed consent for participation in the study.
- Male or female, aged at least 18 years old.
- NIDDM, diagnosed as per standard clinical practice.

3.2.1.1.1 Additional inclusion criteria for Heart Failure Participants

- HFrEF as diagnosed by symptoms and signs of heart failure accompanied by echo or MRI derived measures of ejection fraction (as per European Society of Cardiology 2021 guidelines[1]).

3.2.1.2 Exclusion Criteria

- Participant unwilling or unable to give informed consent.
- Any impediment to communication which, in the opinion of the investigator, might prevent the investigator communicating effectively with the patient during the study which could cause a safety or reliability concern.
- Any other condition which, in the opinion of the investigator, might affect the safety of the participant or reduce the reliability of the study results.
- Involvement in any other research project where the procedures would affect the outcomes of the study.
- Metal clips or metallic foreign body.
- Prior injury to the eye involving fragments of metal.
- Prior shrapnel injuries.
- Any other metallic or electronic implants affected by the magnetic field.
- History of severe claustrophobia.
- Female participant who is pregnant, lactating or planning pregnancy during the course of the study.
- Egg, or soya allergy.
- Disturbances of normal fat metabolism.

- Severe liver damage, TB, pulmonary disease, anaemia, blood coagulation disorders, or recent fracture of pelvis or long bones.

3.2.1.2.1 Additional Exclusion Criteria for Participants with Normal Hearts

- A history of valvular heart disease.
- Impaired LV systolic function.
- Known coronary artery disease.
- Known stomach ulcer.

3.2.1.2.2 Additional Exclusion Criteria for Participants with Heart Failure

- Ischaemia as primary cause of heart failure.

3.2.2 Protocol

All participants attended for 2 visits. Participants were fasted from midnight on the day of visits and also withheld diabetic medication on the morning of visits. Baseline anthropomorphic measurements, blood pressure, ECG and a CMR scan to assess LV volumes and function were recorded at participants' first visit.

Participants were randomised to receive either a 20% Intralipid™ (Fresenius Kabi, UK –'FFA') infusion or an insulin/dextrose ('glucose') infusion, administered as per Chapter 2, section 2.4, with the alternative infusion received at the second visit. Visits were are least 1 week apart. Both infusions were received for at least 1 hour, at the end of which baseline venous blood samples were drawn and subsequently analysed for insulin, glucose, lactate, FFA and BOHB levels. Participants then underwent multi-parametric CMR to assess LV volumes and

function, PCr/ATP ratio and k_f, as per Chapter 2, section 2.5, whilst being maintained on substrate infusion. At the end this protocol, dobutamine was administered as per Chapter 2, section 2.4.3 until 65% predicted maximum heart rate was achieved. Repeat biplane assessment of LVEF and the StreST extension to the TRiST protocol was then performed. Finally, repeat venous blood samples were drawn at the end of the stress protocol. A schematic illustrating the timeline of the protocol is shown in Figure 3.1.

Full datasets were not available for every participant due to either early termination of the protocol before the stress component in some cases, or due to data exclusion due to poor quality recordings as outlined in Chapter 2.

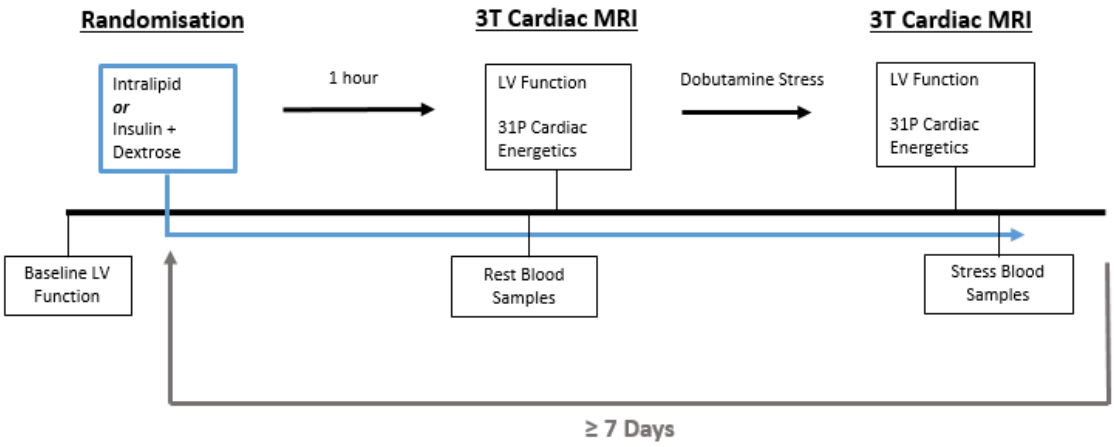

Figure 3.1: *Protocol timeline*

3.3 Results

3.3.1 Baseline Demographics and Clinical Characteristics

Fifteen participants were recruited with NIDDM and normal cardiac function (NHDM cohort) and 10 participants with NIDDM and HFrEF (HFDM cohort). Baseline demographics and clinical characteristics are given in Table 3.1. Participants with heart failure were significantly older, had a higher BMI and a lower LVEF. In addition, 5 of the HFDM cohort had evidence of micro or macrovascular disease (2 with both diabetic retinopathy and peripheral vascular disease, 1 with peripheral vascular disease and non-obstructive coronary disease and 2 with non-obstructive coronary disease alone) versus none in the NHDM cohort.

The majority of participants in both groups were prescribed metformin, with sulphonylureas, SGLT2 inhibitors and dipeptidyl-peptidase 4 (DPP-4) inhibitors also being prescribed and no significant differences between cohorts (Table 3.2). Anti-hypertensive medications were present in both groups, as well as optimised heart failure medication in the HFDM group as expected (Table 3.2).

Table 3.1: Baseline demographic and clinical characteristics

	NHDM Cohort	**HFDM Cohort**	***p***
Recruited *(n)*	15	10	*N/A*
Age *(years)*	62 [56-65]	71 [63-77]	***0.04***
Male *(n, %)*	14 (93)	8 (80)	*0.54*
Weight *(kg)*	87.0 [74.9-91.0]	95.7 [78.6-108.6]	*0.29*
BMI *(kg/m^2)*	27.7 [24.2-30.7]	31.6 [29.0-36.3]	***0.05***
Hip:Waist Ratio	1.0 [1.0-1.1]	1.0 [0.9-1.0]	*0.24*
Systolic BP *(mmHg)*	142 [128-159]	134 [116-149]	*0.15*
Diastolic BP *(mmHg)*	79 [76-84]	77 [67-81]	*0.16*
Hypertension *(n, %)*	8 (53)	8 (80)	*0.23*
Sinus Rhythm *(n, %)*	15 (100)	9 (90)	*0.40*
Baseline LVEF *(%)*	58 [57-62]*	38 [30-44]	***<0.01***
NYHA Class	N/A	2 [1-3]	*N/A*
HBA1c *(mmol/mol)*	53.0 [47.5-56.3]	54.0 [49.8-55.3]	*0.99*

**available for 13 participants*

Table 3.2. Diabetic and cardiac medications at enrolment

		NHDM Cohort	**HFDM Cohort**	***p***
Diabetic Medication *(n, %)*	Metformin	14 (93)	8 (80)	*0.54*
	Sulphonylurea	3 (20)	4 (40)	*0.38*
	SGLT2 Inhibitor	4 (27)	5 (50)	*0.40*
	DPP-4 Inhibitor	1 (7)	0 (0)	*>0.99*
Cardiac Medication *(n, %)*	ACEi/ARB	8 (53)	10 (100)	***0.02***
	β Blocker	1 (7)	7 (70)	***<0.01***
	MRA	0	5 (50)	***<0.01***
	ARNi	0	2 (20)	*0.15*
	Digoxin	0	0	*N/A*
	Ivabridine	0	0	*N/A*
	CCB	1 (7)	2 (20)	*0.54*
	Loop Diuretic	0	6 (60)	***<0.01***
	Amiodarone	0	1 (10)	*0.40*

3.3.2 Blood Results

In both the NHDM and HFDM cohorts, hyperinsulinaemia was achieved as desired on insulin/dextrose infusion, with significantly higher venous insulin levels at both rest and stress compared to on FFA infusion (Tables 3.3 and 3.4 for all). Glucose levels were lower in both groups on insulin/dextrose infusion at rest but with no significant difference at stress. Venous FFA and BOHB levels were significantly higher on FFA infusion in both groups at both rest and stress, whilst venous lactate levels were significantly higher in both groups on insulin/dextrose infusion at rest and non-significantly higher at stress.

Table 3.3: Comparison of venous blood results on glucose and FFA infusions at rest

	NHDM			**HFDM**		
	Glucose Infusion	FFA Infusion	*p*	Glucose Infusion	FFA Infusion	*p*
Glucose *(mmol/l)*	8.11 [5.89-9.23]	8.94 [6.90-9.93]	***0.02***	6.35 [5.41-7.38]	7.06 [6.56-8.27]	***<0.01***
FFA *(mmol/l)*	0.22 [0.16-0.36]	4.68 [3.64-5.83]	***<0.01***	0.27 [0.14-0.36]	3.08 [1.88-4.75]	***<0.01***
Lactate *(mmol/l)*	1.68 [1.34-1.80]	1.16 [1.06-1.34]	***<0.01***	1.52 [1.42-1.67]	1.17 [0.99-1.58]	***0.02***
BOHB *(mmol/l)*	0.00 [0.00-0.00]	0.48 [0.33-0.71]	***<0.01***	0.00 [0.00-0.04]	0.32 [0.10-0.51]	***<0.01***
Insulin *(pmol/l)*	418.2 [321.9-562.8]	59.7 [33.1-105.5]	***<0.01***	520.1 [447.3-591.6]	88.9 [55.1-147.7]	***<0.01***

Table 3.4: Comparison of venous blood results on glucose and FFA infusions at stress

	NHDM			**HFDM**		
	Glucose Infusion	FFA Infusion	*p*	Glucose Infusion	FFA Infusion	*p*
Glucose *(mmol/l)*	8.47 [6.40-9.36]	8.04 [5.55-8.69]	*0.22*	6.33 [5.14-7.03]	6.33 [5.10-6.72]	*0.94*
FFA *(mmol/l)*	0.77 [0.52-0.96]	2.47 [2.01-4.61]	***<0.01***	0.84 [0.57-1.99]	2.88 [1.77-3.85]	***0.02***
Lactate *(mmol/l)*	1.37 [1.08-1.56]	1.19 [1.0-1.41]	*0.11*	1.46 [1.39-1.72]	1.34 [1.26-1.55]	*0.22*
BOHB *(mmol/l)*	0.00 [0.00-0.16]	1.19 [0.77-1.35]	***<0.01***	0.00 [0.00-0.11]	0.56 [0.33-0.90]	***0.02***
Insulin *(pmol/l)*	276.4 [148.3-396.0]	128.2 [107.3-155.7]	***<0.01***	360.8 [262.7-618.6]	203.4 [97.2-443.6]	***0.02***

3.3.3 Cardiac Volumes, Function and Haemodynamics at Rest

There was no difference in the total volume infused on each substrate in either the NHDM (Intralipid^{TM} + heparin: 266 [262-278] ml vs glucose + insulin: 303 [274-328] ml, p = 0.30) or the HFDM (Intralipid^{TM} + heparin: 259 [204-276] ml vs glucose + insulin: 234 [202-287] ml, p = 0.69) cohort.

In the NHDM cohort, FFA infusion resulted in a significantly higher LVEF at rest compared to during glucose infusion, as a result of a significantly lower LVESV but unchanged LVEDV (Table 3.5, Figure 3.2). This was mirrored by similar changes in RVEF and RVESV. These changes represented improved function on FFA infusion rather than a worsened function on glucose infusion, as demonstrated by higher LVEF and RVEF compared to baseline analysis with fasting only (see Appendix). Moreover, whilst HR and BP were similar between infusions, cardiac work and RPP were also higher during FFA infusion compared to during glucose infusion (Table 3.6, Figure 3.2). However, in the HFDM cohort left and right ventricular EF, cardiac work and RPP were no different between substrate infusion (Tables 3.5 and 3.6, Figure 3.2).

Table 3.5: Measures of cardiac dimensions and function at rest

	NHDM			**HFDM**		
	Glucose Infusion	FFA Infusion	*p*	Glucose Infusion	FFA Infusion	*p*
LVEDV *(ml)*	155 [140-182]	159 [133-183]	*0.55*	267 [195-278]	231 [196-255]	***0.03***
LVESV *(ml)*	62 [52-76]	59 [49-66]	***<0.01***	170 [113-195]	141 [112-171]	***0.02***
LVEF *(%)*	60 [58-62]	63 [59-66]	***<0.01***	40 [29-44]	40 [31-49]	*0.10*
3D GCS *(%)*	-19.3 [-22.1-, -18.6]	-20.7 [-22.5-, -19.0]	*0.14*	-11.4 [-14.6, -9.0]	-11.6 [-16.4-,-10.0]	*0.25*
RVEDV *(ml)*	146 [132-176]	150 [120-183]	*0.65*	136 [120-161]	132 [108-159]	***<0.01***
RVESV *(ml)*	61 [53-78]	55 [44-71]	*0.06*	60 [48-79]	58 [45-68]	***0.05***
RVEF *(%)*	59 [55-61]	62 [57-64]	***<0.01***	55 [51-63]	55 [53-64]	*0.13*

Table 3.6: Heart rate, blood pressure and cardiac haemodynamics at rest

	NHDM			**HFDM**		
	Glucose Infusion	FFA Infusion	*p*	Glucose Infusion	FFA Infusion	*p*
Heart Rate *(bpm)*	59 [55-69]	63 [58-68]	*0.13*	63 [54-76]	72 [53-85]	*0.23*
Systolic Blood Pressure *(mmHg)*	127 [121-151]	135 [122-146]	*0.30*	142 [112-148]	135 [107-160]	*0.63*
Diastolic Blood Pressure *(mmHg)*	78 [69-80]	74 [70-80]	*0.22*	66 [58-74]	69 [52-72]	*0.48*
Mean Arterial Pressure *(mmHg)*	93 [88-103]	94 [89-99]	*0.92*	87 [82-98]	90 [76-99]	*0.78*
Cardiac Work *(L.mmHg/min)*	537.1 [489.7-625.8]	595.8 [519.5-625.8]	***0.04***	469.2 [410.1-427.8]	558.9 [427.8-655.6]	*0.69*
Rate Pressure Product *(mmHg.bpm)*	7865 [6552-9248]	8618 [7308-10304]	***0.04***	8733 [7981-9349]	9198 [8533-9600]	*0.30*

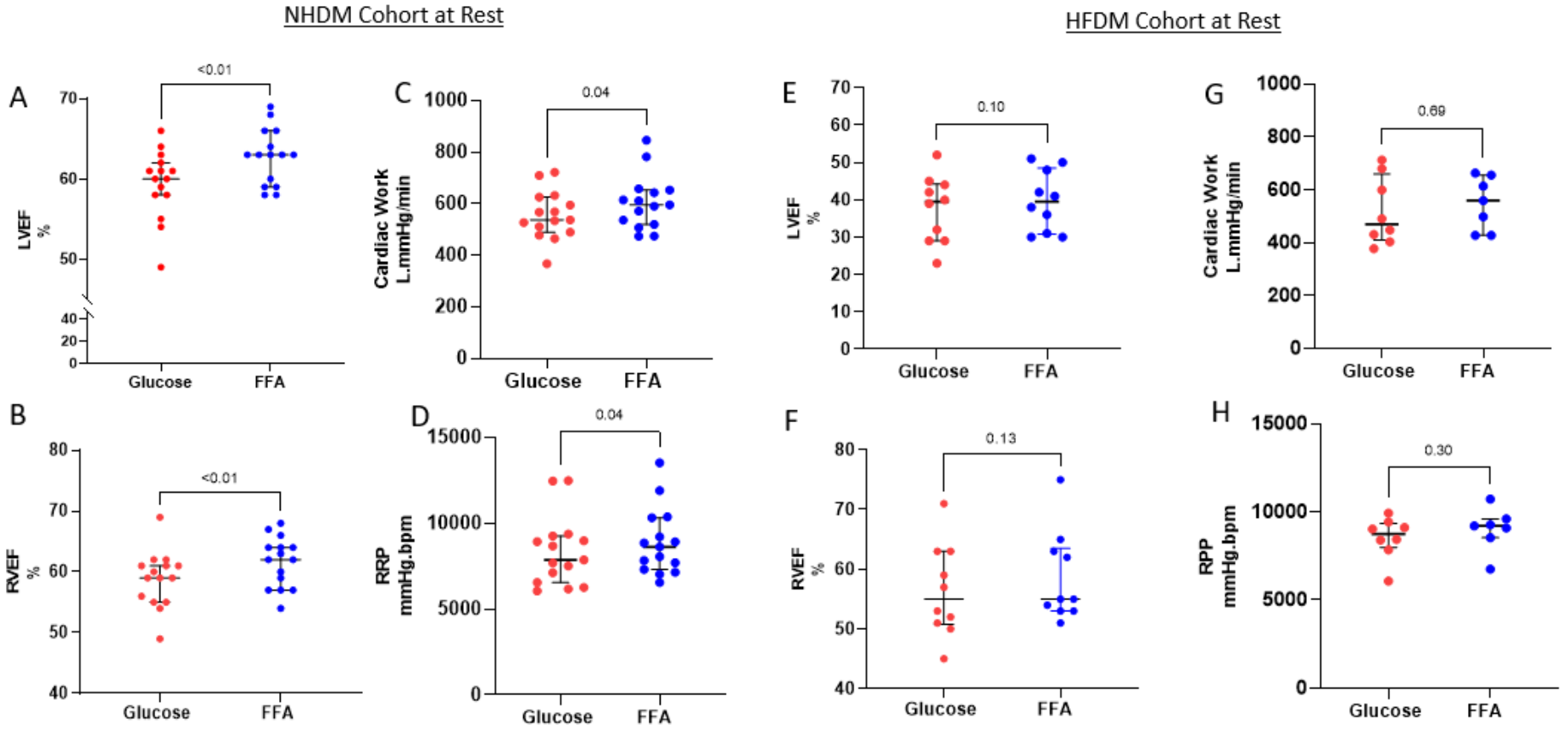

Figure 3.2: *LVEF (A), RVEF (B), cardiac work (C) and RPP (D) in the NHDM cohort at rest. LVEF (E), RVEF (F), cardiac work (G) and RPP (H) in the HFDM cohort at rest*

3.3.4 Cardiac Energetics at Rest

In the NHDM cohort, here was no difference in PCr/ATP at rest between infusions (Table 3.7, Figure 3.3). However, k_f was significantly lower on FFA infusion, resulting in a CK flux which was nearly 40% lower than on glucose infusion (Table 3.7, Figure 3.3). However, in the HFDM cohort there was no significant difference in cardiac energetics at rest between infusions (Table 3.7, Figure 3.3).

Table 3.7: Comparison of cardiac energetics at rest on glucose and FFA infusions

	NHDM			**HFDM**		
	Glucose Infusion	FFA Infusion	*p*	Glucose Infusion	FFA Infusion	*p*
PCr/ATP	1.94 [1.72-2.11]	1.98 [1.80-2.05]	*0.43*	1.76 [1.58-2.37]	1.91 [1.81-2.39]	*0.32*
k_f (s^{-1})	0.261 [0.181-0.451]	0.175 [0.092-0.277]	***<0.01***	0.143 [0.016-0.275]	0.313 [0.094-0.404]	*0.63*
CK Flux *(µmol (g wet weight)$^{-1}$ s^{-1})*	3.20 [1.78-4.92]	1.98 [1.17-3.22]	***0.02***	1.35 [0.21-2.31]	3.62 [1.03-4.00]	*>0.99*

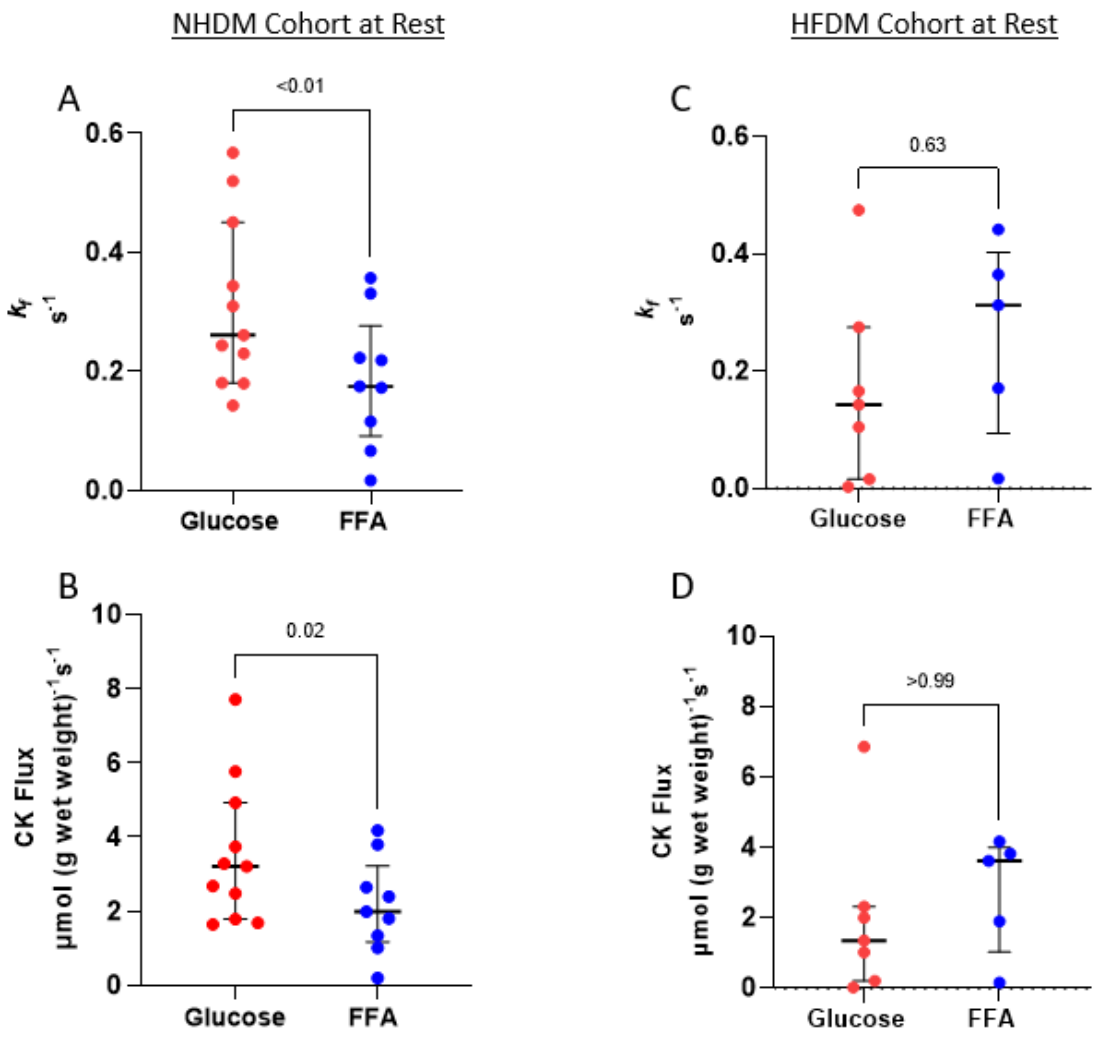

Figure 3.3: *k_f (A) and CK flux (B) for the NHDM cohort at rest. k_f (C) and CK flux (D) for the HFDM cohort at rest*

3.3.5 Cardiac Volumes, Function and Haemodynamics at Stress

In the NHDM cohort, dobutamine stress significantly increased biplane LVEF from rest on both the glucose and FFA infusions (Figure 3.4). Heart rate, cardiac work and RPP were also all increased by stress on both infusions (Figure 3.4). There was no difference between infusions in stress LVEF, cardiac work, RPP or any other haemodynamic parameter (Table 3.8).

However, in the HFDM cohort, whilst dobutamine stress significantly increased heart rate, LVEF and cardiac work were only significantly increased when on the FFA infusion and not when on the glucose infusion (Figure 3.4). There was no difference in any other haemodynamic parameter during stress between either infusion (Table 3.8).

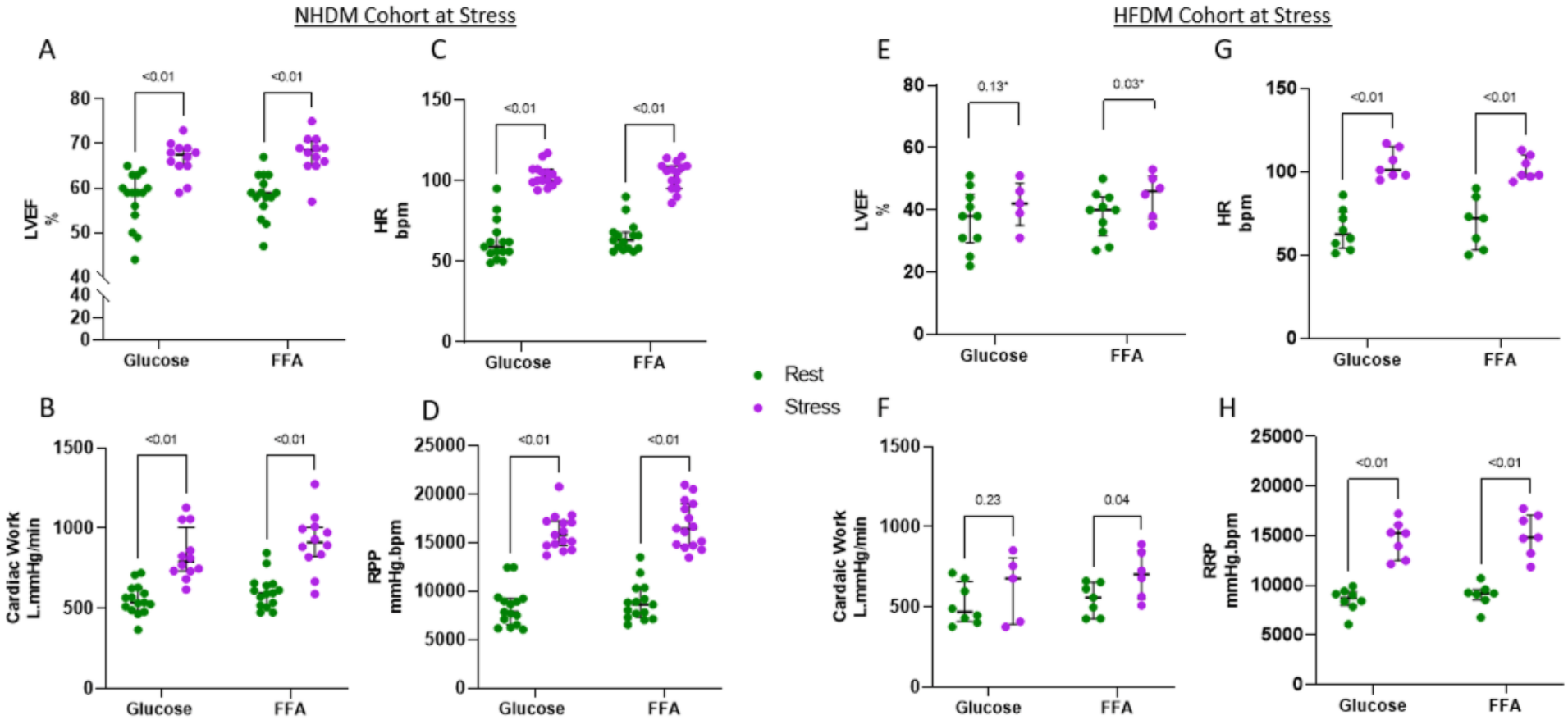

Figure 3.4: *Rest and stress LVEF, cardiac work, HR and RPP for the NHDM cohort (A-D respectively) and the HFDM cohort (E-H respectively) at stress, compared by substrate infusion. *paired Wilcoxon signed rank tests as insufficient data for mixed effect analysis*

Table 3.8: Left ventricular volumes and function and cardiac haemodynamics at stress

	NHDM			**HFDM**		
	Glucose Infusion	FFA Infusion	*p*	Glucose Infusion	FFA Infusion	*p*
LVEDV *(ml)*	125 [106-143]	128 [107-151]	0.63	185 [142-188]	178 [158-209]	*0.31*
LVESV *(ml)*	42 [34-48]	43 [32-45]	*0.65*	101 [75-122]	100 [75-127]	*0.50*
LVEF *(%)*	68 [65-69]	69 [65-71]	*0.56*	42 [35-49]	46 [37-51]	*0.31*
Heart Rate *(bpm)*	100 [95-109]	106 [95-109]	*0.95*	98 [97-110]	101 [98-115]	*0.16*
Systolic Blood Pressure *(mmHg)*	155 [147-170]	165 [145-179]	*0.06*	135 [127-166]	135 [126-169]	*>0.99*
Diastolic Blood Pressure *(mmHg)*	69 [63-72]	66 [65-74]	*0.57*	58 [52-66]	58 [51-62]	*0.28*
Mean Arterial Pressure *(mmHg)*	96 [94-100]	99 [96-105]	*0.10*	89 [80-93]	86 [77-95]	*0.38*
Cardiac Work *(L.mmHg/min)*	792.1 [732.6-1007.0]	912.5 [824.4-1007.0]	*0.28*	678.5 [392.7-805.6]	704.4 [551.6-852.4]	*0.31*
Rate Pressure Product *(mmHg.bpm)*	15808 [14725-17220]	16459 [14725-19000]	*0.10*	15255 [12502-16102]	14835 [13230-17069]	*0.22*

3.3.6 Cardiac Energetics at Stress

In the NHDM cohort, PCr/ATP at stress was significantly higher than at rest during glucose infusion but not FFA infusion, although there was no difference between rest and stress k_f or CK flux (Figure 3.5). There were also no significant differences between infusions in the values at stress (Table 3.9). However, in the HFDM cohort, neither PCr/ATP, k_f or CK flux were increased during stress on either infusion.

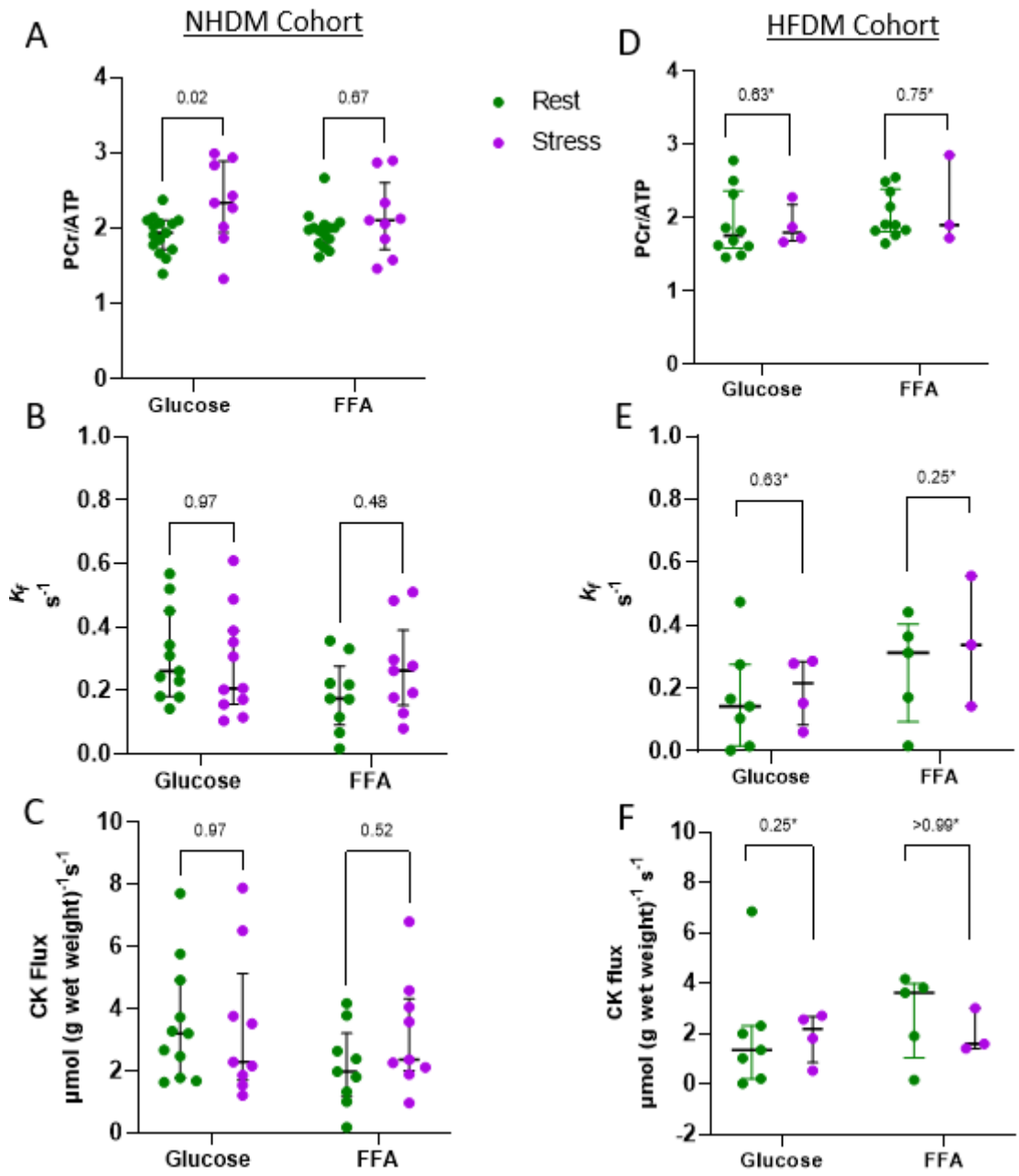

Figure 3.5: *Rest and stress PCr/ATP, k_f and CK flux for the NHDM cohort (A-C respectively) and the HFDM cohort (D-F respectively), compared by infusion. *paired Wilcoxon signed rank tests as insufficient data for mixed effect analysis*

Table 3.9: Comparison of cardiac energetics at stress on glucose and FFA infusions

	NHDM			**HFDM**		
	Glucose Infusion	FFA Infusion	*p*	Glucose Infusion	FFA Infusion	*p*
PCr/ATP*	2.34 [1.95-2.89]	2.11 [1.72-2.61]	*0.19*	1.80 [1.68-2.18]	1.90 [1.72-2.85]	*0.50*
k_f (s^{-1})	0.207 [0.156-0.389]	0.263 [0.154-0.391]	*0.20*	0.216 [0.084-0.284]	0.338 [0.143-0.557]	*0.75*
CK Flux *(µmol (g wet weight)$^{-1}$ s^{-1})*	2.29 [1.70-5.14]	2.36 [2.00-4.32]	*0.09*	2.19 [0.85-2.67]	1.59 [1.41-2.01]	*>0.99*

**PCr/γ-ATP*

3.3.7 Comparison of Energetics between NHDM and HFDM

When cardiac energetics were compared between cohorts at both rest and stress, matched for infusion, there were no significant differences, although there was a trend towards lower k_f and CK flux at rest during glucose infusion for the HFDM cohort (Figure 3.6).

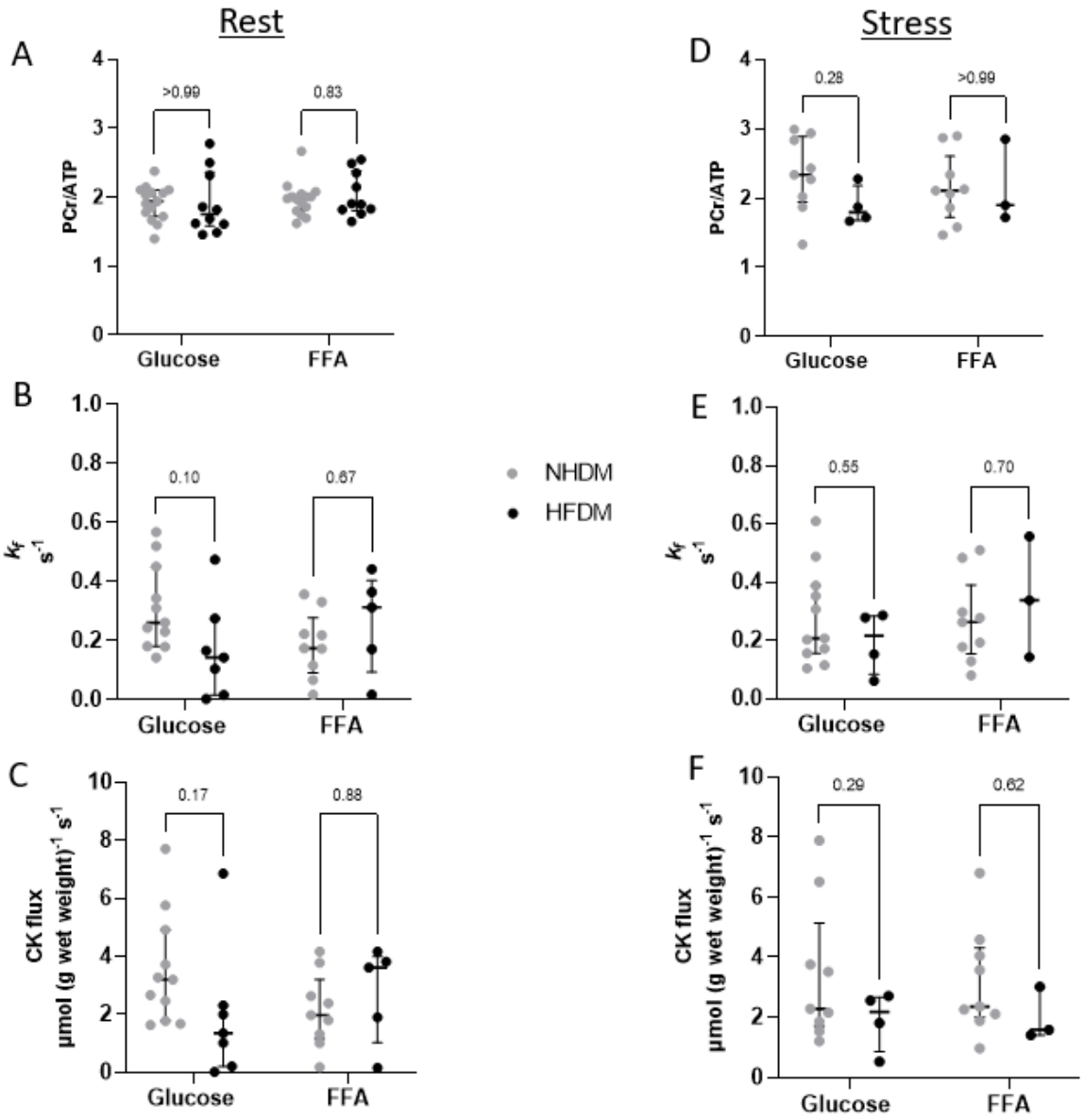

Figure 3.6: *Comparison of cardiac energetics between cohorts, matched for infusion, for rest PCr/ATP (A), rest k_f (B), rest CK flux (C), stress PCr/ATP (D), stress k_f, (E) and stress CK flux (F)*

3.3.8 Correlations Between Cardiac Haemodynamics and Energetics

There were no significant correlations between haemodynamics and energetics at rest in the NHDM cohort, although with data combined from both infusions stroke work did correlate with PCr/ATP in the HFDM cohort (R = 0.53, p = 0.05). However, in the NHDM cohort at stress, k_f correlated positively with cardiac work on both infusions (R = 0.74, p = 0.05 for both), with CK flux also correlating positively with cardiac work on FFA infusion (R = 0.74, p = 0.05). These correlations were not observed in the HFDM cohort. The results for both infusions combined are shown in Figure 3.7.

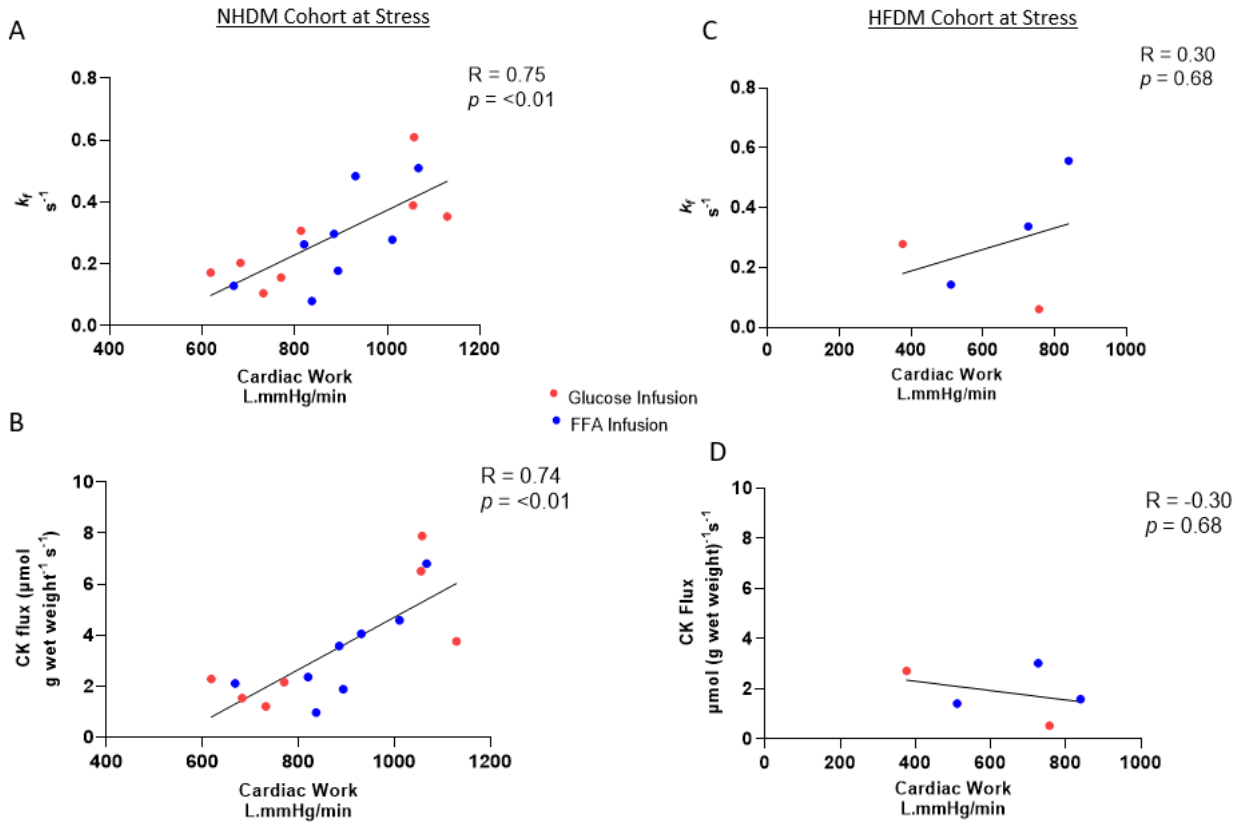

Figure 3.7: *Significant positive correlations of k_f (A) and CK flux (B) with cardiac work in the NHDM cohort at stress, which are not present in the HFDM cohort at stress (C+D respectively). Combined data from both infusions*

3.4 Discussion

The main findings of this chapter are:

1. Free fatty acid infusion increased LV systolic function and cardiac work at rest in the NHDM cohort, compared to a glucose infusion. This was associated with a decrease in k_f and CK flux, implying improved energetic efficiency.
2. This was not observed in the HFDM cohort, where substrate manipulation was unable to alter cardiac function or energetics at rest, suggesting impaired metabolic flexibility.
3. During dobutamine stress, LV systolic function and cardiac work is increased regardless of substrate infusion in the NHDM cohort. The increase in cardiac work correlates with the increase in k_f and CK flux, with a glucose infusion obtaining a higher PCr/ATP ratio compared to at rest. This suggests that metabolic flexibility is preserved.
4. This was not observed during stress in the HFDM cohort, where an increase in LV systolic function and cardiac work was only observed with FFA infusion, without a change in energetics.

Overall, our data is consistent with the hypothesis that metabolic flexibility is preserved both at rest and stress in the NHDM cohort, but that it is not, even at rest, in the HFDM cohort.

3.4.1 Improved Cardiac Function and Work on FFA Infusion

The finding that overall FFA infusion appears to be associated with improved measures of cardiac contractility in the NHDM cohort is in keeping with previous findings in our group in non-diabetic participants with both normal heart function and systolic heart failure (unpublished). However, this was not seen in the HFDM cohort at rest. Importantly, this occurred without any significant difference in infusion volume between arms and so cannot be accounted for by differences in preload.

Fatty acid oxidation generates more ATP per mole than glucose oxidation[247]. Whilst it is less efficient in terms of oxygen efficiency[234, 249, 251], in the absence of oxygen limitation (as could be expected in both the cohorts here), this would not be expected to be a disadvantage, with the increased ATP generation being beneficial. In addition, however, BOHB levels on FFA infusion were also significantly higher at rest and stress in both cohorts. Ketones are taken up in a concentration dependent manner from plasma and so it is possible that ketone uptake was also increased[223]. Furthermore, they are more oxygen efficient than FFA oxidation[256] and infusion of ketones intravenously has been shown to increase cardiac output and ejection fraction in a heart failure cohort[292]. The increase in venous BOHB levels seen on FFA infusion could therefore account for some of the improvements in cardiac systolic function. Finally, FFA infusion has previously been shown to be associated with increased blood pressure, systemic vascular resistance and heart rate[375], as well as stimulation of the autonomic nervous system[376], which may be another mechanism accounting for these findings.

3.4.2 Metabolic Flexibility is Maintained at Rest in NHDM

In the NHDM cohort, FFA infusion results in increased cardiac systolic function and work compared to glucose infusion. Furthermore, CK flux is decreased, implying improved energetic efficiency, and so metabolic flexibility appears to be maintained. However, in the HFDM cohort substrate manipulation does not appear to affect either systolic function, work or energetics, suggesting in general a loss of metabolic flexibility in line with our hypothesis. This may in part explain the decreased response rates to CRT that are seen in diabetic populations[65, 122].

3.4.3 Improved Energetic Efficiency on FFA infusion

The finding of decreased k_f and CK flux at rest in the NHDM cohort despite increased cardiac work is interesting. It implies that there is less ATP delivery through the PCr shuttle to generate the same mechanical cardiac work. If this is due to decreased ATP hydrolysis then it implies that 'efficiency' (in terms of ATP usage rather than cardiac oxygen consumption) is improved. This is different to our findings in a healthy non-diabetic population, which showed that both k_f and CK flux were increased in response to FFA infusion. Conceptually, this could make sense in a diabetic heart which is adapted to predominant FA metabolism. Similarly, an increase in cardiac systolic function during dobutamine stress only occurred on FFA infusion in the HFDM cohort, but not on glucose infusion, and this occurred without a change in energetics, again suggesting improved efficiency. There are different possible mechanisms which could explain decreased flux despite increased work.

3.4.3.1 Alternative Routes of ATP Delivery

Only ATP delivery through the PCr shuttle is assessed in this study. However, it should be remembered that ATP provision can also occur via adeylate kinase, which normally accounts for 10-20%, as well as by glycolysis[245, 246]. While it would seem unlikely that glycolysis is increased on an FFA infusion, it is possible that transfer via adenylate kinase is increased, accounting for the apparent shortfall in ATP delivery.

3.4.3.2 Decreased Basal Metabolic Work

It may be that basal metabolic work was reduced on FFA infusion. Thus, even if ATP delivery was reduced, the amount used in excitation-contraction coupling to generate mechanical work could be unchanged or even increased. However, previous studies have actually suggested that the increased MVO_2 associated with FFA metabolism is due to an increase in ATP demand for basal metabolism due to enhanced Ca^{2+} pump activity[251] and futile cycling associated with FA oxidation is also associated with ATP consumption in order to re-esterify exported FA anions to an acyl-CoA for re-entry to the mitochondrion[255]. Therefore reduced basal metabolic work would seem unlikely.

3.4.4 Correlations

The finding that overall k_f and CK flux positively correlated cardiac work in the NHDM cohort at stress demonstrates the utility of ^{31}P spectroscopy in measuring CK flux and ATP delivery at differing workloads and again suggests that metabolic flexibility is maintained. Furthermore, resting PCr/ATP in the HFDM cohort, but not the NHDM cohort, correlated with measures of contractility. This is similar to our findings in participants with HFrEF without

DM, where we hypothesised that it indicated that impaired resting energetics were a limiting factor on cardiac contractility. Therefore, this also seems to be the case in participants with NIDDM and HFrEF, although the impaired metabolic flexibility we have shown in these participants is preserved in HFrEF without DM (unpublished).

3.5 Limitations

Although 10 participants were recruited in the HFDM group, due to more extensive comorbidity interpretable data on cardiac energetics was only obtained in a small proportion of these. The emphasis which can be placed on those results in that cohort is therefore likely to be limited.

Both cohorts likely represent a relatively 'mild' diabetic phenotype, as indicated by the relatively low HbA1c levels in both. Indeed, the exclusion of insulin-dependent participants would tend to exclude those at the more severe end of the diabetic spectrum. Therefore, whether flexibility is preserved across the full range of diabetic severity is unknown.

Although venous insulin and metabolite levels were significantly altered by the Intralipid™ and insulin/dextrose infusions, we cannot be certain that this affected substrate uptake and metabolism. However, a hyperinsulinaemic state would be expected to result in increased systemic glucose uptake even in insulin resistant states and the need for significant volumes of dextrose infusion to maintain fasting glucose levels would support this. In addition, a previous study has shown that myocardial FFA uptake and oxidation is proportional to arterial

concentration[235] and ketone bodies are also freely diffusible and taken up in proportion to concentration[223].

Although there was no significant difference between cohorts in terms of HbA1c levels, half of the HFDM cohort had evidence of micro or macrovascular disease. Whilst significant epicardial coronary artery disease causing ischaemic cardiomyopathy was an exclusion criteria for the study, microvascular disease could remain a possibility. Similarly, it is possible that undiagnosed autonomic neuropathy and dysfunction was more prevalent in this cohort.

3.6 Summary

This chapter demonstrates that the increased cardiac contractility in response to a FFA infusion, which we have previously shown in participants with HFrEF and without diabetes, is replicated in participants with NIDDM and normal cardiac function. These participants also appear to have preserved metabolic flexibility and improved energetic efficiency when FA metabolism is maximised. These findings were not seen in NIDDM participants with HFrEF, suggesting that metabolic flexibility is impaired. However, the correlation of resting PCr/ATP with cardiac contractility does imply that cardiac energetics may be a limiting factor on cardiac contractility in these patients.

Chapter 4:

Acute Changes in Cardiac Work, Efficiency and Substrate Uptake in Response to Cardiac Resynchronisation Therapy

---

4.1 Introduction

Cardiac resynchronisation therapy acutely rebalances the electrical and mechanical dyssynchrony associated with LBBB, resulting in improved acute haemodynamics[55-58, 63]. Additionally, it appears to achieve this without an increase (or even with a decrease) in MVO_2 and so myocardial efficiency as defined by oxygen usage (cardiac work / MVO_2) is improved[340, 341, 346]. Even in a study which demonstrated increased MVO_2 with CRT, cardiac work was more than proportionally increased and so efficiency was still improved[347].

Use of FDG-PET has also demonstrated that CRT influences regional cardiac glucose uptake, with homogenisation of uptake to match the rebalancing of cardiac work between the septum and lateral wall which is seen with CRT[337, 338]. Whilst other chronic metabolic effects of CRT have been studied, e.g. analysis of effects on the metabolome[353], acute effects on metabolic

substrate uptake overall are unknown and no studies to date have assessed and quantified cardiac metabolic substrate uptake invasively using paired A-V samples. Given the differential effect of substrate metabolism on cardiac efficiency, with FA metabolism requiring greater oxygen usage per mole of ATP generated[226], substrate usage would be expected to impact on efficiency calculations. Furthermore, acute changes in substrate uptake in response to CRT would imply a degree of preserved substrate flexibility, challenging one of the central premises of the energetic theory of heart failure, which is that the failing heart is metabolically inflexible[249]. Finally, heart failure symptoms are frequently experienced on exertion, illustrating the importance of assessing interventions under conditions of stress.

We therefore aimed to invasively assess and quantify cardiac work, cardiac efficiency and metabolic substrate uptake in response to acute CRT, while cardiac substrate supply was manipulated to either increase glucose uptake (insulin/dextrose clamp) or FFA uptake (Intralipid™ infusion). We also aimed to assess this during CRT at stress as simulated using rapid pacing, as well as at rest.

4.2 Methods

4.2.1 Recruitment

Participants with severe non-ischaemic heart failure with reduced ejection fraction (HFrEF) who were scheduled for a CRT device implantation were recruited from cardiology services of the Oxford University Hospitals NHS Foundation Trust.

4.2.1.1 Inclusion Criteria

- Participant willing and able to give informed consent for participation in the study.
- Male or female, aged at least 18 years old.
- Non–ischaemic cardiomyopathy (based on either no flow-limiting disease on coronary angiography or negative non-invasive functional test, with a non-ischaemic pattern of (or no) late gadolinium enhancement on CMR).
- HFrEF as diagnosed by the combination of symptoms and signs of heart failure accompanied by echo or CMR LVEF <40% (as per European Society of Cardiology 2021 guidelines[1]).
- Scheduled for a CRT implantation as part of routine clinical care, according to the European Society of Cardiology 2021 guidelines[1].

4.2.1.2 Exclusion Criteria

- Participant unwilling or unable to give informed consent.
- Any impediment to communication which, in the opinion of the investigator, might prevent the investigator communicating effectively with the patient during the study which could cause a safety or reliability concern.
- Any other condition which, in the opinion of the investigator, might affect the safety of the participant or reduce the reliability of the study results.
- Involvement in any other research project where the procedures would affect the outcomes of this study.
- Patient with known iodine contrast hypersensitivity.

- Patient with uncontrolled AF or a baseline heart rate judged by the investigators to preclude the ability to pace at a heart rate simulating resting conditions.
- Egg or soya allergy.
- Disturbances of normal fat metabolism.
- Severe liver damage, TB, pulmonary disease, anaemia, blood coagulation disorders, or recent fracture of pelvis or long bones.
- Female participant who was pregnant, lactating or planning pregnancy during the course of the study.

4.2.2 Protocol

Participants were fasted from midnight on the day of their procedure as per clinical protocol. At least 1 hour before the start of their CRT procedure they were started on a hyperinsulinaemic euglycaemic clamp, as outlined in Chapter 2, section 2.4.2.

Once all pacing leads had been placed during the implant procedure, 8Fr femoral and 6Fr radial arterial access was established. As detailed in Chapter 2, section 2.6, a PV loop catheter (CD Leycom, NL) was placed at the apex of the LV and intra-arterial heparin was given to keep the ACT ≥250 seconds. A coronary guide catheter was placed in the LMS, diagnostic angiography performed and finally a Volcano^{TM} Doppler guide wire (Phillips, NL) was placed in the distal LMS (in one case this was not possible and so it was placed instead in the proximal LAD). Pacing leads were connected to the pulse generator and biventricular pacing settings (i.e. AV and VV delays) were optimised as per standard clinical protocol. Following this, a pacing protocol was performed as shown in Figure 4.1.

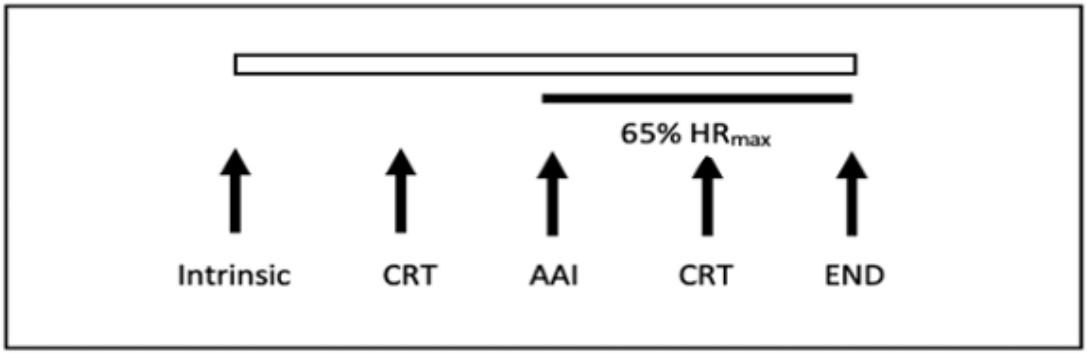

Figure 4.1: *Pacing protocol performed on each substrate infusion, consisting of intrinsic rhythm, biventricular pacing with CRT, AAI pacing at 65% maximal predicted heart rate and BiV pacing at 65% maximal predicted heart rate*

This consisted of intrinsic rhythm with no pacing, optimised BiV pacing at intrinsic heart rate (atrial sensed), AAI pacing at 65% predicted maximal heart rate and optimised BiV pacing at 65% predicted maximal heart rate. One participant was pacing dependent and so right ventricular pacing was performed instead of intrinsic rhythm/AAI pacing, with RV pacing also used instead of AAI in a second participant due to high degree AV block at higher heart rates. After one minute established at each setting, simultaneous recordings were taken from the PV loop catheter and doppler wire for a further minute. Previous studies have shown that changes in coronary flow and cardiac oxygen consumption in response to acute mechanical changes stabilise within 60 to 90 seconds[377, 378]. At the end of this minute of recording, paired arterial and venous blood samples (serum, plasma and blood gas) were taken from the guide catheters in the LMS and CS ostium, respectively. At the end of the protocol, the insulin/dextrose infusion was stopped and a 20% Intralipid^{TM} infusion started at 60ml/hr. After at least 15 minutes on this infusion, the above pacing protocol, measurements and

blood sampling were repeated. Within each substrate infusion, paired measurements were compared between intrinsic rhythm and CRT with atrial sensing (Rest) and between AAI pacing at 65% predicted HR and CRT at 65% predicted HR (Stress). A schematic illustrating catheter and guidewire placement and blood sampling is shown in Figure 4.2.

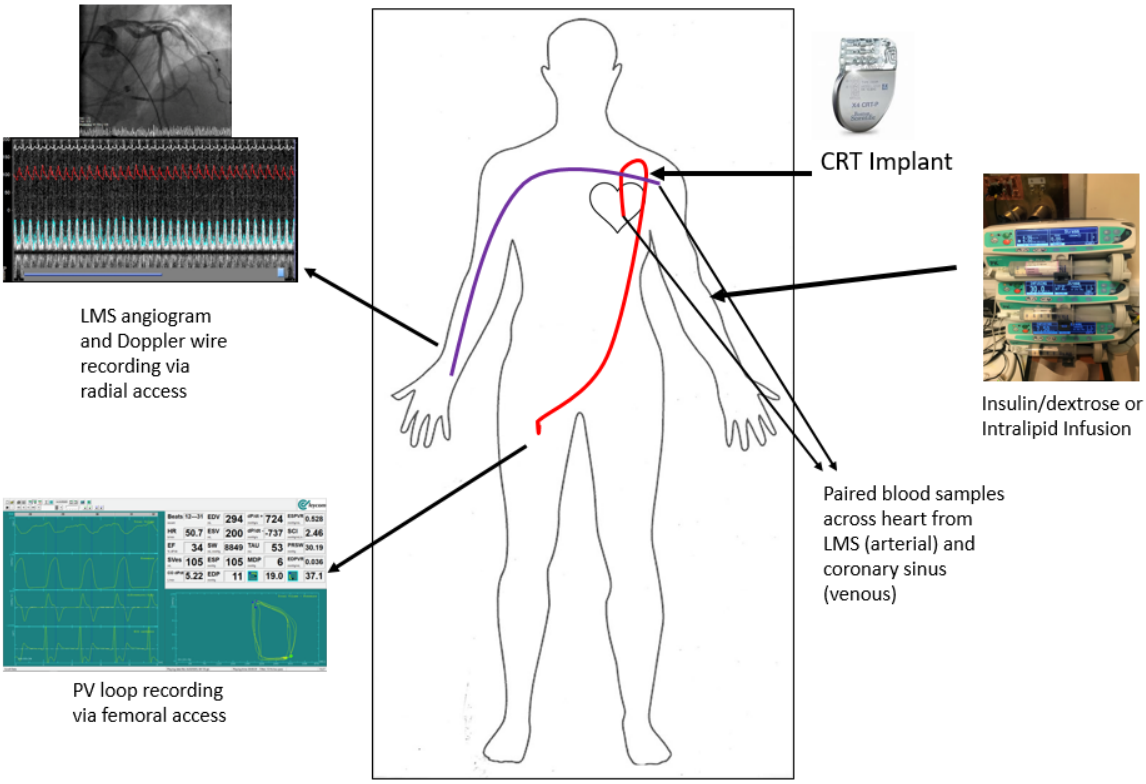

Figure 4.2: *Schematic showing positioning of catheters and guidewires and measurements obtained during the protocol.*

Measures of stroke work, cardiac work, LVEF and dyssynchrony were available for 7 of the participants and dP/dt_{max} for 10 participants, due to either an inability to place the PV loop

catheter or poor quality recordings. For one additional participant paired A-V blood samples were only obtained on glucose infusion.

4.3 Results

4.3.1 Baseline Demographics and Clinical Characteristics

Eleven participants were recruited in total. Baseline demographics and clinical details are given in Table 4.1. All participants were on optimal heart failure medication, as shown in Table 4.2.

Table 4.1: Baseline demographics and clinical characteristics

Recruited *(n)*	**11**
Age *(years)*	63 [60-74]
Male *(n)*	6
Weight *(kg)*	87.6 [73.0-99.4]
BMI *(kg/m^2)*	28.6 [23.6 -33.4]
Hip:Waist Ratio	1.1 [0.1-1.2]
NIDDM *(n)*	2
Hypertension *(n)*	6
Systolic Blood Pressure *(mmHg)*	115 [110-129]
Diastolic Blood Pressure *(mmHg)*	76 [65-88]
Sinus Rhythm *(n)*	11
LBBB *(n)*	11
QRS duration *(ms)*	168 [162-184]
Baseline LVEF *(%)*	30 [26-33]
NYHA Class	2 [2-3]

Table 4.2: Cardiac medication at enrolment

ACEi/ARB	11 (100)
β Blocker	9 (82)
ARNi	7 (64)
MRA	8 (73)
SGLT2i	1 (9)
Digoxin	0 (0)
Ivabridine	0 (0)
Loop Diuretic	7 (64)
Amiodarone	1 (9)

Figures as total number and (%)

4.3.2 Acute Electrical Resynchronisation

Optimised CRT resulted in effective electrical resynchronisation, as demonstrated by significant acute narrowing of the QRSd from 168 [162-184] to 129 [126-144] ms (p = <0.01 – data available for 9 participants).

4.3.3 Substrate Manipulation

Insulin/Dextrose infusion resulted in hyperinsulinaemia, as desired, with a higher average arterial insulin concentration across pacing protocols compared to FFA infusion (151.9 [87.9-259.3] vs 54.3 [30.3-67.0] pmol/l, p = <0.01). This corresponded with higher absolute glucose uptake on glucose infusion across pacing protocols, whilst FFA infusion resulted in a higher FFA uptake, confirming substrate manipulation (Table 4.3).

Table 4.3: Comparison of glucose and FFA uptake on respective infusions.

	Glucose Infusion				**FFA Infusion**				
	Intrinsic	CRT	AAI	Fast CRT	Intrinsic	CRT	AAI	Fast CRT	*p*
Glucose Uptake *(µmol/min)*	59.8 [40.4-113.4]	45.5 [33.9-71.8]	58.7 [19.9-114.7]	75.9 [29.0-138.1]	39.5 [15.3-81.9]	37.4 [5.3-74.5]	17.6 [4.1-46.7]	25.7 [3.8-71.4]	***0.01***
FFA Uptake *(µmol/min)*	1.8 [-6.0-15.4]	14.0 [4.9-41.6]	17.4 [7.2-31.6]	7.9 [-0.5-27.7]	52.4 [25.1-119.0]	57.6 [1.2-61.1]	37.2 [1.2-61.1]	67.8 [15.6-134.3]	***0.03***

p value = mixed effects model across pacing protocol

4.3.4 Effects of CRT on Cardiac Work and Efficiency

There was no difference in LV end-diastolic pressure (LVEDP) with CRT on either infusion (Table 4.4). However, regardless of whether on glucose or FFA infusion, invasive measures of cardiac contractility and work were improved with CRT, both at rest and at stress (Table 4.4, Figures 4.3, 4.4 and 4.5), although LVEF at rest was not significantly different. This was associated with a non-significant trend to decreased systolic dyssynchrony, especially at stress (Table 4.5).

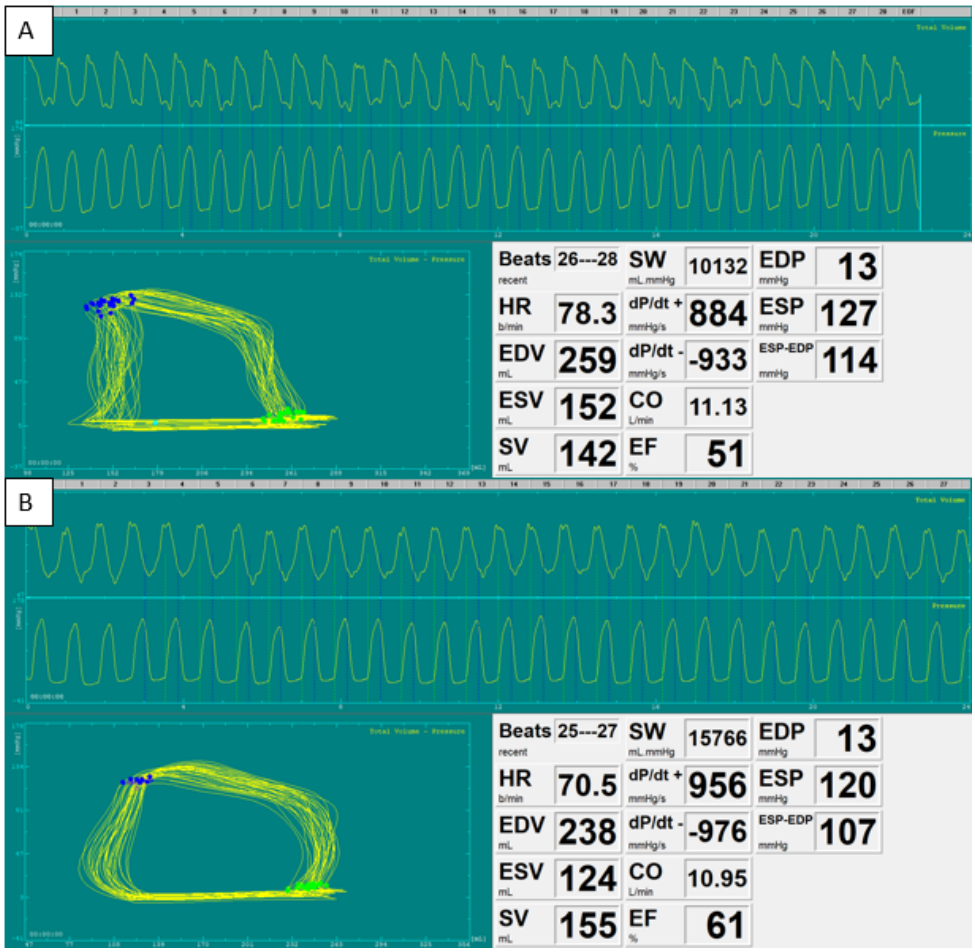

Figure 4.3: *Example PV catheter recordings from the same patient, with intrinsic rhythm (A) and optimised CRT (B). Top trace shows total volume, bottom trace shows pressure, with derived PV loop bottom left and derived indices bottom right. Note the change in shape of the PV loop with CRT, along with a 56% increase in stroke work (SW) and increases in* dP/dt_{max} *and LVEF*

Table 4.4: Measures of cardiac function and dyssynchrony on glucose and FFA infusion

	Glucose Infusion			**FFA Infusion**			**Glucose Infusion**			**FFA Infusion**		
	Intrinsic	CRT	*p*	Intrinsic	CRT	*p*	AAI	Fast CRT	*p*	AAI	Fast CRT	*p*
LVEDP *(mmHg)*	14.3 [9.6-18.4}	11.9 [8.9-15.5]	*0.48*	11.4 [8.8-20.2]	13.7 [9.9-19.2]	*0.32*	9.8 [6.5-13.7]	10.7 [7.6-16.3]	*0.09*	9.8 [8.0-12.0]	9.9 [6.4-18.3]	*0.54*
Stroke Work *(ml.mmHg)*	10304 [6649-11440]	10979 [6975-16316]	***0.05***	8160 [5828-9104]	10791 [7067-15848]	***0.03***	5218 [3817-8803]	9790 [5997-13783]	***0.02***	5026 [4119-7590]	9874 [6439-13362]	***0.03***
Cardiac Work *(L.mmHg/min)*	552 [444-856]	715 [550-1163]	***0.02***	507 [468-666]	638 [540-1084]	***0.02***	553 [387-883]	1079 [632-1380]	***0.02***	534 [367-724]	941 [679-1342]	***0.03***
dP/dt$_{max}$ *(mmHg/s)*	639 [555-723]	735 [623-807]	***<0.01***	698 [598-724]	804 [690-882]	***<0.01***	746 [653-853]	804 [723-1002]	***<0.01***	796 [662-940]	925 [797-1051]	***<0.01***
LVEF *(%)*	40.6 [35.1-48.8]	37.6 [35.6-64.2]	*0.22*	40.3 [30.2-50.0]	42.4 [40.3-55.5]	*0.16*	34.5 [30.0-38.9]	37.9 [34.0-66.4]	***0.02***	34.0 [30.9-48.3]	47.3 [39.7-53.4]	***0.03***
Systolic Dyssynchrony *(%)*	16.5 [11.8-21.7]	12.4 [8.9-23.4]	*0.16*	17.7 [14.4-24.4]	14.6 [11.7-29.2]	*0.22*	21.8 [15.7-29.3]	13.3 [7.8-23.5]	*0.08*	21.7 [18.04-30.3]	14.4 [10.5-28.8]	*0.08*

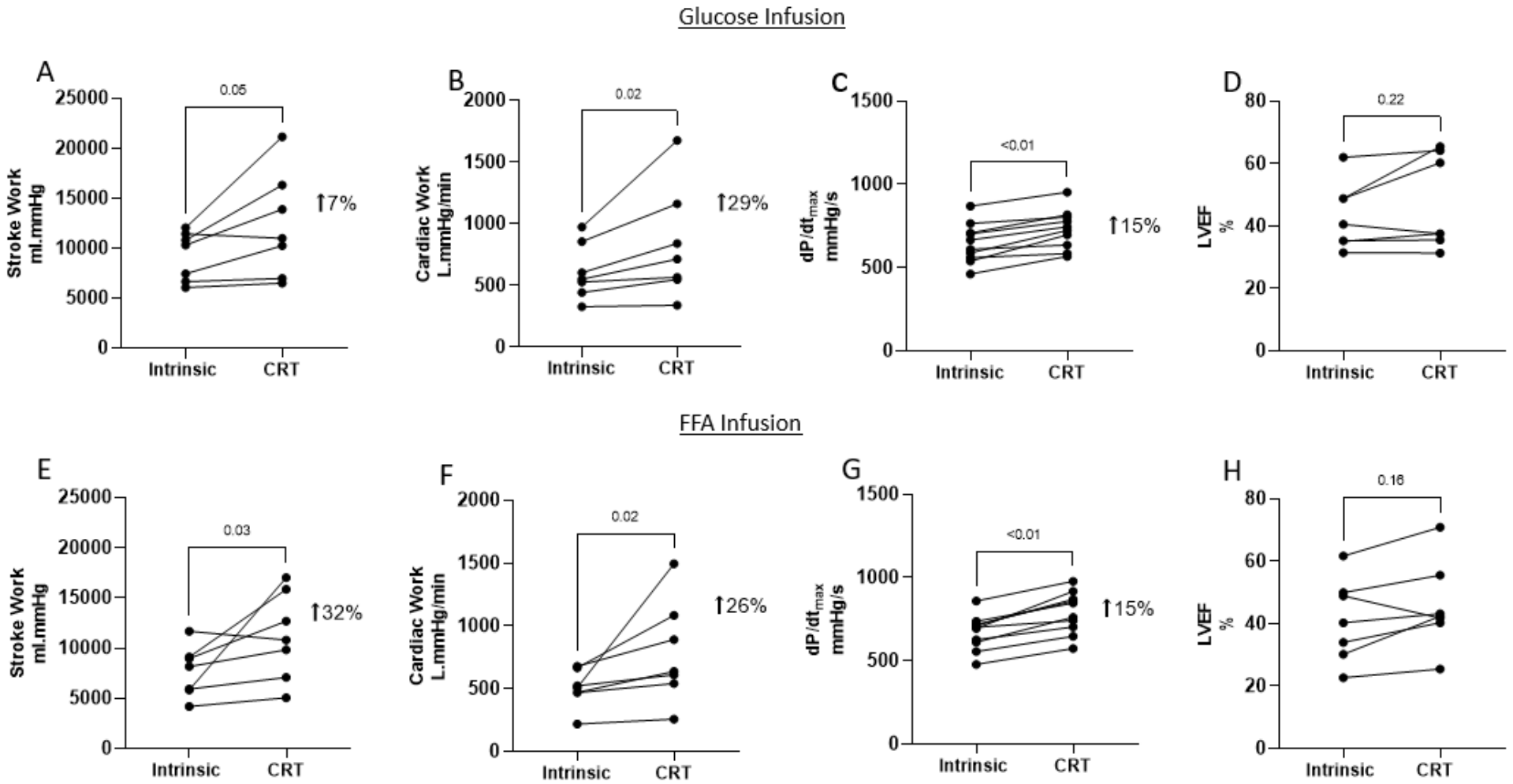

Figure 4.4: *Changes in cardiac contractility with CRT at rest, on glucose (A-D) and FFA (E-H) infusion*

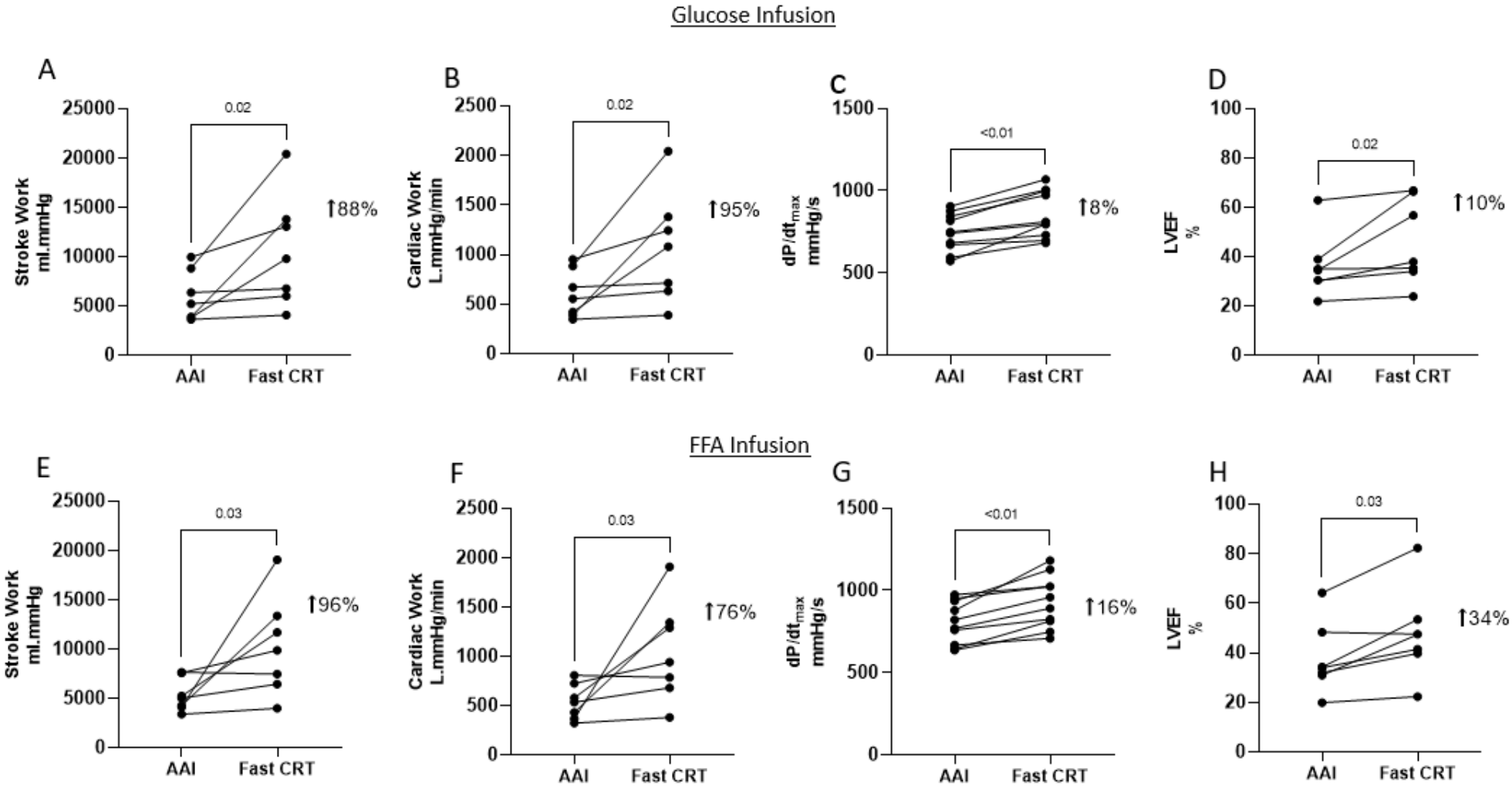

Figure 4.5: *Changes in cardiac contractility with CRT at stress, on glucose (A-D) and FFA (E-H) infusion*

Although LMS flow during CRT at rest was significantly lower during glucose infusion and significantly higher during FFA infusion, there was no difference at stress and no differences in oxygen extraction (Table 4.5). Overall, there was no significant difference in MVO_2 with CRT at any point despite the increase seen in cardiac work. As a result cardiac efficiency, calculated as cardiac work / MVO_2, was increased (Glucose: Intrinsic 65.5 [22.1-78.2]; CRT 70.7 [29.7-128.1], p = 0.02; AAI 45.7 [20.7-57.1], Fast CRT 76.5 [31.7-122.5], p = 0.03; FFA: Intrinsic 32.8 [22.7-42.5], CRT 43.0 [30.7-61.1], p = 0.02, AAI 26.7 [19.4-61.7], Fast CRT 42.0 [31.1-83.0] L.mmHg/ml, p = 0.09) (Figure 4.6).

Table 4.5: Measures of LMS flow, O_2 extraction and MVO_2 on glucose and FFA infusion

	Glucose Infusion			**FFA Infusion**			**Glucose Infusion**			**FFA Infusion**		
	Intrinsic	CRT	*p*	Intrinsic	CRT	*p*	AAI	Fast CRT	*p*	AAI	Fast CRT	*p*
LMS Flow *(ml/s)*	2.9 [2.0-3.9]	2.6 [1.7-3.3]	***0.03***	3.0 [2.6-3.3]	3.3 [2.5-3.7]	***0.04***	3.3 [2.8-4.3]	3.3 [2.7-4.3]	*0.56*	3.7 [3.1-4.1]	4.3 [3.0-4.8]	*0.24*
O_2 Extraction *(ml/dl)*	6.6 [4.7-10.4]	7.5 [4.6-11.2]	*0.10*	8.2 [6.2-13.7]	9.3 [5.3-12.9]	*0.49*	7.5 [5.4-12.1]	8.3 [6.4-11.5]	*0.90*	9.1 [4.7-13.3]	8.4 [5.7-13.1]	*0.36*
MVO_2 *(ml/min)*	11.0 [4.9-14.9]	9.9 [6.2-19.2]	*0.32*	16.6 [11.5-22.2]	16.6 [11.0-26.0]	*0.63*	18.2 [7.4-21.5]	16.3 [10.2-25.0]	*0.90*	19.1 [10.3-31.7]	20.8 [14.5-29.5]	*0.36*

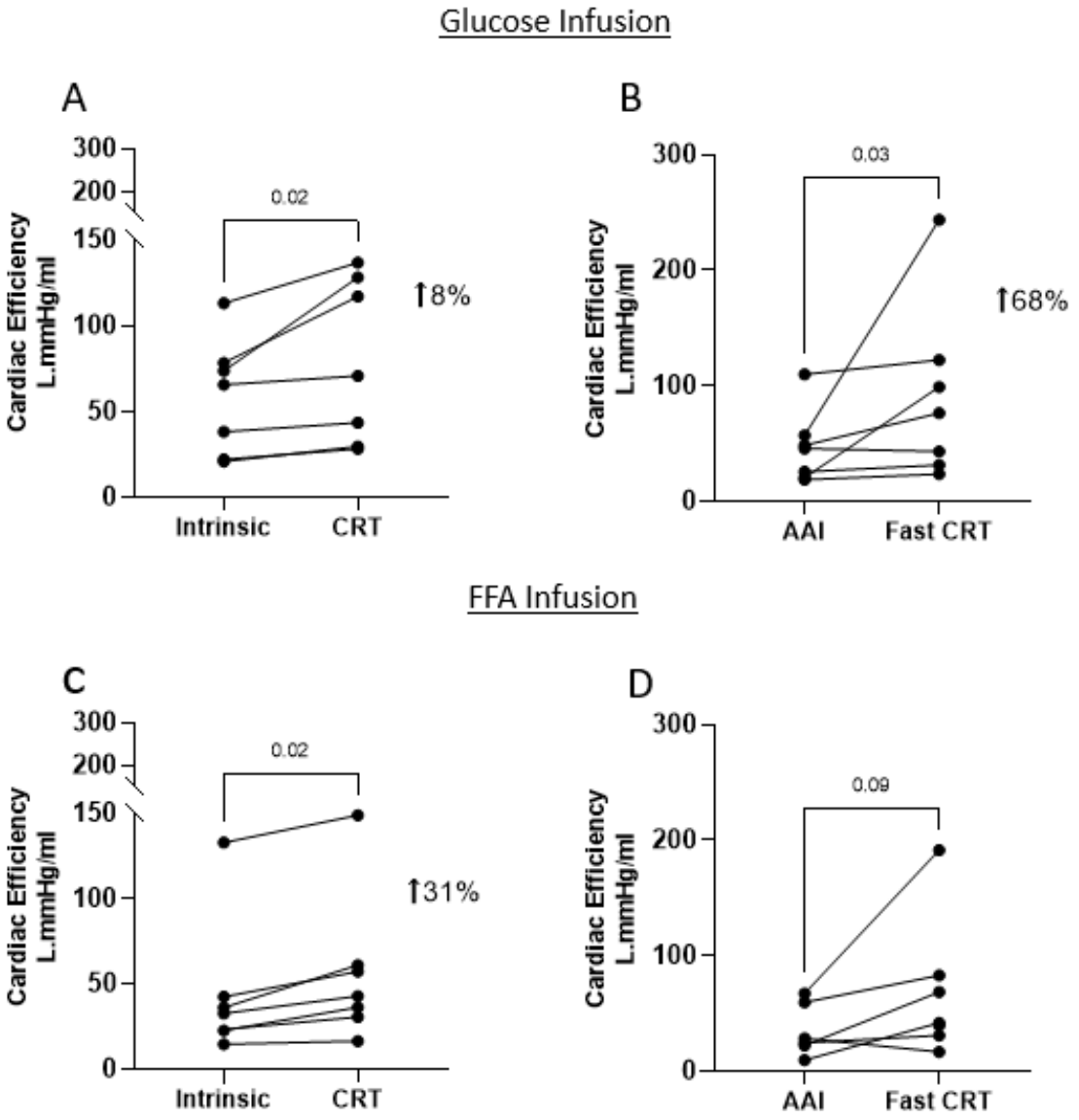

Figure 4.6: *Improvement in cardiac efficiency (cardiac work / MVO_2) during glucose infusion with CRT at rest (A) and at stress (B) and during FFA infusion with CRT at rest (C) and at stress (D)*

4.3.5 Effects of CRT on Cardiac Substrate Uptake

4.3.5.1 During Glucose Infusion

During glucose infusion, there was no difference in arterial glucose, lactate, FFA or BOHB with any pacing parameter (Table 4.6). However, despite there being no difference in substrate supply, CRT at rest resulted in a significant increase in cardiac FFA uptake, while CRT at stress resulted in a significant increase in cardiac lactate uptake (Table 4.6, Figure 4.7). There was no difference in Respiratory Quotient (RQ) with CRT at rest or at stress (Intrinsic: 1.01 [0.70-1.22] vs CRT: 0.96 [0.78-1.40], p = 0.97; AAI: 0.94 [0.67-1.03] vs Fast CRT: 0.92 [0.76-1.08], p = 0.46).

Table 4.6: Arterial metabolic substrate concentrations and absolute cardiac uptake, during glucose and FFA infusion

	Glucose Infusion			**FFA Infusion**			**Glucose Infusion**			**FFA Infusion**		
	Intrinsic	CRT	*p*	Intrinsic	CRT	*p*	AAI	Fast CRT	*p*	AAI	Fast CRT	*p*
Arterial Glucose *(mmol/l)*	5.9 [5.1-7.0]	5.6 [5.3-7.1]	*0.56*	5.5 [4.9-6.4]	5.3 [4.9-6.3]	*0.48*	5.9 [5.2-7.0]	5.8 [5.1-7.1]	*0.66*	5.3 [4.7-6.5]	5.3 [4.9-6.8]	*0.38*
Glucose Uptake *(µmol/min)*	59.8 [40.4-113.4]	45.5 [33.9-71.8]	*0.28*	39.5 [15.3-81.9]	37.4 [5.3-74.5]	*0.32*	58.7 [19.9-114.7]	75.9 [29.0-138.1]	*0.46*	17.6 [4.1-46.7]	25.7 [3.8-71.4]	*0.19*
Arterial Lactate *(mmol/l)*	0.8 [0.7-1.0]	0.8 [0.7-1.0]	*0.94*	0.8 [0.7-1.0]	0.7 [0.6-0.9]	***0.03***	0.8 [0.7-1.0]	0.8 [0.7-1.0]	*0.12*	0.7 [0.7-0.9]	0.7 [0.7-0.8]	*0.05*
Lactate Uptake *(µmol/min)*	38.4 [12.3-40.4]	23.3 [0.0-31.7]	*0.32*	27.5 [5.1-39.7]	21.6 [8.2-40.0]	*0.23*	23.5 [-2.7-31.2]	33.1 [19.3-57.5]	***0.02***	19.1 [2.5-50.3]	22.9 [6.9-43.1]	*0.63*
Arterial FFA *(mmol/l)*	0.9 [0.4-1.3]	0.7 [0.4-1.3]	*0.88*	3.0 [2.5-3.9]	3.7 [2.4-4.5]	*0.11*	0.9 [0.4-1.2]	0.7 [0.3-1.1]	*0.24*	3.9 [2.5-4.5]	4.3 [2.6-5.5]	***<0.01***
FFA Uptake *(µmol/min)*	1.8 [-6.0-15.4]	14.0 [4.9-41.6]	***0.02***	52.4 [25.1-119.0]	57.6 [14.1-77.1]	*0.70*	17.4 [7.2-31.6]	7.9 [-0.5-27.7]	*0.56*	37.2 [1.2-61.1]	67.8 [15.6-134.3]	*0.19*
Arterial BOHB (*mmol/l)*	0.0 [0.0-0.0]	0.0 [0.0-0.0]	*N/A*	0.0 [0.0-0.1]	0.1 [0.0-0.2]	***0.02***	0.0 [0.0-0.0]	0.0 [0.0-0.0]	*N/A*	0.2 [0.0-0.3]	0.3 [0.1-0.4]	***<0.01***
BOHB Uptake *(µmol/min)*	0.0 [0.0-0.0]	0.0 [0.0-0.0]	*N/A*	0.0 [0.0-5.9]	8.3 [0.0-30.1]	*0.08*	0.0 [0.0-0.0]	0.0 [0.0-0.0]	*N/A*	2.2 [0.0-16.7]	8.1 [0.0-26.4]	*0.15*

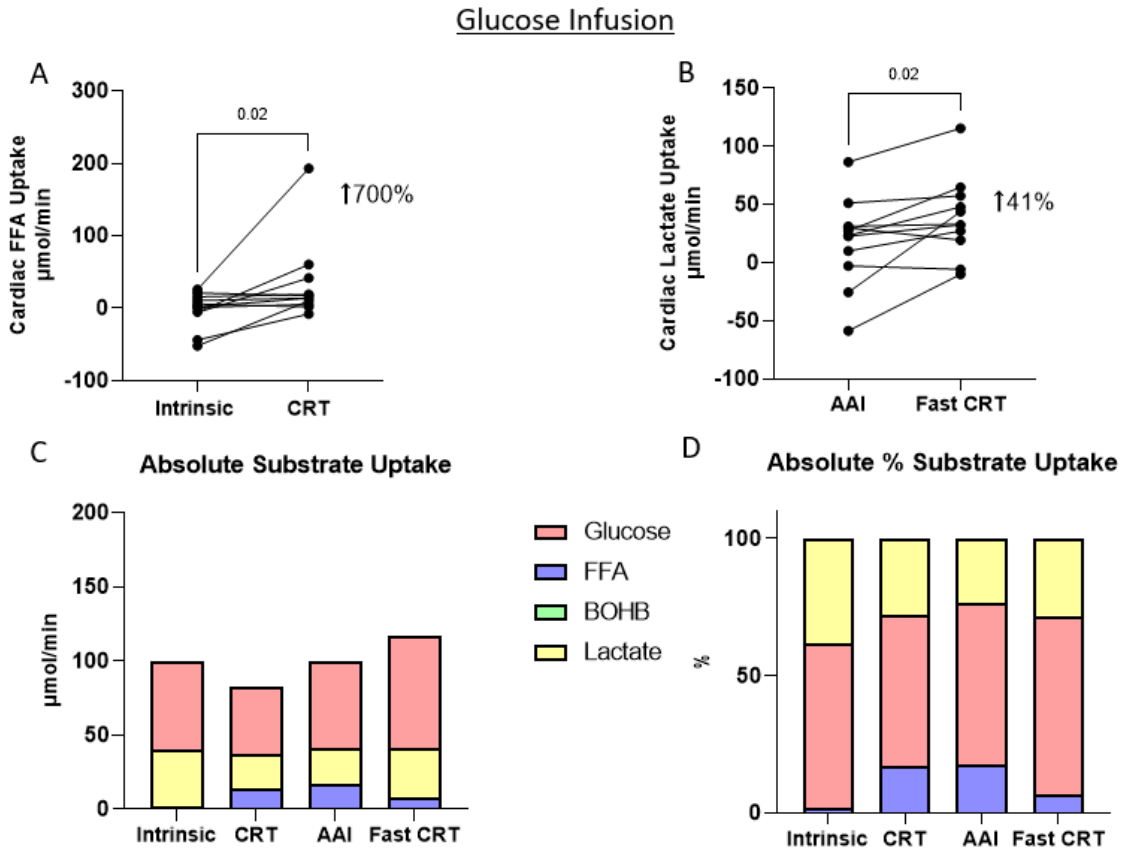

Figure 4.7: *Increased cardiac FFA uptake with CRT at rest (A) and lactate uptake with CRT at stress (B), during glucose infusion. Absolute total (C) and percentage (D) substrate uptakes with each pacing protocol during glucose infusion.*

4.3.5.2 During FFA Infusion

During FFA infusion, arterial lactate was lower on CRT at both rest and stress (Table 4.6). In addition, there was higher arterial BOHB with CRT at rest and arterial FFA and BOHB with CRT at stress. Despite this, there was no significant difference seen in substrate uptake with CRT whilst on FFA infusion. However, FFA uptake was numerically higher with CRT at rest and stress and there was also a non-significant trend towards higher BOHB uptake with CRT at

rest and stress (Figure 4.8). There was no difference in RQ with CRT at rest or at stress (Intrinsic: 0.91 [0.64-1.03] vs CRT: 0.85 [0.61-1.34], p = >0.99; AAI: 0.91 [0.66-1.17] vs Fast CRT: 0.84 [0.48-1.27], p = 0.56).

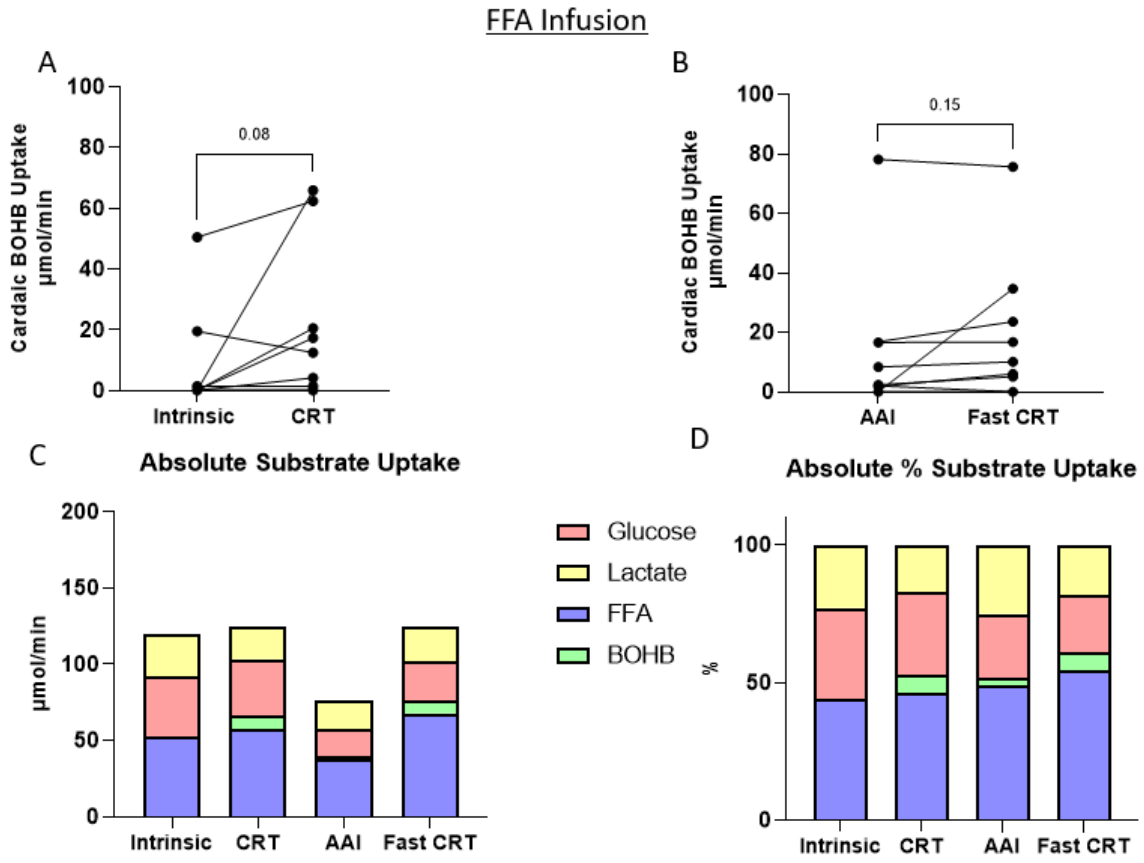

Figure 4.8: *Increased cardiac BOHB uptake with CRT at rest (A) and stress (B) during FFA infusion. Absolute total (C) and percentage (D) substrate uptakes with each pacing protocol during FFA infusion*

4.3.6 Comparison of Substrate Infusion

4.3.6.1 Cardiac Work and Efficiency

During FFA infusion, dP/dt_{max} was higher with CRT at rest and stress, compared to during glucose infusion (Figure 4.9) but with no significant difference in stroke work or cardiac work. There was no difference between substrate infusions in the change (delta, Δ) in cardiac work, stroke work or dP/dt_{max} seen with CRT, either at rest or at stress (Figure 4.10).

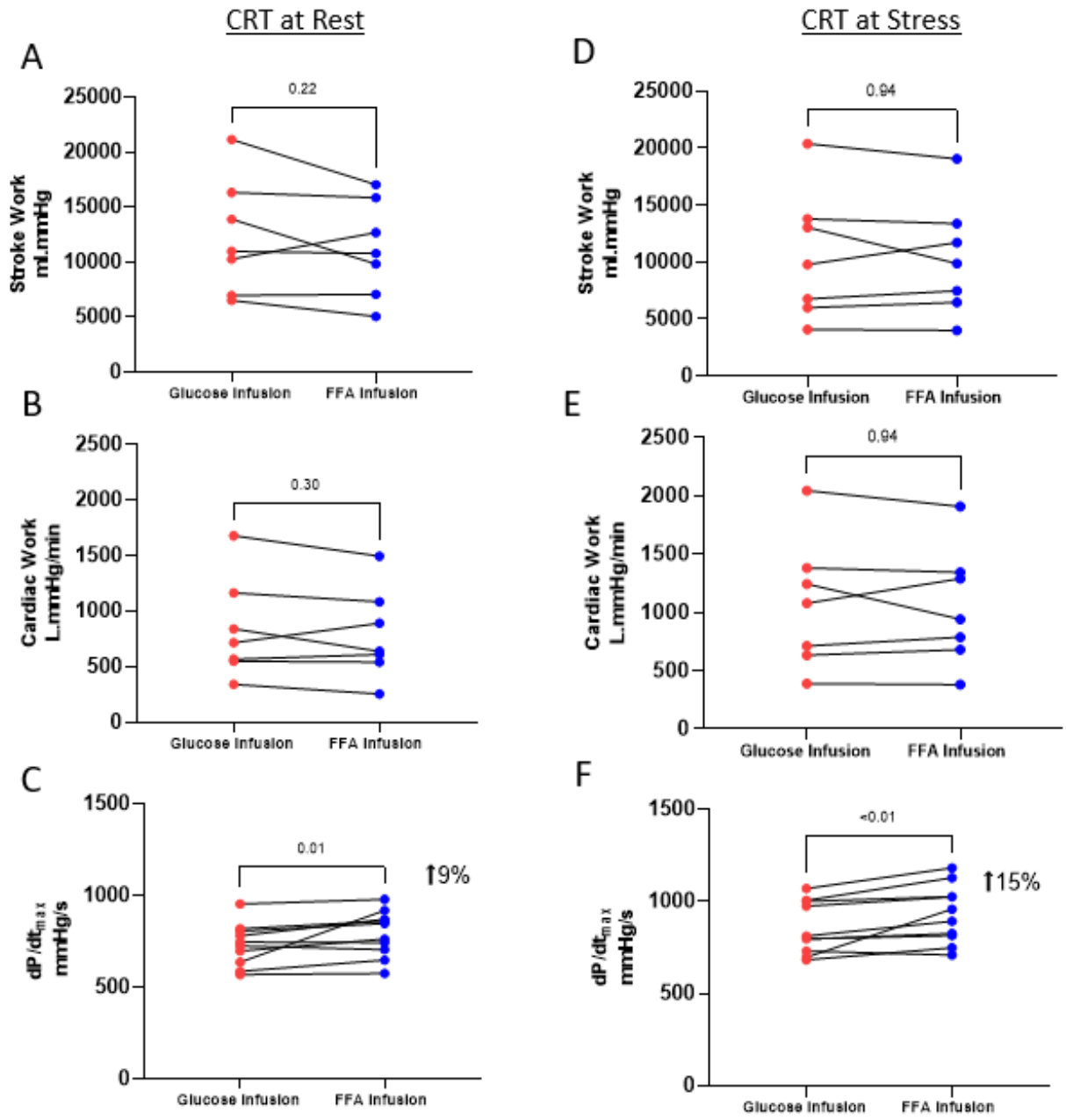

Figure 4.9: *Stroke work (A), cardiac work (B) and dP/dt_{max} (C) during CRT at rest, and at stress (D-F respectively), compared by substrate infusion*

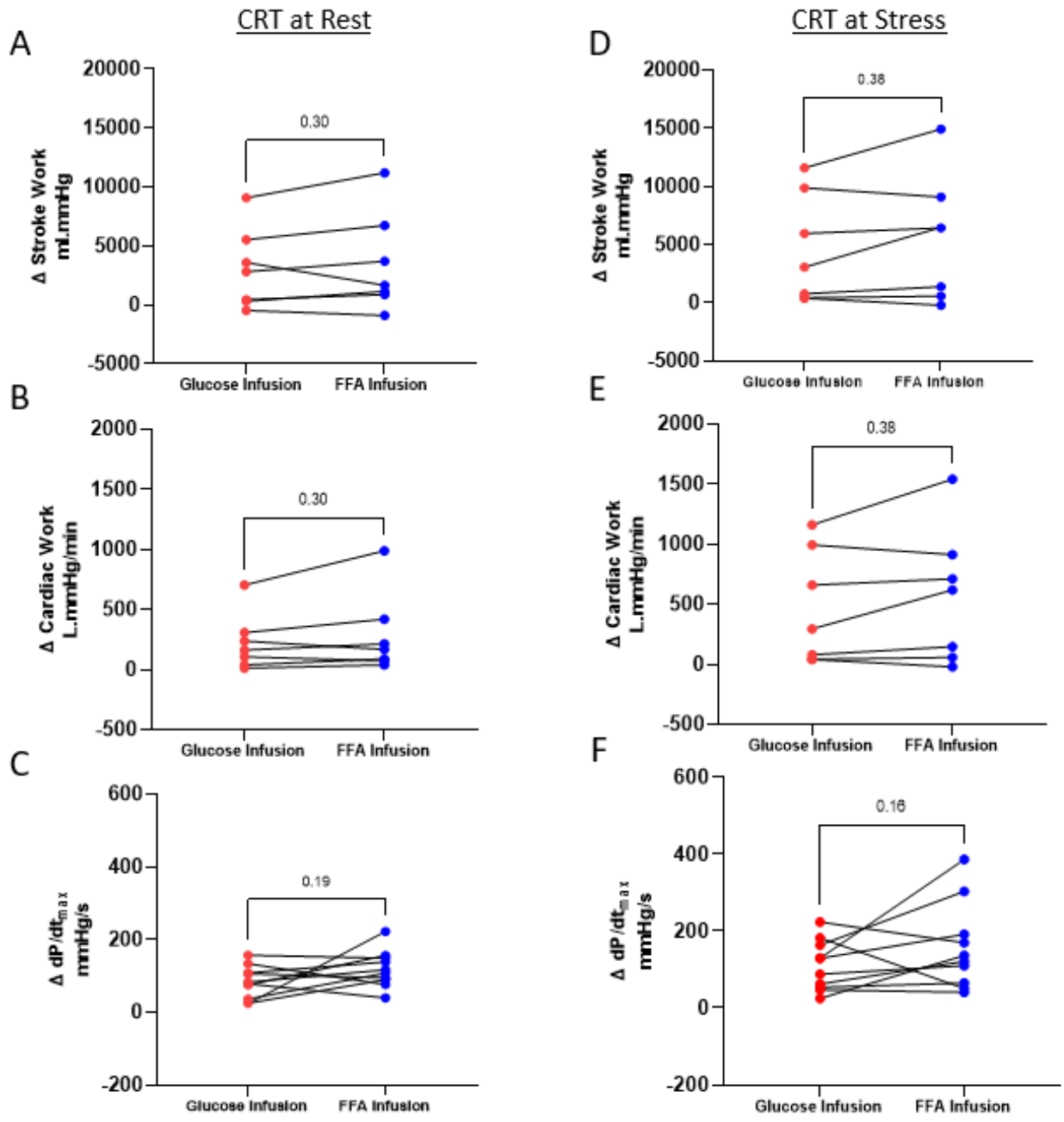

Figure 4.10: *Changes (Δ) in stroke work (A), cardiac work (B) and dP/dt_{max} (C) with CRT at rest, and at stress (D-F respectively), compared by substrate infusion*

As would be expected, MVO_2 was higher during FFA infusion than during glucose infusion at all pacing settings (Intrinsic: 16.6 [11.5-22.2] vs 11.0 [4.9-14.9], p = 0.03; CRT: 16.6 [11.0-26.0] vs 9.9 [6.2-19.2] p = <0.01; AAI: 19.1 [10.3-31.7] vs 18.2 [7.4-21.5], p = 0.05; fast CRT: 20.8 [14.5-29.5] vs 16.3 [10.2-25.0] ml/min, p = <0.01, respectively). This combination resulted in a significant reduction in efficiency for CRT at stress on FFA infusion compared to on glucose infusion and also a trend to reduction for CRT at rest which, whilst it did not reach significance, was almost identical in proportion to that seen at stress (Figure 4.11).

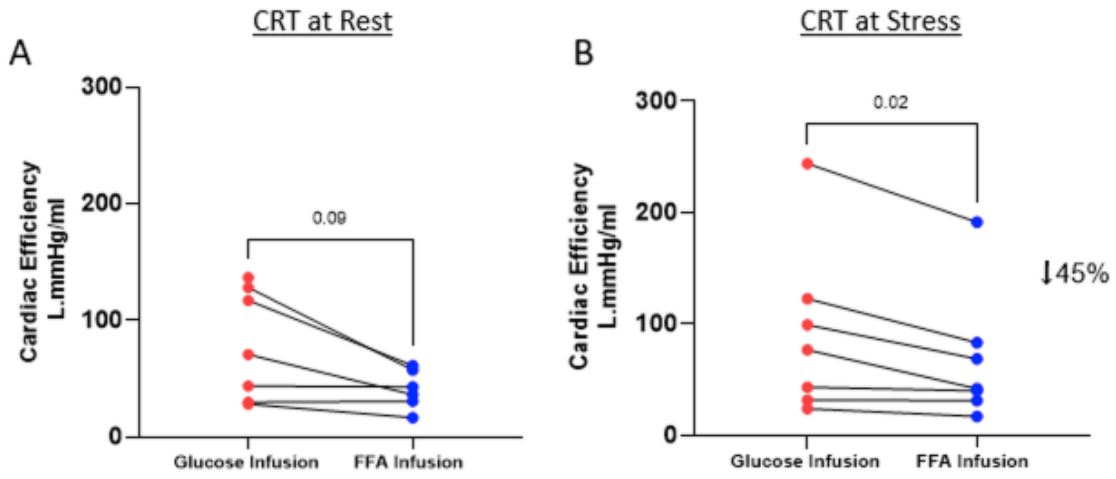

Figure 4.11: *Cardiac efficiency with CRT at rest (A) and at stress (B), compared by substrate infusion*

4.3.6.2 Substrate Uptake

Cardiac resynchronisation therapy at stress during FFA infusion resulted in an increase in FFA uptake which was significantly greater than during glucose infusion, where essentially no increase was seen (Figure 4.12). There was no difference in the degree of change in FFA uptake with CRT at rest, glucose uptake with CRT at rest or stress, or lactate uptake with CRT

at rest. Change in lactate uptake with CRT at stress was significantly higher during glucose infusion. When results from both substrate infusions were combined, there was a positive correlation between the change in FFA uptake and the change in glucose uptake with CRT at rest (Figure 4.13).

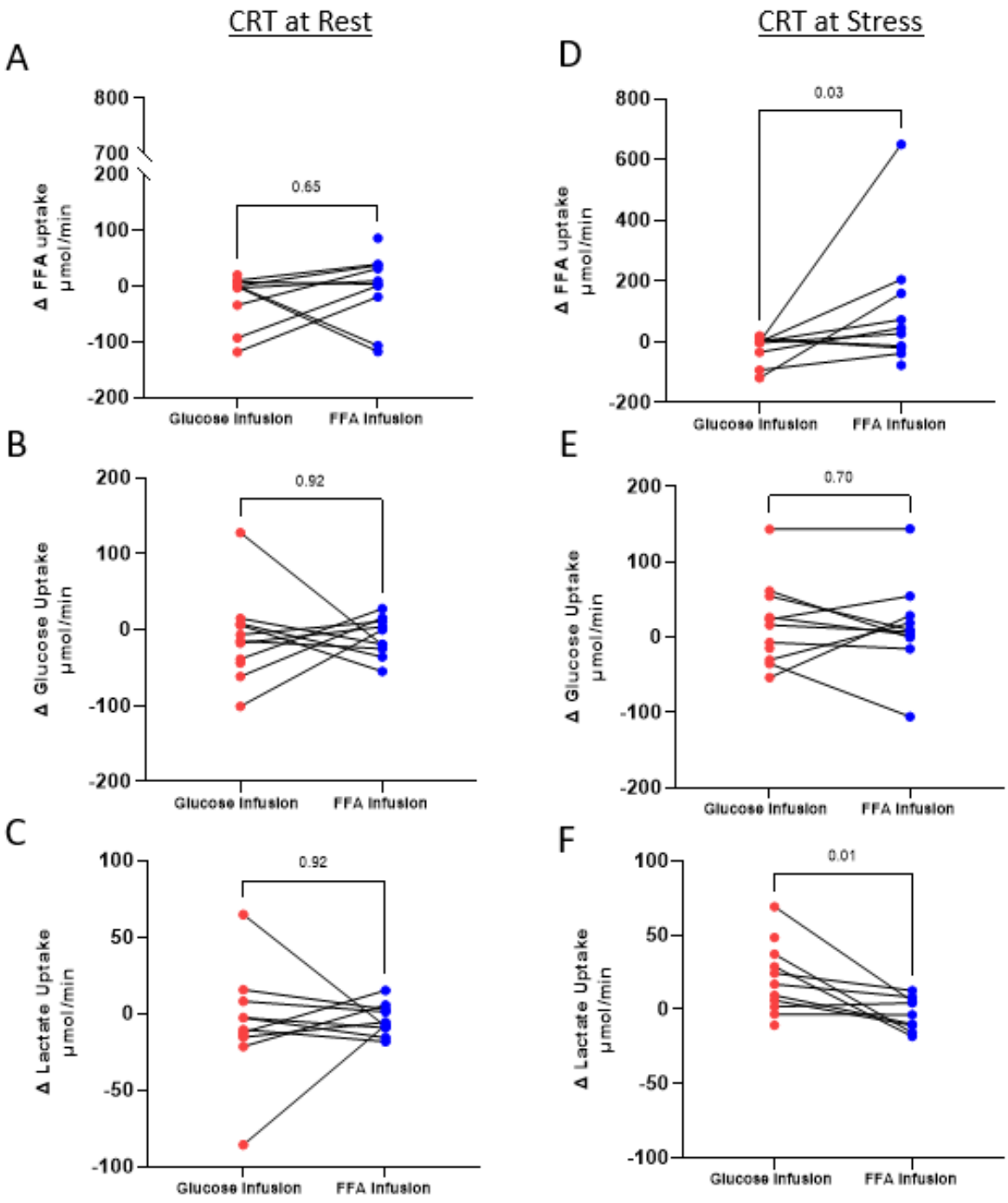

Figure 4.12: *Changes (Δ) in FFA uptake (A) glucose uptake (B) and lactate uptake (C) on CRT at rest, and at stress (D-F respectively), compared by substrate infusion*

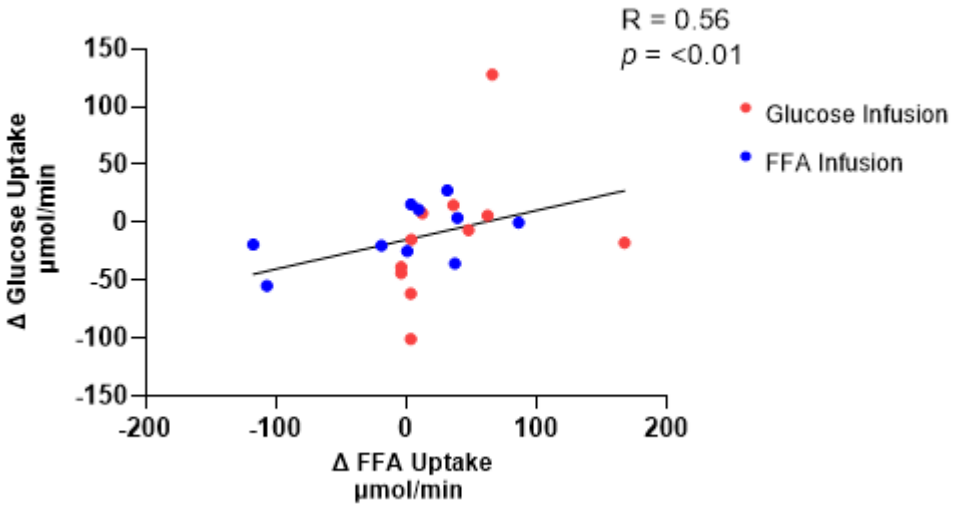

Figure 4.13: *Combined measurements from during both substrate infusions, showing positive correlation between changes (Δ) in glucose and FFA uptake with CRT at rest*

4.3.7 Correlations of Cardiac Work and Substrate Uptake

During glucose infusion, the change in FFA uptake seen with CRT at rest positively correlated with the change in LVEF with CRT, with a trend towards a positive correlation with the change in stroke work (Figure 4.14). With CRT at stress, the change in FFA uptake positively correlated with the change in dP/dt_{max} (Figure 4.14). There was no significant correlation between measures of cardiac contractility and other substrate uptakes.

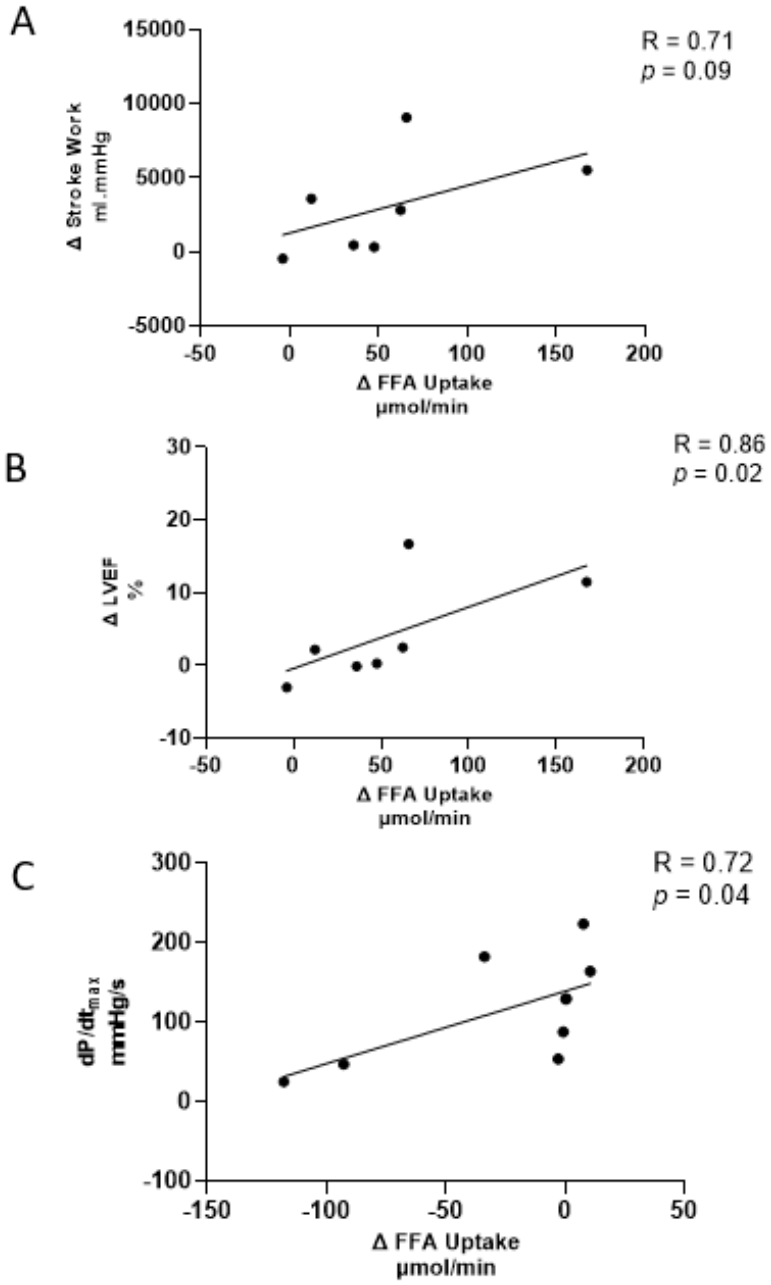

Figure 4.14: *During glucose infusion, positive correlations between change (Δ) in FFA uptake and: (A) change in stroke work with CRT at rest; (B) change in LVEF with CRT at rest; (C) change in* dP/dt_{max} *with CRT at stress*

However, during FFA infusion, the change in BOHB uptake with CRT at rest positively correlated with the change in stroke work and cardiac work, with a trend towards a positive

correlation with dP/dt_{max} (Figure 4.15). There was no significant correlation between measures of cardiac contractility with other changes in substrate uptake at rest. Whilst there was no significant correlation between changes in substrate uptake and measures of systolic function at stress while on FFA infusion, if both rest and stress CRT comparisons were combined then change in BOHB uptake once again correlated with change in both stroke work and cardiac work (Figure 4.15).

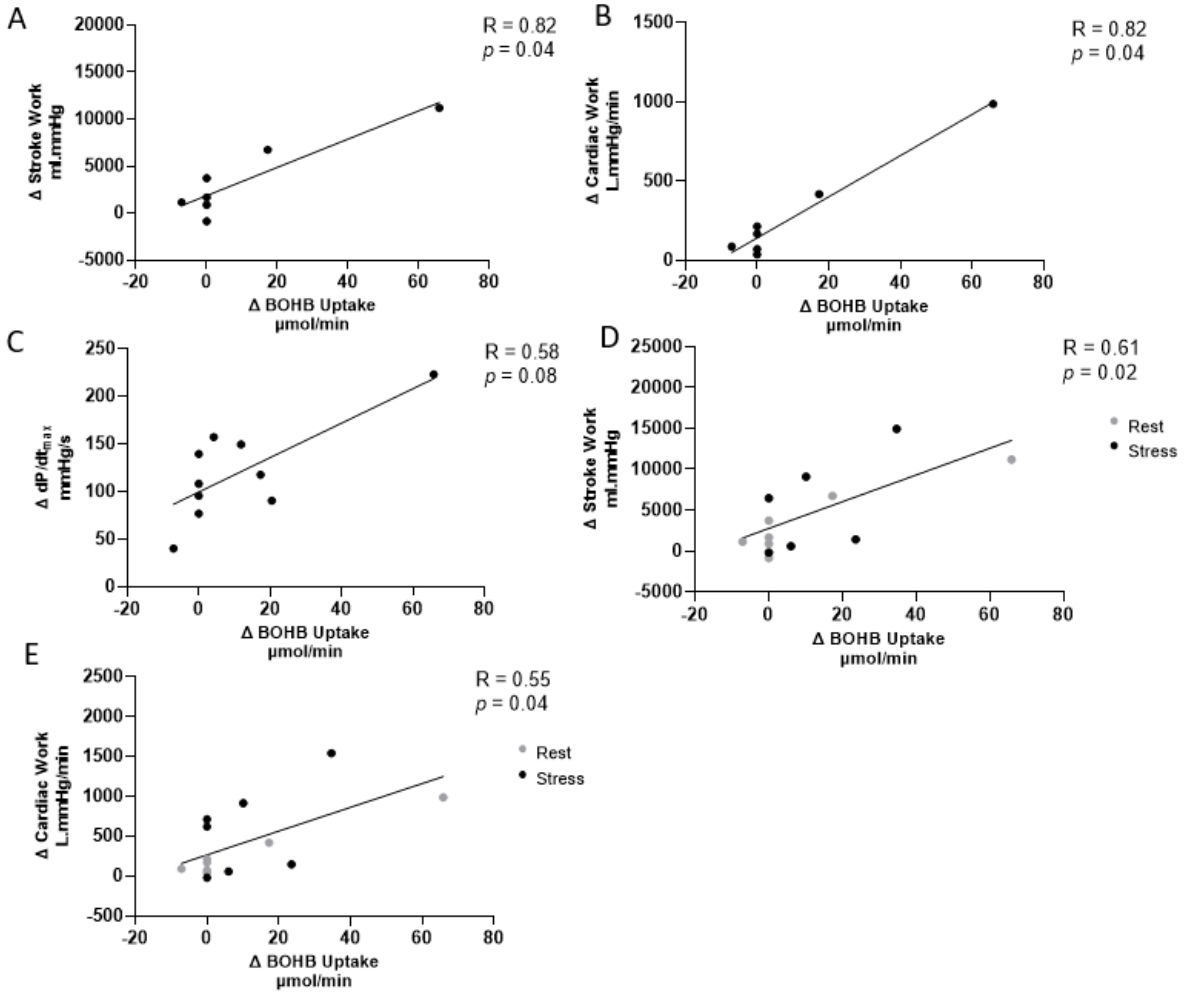

Figure 4.15: *During FFA infusion, positive correlations between change (Δ) in BOHB uptake and: (A) change in stroke work with CRT at rest; (B) change in cardiac work with CRT at rest; (C) change in dP/dt$_{max}$ with CRT at stress. During FFA infusion, positive correlations between change in BOHB uptake and: (D) stroke work; (E) cardiac work with combined measurements of CRT at rest and stress*

Finally, with combination of measurements from both substrate infusions on CRT at stress, change in FFA uptake again correlated with change in dP/dt$_{max}$ (Figure 4.16).

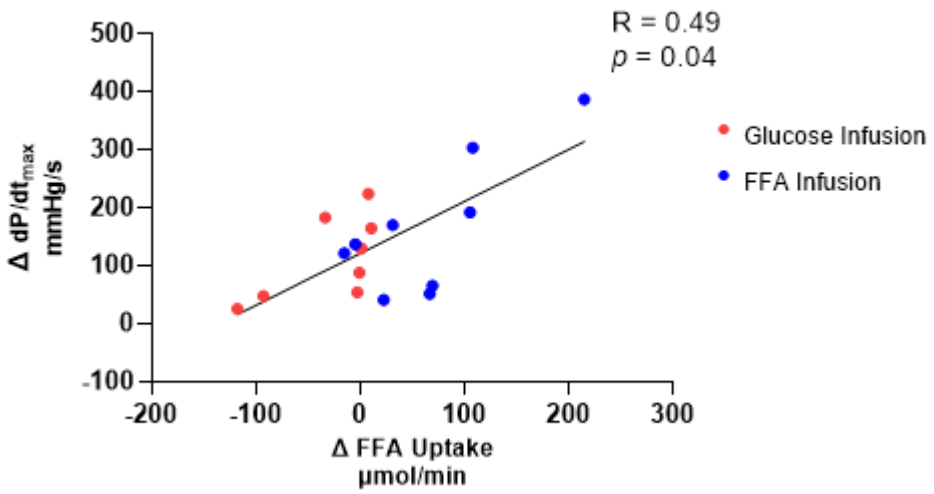

Figure 4.16: *Combined measurements from both substrate infusions for CRT at stress, showing change in FFA uptake against change in* dP/dt_{max}

4.4 Discussion

The main findings of this chapter are that:

1. CRT acutely improves cardiac work regardless of substrate manipulation.
2. CRT improves cardiac efficiency regardless of substrate manipulation.
3. With predominant glucose uptake, CRT at rest increases cardiac FFA uptake while at stress it increases lactate uptake. Change in FFA uptake correlates with change in cardiac contractility.
4. With predominant FFA uptake, CRT at rest and stress appears to increase BOHB uptake. Change in BOHB uptake correlates with change in cardiac contractility.

4.4.1 CRT Acutely Alters Cardiac Substrate Uptake

Regional changes in myocardial glucose uptake have been demonstrated using FDG-PET, as previously discussed. However, this is the first time to our knowledge that absolute cardiac metabolic substrate uptake has been assessed invasively during CRT. Despite increased glucose uptake during the hyperinsulinaemic euglycaemic clamp, when CRT was commenced this caused an increase in resting FFA uptake. Importantly, this increase in FFA uptake occurred without change in arterial FFA supply. This suggests not only that the heart has displayed metabolic flexibility, but also that there was an active element to substrate selection. Furthermore, this change also suggests that CRT is potentially reversing the metabolic phenotype associated with heart failure back towards a more normal phenotype. This is in line with recent work by Martens *et al.*[349] which showed a shift towards FA metabolism induced by CRT after 6 months, associated with improved mitochondrial function, although neither arterial blood sampling nor coronary flows were assessed and so this study could not quantify cardiac substrate uptake.

Whilst MVO_2 was not significantly increased in line with this increase in FFA uptake in our study, and RQs were not significantly lower, it is possible that the effects of increased mechanical efficiency as a result of CRT could outweigh any increases in MVO_2 as a result of increased FFA uptake, with the combination leading to an overall neutral effect on MVO_2. Additionally, whilst the relative increase in FFA uptake is large, it is more modest in absolute terms. It may therefore be that the increase alone is not sufficient to result in a measurable change in MVO_2 or RQ.

At stress, the situation appears to be different. The heart appears to instead preferentially take up lactate. It is plausible that, as it requires additional ATP, it utilises lactate as a readily available and freely diffusible glucose-like substrate at high levels of work. On FFA infusion, FFA uptake with rest and stress CRT was not significantly increased. This may be because uptake is already sufficient and does not need to be increased, or because uptake is already maximised. However, there is a trend towards increased BOHB uptake at rest and stress.

The fact that these changes in uptake occur within 2 minutes of CRT being initiated demonstrates that metabolic flexibility is at least partially preserved, challenging the prevailing thought that it is impaired in heart failure[249]. While it is possible that these substrate increases merely reflect a passive process to match supply to the increased cardiac work during CRT, if this was the case then a more general increase in substrate uptake could be expected, in particular glucose, rather than an active preference for FA or ketone metabolism.

Overall therefore, in conditions where FFA supply is limited, CRT appears to switch metabolic uptake to attempt to take up more FFA if possible. If this is not sufficient, as with CRT at stress, it also increases lactate uptake. However, if FFA supply is maximised CRT instead appears to increase BOHB uptake and it is notable that cardiac ketone metabolism in patients with HFrEF has recently been shown to correlate with increased LVEF and cardiac output, without effecting cardiac efficiency[292].

4.4.2 CRT Improves Cardiac Work and Efficiency Regardless of Substrate

These results confirm that CRT improves measures of cardiac systolic function and work, at both rest and stress. Furthermore, MVO_2 is not increased and so cardiac efficiency is improved. Whilst improved cardiac efficiency with CRT has been shown previously, these studies have mainly used ^{11}C-acetate PET, as discussed in Chapter 1. Nelson *et al.*[346] have demonstrated increased efficiency invasively using paired A-V blood sampling across the heart and a PV loop catheter, but it should be noted that this study only included 3 usable PV loop recordings, with the main determinant of systolic function being dP/dt_{max}. In addition few studies have assessed efficiency at stress and they have often relied on use of dobutamine, which has vascular, inotropic and chronotropic effects[379].

Importantly, no previous studies have to our knowledge assessed cardiac efficiency on different metabolic substrate infusions. This is key, as FA metabolism is less efficient at ATP production per mole of oxygen required and also decreases efficiency due to futile cycling[226, 234]. Therefore the balance of substrate utilisation would be expected to influence cardiac efficiency. Our finding that oxygen efficiency is increased regardless of predominate FFA or glucose uptake is novel.

Whilst dP/dt_{max} was higher on FFA infusion compared to glucose infusion with CRT at rest and stress, there was no significant difference in cardiac work or in the degree of change (delta) of measures of cardiac work with CRT on FFA infusion. Due to the increased MVO_2 associated with FA metabolism[226, 234, 251], however, cardiac efficiency was lower with FFA infusion, especially at stress.

4.4.3 Oxygen Supply is Not Limited

During CRT on both substrate infusions lactate uptake, rather than production, was seen. Indeed, with an increasing level of cardiac work seen with CRT at stress on a glucose infusion, lactate uptake is increased. This suggests that the heart was not oxygen limited. This correlates with previous CMR data which demonstrated that there is no evidence of oxygen limitation in non-ischaemic cardiomyopathy[380].

4.4.4 FFA Infusion Results in a Lesser Increase in Efficiency than Glucose Infusion

As already discussed, the inherently higher MVO_2 associated with FA metabolism inevitably results in a relatively lower improvement in cardiac efficiency seen with CRT than during glucose infusion. Given this, a preference for FFA uptake may be counter-intuitive and indeed this is the reason that decreasing FA metabolism and increasing glucose metabolism has classically been the target of metabolic heart failure treatments[381-383]. However, if the heart is not oxygen limited, as might be expected in a non-ischaemic cardiomyopathy and as demonstrated above, then the increased oxygen requirements associated with FA metabolism would not be detrimental. This is seen in the healthy heart during overnight fasting, where the heart oxidizes fat to generate ATP, has a reduced oxygen efficiency, but is able to generate sufficient ATP as oxygen is not limiting. Indeed, whilst FA metabolism is less oxygen efficient, there is increased ATP generated per mole of FA[247] and this is likely to be the underlying reason for the increased cardiac work seen with increased FFA uptake. This may be why there appears to be a switch back towards FA metabolism when CRT is commenced, with the heart attempting to shift back towards the predominant FA metabolism

seen in healthy conditions. Whilst the decreased oxygen efficiency is unlikely to be deleterious in non-ischaemic cardiomyopathies where oxygen is not a limiting factor, in ischaemic heart disease CRT may increase mechanical efficiency but concurrently increase FA metabolism and so oxygen demand. Whether these 2 opposite effects on oxygen efficiency cancel each other out is unknown, however it is tempting to speculate whether this could be one underlying mechanism responsible for worse responder rates for CRT in ischaemic populations[126, 127].

4.4.5 Challenging the use of Oxygen Efficiency as the Metric of Cardiac Efficacy

As detailed above, the traditional metric of efficiency used in the literature is derived as cardiac work / MVO_2, and generates an oxygen efficiency of contraction. Whilst this is a useful metric in situations where oxygen is limited, this study highlights that this metric is not appropriate for conditions where oxygen is not limiting. This is shown here in this study where cardiac function (dP/dt_{max}), is 15% higher during CRT at stress on FFA infusion compared to on glucose infusion, but oxygen efficiency is lower. In the setting where oxygen is not limited, rather than focusing on the oxygen efficiency of contraction, if the aim is to increase ATP production and contraction, a better metric to use may be cardiac work / ATP delivery.

4.5 Limitations

These findings are from a relatively small number of participants and due to the complexity of the protocol, full datasets were not available for every participant. However, we believe that the strength of the data lies firstly in its uniqueness and also in the amount obtained

from each participant, with paired data not only on different substrate infusions, but also at rest and stress.

Measured coronary flow and arterial blood sampling was only from the LMS and so does not take into account right coronary artery blood flow and substrate/oxygen delivery. Similarly, CS venous sampling does not account for all venous drainage, with 20-30% of venous blood draining directly into the cardiac chambers via the Thebesian veins in the lesser cardiac venous system[384]. However, these predominantly drain into the right side of the heart and so the combination of LMS flow and CS drainage should account for the majority of LV perfusion/drainage. Additionally, whilst this may affect absolute substrate / oxygen uptake measurements, the main findings of this study relate to relative changes between time points, which should therefore be unaffected.

The increased FFA and BOHB uptake seen on CRT when on FFA infusion may be caused to some extent by the increased arterial concentrations seen. This may result from the non-randomised nature of the pacing protocol and so longer duration of Intralipid^{TM} infusion at the CRT time points, which occurred after the intrinsic/AAI measurements and indeed an increase in arterial BOHB and FFA concentration is seen as time progresses from intrinsic rhythm to fast CRT. It may therefore not represent a cardiac preference *per se*. However, this does not detract from the correlation which is seen between change in FFA or BOHB uptake and measures of cardiac work.

Finally, whilst we have measured differences in metabolic substrate uptake across the heart, this may not reflect actual substrate usage, as substrates may have difference metabolic fates.

For example glucose may be used for glyconeogenesis and FFA may be converted into TAG stores in the myocyte, rather than undergoing oxidation.

4.6 Summary

The findings of this chapter confirm that CRT improves efficiency, regardless of predominant substrate uptake and at both rest and stress. In addition, it appears to acutely alter metabolic substrate uptake, with a shift back towards the predominant lipid-derived metabolism (FFA or BOHB) seen in the healthy heart. This demonstrates preserved metabolic flexibility and is likely to be advantageous as the degree of change of uptake correlates with improvement in measures of cardiac work/systolic function. This may therefore open up new avenues for improving CRT response via metabolic manipulation.

Chapter 5:

Metabolic Flexibility and Predictors of Chronic Left Ventricular Reverse Remodelling

5.1 Introduction

Left ventricular remodelling encompasses the progressive changes in geometry (generally LV dilatation and impairment of systolic function) and in cellular and extracellular composition (hypertrophy and fibrosis) which occur in HrEF[66]. Reverse remodelling is the reversal of this process, which can occur with removal of the underlying cause of heart failure, commencement of heart failure therapy, or occasionally spontaneously[67], resulting in improvement or even normalisation of LV geometry and systolic function. The mechanical dyssynchrony and subsequent altered regional myocardial workload, which results from electrical dyssynchrony, can also result in LV remodelling[18, 77] and it is well established that CRT can correct this process and induce reverse remodelling in CRT

responders[81-83]. However, approximately one third of patients do not respond to CRT, for reasons which remain largely unclear[88, 89].

Meanwhile, the energetic theory of heart failure is attracting increasing attention[281]. It has been recognised for decades that myocardial energetics are impaired in HFrEF, with the development and use of ^{31}P-MRS showing both a reduction in the PCr/ATP ratio[273, 275] and more recently a reduction in overall CK flux and ATP delivery[278]. In addition to this, changes in myocardial substrate uptake and usage in HFrEF, with an overall shift towards glucose metabolism, have led to the concept of the failing heart being metabolically inflexible[249]. Whilst these changes were initially thought to result as a consequence of the HFrEF disease process, with changes in substrate usage being adaptive, increasingly they are thought to potentially have a causal role in HFrEF, with the heart being ATP-starved[262, 281].

Linking these fields, there is also increasing evidence that CRT and cardiac metabolism have reciprocal influences, with effective CRT inducing beneficial myocardial metabolic changes[323, 324] and baseline metabolism and flexibility possibly affecting the degree of CRT response[348]. However, the influence of metabolism on CRT response has not yet been fully investigated.

We therefore sort to examine whether either baseline cardiac energetics (as assessed by cardiac ^{31}P-MRS) or acute changes in cardiac metabolic substrate uptake induced by CRT, correlated with reverse remodelling at 6 months.

5.2 Methods

5.2.1 Recruitment

Participants are the same as those presented in Chapter 4, with the addition of 2 participants who took part in the CMR protocol prior to CRT implantation but not in the invasive protocol, who were recruited in the same way. Additionally, one participant from Chapter 4 had subsequent displacement of her LV lead and so was excluded from 6 month follow up.

5.2.1.1 Inclusion Criteria

Inclusion criteria were the same as those listed in Chapter 4.

5.2.1.2 Exclusion Criteria

Exclusion criteria were the same as those listed in Chapter 4. In addition, those participants who took part in the CMR protocol prior to CRT implantation were subject to the following additional exclusion criteria:

- Metal clips or metallic foreign body.
- Prior injury to the eye involving fragments of metal.
- Prior shrapnel injuries.
- Any other metallic or electronic implants affected by the magnetic field.
- History of severe claustrophobia.
- Implanted pacemaker prior to commencement of trial.

5.2.2 Protocol

Prior to CRT implantation, participants had baseline ECG, 6MWT, NYHA class and EQ-5D-3L score recorded, as described in Chapter 2. Seven participants underwent the multi-parametric CMR protocol on Intralipid^{TM} and insulin/dextrose infusions, as set out for the cohort in Chapter 3. Of these 7 participants, 5 participants plus an additional 5 underwent the invasive protocol with PV loop and coronary flow measurements with paired A-V blood sampling, as set out in Chapter 4. For the additional 5 participants who did not have a research CMR scan prior to CRT, baseline LV function was either obtained via echocardiography (using Simpson's biplane measurements) or taken from a clinical CMR scan if available. All participants were followed up 6 months after CMR implantation, with repeat assessment of LV function by CMR (n = 10, as per Chapter 2) or echocardiography (n = 2) and repeat assessment/recording of NYHA class, ECG, 6MWT and EQ-5D-3L score. Follow-up assessments of LV function with CMR were performed with both AOO pacing ('Intrinsic') and DOO with BiV pacing ('BiV') (in a randomised order), with asynchronous pacing set 10 bpm above the participant's intrinsic heart rate to prevent competitive pacing. Only CMR measurements were used for assessment of LV volumes. It was not always possible to obtain full data sets for each participant.

A flow diagram illustrating the overall study protocol is shown in Figure 5.1.

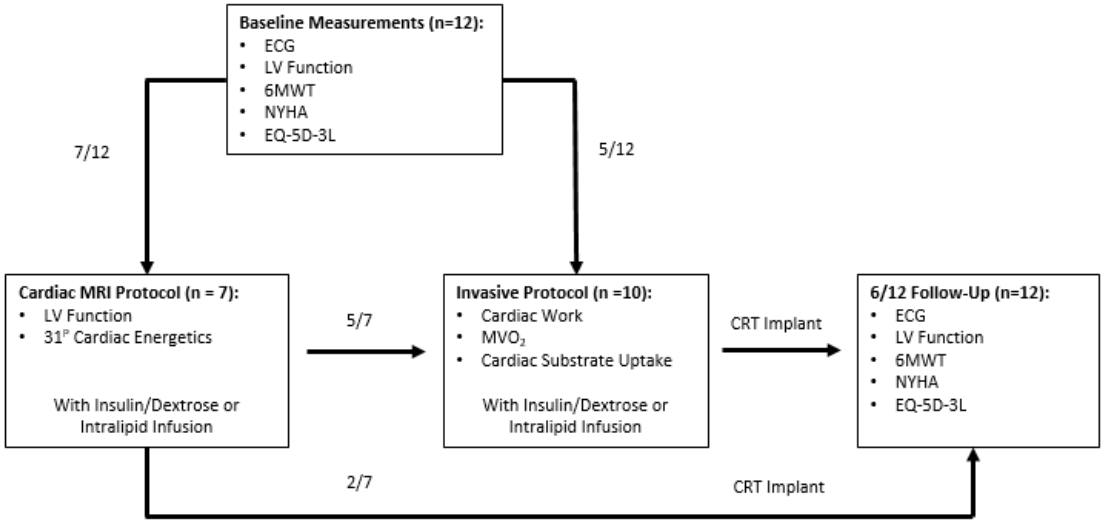

Figure 5.1: *Study flow diagram*

5.3 Results

5.3.1 Baseline Demographics and Clinical Characteristics

In total, twelve participants with non-ischaemic DCM were recruited to the study. Baseline demographics and clinical details are given in Table 5.1. All participants were on optimal heart failure medication, as shown in Table 5.2.

Table 5.1: Baseline demographics and clinical characteristics

Recruited *(n)*	**12**
Age *(years)*	64 [60-71]
Male *(n)*	7
Weight *(kg)*	90.6 [78.6-101.4]
BMI *(kg/m^2)*	30.7 [25.5-34.2]
Hip:Waist Ratio	1.1 [1.0-1.10]
Systolic Blood Pressure *(mmHg)*	119 [110-128]
Diastolic Blood Pressure *(mmHg)*	75 [65-87]
NIDDM *(n)*	2
Hypertension *(n)*	7
Sinus Rhythm *(n)*	12
LBBB *(n)*	12
QRSd *(ms)*	169 [162-183]
LVEF (%)	29 [25-31]
NYHA Class	2 [2-3]

Table 5.2: Cardiac medication at enrolment

ACEi/ARB	12 (100)
β Blocker	10 (83)
ARNi	8 (67)
MRA	9 (75)
SGLT2i	2 (17)
Digoxin	0 (0)
Ivabridine	0 (0)
Loop Diuretic	9 (75)
Amiodarone	1 (8)

Figures as total number and (%)

5.3.2 Reverse Remodelling

Participants were followed up at least 6 months post-CRT implant (219 [206-231] days). There was marked significant reverse remodelling of LV cavity size and function across the cohort, with a 54% reduction in LVEDV and a 38% relative increase in LVEF (using follow up scans with BiV pacing) (Table 5.3, Figure 5.2).

Table 5.3: Baseline and follow-up Left ventricular volumes and function

	Baseline (CMR)	**Follow Up (BiV)**	***p***
LVEDV *(ml)*	276 [258-334]	127 [100-178]	***<0.01***
LVESV *(ml)*	202 [178-221]	80 [49-107]	***<0.01***
LVEF *(%)*	29 [25-31]*	40 [33-50]*	***<0.01***

** Includes 2 results from echocardiographic follow up assessment*

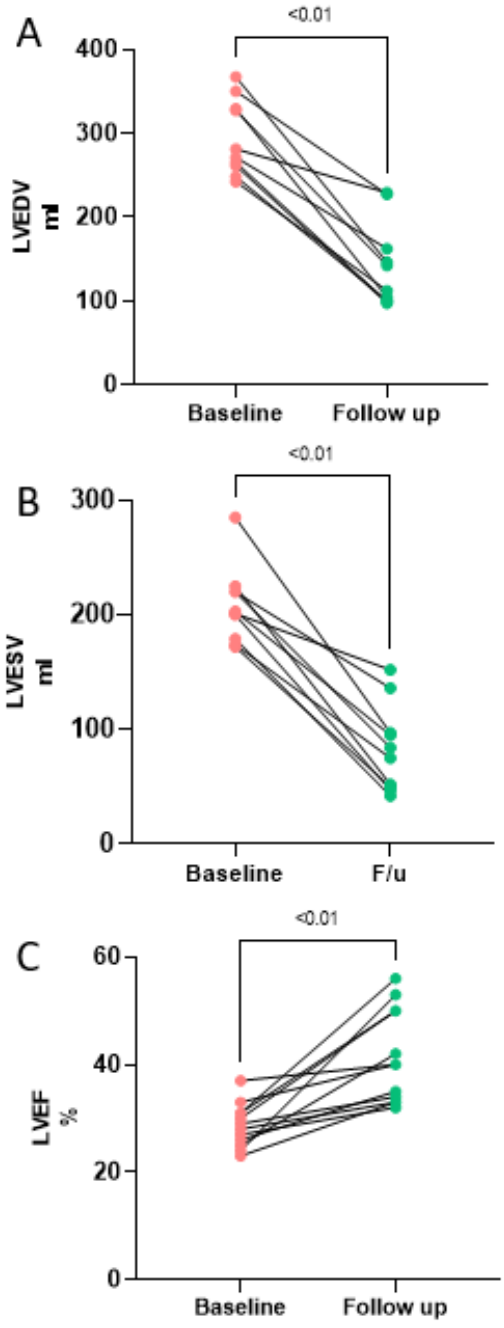

Figure 5.2: *LVEDV (A), LVESV (B) and LVEF (C) at baseline and follow up (with BiV pacing)*

5.3.2.1 Electrical and Volumetric Remodelling

QRS durations were assessed pre-CRT implant ('baseline intrinsic'), at CRT implant with optimised BiV pacing ('baseline BiV') and at follow up with both intrinsic rhythm ('f/u intrinsic') and optimised BV pacing ('f/u BiV'). There was significant intrinsic electrical remodelling, with intrinsic QRSd at follow up significantly shorter than with intrinsic rhythm at baseline. In addition, QRSd with optimised BiV pacing was significantly shorter than with intrinsic rhythm, both at baseline and follow up, but there was no difference between BiV pacing at baseline and at follow up (Table 5.4 and Figure 5.3 for all).

LVEDV at the same time points (invasive PV loop volumes on glucose infusion used at baseline), showed a small significant reduction in volume with acute BiV pacing at baseline, with a much larger reduction at 6 month follow up (Table 5.4 and Figure 5.3). Furthermore, LVEDV was unchanged between intrinsic rhythm and BiV pacing at follow up (Figure 5.3 and 5.4), despite the continuing significant reduction in QRSd. There was also no significant difference in LVESV or LVEF with BiV pacing at follow up (Figure 5.4).

Table 5.4: QRS duration and cardiac volumes at baseline and follow up, with both intrinsic rhythm and BiV pacing

	Baseline (Intrinsic)	**Baseline (BiV)**	**Follow Up (Intrinsic)**	**Follow Up (BiV)**	***p***
QRSd *(ms)*	169 [162-183]	132 [126-144]	164 [150-171]	138 [123-149]	***<0.01***
LVEDV *(ml)*	311 [269-377]	303 [256-355]	137 [102-186]	127 [100-178]	***<0.01***
LVESV *(ml)*	213 [174-231]	181 [158-226]	86 [47-112]	80 [49-107]	***<0.01***

p = mixed effect model across groups

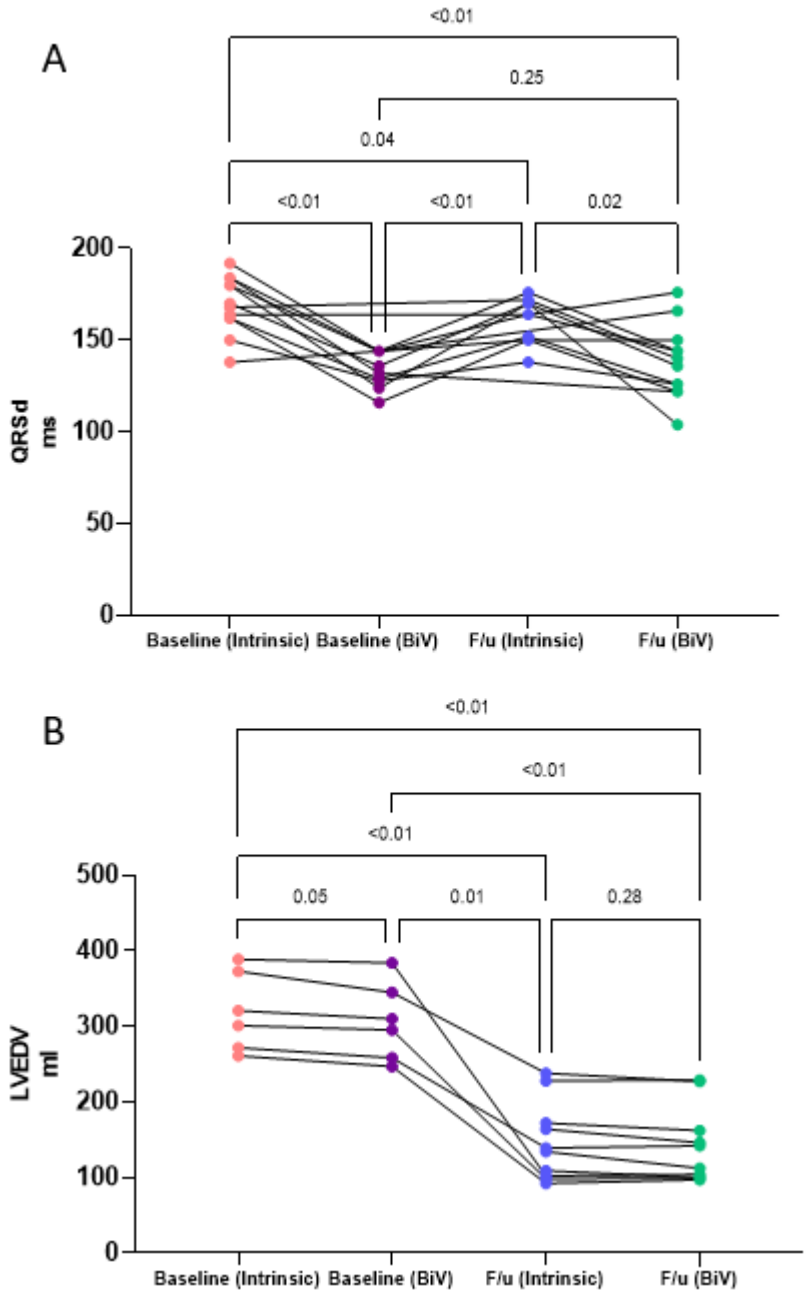

***Figure 5.3**: QRSd (A) and LVEDV (B) at baseline implant and follow up, with intrinsic rhythm and BiV pacing.*

p = mixed effect analysis

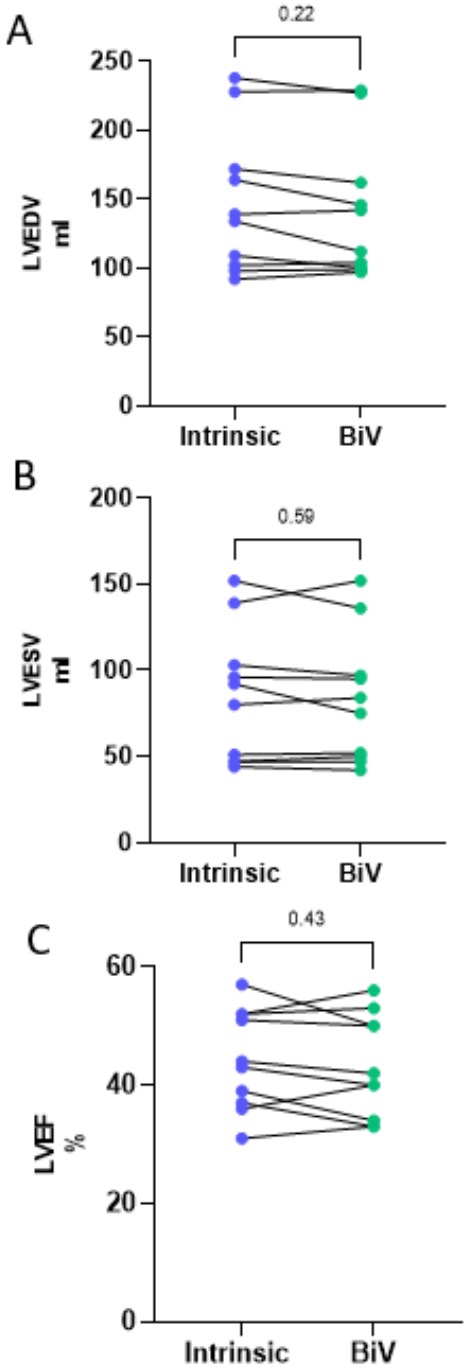

Figure 5.4: *LVEDV (A), LVESV (B) and LVEF (C) at follow up with intrinsic rhythm (AOO) and BiV pacing*

Finally, electrical and volumetric reverse remodelling were also significantly positively correlated, with absolute change in LVEDV correlating with both change in intrinsic QRSd and change in QRSd with BiV pacing (i.e. follow up BiV QRSd minus baseline intrinsic QRSd) at follow up, as shown in Figure 5.5. Although acute change in QRSd with BiV pacing at implant positively correlated with the QRSd change with BiV pacing at follow up (R = 0.88, p = <0.01), it did not correlate with change in LVEDV at follow up (Figure 5.5, available for 7 participants with matched CMR follow up volumes).

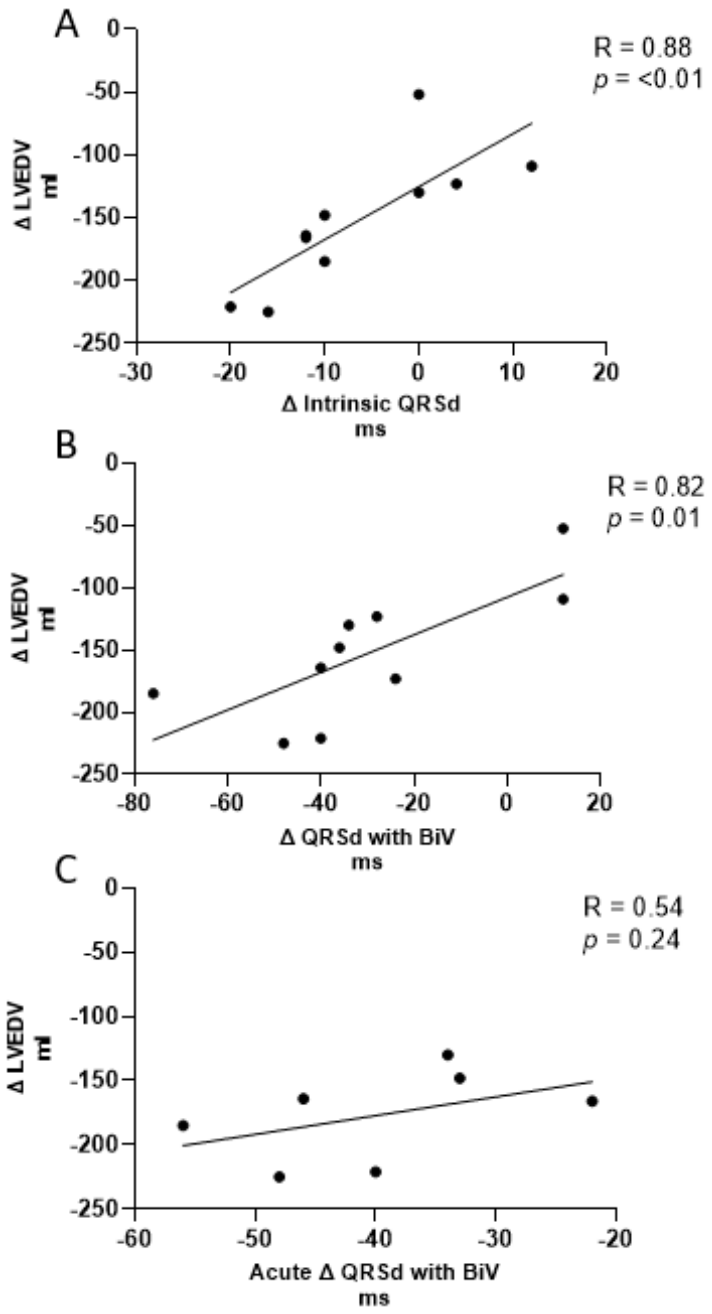

Figure 5.5: *Significant positive correlations between change (Δ) in LVEDV and both Δ intrinsic QRSd (A) and Δ QRSd with BiV pacing (B) at follow up. No significant correlation between acute Δ QRSd with BiV at implant and Δ LVEDV at follow up (C)*

5.3.2.2 Functional/Symptomatic Improvement

There was significant functional/symptomatic improvement at follow up, with increased 6MWT distance and increased EQ-5D visual analogue scale (VAS) score (a participant's self-rating of overall health on a scale of 0-100 – see Appendix) (Table 5.5). In 42% of participants there was also an improvement by at least 1 NYHA class. There was also a decrease in level at which participants scored themselves for each of the 5 categories of the EQ-5D-3L (Table 5.6).

Table 5.5: Functional/symptomatic assessment at start and follow up

	Start	**Follow Up**	***p***
6MWT	402 [345-443]	413 [399-480]	***0.02***
EQ-5D VAS score	72.5 [61.3-78.8]	80.0 [72.5-93.8]	***0.02***

Table 5.6: EQ-5D-3L results, showing *n* (%) at each level for each category, at the start and at follow up

	Mobility		**Self-Care**		**Usual Activities**		**Pain/ Discomfort**		**Anxiety/ Depression**	
	Start	F/u	Start	F/u	Start	F/u	Start	F/u	Start	F/u
Level 1	4 (33)	7 (58)	11 (92)	12 (100)	5 (42)	10 (83)	4 (33)	7 (58)	10 (83)	12 (100)
Level 2	8 (67)	5 (42)	0 (0)	0 (0)	7 (58)	2 (17)	8 (67)	5 (42)	2 (17)	0 (0)
Level 3	0 (0)	0 (0)	1 (8)	0 (0)	0 (0)	0 (0)	0 (0)	0 (0)	0 (0)	0 (0)

Level 1 = no problems; Level 2 = some problems; Level 3 = extreme problems

5.3.3 Correlations of Baseline Energetics with Reverse Remodelling

Cardiac work derived during CMR and cardiac energetics pre-CRT implant are given in Table 5.7.

Table 5.7: Baseline cardiac work and energetics

	Glucose Infusion	**FFA Infusion**	***p***
Cardiac Work *(L.mmHg/min)*	496 [429-544]	556 [496-701]	*0.06*
PCr/ATP	1.93 [1.58-2.04]	1.99 [1.66-2.49]	***0.03***
Rest k_f *(s^{-1})*	0.193 [0.106-0.324]	0.265 [0.093-0.364]	*>0.99*
Rest CK Flux *(µmol (g wet weight)$^{-1}$ s^{-1})*	2.05 [1.08-2.55]	2.28 [1.10-3.74]	*0.81*
Stress PCR/ATP*	1.82 [1.54-2.32]	1.94 [1.37-2.34]	*>0.99*
Stress k_f *(s^{-1})*	0.370 [0.173-0.926]	0.179 [0.100-0.616]	*0.50*
Stress CK Flux *(µmol (g wet weight)$^{-1}$ s^{-1})*	4.02 [1.54-7.64]	1.30 [1.28-6.24]	*0.50*

**PCR/y-ATP*

Whilst there were no apparent significant correlations between standard baseline cardiac energetics and LV reverse remodelling (Table 5.8, Figure 5.6), the small numbers of participants are insufficient to allow a conclusion to be drawn as to whether there are any significant correlations or not.

Table 5.8: Correlations between baseline energetics and reverse remodelling

		Δ LVEDV at Follow Up		Δ LVEF at Follow Up	
		R	***p***	**R**	***p***
Glucose Infusion	**PCr/ATP**	-0.32	*0.50*	0.29	*0.54*
	Rest k_f *(s^{-1})*	0.50	*0.45*	0.20	*0.78*
	Rest CK Flux *(µmol (g wet weight)$^{-1}$ s^{-1})*	0.30	*0.68*	0.50	*0.45*
	Stress PCR/ATP	0.00	*>0.99*	-0.30	*0.68*
	Stress k_f *(s^{-1})*	-0.60	*0.42*	0.80	*0.33*
	Stress CK Flux *(µmol (g wet weight)$^{-1}$ s^{-1})*	-0.10	*0.95*	0.10	*0.95*
	Δ k_f on stress *(s^{-1})*	-0.60	*0.35*	-0.10	*0.95*
	Δ CK Flux on stress *(µmol (g wet weight)$^{-1}$ s^{-1})*	-0.20	*0.78*	-0.30	*0.68*
FFA Infusion	**PCr/ATP**	-0.39	*0.40*	-0.04	*0.95*
	Rest k_f *(s^{-1})*	0.10	*0.95*	-0.70	*0.23*
	Rest CK Flux *(µmol (g wet weight)$^{-1}$ s^{-1})*	0.10	*0.95*	-0.70	*0.23*
	Stress PCR/ATP	-0.43	*0.42*	-0.14	*0.80*
	Stress k_f *(s^{-1})*	0.50	*>0.99*	-0.50	*>0.99*
	Stress CK Flux *(µmol (g wet weight)$^{-1}$ s^{-1})*	-0.50	*>0.99*	0.50	*>0.99*
	Δ k_f on stress *(s^{-1})*	-0.50	*>0.99*	0.50	*>0.99*
	Δ CK Flux on stress *(µmol (g wet weight)$^{-1}$ s^{-1})*	-0.50	*>0.99*	0.50	*>0.99*

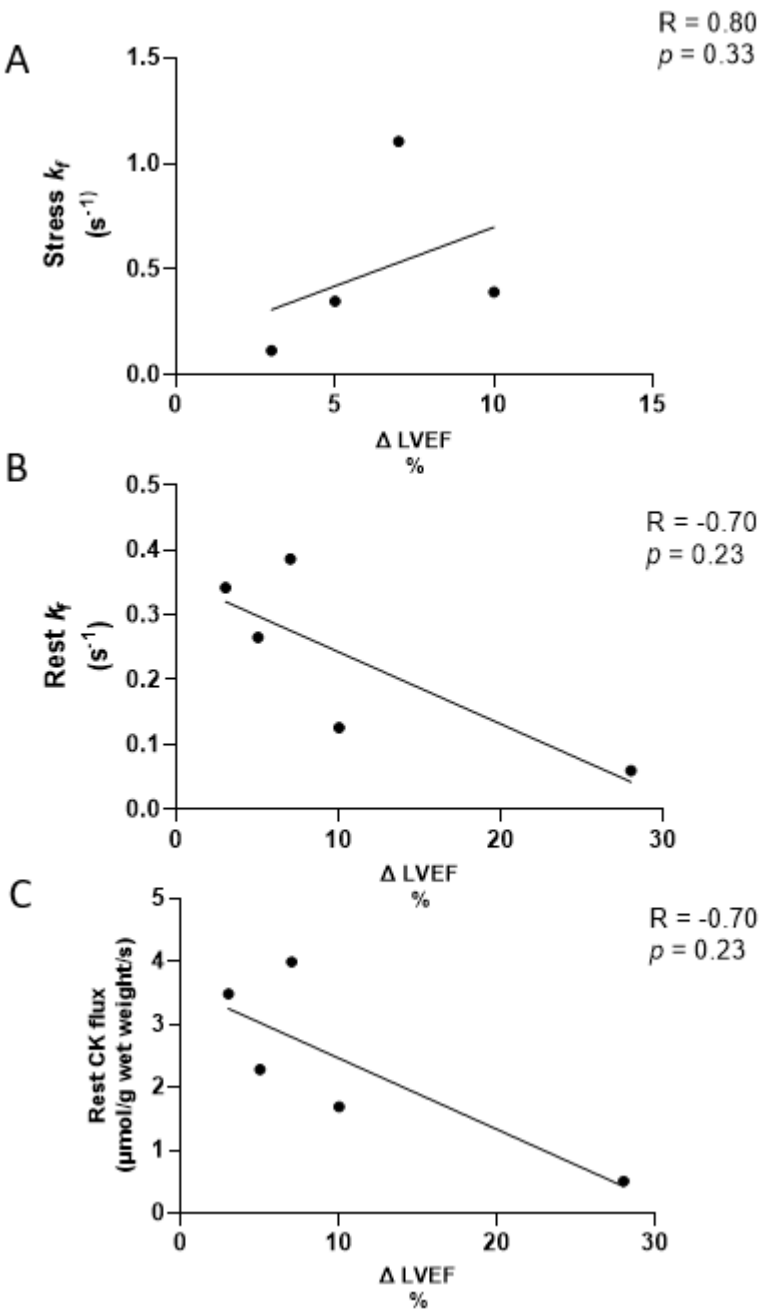

Figure 5.6: *Correlations between stress k_f during glucose infusion (A) and rest k_f (B) and CK flux (C) during FFA infusion, and change in LVEF at follow up. The n numbers are insufficient to draw a conclusion as to whether there is a significant correlation or not*

However, there was a significant positive correlation between CMR derived cardiac work / CK flux at rest (i.e. 'efficiency' as defined by ATP supply) during glucose infusion, with change in LVEF at follow up (Figure 5.7).

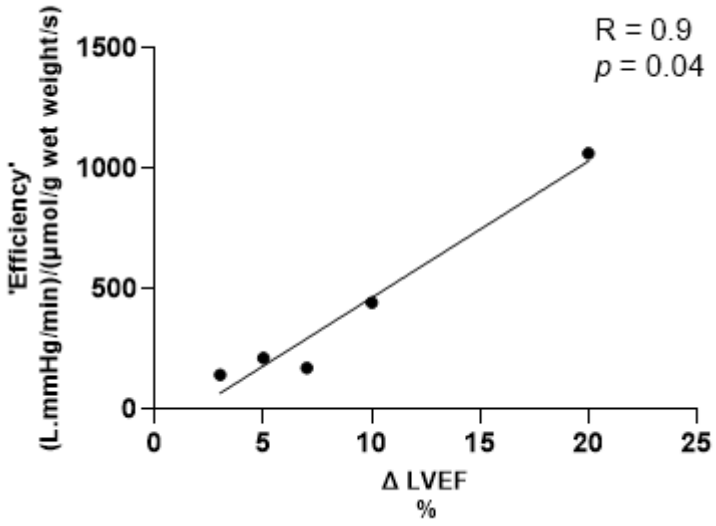

Figure 5.7: *Positive correlation between CMR derived cardiac work / CK flux at rest during glucose infusion and change in LVEF at follow up*

5.3.4 Correlations of Invasive Measurements at Implant with Reverse Remodelling

The acute change with CRT in both stroke work and cardiac work measured at implant significantly negatively correlated with the change in LVEDV at follow up, at both rest and stress and during both glucose and FFA infusions (Figure 5.8). There were no significant correlations with LVEF at follow up.

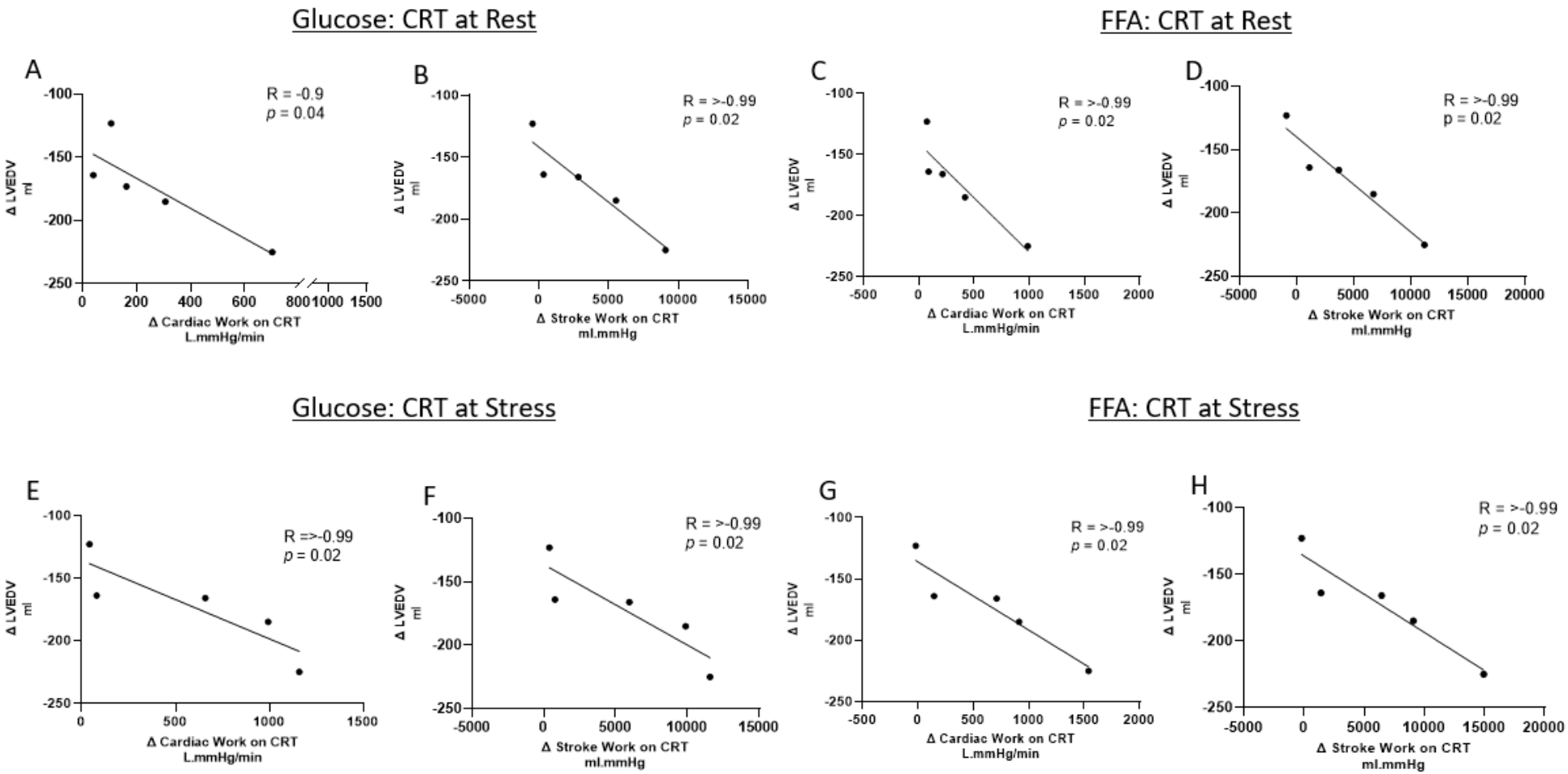

Figure 5.8: *Significant negative correlations between change (Δ) in LVEDV at follow up and acute change in cardiac work and stroke work with CRT at rest during glucose infusion (A+B respectively) and FFA infusion (C+D); and with CRT at stress during glucose infusion (E+F) and FFA infusion (G+H)*

There was a significant negative correlation between change in cardiac FFA uptake with CRT at rest during glucose infusion and change in LVEDV at 6 months (Figure 5.9). In addition, there was a significant negative correlation between change in cardiac BOHB uptake with CRT at rest during FFA infusion and change in LVEDV at follow up (Figure 5.10). There were no significant correlations with LVEF at follow up and no correlations with changes in other substrate uptake. Cardiac efficiency (cardiac work / MVO_2) at implant did not correlate with LVEDV at follow up (Glucose (Rest): R = -0.50, *p* = 0.45; Glucose (Stress): R = -0.50, *p* = 0.45; FFA (Rest): R = -0.01, *p* = 0.95; FFA (Stress): R = -0.50, *p* = 0.45).

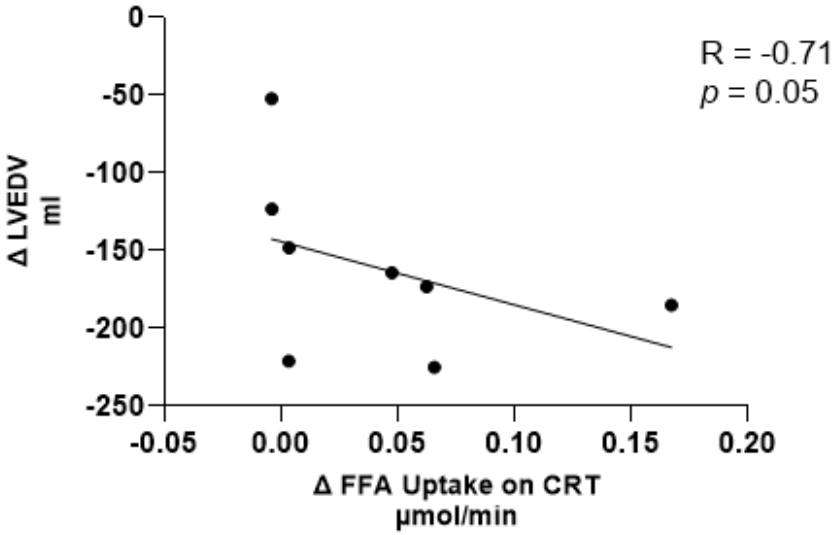

Figure 5.9: *Change in cardiac FFA uptake at rest during glucose infusion significantly negatively correlates with change in LVEDV at follow up*

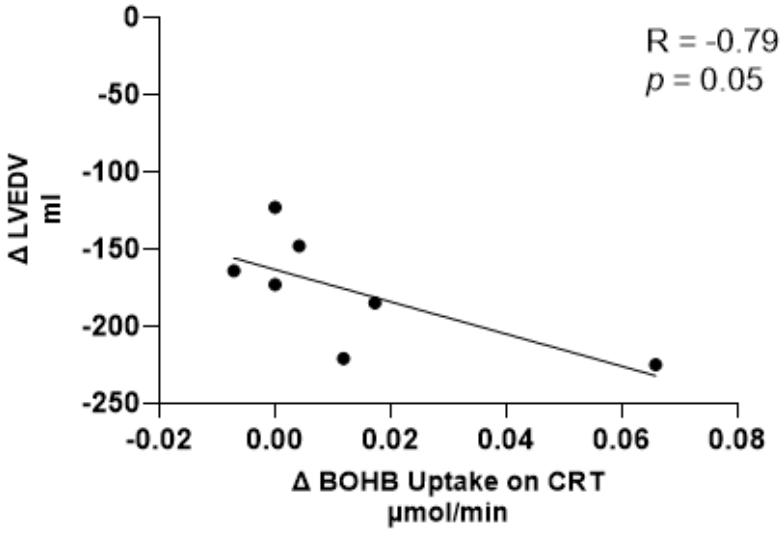

Figure 5.10: *Change in cardiac BOHB uptake at rest during FFA infusion significantly negatively correlates with change in LVEDV at follow up*

5.4 Discussion

The main findings of this chapter are:

1. CRT induced significant electrical and geometric reverse remodelling at 6 month follow up beyond that achievable via acutely changing QRSd.
2. Whilst baseline cardiac energetics assessed by ^{31}P-MRS (PCR/ATP, k_f and CK flux) did not correlate with reverse remodelling, CMR derived measures of cardiac efficiency did.
3. Acute changes in stroke work and cardiac work with CRT at implant correlated with reverse remodelling (as defined by reduction in LVEDV).

4. Change in cardiac FFA uptake with CRT correlated with reverse remodelling, while change in BOHB uptake when FFA uptake was maximised on a FFA infusion correlated with reverse remodelling.

Overall, in DCM those hearts that are more efficient and able to increase FFA uptake and improve cardiac work with CRT are more likely to undergo significant reverse remodelling.

5.4.1 Reverse Remodelling

Both improvement in LVEF and reduction in LVEDV have commonly been used to define reverse remodelling[68]. Our use of absolute reduction in LVEDV and improvement in LVEF to assess the degree of reverse remodelling is in line with a number of CRT trials, which have similarly used LVEF and measurements of LV size (relative or absolute reduction in LVEDV, LV end-diastolic dimension (LVEDd), LVESV or LVESV index) to assess reverse remodelling[40, 42, 92, 385-388]. In particular, the MADIT-CRT[42] and MIRACLE[386] studies utilised absolute reduction in LVEDV as one of their outcome measures. The degree of reverse remodelling in our cohort is generally greater than that which has been found in these trials, with a 54% reduction in LVEDV vs (for example) approximately a 10-20% reduction in MADIT-CRT and MIRACLE. There was also a 38% relative (11% absolute) improvement in LVEF, which was greater than in MIRACLE (15% relative) but similar to MADIT-CRT (45% relative and 11% absolute), although this was at 1 year follow up rather than 6 months as in our study.

One explanation for this may be due to participant demographics, with all of the participants in our study having a non-ischaemic aetiology of heart failure and LBBB, both of which are

associated with improved CRT response rates[127, 131]. However, it should also be noted that these historical trials used echocardiography to assess reverse remodelling. Cardiac MRI is now recognized as the gold standard for assessment of cardiac volumes and systolic function[389], with echocardiography underestimating volumes and LVEF[390]. The advent of MRI-conditional CRT devices has therefore allowed us to use CMR at follow up to calculate both LV volumes and LVEF, which would be expected to give a more accurate assessment of reverse remodelling. We believe that this is the first study to assess reverse remodelling following CRT using CMR.

In addition to this, all our participants had Boston CRT devices implanted, which were unique (until the recent release of the Gallant™ CRT-D devices by Abbott) in allowing BiV pacing during MRI-safe mode. Use of BiV pacing during CMR scanning has been shown to result in a higher measured LVEF and smaller LV volumes as opposed to intrinsic rhythm (with AOO pacing)[391], although the deterioration in LVEF values with intrinsic rhythm is not to pre-CRT levels. Therefore, use of BiV pacing during follow-up assessment likely allowed a more accurate assessment of reverse remodelling than if scanning during intrinsic rhythm alone had been used, although no significant differences between pacing settings were found in our participants.

Our finding of electrical reverse remodelling in response to CRT, with significant shortening of intrinsic QRSd, is in keeping with previous studies[392-394]. However, an immediate deterioration in LVEDV and LVEF is not seen in going from BiV pacing to intrinsic rhythm at 6 month follow up, despite BiV paced QRSd still being significantly shorter than with intrinsic rhythm. Conversely, shortening of the QRSd with BiV pacing at implant only led to a modest reduction in LVEDV. Together, these suggest that while acute narrowing of QRSd is

responsible for initiating reverse remodelling, by 6 months significant cellular and extra-cellular reverse remodelling with structural changes have occurred, beyond the acute improvements seen by improvement of QRSd alone. Whilst the lack of acute change in LV volumes and LVEF with BiV pacing at follow up is contrary to some other studies[391, 395], it could be hypothesised that this is in part due to the large degree of chronic reverse remodelling seen in our cohort, with electrical resynchronisation therefore playing less of an acute role. In this case, at least at follow up, CRT could be seen to be simply maintaining reverse remodelling. This would correlate with the gradual decline in LV function which has been demonstrated when CRT is discontinued in super-responders[396, 397], albeit with variable results in terms of LVEDV deterioration. This is the first study to use both PV loop catheter measurements at CRT implant and CMR measurements at follow up to attempt to differentiate and quantify the acute and chronic changes in QRSd and LV volumes which are associated with reverse remodelling.

Finally, the degree of improvement in acute haemodynamics is known to predict long term response to CRT[57, 62, 63]. Our finding that acute improvements in cardiac work and stroke work correlate with degree of reduction in LVEDV is therefore in keeping with this.

5.4.2 Acute Cardiac Substrate Uptake and Reverse Remodelling

Our finding that changes in acute cardiac substrate uptake with commencement of CRT correlated with the change in LVEDV at follow up is interesting, particularly as it is similar to the changes seen acutely which were discussed in Chapter 4. In that Chapter, we showed that cardiac uptake of FFA was acutely increased by commencement of CRT at rest during

glucose infusion and that this correlated with the improvement in markers of systolic function. Here, it is again the increase in uptake of FFA with commencement of CRT during glucose infusion which significantly positively correlated with the improvement in LVEDV at follow up. Similarly, it was the increase in BOHB uptake with commencement of CRT on a FFA infusion (when FFA uptake was likely maximised) which was shown to correlate with acute improvements in cardiac work and it is again this which correlated with improvements in LVEDV at follow up.

These results therefore add to the initial conclusions of Chapter 4, that CRT increases cardiac FFA uptake at rest or, if this is already maximised, increases BOHB uptake instead. As previously discussed, although FA oxidation is less oxygen efficient[226], this is likely to be outweighed by the increased ATP generation per mole of FA[247]. In addition, BOHB metabolism has been shown to be associated with improved cardiac function in heart failure[292]. If the failing heart is indeed ATP starved, then it can be hypothesised that any significant reverse remodelling must be dependent upon an ability to first increase or improve the ATP supply, or the efficiency of ATP use. As the ability of CRT to acutely increase the cardiac uptake of FFA and BOHB demonstrates a degree of preserved metabolic flexibility (and indeed, metabolic preference), and substrate oxidation is linked directly to ATP production, it would therefore be logical that this would correlate with the degree of reverse remodelling.

A recent study by Martens *et al.*[349] has similarly shown a potential switch to FA oxidation at 6 months post-CRT, as assessed with peripheral blood samples, and that this is associated with improved mitochondrial function as assessed by ^{99}Technetium-sestamibi scanning. Whilst a previous study by Obrzut *et al.*[348] suggested that increased cardiac FFA uptake in a non-ischaemic cardiomyopathy cohort was associated with poorer response to CRT, it should be

emphasised that this study assessed baseline (i.e. pre-existing) uptake rather than changes in uptake in response to CRT. It is therefore plausible that a higher pre-existing cardiac FFA uptake would mean that the heart is less able to increase uptake in response to CRT and so less able to reverse remodel. Indeed, this has been hypothesised by Antoniou *et al.*[323].

5.4.3 Baseline Cardiac Energetics

Due to the lengthy and complex nature of the protocol, the number of participants in the CMR arm of the study prior to CRT was unfortunately few, which limits the strength of any conclusions which can be drawn about correlations between energetics and reverse remodelling. However, it is interesting that there was a significant positive correlation between energetic efficiency (cardiac work / CK flux) and change in LVEF at follow up. Energetic efficiency in this manner should be differentiated from oxygen efficiency (cardiac work / MVO^2, commonly used when referring to 'cardiac efficiency') and the mechanical efficiency of the coupling of cardiac contraction to ejection. Although there was no correlation between degree of reverse remodelling and oxygen efficiency as measured at implant, this may in fact be logical given the limitations of the use of oxygen efficiency as a metric, as discussed in Chapter 4. If the heart is not oxygen limited in a non-ischaemic cardiomyopathy, then oxygen efficiency might be expected not to significantly influence reverse remodelling. However, energetic efficiency as determined by ATP supply and use might be expected to influence remodelling if ATP supply is a limiting factor on cardiac function, as has previously been hypothesised by our group (unpublished). It is likely that further studies with larger

numbers are required to see if this correlation is reproducible and if any other correlations emerge.

5.5 Limitations

As discussed above, the numbers involved in this study were low. However, we believe that the combination of investigations carried out in the same cohort is unique, and that the correlations shown are thought provoking and merit further investigation.

All follow up CMR scans were carried out with pacing at 10 bpm above intrinsic heart rate to ensure lack of competition. They therefore may have been at a higher heart rate than baseline scans, but it is unlikely that this degree of difference in rate significantly influenced results. In addition, BiV pacing in MRI-safe mode in the Boston models implanted in our participants is carried out with a non-programmable fixed AVD (100 ms) and no VVD. It therefore does not represent optimised BiV pacing. However, no manufacturer currently allows programmable offsets in MRI-safe mode. In addition, there was no significant difference in QRSd between optimised BiV pacing and MRI-safe mode BiV pacing in our cohort ($p = 0.11$).

5.6 Summary

This chapter confirms that CRT induces significant electrical and volumetric reverse remodelling beyond that achieved by acutely changing the QRSd and is the first study to do so using CMR, including BiV pacing during follow up scanning. This reverse remodelling correlates with acute haemodynamic improvement in response to CRT. This chapter also suggests that the acute changes in cardiac substrate uptake seen in response to CRT, namely increased FFA uptake or increased BOHB uptake when FFA uptake is maximised, are positively correlated with the degree of reverse remodelling.

Chapter 6:

Influence and Effectiveness of Fusion Pacing During Exercise

6.1 Introduction

Cardiac resynchronisation therapy provides electrical and mechanical resynchronisation in HFrEF with a widened QRSd, improving morbidity and mortality[21], with the degree of QRSd narrowing correlating with degree of response[101-103]. However, achieving maximal electrical resynchronisation via optimised CRT entails more than a simple 'on or off' function of BiV pacing. Selection of appropriate CRT algorithms along with optimised individual programming are key to maximising response.

Fusion pacing in CRT utilises timing of the LV pacing impulse to allow fusion of its wave-front with intrinsic conduction +/- the wave-front from RV pacing[176, 205]. For this to occur effectively requires sinus rhythm and relatively preserved intrinsic AV conduction, as well as optimisation of the AVD to allow LV pacing to time correctly with either an atrial sensed or paced impulse. Manufacturer specific algorithms therefore allow dynamic assessment of intrinsic AV

conduction, with subsequent adjustment of the AVD. One such algorithm is SyncAV™ (Abbott), which measures intrinsic conduction on the third of 3 intrinsic beats which are conducted every 256 beats. A delta offset (adjustable but nominally -50 ms) is then programmed, with the AVD being intrinsic conduction minus the delta.

However, it is unknown to what extent SyncAV™ is able to maintain fusion pacing during exercise and whether this could therefore influence exercise capacity. Intrinsic AV conduction commonly changes with exercise, normally shortening with increasing HR[172], but importantly there is evidence that in heart failure patients increasing HR can result in a greater degree of shortening than in normal controls[195] or conversely even in lengthening of conduction[221]. This lack of uniform response combined with the subtraction of a fixed delta could result in loss of fusion during exercise and so lack of effective CRT.

Cardio-pulmonary exercise testing is an established method of measuring exercise capacity via measurement of ventilation, oxygen consumption ($\dot{V}O_2$) and carbon dioxide production, including in the heart failure population[398, 399]. Calculation of peak oxygen consumption on exercise (peak $\dot{V}O_2$, or $\dot{V}O_2^{PEAK}$), first and second ventilatory thresholds (VT1 and VT2), peak respiratory exchange ratio (RER) and other CPET variables such as blood lactate level allows an objective assessment of the anaerobic threshold and peak exercise capacity to be made. Furthermore, the combination of heart rate and oxygen uptake (O_2 pulse) provides a surrogate marker for stroke volume. In addition, the BORG rating of perceived exertion (RPE) scale is a recognised method by which patients can report perceived exercise intensity[372, 373]. In the heart failure population, quality of life and exercise capacity are inextricably linked, making CPET combined with subjective symptom reporting an ideal method to assess this and CRT is known to improved exercise capacity in responders, as assessed by CPET[400, 401].

In order to assess whether fusion pacing is maintained on exercise and whether this influences exercise capacity, we therefore used CPET with 12 lead ECG monitoring to compare the SyncAV™ algorithm to conventional BiV pacing, in a double-blinded randomised crossover study.

6.2 Methods

6.2.1 Recruitment

Participants were recruited from those with a suitable CRT device under current follow up in the cardiac devices clinic at Oxford University Hospitals NHS Foundation Trust.

6.2.1.1 Inclusion Criteria

- Age ≥18 and able to give informed consent.
- Existing CRT devices able to utilise the SyncAV™ algorithm, implanted ≥6 months and under follow up at Oxford University Hospitals NHS Foundation Trust.
- Evidence of response to CRT, defined as functional improvement or LV remodelling on imaging within the last 1 year or at least 6 months post-CRT implant.
- Sinus rhythm and PR interval <250 ms.
- Able to exercise to perform CPET.

6.2.1.2 Exclusion Criteria

- Pregnancy or breast feeding.
- Atrial fibrillation or atrial tachycardia.
- Underlying 2nd or 3rd degree heart block.

- PR interval ≥250 ms.
- Chronotropic incompetence, defined as use of a rate-response algorithm or ≥80% atrial pacing.
- Any concurrent condition contraindicating use of CPET.

6.2.2 Protocol

All recruited participants underwent 2 visits. At the first visit, they underwent optimisation of CRT programming other than the AVD. In brief, Q-LV was first tested on each pole, with the pole with the longest Q-LV used for all subsequent testing unless there was phrenic nerve stimulation near the threshold, in which case next-best Q-LVs were used sequentially instead. AVDs were set to 120/120 ms as this previously been shown to be non-inferior to a fusion-based AV optimisation algorithm at rest in the SmartAV study[194]. For VV optimisation the VVD (i.e. delay between RV and LV pacing) was altered in 10 ms intervals to achieve the narrowest QRSd. Other settings (e.g. multipoint pacing in n = 1) were left unchanged from pre-existing settings. Participants were then randomised to either fixed AVD or SyncAV™. For the fixed AVD setting, AVDs were also set to 120/120 ms unless there was evidence of fusion, in which case they were shortened in 10 ms intervals until there was no fusion (n = 1). For the SyncAV™ setting, the delta was adjusted in 10 ms intervals to give the narrowest QRSd.

Participants then underwent CPET testing with 12 lead ECG monitoring at each visit, as per Chapter 2, section 2.7, whilst programmed with either fixed AVD or SyncAV™. A standard 15W step protocol was used and venous blood was withdrawn from a cannula at baseline, end of 15W stage, peak exercise and after 15 minutes of a recovery stage, to measure lactate

concentration. Participants also indicated their BORG-RPE rating at the end of each stage. Tests were terminated at participants' request at perceived maximal exercise. Participants crossed over to perform CPET at the other setting at the second visit, with visits carried out at least 1 week apart. At the end of both visits 1 and 2 CRT settings were reset to the participant's pre-existing, baseline, settings and so changes to programming were only for the duration of each CPET. Cardiopulmonary exercise test operators and participants were blinded to randomisation.

A power calculation estimated a sample size of 18 participants, assuming an alpha-value of 0.05 and a beta-value of 0.8, for an estimated difference in mean QRSd between groups of 10 ms and a standard deviation of 15 ms and with paired samples. To allow for a 10% drop-out rate, we aimed to recruit 20 participants.

A summary flow diagram of the study is given in Figure 6.1.

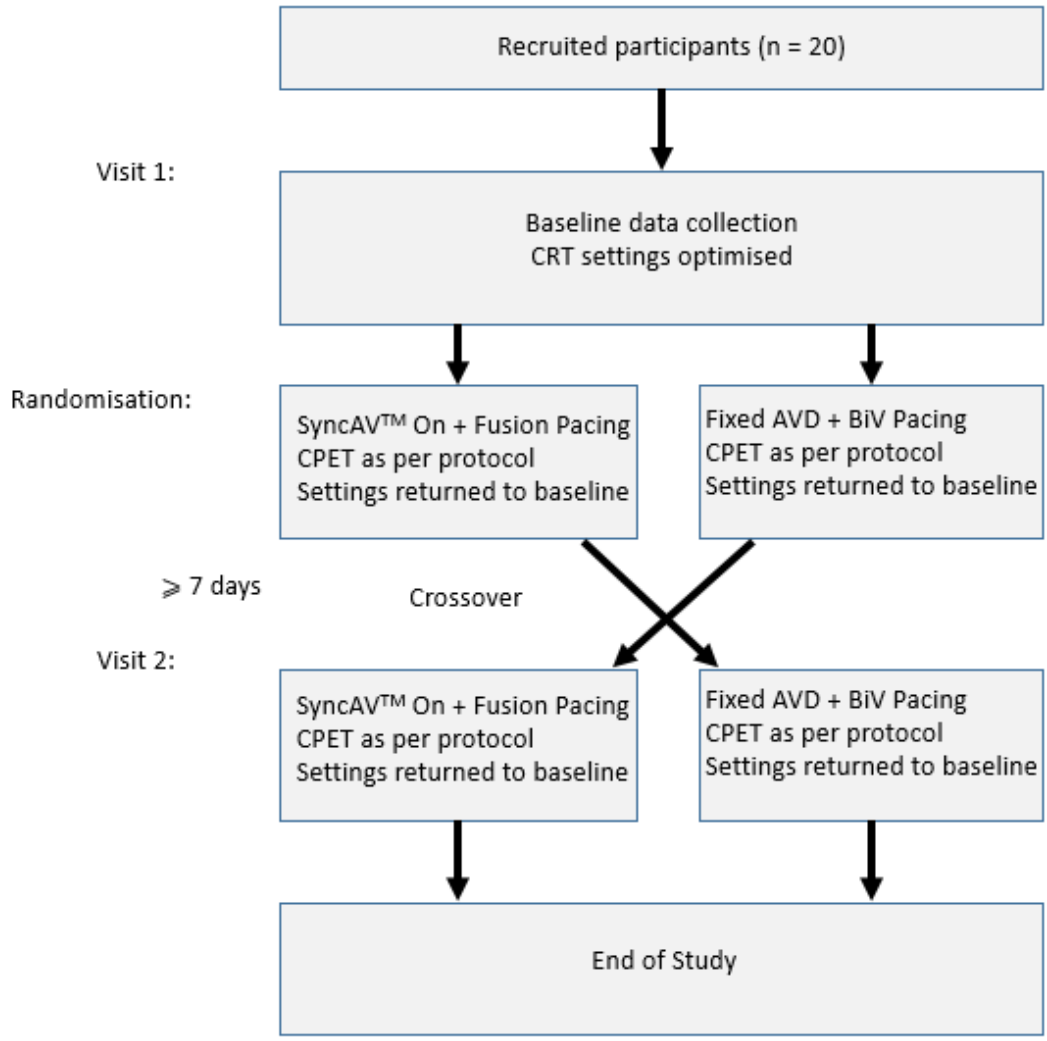

Figure 6.1: *Study Protocol*

6.3 Results

6.3.1 Baseline Demographics and Clinical Characteristics

Twenty participants were recruited in total, all with either a Quadra Allure™ or Quadra Assura™ CRT device and with an average of approximately 2 years since CRT implantation.

Baseline demographics and clinical details are given in Table 6.1. All were well optimised on standard heart failure medication (Table 6.2).

Table 6.1: Cohort baseline demographics and clinical characteristics

Recruited *(n)*		**20**
Age *(years)*		71 [65-77]
Male *(n)*		11
Weight *(kg)*		90.1 [80.5-99.2]
BMI *(kg/m^2)*		31.8 [27.3-36.2]
NIDDM *(n)*		9
HF Aetiology	Ischaemic *(n)*	5
	Non-ischaemic *(n)*	12
	Mixed *(n)*	3
Time from Diagnosis *(years)*		5 [2.3-14.5]
Time from CRT Implant *(days)*		724 [471-1331]
Intrinsic QRSd *(ms)*		162 [144-181]
Intrinsic PR *(ms)*		172 [160-200]

Table 6.2: Cardiac medication at enrolment

ACEi/ARB	20 (100)
β Blocker	20 (100)
ARNi	4 (20)
MRA	13 (65)
SGLT2i	3 (15)
Digoxin	0 (0)
Ivabridine	0 (0)
ISMO	1 (5)
Alpha blocker	1 (5)
Loop Diuretic	5 (25)

Figures as n (%)

In addition, all participants had evidence of either symptomatic improvement since CRT implant, or LV reverse remodelling with an increase in LVEF and decrease in LV internal diameter in diastole (LVIDd), as set out in Table 6.3.

Table 6.3: Reverse remodelling or improvement in NYHA class since CRT implant

	Pre-CRT	**Post-CRT**	***p***
LVEF *(%)*	31 [23-35]	44 [36-50]	***<0.01***
LVIDd *(cm)*	5.6 [5.3-6.5]	5.3 [4.4-5.6]	***<0.01***
NYHA Class	3 [2-3]	2 [1-2]	***<0.01***

6.3.2 Comparison Between Fixed AVD and SyncAV™

The median SyncAV™ delta used was -50 [IQR -50 to -40] ms, with a range of -30 to -80ms.

6.3.2.1 CPET Results

There was no difference between fixed AVD settings and SyncAV™ in terms of any CPET outcome (Table 6.4, Figure 6.2). There was no difference in $\dot{V}O_2$ at peak exercise ($\dot{V}O_2^{PEAK}$), VT1 ($\dot{V}O_2^{VT1}$) or VT2 ($\dot{V}O_2^{VT2}$), or in the time to reach either $\dot{V}O_2^{PEAK}$ or VT1. O_2 pulse was also not difference at peak (O_2 $Pulse^{PEAK}$), VT1 (O_2 $Pulse^{VT1}$) or VT2 (O_2 $Pulse^{VT2}$). Finally, there was no difference in RER at peak (RER^{PEAK}) or in efficiency at peak (peak work / $\dot{V}O_2^{PEAK}$).

Table 6.4: Comparison of CPET measurements between Fixed AVD and SyncAV^{TM} groups

	Fixed AVD	**SyncAV^{TM}**	***p***
$\dot{V}O_2^{PEAK}$ *(ml/kg/min)*	14.91 [12.61-18.16]	15.61 [12.18-19.70]	*0.19*
$\dot{V}O_2^{VT1}$ *(ml/kg/min)*	7.36 [6.93-8.94]	7.87 [6.77-9.24]	*0.42*
$\dot{V}O_2^{VT2}$ *(ml/kg/min)*	11.92 [10.61-14.97]	11.43 [10.50-16.17]	*0.71*
O_2 Pulse^{PEAK} *(ml/beat)*	12 [10-13]	12 [10-14]	*0.67*
O_2 Pulse^{VT1} *(ml/beat)*	9 [7-9]	8 [7-10]	*0.81*
O_2 Pulse^{VT2} *(ml/beat)*	12 [9-13]	11 [9-14]	*0.88*
Time to $\dot{V}O_2^{PEAK}$ *(secs)*	1241 [1096-1637]	1267 [1041-1730]	*0.81*
Time to VT1 *(secs)*	473 [326-621]	538 [311-753]	*0.39*
Work Rate^{PEAK} *(watts)*	75 [64-116]	90 [60-116]	*0.99*
RER^{PEAK}	1.03 [0.99-1.08]	1.03 [0.97-1.11]	*>0.99*
Efficiency^{PEAK} (*watts/ml/kg/min)*	5.59 [4.47-6.21]	5.25 [4.76-6.05]	*0.41*
BORG-RPE at median stage	11 [10-13]	11 [9-12]	*0.61*
BORG-RPE at peak	19 [17-19]	18 [17-19]	*0.06*
HR at median stage *(bpm)*	92 [83-98]	89 [84-98]	*0.79*
HR at peak *(bpm)*	119 [102-134]	110 [102-142]	*0.51*
HR Recovery *(bpm)*	10.2 [5.9-13.6]	9.9 [6.9-17.2]	*0.14*

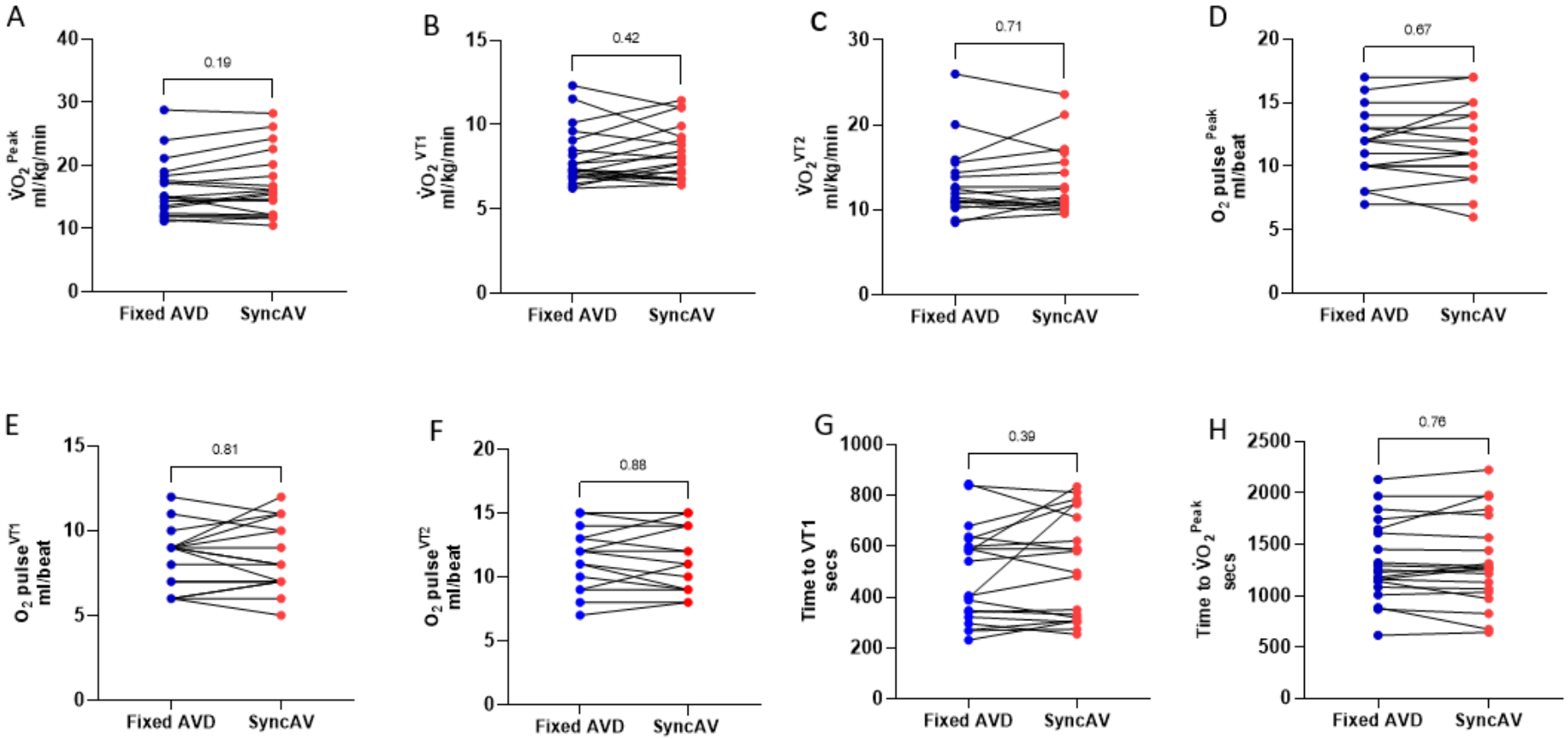

Figure 6.2: *Comparisons of CPET results between fixed AVD and SyncAV™ settings, showing: $\dot{V}O_2^{PEAK}$ (A), $\dot{V}O_2^{VT1}$ (B), $\dot{V}O_2^{VT2}$ (C), O_2 Pulse^{PEAK} (D), O_2 Pulse^{VT1} (E), O_2 Pulse^{VT2} (F), time to VT1 (G) and time to $\dot{V}O_2^{PEAK}$ (H)*

On average, venous lactate was significantly higher at peak than at rest (4.92 [3.70-6.06] vs 1.52 [1.32-2.28] mmol/l, p = <0.01), demonstrating that anaerobic thresholds were reached during exercise. Lactate at peak exercise was higher in the SyncAV™ group (Figure 6.3). There was no difference in BORG-RPE scare at the median stage of exercise, although there was a trend towards a higher peak score in the fixed AVD group, driven by a single outlier (Table 6.4, Figure 6.4). There was no difference in the median heart rate at the median stage of exercise, peak HR, or in HR recovery in the first minute of exercise (Table 6.4, Figure 6.5).

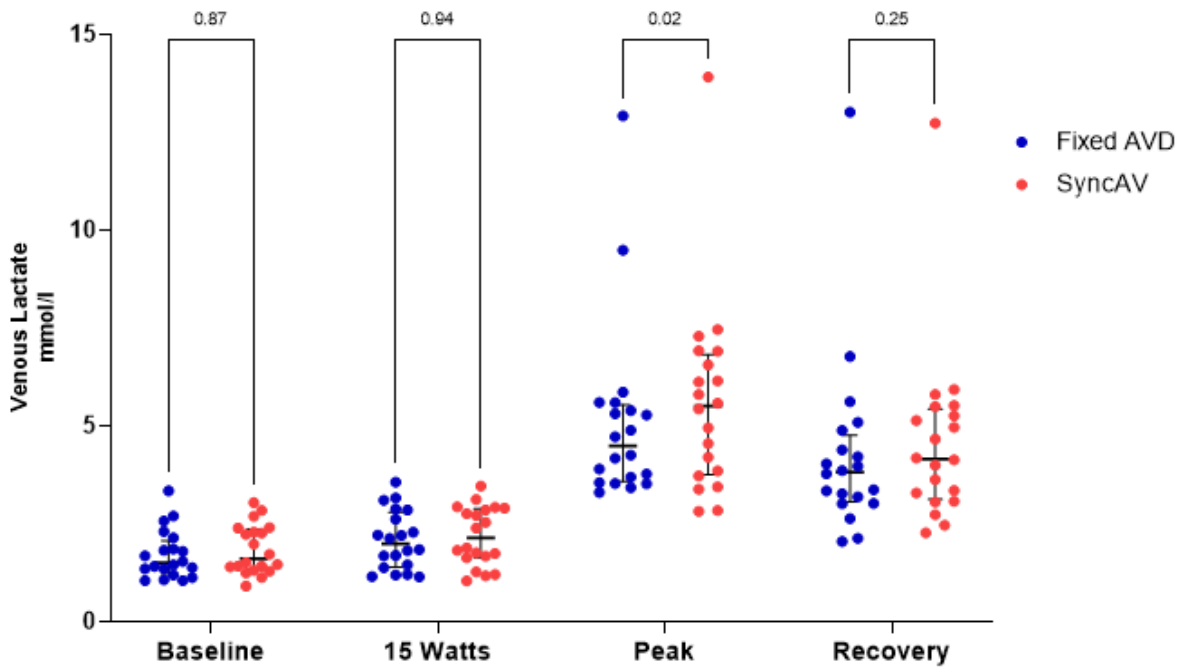

***Figure 6.3**: Comparisons of venous lactate at each measured time point. p = 2 way ANOVA*

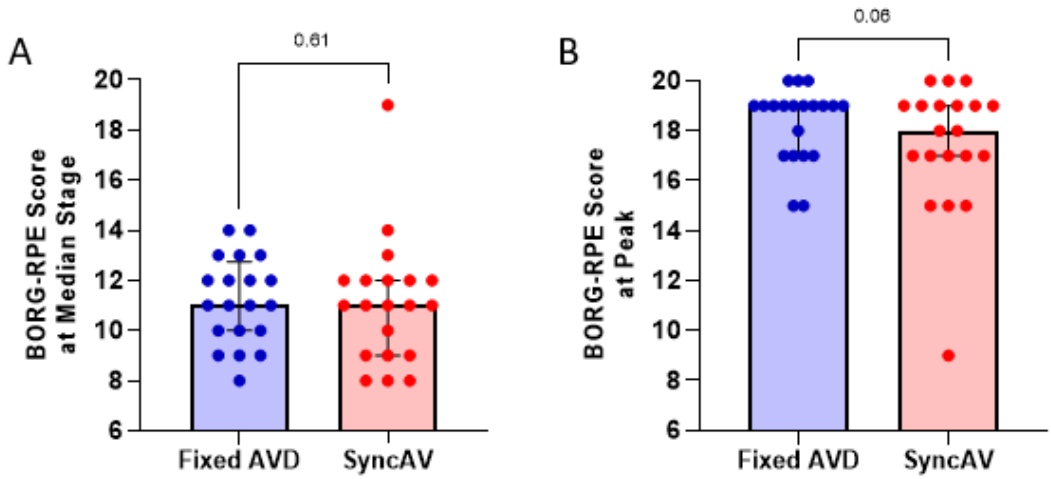

Figure 6.4: *BORG-RPE score at the median stage of exercise (A) and at peak exercise (B)*

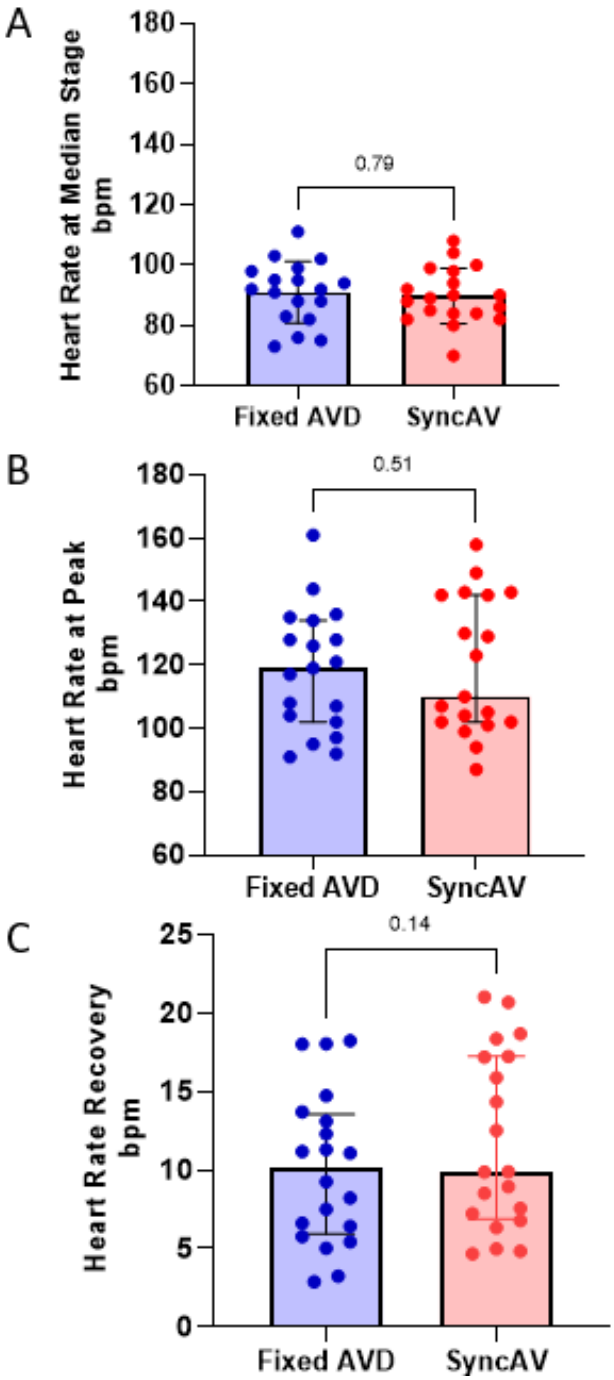

Figure 6.5: *Heart rate at the median stage of exercise (A) and peak heart rate (B). Heart rate recovery in the first minute of recovery (C)*

6.3.2.2 ECG Results

Fixed AVD and SyncAV™ resulted in similar narrowing of QRSd from intrinsic rhythm, with average optimised QRSd which were not significantly different at rest (Table 6.5). In addition, median QRSd either over the duration of each CPET in total (Table 6.5) or compared at each exercise stage (Figure 6.6) was also not significantly different. On analysis of only those exercise stages at which HR was significantly increased (stress stages, defined as HR ≥ 20 bpm above resting HR), there was also no significant difference in QRSd (Figure 6.6).

Table 6.5: QRS duration at rest and during exercise

	Fixed AVD	**SyncAV™**	***p***
QRSd at Rest *(ms)*	131 [103-137]	134 [110-137]	*0.85*
Median QRSd (CPET excluding recovery) *(ms)*	132 [122-143]	132 [121-141]	*0.38*

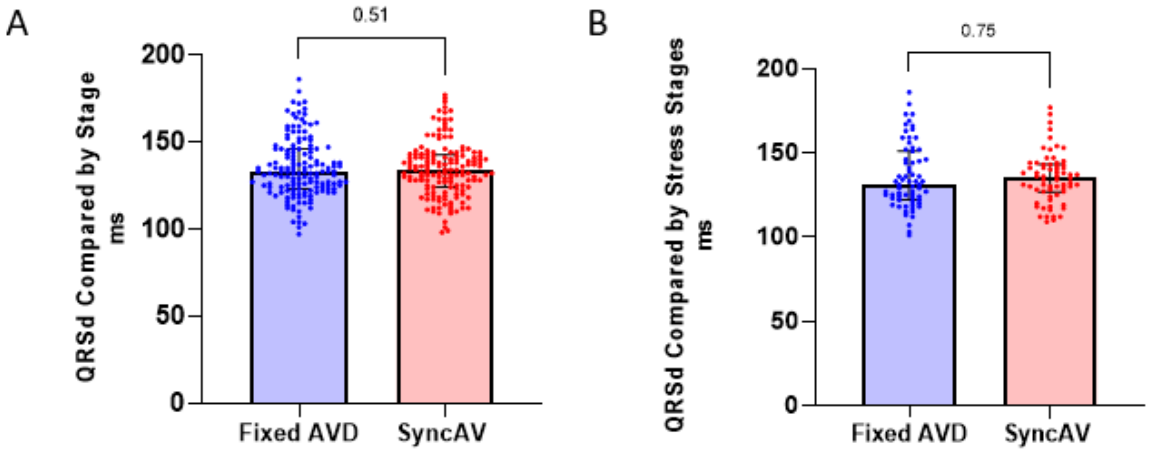

Figure 6.6: *QRSd compared by each stage of CPET (excluding recovery) (A) and by stress stages (HR ≥ 20bpm above resting) (B)*

Where it was possible to manually identify SyncAV™ re-assessments on the ECG by identifying the 3 intrinsic beats on which the algorithm measures intrinsic AV conduction, QRSd during exercise was also assessed immediately pre and post the assessment to identify if there was a significant change. No significant difference was seen (Pre: 137 [124-144]; Post: 135 [123-146] ms, $p = 0.89$) (Figure 6.7). An average of 7 [5-8] adjustments were carried out during the exercise stages.

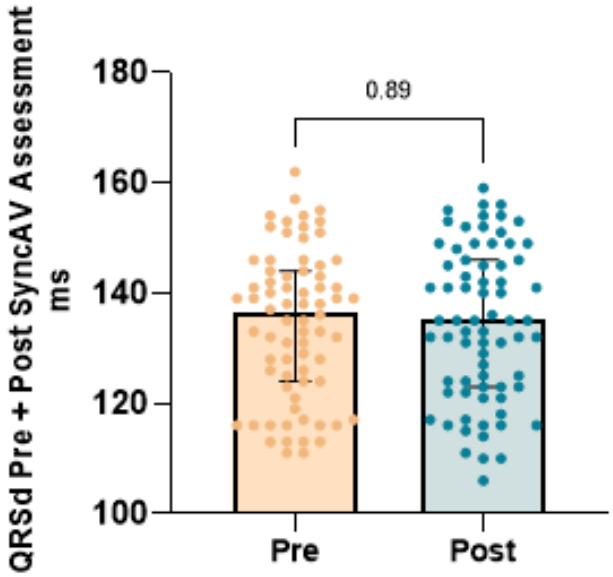

Figure 6.7: *QRSd pre and post SyncAV™ re-assessment*

6.3.3 Comparison of Narrowest vs Widest QRSd Programming at Rest

The total cohort was divided by comparing QRSd at rest (narrowest vs widest) regardless of programming (i.e. by best programming at rest). Eight were narrower with fixed AVD, 8 with SyncAV™ and in 4 there was no difference.

6.3.3.1 CPET Results

Peak cardiac efficiency and O_2 $Pulse^{PEAK}$ were improved in the narrowest QRSd group, although there was no difference in any other CPET parameters (Table 6.7, Figures 6.8-6.11). In addition, lactate at peak was significantly higher in the narrowest QRSd group (Figure 6.12).

Table 6.7: Comparison of CPET measurements based on QRS duration at rest, regardless of programming

	Narrowest QRSd	**Widest QRSd**	***p***
$\dot{V}O_2^{PEAK}$ *(ml/kg/min)*	15.05 [12.41-18.04]	15.11 [12.01-17.46]	*0.18*
$\dot{V}O_2^{VT1}$ *(ml/kg/min)*	7.76 [6.83-8.73]	7.70 [7.01-9.54]	*0.95*
$\dot{V}O_2^{VT2}$ *(ml/kg/min)*	11.43 [10.33-15.77]	11.08 [10.55-14.72]	*0.47*
O_2 Pulse^{PEAK} *(ml/beat)*	12 [10-15]	12 [9-14]	***0.03***
O_2 Pulse^{VT1} *(ml/beat)*	9 [7-10]	9 [6-11]	*0.33*
O_2 Pulse^{VT2} *(ml/beat)*	12 [9-14]	12 [9-13]	*0.27*
Time to $\dot{V}O_2^{PEAK}$ *(secs)*	1267 [1039-1535]	1215 [986-1566]	*0.38*
Time to VT1 *(secs)*	473 [302-626]	489 [318-660]	*0.23*
Work Rate^{PEAK} *(watts)*	90 [64-105]	75 [60-101]	*0.13*
RER^{PEAK}	1.02 [0.98-1.11]	1.05 [0.97-1.12]	*0.85*
Efficiency^{PEAK} (*watts/ml/kg/min)*	5.24 [4.81-6.11]	5.12 [4.47-5.90]	***0.04***
BORG-RPE at median stage	11 [9-12]	12 [9-12]	*0.38*
BORG-RPE at peak	19 [17-20]	19 [17-19]	*0.19*
HR at median stage *(bpm)*	92 [85-97]	91 [82-99]	*0.32*
HR at peak *(bpm)*	120 [101-134]	123 [100-141]	*0.54*
HR Recovery *(bpm)*	9.6 [6.4-13.0]	11.2 [6.5-16.9]	*0.37*

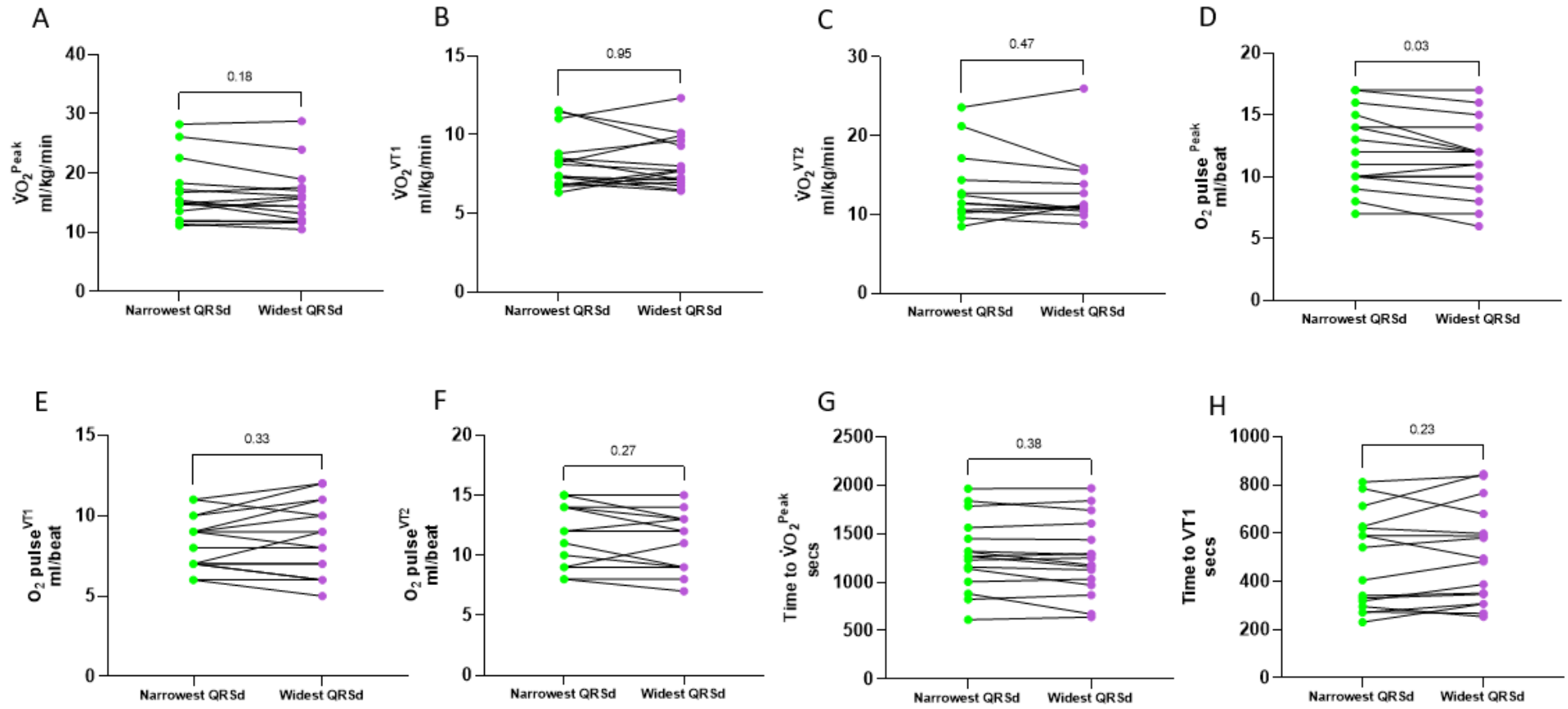

Figure 6.8: *Comparisons of CPET results compared by QRSd at rest, showing: $\dot{V}O_2^{PEAK}$ (A), $\dot{V}O_2^{VT1}$ (B), $\dot{V}O_2^{VT2}$ (C), O_2 $Pulse^{PEAK}$ (D), O_2 $Pulse^{VT1}$ (E), O_2 $Pulse^{VT2}$ (F), time to VT1 (G) and time to $\dot{V}O_2^{PEAK}$ (H)*

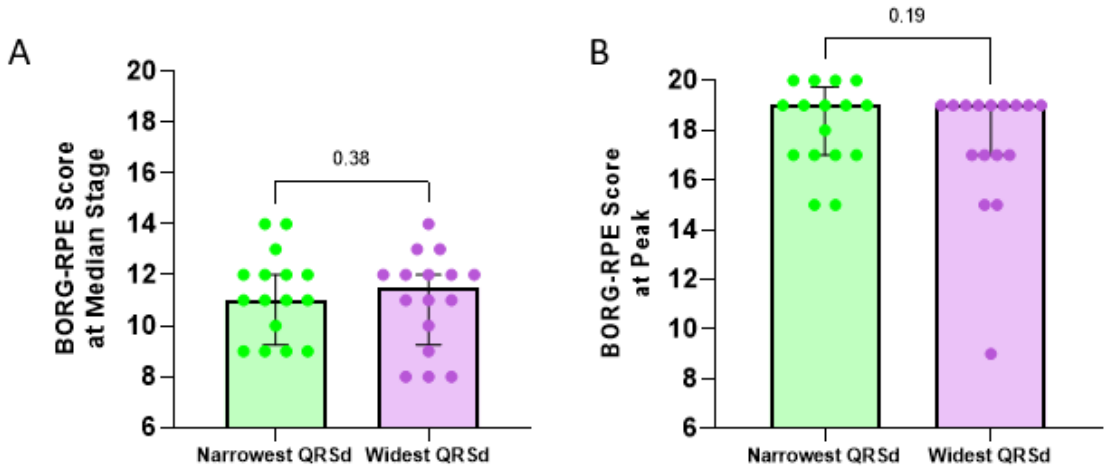

Figure 6.9: *BORG-RPE score at median stage of exercise (A) and peak exercise (B), compared by QRSd at rest*

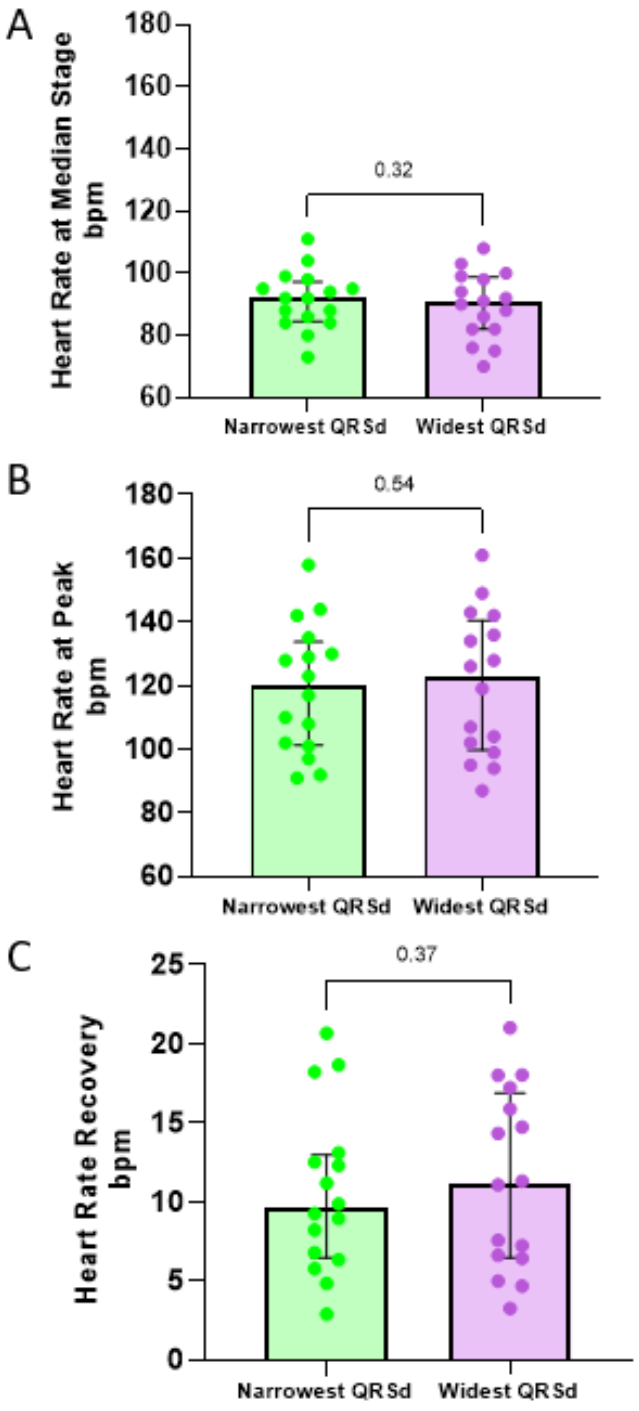

Figure 6.10: *Heart rate at median stage of exercise (A), peak heart rate (B) and heart rate recovery (C), compared by QRSd at rest*

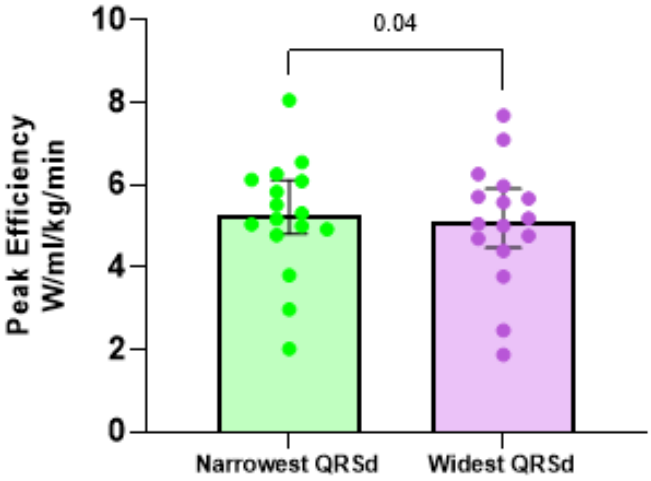

Figure 6.11: *Peak efficiency compared by QRSd at rest*

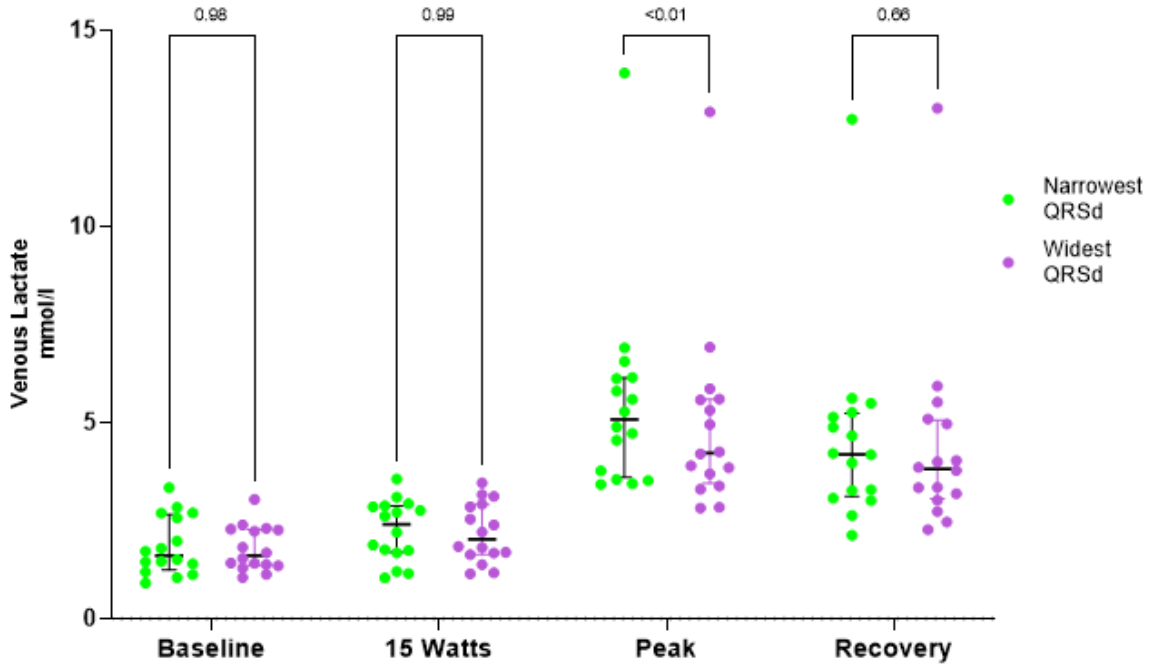

Figure 6.12: *Comparisons of venous lactate at each measured time point, compared by QRSd at rest. p = 2 way ANOVA*

6.3.3.2 ECG Results

QRS duration at rest was narrower by 15 ms in the narrowest QRSd group (Table 6.8). Neither median QRSd over each CPET overall or QRSd compared by stage (excluding recovery) were significantly different (Table 6.8, Figure 6.12). However, QRSd compared by stress stages alone was significantly shorter by 2 ms (Figure 6.12).

Table 6.8: QRSd at rest and during exercise, compared by QRSd at rest

	Narrowest QRSd	**Widest QRSd**	***p***
QRSd at Rest *(ms)*	119 [96-136]	134 [119-142]	***<0.01***
Median QRSd (CPET excluding recovery) *(ms)*	132 [124-141]	132 [121-142]	*0.35*

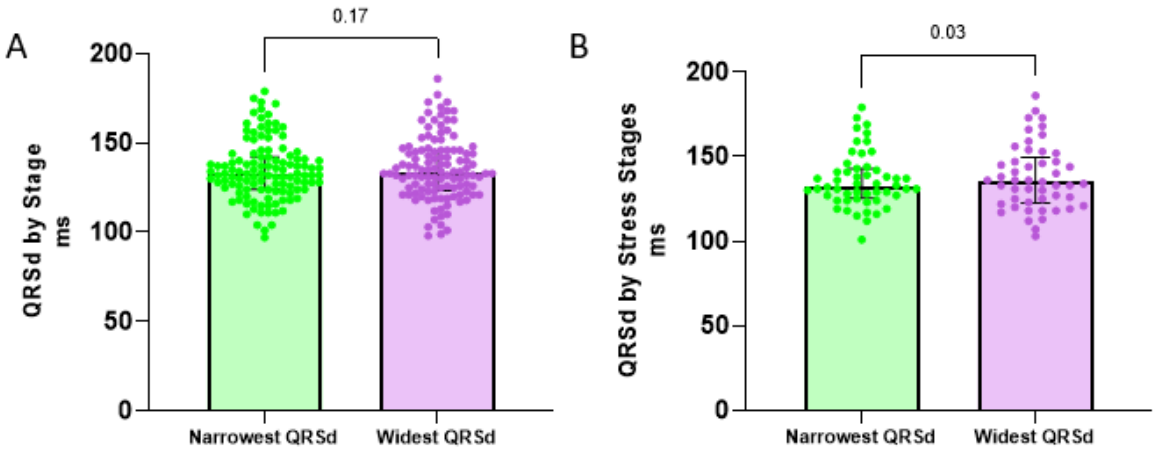

Figure 6.12: *QRSd at each stage of CPET (excluding recovery) (A) and at stress stages (HR ≥ 20bpm above resting) (B), compared by QRSd at rest*

6.4 Discussion

The main findings of this chapter are that:

1. There is no difference in exercise capacity or QRSd at rest or at exercise between optimised fixed AVD and SyncAV^{TM}.
2. If results are compared based on whichever programming gives the narrowest QRSd at rest, then narrower QRSd at rest is associated with a narrower QRSd at stress, higher O_2 Pulse^{PEAK} and higher peak cardiac efficiency.

6.4.1 Comparison Between Fixed AVD and SyncAV^{TM}

The finding that there is no significant difference overall in terms of exercise duration or QRSd during exercise between programming arms suggests that SyncAV^{TM} maintains fusion pacing during exercise. This provides reassurance for its use in active individuals, who are likely to achieve significant increases in their HR. Peak lactate is higher with SyncAV^{TM}, which may indicate higher anaerobic work, although the lack of significant differences with other CPET parameters such as peak $\dot{V}O_2$ makes the significance of this uncertain.

6.4.2 Analysis Based on Best Programming.

Narrower QRSd at rest, regardless of programming, is associated with a narrower QRSd at stress, as well as higher O_2 Pulse^{PEAK} (a surrogate of stroke volume) and higher peak cardiac efficiency. Peak lactate was significantly higher in the narrowest QRSd group, although again the significance of this is uncertain given the lack of difference in measures of O_2

consumption. This is in keeping with the breadth of evidence that narrower QRSd in response to CRT improves haemodynamics and responder rates, as discussed in Chapter 1. Of note, 40% of our study participants has a narrower QRSd at rest with SyncAV™ and so we would advocate its use where this can be achieved.

This is the first study to show that a narrower QRSd during exercise correlates to better CPET performance and gives reassurance that CPET is able to detect the impact of a narrower QRSd on performance.

6.4.3 Other Fusion Pacing Algorithms

As discussed in Chapter 1, the newer SyncAV Plus™ algorithm from Abbott utilises a delta which is a percentage of intrinsic AV conduction, rather than a fixed value. Although our study has not shown evidence of loss of fusion on exercise with SyncAV™, use of a percentage narrowing in this way with SyncAV Plus™ would intuitively seem to be more physiological and maintain better AV optimisation. For example, in a patient with short intrinsic AV conduction at rest and then further shortening on exercise, it would help prevent AVDs being too short, leading to impairment of diastolic filling[191]. In addition, as well as SyncAV™, the other main fusion pacing algorithm available is AdaptivCRT™ from Medtronic (as Boston's SmartAV™ does not provide dynamic optimisation). This paces at approximately 70% of intrinsic conduction, but importantly can switch between LV-only pacing and BiV pacing (still with adaptive AVD, adjusted every minute). If intrinsic AV conduction is prolonged or if HR goes above 100 bpm, then it will automatically switch to optimised BiV pacing, eliminating any uncertainty over potential loss of fusion at higher heart rates.

6.4.4 Use of CPET to Evaluate Pacing Algorithms

Cardiopulmonary exercise testing has been used previously to attempt to identify those patients most likely to respond to CRT and so aid patient selection[402, 403]. In addition, it has been used to assess changes in exercise capacity as a result of rate responsive pacing algorithms [404] and RAAVDs[173] in CRT, and the use of non-invasive haemodynamic monitoring to optimise AV and VV delays[405]. However, to our knowledge this is the first time that 12 lead ECG recordings and measures of exercise capacity have been combined by CPET in the evaluation of fusion pacing algorithms. This combination allows for the assessment of maintenance of effective fusion as determined by QRSd as well as exercise capacity, and the finding in our study of increased O_2 $Pulse^{PEAK}$ and higher peak cardiac efficiency along with narrower QRSd at stress in those with narrowest QRSd at rest shows the utility of combining these outcomes. This may therefore provide a novel method of initially assessing new dynamic pacing algorithms, prior to conducting large, expensive randomised controlled trials.

Several measures obtained during CPET, such as peak $\dot{V}O_2$, $\dot{V}O_2$ at VT1 and exercise duration[399, 406-408], have been shown to be predictors of mortality in heart failure, although there doesn't appear to be a clear cut-off for peak $\dot{V}O_2$ to predict survival[407]. In addition, heart rate recovery in the first minute after exercise has been shown to be a predictor of overall mortality in a non-heart failure cohort[409]. Therefore, it would seem reasonable to think that such parameters could be important measures against which to routinely assess dynamic pacing protocols, especially given that the key function of such protocols is to optimise CRT during changes in HR, as during exercise.

6.5 Limitations

This is a relatively small crossover study for comparison of acute CRT programming changes. However, we believe that the paired nature of the data, with the same participants undergoing repeated testing in a double-blinded manner, is a significant strength and that the cohort size is therefore sufficient to draw the above conclusions.

Given that SyncAV^{TM} only reassesses every 256 beats, it could be that the length of CPET test does not allow enough time for a sufficient number of reassessments and readjustments to take place. However, where it was possible to identify the adjustments based on visualisation of the intrinsic beats, an average of 7 were carried out per test during the exercise stages, which should be sufficient for any adjustments to have an effect on overall QRSd. Furthermore, a greater proportion of these would be at stages with higher HRs, which is when there would presumably be the greatest benefit to reassessment and readjustment.

Finally, recruited participants had to have either subjective or objective evidence of response to CRT, which could limit the applicability of these findings to patients at initial implant. However, responders are more likely to be undergoing exercise with resultant significant changes in their HR and so are likely to be the cohort for whom concerns about lack of fusion on exercise are greatest.

6.6 Summary

There is no significant difference in exercise capacity or QRSd between the use of optimised fixed AVD or SyncAV™ and so it appears that fusion pacing is adequately maintained on exercise, lending reassurance to its use. In addition, programming with whichever algorithm gives the narrowest QRSd at rest is associated with a narrower QRSd during significant exercise, higher peak stroke volume and improved cardiac efficiency. This supports the use of SyncAV™ in the 40% of patients where this gave the narrowest QRSd at rest.

Summary and Future Directions

This thesis aims to explore and develop the links the between CRT and myocardial metabolism. A further appreciation of the metabolic influences of CRT may lead to better CRT optimisation and reverse remodelling. In addition, a further understanding of why some patients fail to respond to CRT could potentially aid patient selection, thus preventing procedures from being undertaken which are unlikely to provide clinical benefit.

Chapter 1 set out a summary of heart failure, cardiac conduction and the history and mechanisms of CRT, including newer developments in CRT programming which allow for fusion pacing. In addition, myocardial metabolism in the healthy heart as well as in heart failure and DM were discussed, along with the current evidence for the influence of CRT on cardiac efficiency and substrate usage. Both PET imaging and invasive A-V blood sampling have been previously used to assess myocardial metabolism in the context of CRT, but no studies to date have quantified acute changes in cardiac metabolic substrate uptake in response to CRT, both at rest and at stress.

Chapter 2 discussed the experimental methods used in this thesis. The use of advanced ^{31}P-MRS to assess myocardial energetics *in vivo* is explained, along with invasive measurement of cardiac contractility using PV loop catheters and quantification of cardiac substrate uptake using A-V blood sampling across the heart and assessment of coronary blood flow. The combination of these techniques in order to assess myocardial metabolism in CRT patients has not previously been performed.

Chapter 3 discussed the assessment of substrate manipulation using either a FFA or insulin/dextrose infusion in participants with non-insulin dependent diabetes mellitus. Two participant cohorts were assessed; those with normal cardiac function and those with systolic heart failure. Metabolic flexibility appears to be maintained in participants with DM alone, with increased contractility on an FFA infusion. Furthermore, this appears to be associated with improved energetic efficiency, with decreased metabolic flux at rest, which may be due to diabetic hearts being optimised for predominant FA oxidation. However, metabolic flexibility is decreased or absent in participants with both DM and heart failure, which might be expected given that both of these are classically felt to represent metabolically inflexible states. This may in part explain decreased CRT responder rates in diabetic populations. Further work in assessing and potentially increasing metabolic flexibility in these patients may therefore help to improve CRT response rates.

In Chapter 4, the acute changes in cardiac contractility, efficiency and metabolic substrate uptake in response to CRT were explored. It was demonstrated that CRT improves oxygen efficiency regardless of substrate manipulation and that in non-ischaemic cardiomyopathy the heart is not oxygen limited. Furthermore, CRT induces acute changes in cardiac substrate uptake, with FFA uptake increased. If further FFA uptake is not possible, i.e. if supply is limited or uptake is already maximised, then either lactate or ketone uptake is increased. Therefore, CRT appears to acutely rebalance substrate uptake towards a more physiological picture of lipid based metabolism, as seen in the healthy heart. In addition, these changes in uptake positively correlate with acute improvements in cardiac contractility. Quantified changes in acute cardiac substrate uptake in response to CRT at both rest and stress in this way has not previously been assessed. Chapter 5 takes these

findings further, and correlates the changes in acute substrate uptake to reverse remodelling at 6 months, where the increase in FFA uptake positively correlates with change in LVEDV. Together, these findings suggest that in non-ischaemic cardiomyopathies the increased ATP supply associated with FA oxidation may improve CRT response. Further work should therefore include pharmacological efforts to maximise FFA uptake and oxidation (e.g. through the use of fibrates which act as PPAR-α agonists), to assess whether this could therefore, in combination with CRT, improve reverse remodelling rates. In addition, although CRT increases FFA uptake its final intracellular fate is not currently known and should be assessed. Metabolomic assessment of blood samples would enable this to be further investigated, along with further detail regarding which FA chain lengths are utilised and fates of other metabolic substrates.

Chapter 5 also assessed baseline energetic status to see if this correlated with CRT response, with a ^{31}P-MRS measure of energetic efficiency (cardiac work / CK flux) appearing to positively correlate with reverse remodelling. Given that acute oxygen efficiency did not correlate with reverse remodelling, this again suggests that it is ATP supply which may influence response, regardless of the oxygen efficiency of the substrate used. Further studies correlating baseline metabolic flexibility and energetic efficiency with CRT response are needed to see if this may represent a viable method of optimising patient selection for CRT. Finally, Chapter 5 attempted to separate out the acute effects of QRS narrowing by CRT from longer term volumetric reverse remodelling. At implant, there were only modest acute improvements in LVEDV despite significant QRS narrowing with BiV pacing, whilst after 6 months LVEDV had reduced by a much greater extent compared to at implant. However, there was little change in LVEDV after 6 months when QRSd was allowed to

acutely broaden going from BiV pacing to intrinsic rhythm. This demonstrated that structural reverse remodelling had taken place beyond the acute effect of QRS narrowing and suggests that once reverse remodelling has occurred, the mechanism of CRT is to maintain this by preventing reversion to the inhomogeneous workload which is seen with dyssynchronous heart failure. Use of PV loops and CMR to assess the acute and chronic effects of CRT in this way has not been done before.

Chapter 6 was a double-blind, randomised crossover study using CPET to assess the effectiveness of fusion pacing during exercise. Whilst there was no difference in exercise capacity between fusion pacing with SyncAV^{TM} compared to fixed AVD, this in itself shows that fusion is not lost on exercise and so lends reassurance to its use in this situation. Furthermore, using whichever programming gave the narrowest QRSd at rest led to a narrower QRSd on exercise and improvement in CPET parameters such as oxygen pulse (a surrogate of stroke volume) and peak cardiac efficiency. This confirms that maximal narrowing of QRSd at rest should be the aim of CRT optimisation, regardless of algorithm used. Future trials looking at optimal device programming may therefore be better focussed on achieving this in a personalised approach, rather than assessing individual algorithms in a 'one size fits all' way. Ideally, such studies would involve all, rather than specific, device manufacturers. In addition, the utility of CPET in allowing assessment not only of the 12 lead ECG at rest and stress but also of exercise capacity, could be useful to assess the effectiveness of future pacing algorithms. This could be more cost effective than going straight to large scale randomised control trials, which may show no benefit.

In summary, this thesis demonstrates the interwoven nature of CRT and myocardial metabolism. Future studies which further investigate this relationship may pave the way for

a better understanding of the mechanisms of CRT, along with methods for improving rates of reverse remodelling. Given the ongoing challenges associated with the burden of heart failure, this could represent an important avenue for optimising treatment.

Appendix

A. EQ-5D-3L Questionnaire, EuroQol Research Foundation, UK (English) V2.1:

Under each heading, please tick the ONE box that best describes your health TODAY.

MOBILITY

I have no problems in walking about ❑

I have some problems in walking about ❑

I am confined to bed ❑

SELF-CARE

I have no problems with self-care ❑

I have some problems washing or dressing myself ❑

I am unable to wash or dress myself ❑

USUAL ACTIVITIES *(e.g. work, study, housework, family or leisure activities)*

I have no problems with performing my usual activities ❑

I have some problems with performing my usual activities ❑

I am unable to perform my usual activities ❑

PAIN / DISCOMFORT

I have no pain or discomfort ❑

I have moderate pain or discomfort ❑

I have extreme pain or discomfort ❑

ANXIETY / DEPRESSION

I am not anxious or depressed ❑

I am moderately anxious or depressed ❑

I am extremely anxious or depressed ❑

We would like to know how good or bad your health is TODAY.

This scale is numbered from 0 to 100.

100 means the best health you can imagine.
0 means the worst health you can imagine.

Please mark an X on the scale to indicate how your health is TODAY.

Now, write the number you marked on the scale in the box below.

YOUR HEALTH TODAY = ☐

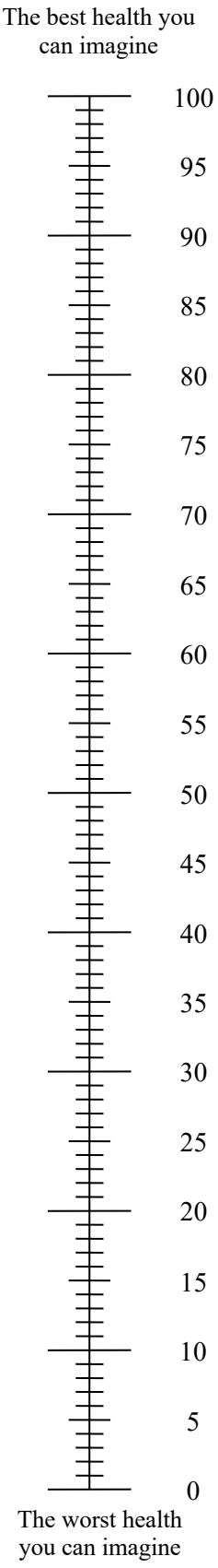

B. BORG-RPE Scale

Borg Scale (6-20)

Rating	How Hard you are Exercising
6	No, exertion at all
7	Very, very light
8	
9	Very light
10	
11	Light
12	
13	Somewhat hard
14	
15	Hard
16	
17	Very hard
18	
19	Extremely hard
20	Maximal Exertion

C. Chapter 3 - Table 3.5

Baseline fasting values off substrate infusion included:

	NHDM				HFDM			
	Baseline*	Glucose Infusion	FFA Infusion	*p*	Baseline	Glucose Infusion	FFA Infusion	*p*
LVEDV *(ml)*	149 [131-188]	155 [140-182]	159 [133-183]	*0.58*	242 [197-282]	267 [195-278]	231 [196-255]	***0.04***
LVESV *(ml)*	65 [56-73]	62 [52-76]	59 [49-66]	***0.01***	156 [118-185]	170 [113-195]	141 [112-171]	***0.01***
LVEF *(%)*	58 [57-62]	60 [58-62]	63 [59-66]	***<0.01***	38 [30-44]	40 [29-44]	40 [31-49]	***0.05***
3D GCS *(%)*	-19.5 [-20.3-, -17.4]	-19.3 [-22.1-, -18.6]	-20.7 [-22.5-, -19.0]	*0.06*	-12.8 [-14.1-, -11.1]	-11.4 [-14.6-, -9.0]	-11.6 [-16.4-, -10.0]	*0.18*
RVEDV *(ml)*	156 [129-185]	146 [132-176]	150 [120-183]	*0.44*	136 [117-155]	136 [120-161]	132 [108-159]	*0.11*
RVESV *(ml)*	66 [49-78]	61 [53-78]	55 [44-71]	***0.05***	56 [50-62]	60 [48-79]	58 [45-68]	***0.04***
RVEF *(%)*	58 [54-61]	59 [55-61]	62 [57-64]	***<0.01***	58 [55-62]	55 [51-63]	55 [53-64]	***0.04***

**n = 13 participants. p value = mixed effect analysis for NHDM cohort and one-way ANOVA for HFDM cohort (except for RVEF - Friedman test)*

D. Chapter 4 - Figure 4.11

Significant outlier in panel A (grey point) included and updated *p* value:

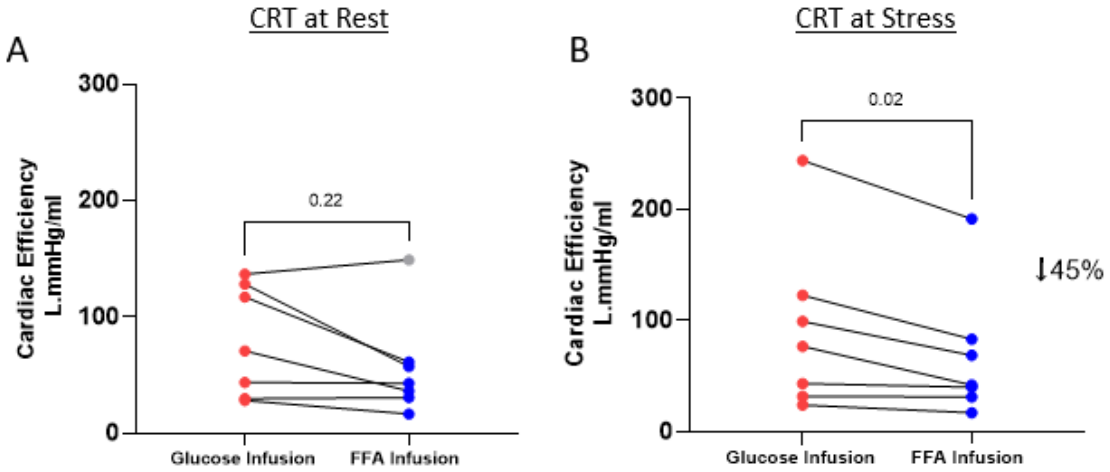

E. Chapter 4 - Figure 4.12

Significant outlier in panel F (grey point) included and updated *p* value:

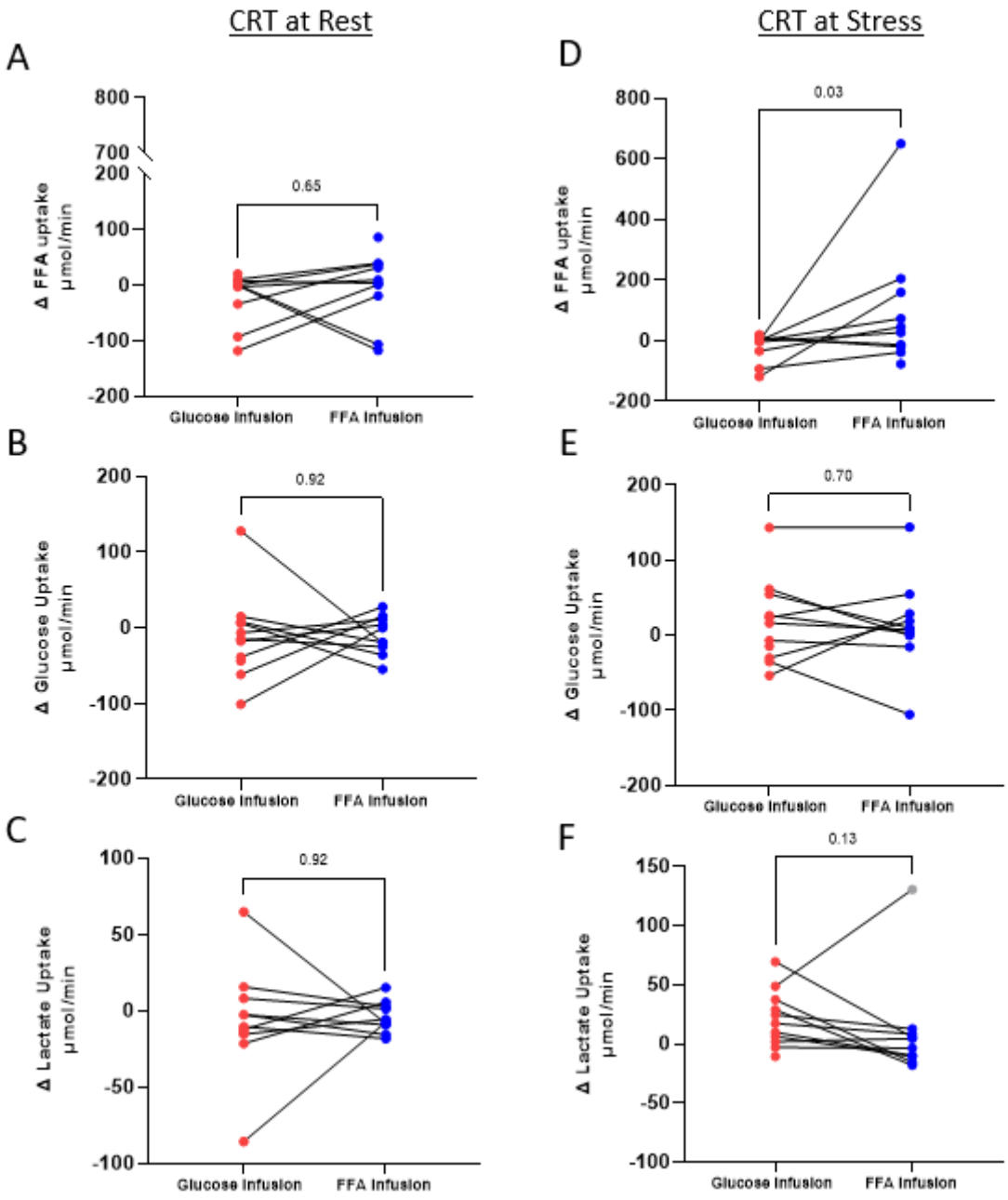

References

1. McDonagh, T.A., Metra, M., Adamo, M.*, et al.*, *2021 ESC Guidelines for the diagnosis and treatment of acute and chronic heart failure.* Eur Heart J, 2021. **42**(36): p. 3599-3726.
2. Schultheiss, H.-P., Fairweather, D., Caforio, A.L.P.*, et al.*, *Dilated cardiomyopathy.* Nature Reviews Disease Primers, 2019. **5**(1): p. 32.
3. Connolly, M., Beattie, J., Walker, D., and Dancy, M., *End of life care in heart failure: A framework for implementation*, H.I. Programme, Editor. 2014, NHS Improvement.
4. *The National Heart Failure Audit*. 2020.
5. Silverman, M.E. and Upshaw, C.B., *Walter gaskell and the understanding of atrioventricular conduction and block.* Journal of the American College of Cardiology, 2002. **39**(10): p. 1574-1580.
6. Keith, A. and Flack, M., *The Form and Nature of the Muscular Connections between the Primary Divisions of the Vertebrate Heart.* Journal of anatomy and physiology, 1907. **41**(Pt 3): p. 172-189.
7. Silverman, M.E. and Hollman, A., *Discovery of the sinus node by Keith and Flack: on the centennial of their 1907 publication.* Heart (British Cardiac Society), 2007. **93**(10): p. 1184-1187.
8. Silverman, M.E., Grove, D., and Upshaw, C.B., *Why Does the Heart Beat?* Circulation, 2006. **113**(23): p. 2775-2781.
9. Iaizzo, P.A., *Handbook of Cardiac Anatomy, Physiology, and Devices*. 2015: Springer.
10. Tan, N.Y., Witt, C.M., Oh, J.K., and Cha, Y.M., *Left Bundle Branch Block: Current and Future Perspectives.* Circ Arrhythm Electrophysiol, 2020. **13**(4): p. e008239.
11. Surawicz, B., Childers, R., Deal, B.J.*, et al.*, *AHA/ACCF/HRS recommendations for the standardization and interpretation of the electrocardiogram: part III: intraventricular conduction disturbances: a scientific statement from the American Heart Association Electrocardiography and Arrhythmias Committee, Council on Clinical Cardiology; the American College of Cardiology Foundation; and the Heart Rhythm Society: endorsed by the International Society for Computerized Electrocardiology.* Circulation, 2009. **119**(10): p. e235-40.
12. Auffret, V., Martins, R.P., Daubert, C.*, et al.*, *Idiopathic/Iatrogenic Left Bundle Branch Block-Induced Reversible Left Ventricle Dysfunction: JACC State-of-the-Art Review.* J Am Coll Cardiol, 2018. **72**(24): p. 3177-3188.
13. Wiggers, C.J., *The muscular reactions of the mammalian ventricles to artificial surface stimuli.* American Journal of Physiology, 1925. **73**(2): p. 346-378.
14. Ghani, A., Delnoy, P., Adiyaman, A.*, et al.*, *Septal rebound stretch as predictor of echocardiographic response to cardiac resynchronization therapy.* Int J Cardiol Heart Vasc, 2015. **7**: p. 22-27.

15. Gorcsan, J., 3rd, Anderson, C.P., Tayal, B.*, et al.*, *Systolic Stretch Characterizes the Electromechanical Substrate Responsive to Cardiac Resynchronization Therapy.* JACC Cardiovasc Imaging, 2019. **12**(9): p. 1741-1752.
16. De Boeck, B.W., Teske, A.J., Meine, M.*, et al.*, *Septal rebound stretch reflects the functional substrate to cardiac resynchronization therapy and predicts volumetric and neurohormonal response.* Eur J Heart Fail, 2009. **11**(9): p. 863-71.
17. Sörensen, J., Harms, H.J., Aalen, J.M.*, et al.*, *Myocardial Efficiency: A Fundamental Physiological Concept on the Verge of Clinical Impact.* JACC: Cardiovascular Imaging, 2020. **13**(7): p. 1564-1576.
18. Nguyen, U.C., Verzaal, N.J., van Nieuwenhoven, F.A., Vernooy, K., and Prinzen, F.W., *Pathobiology of cardiac dyssynchrony and resynchronization therapy.* Europace, 2018. **20**(12): p. 1898-1909.
19. Grines, C.L., Bashore, T.M., Boudoulas, H.*, et al.*, *Functional abnormalities in isolated left bundle branch block. The effect of interventricular asynchrony.* Circulation, 1989. **79**(4): p. 845-53.
20. Prinzen, F.W., Hunter, W.C., Wyman, B.T., and McVeigh, E.R., *Mapping of regional myocardial strain and work during ventricular pacing: Experimental study using magnetic resonance imaging tagging.* J Am Coll Cardiol, 1999. **33**(6): p. 1735-1742.
21. Leyva, F., Nisam, S., and Auricchio, A., *20 years of cardiac resynchronization therapy.* J Am Coll Cardiol, 2014. **64**(10): p. 1047-58.
22. Shenkman, H.J., Pampati, V., Khandelwal, A.K.*, et al.*, *Congestive heart failure and QRS duration: establishing prognosis study.* Chest, 2002. **122**(2): p. 528-34.
23. Witt, C.M., Wu, G., Yang, D.*, et al.*, *Outcomes With Left Bundle Branch Block and Mildly to Moderately Reduced Left Ventricular Function.* JACC Heart Fail, 2016. **4**(11): p. 897-903.
24. Baldasseroni, S., Opasich, C., Gorini, M.*, et al.*, *Left bundle-branch block is associated with increased 1-year sudden and total mortality rate in 5517 outpatients with congestive heart failure: a report from the Italian network on congestive heart failure.* Am Heart J, 2002. **143**(3): p. 398-405.
25. Tabrizi, F., Englund, A., Rosenqvist, M., Wallentin, L., and Stenestrand, U., *Influence of left bundle branch block on long-term mortality in a population with heart failure.* Eur Heart J, 2007. **28**(20): p. 2449-55.
26. Silvet, H., Amin, J., Padmanabhan, S., and Pai, R.G., *Prognostic implications of increased QRS duration in patients with moderate and severe left ventricular systolic dysfunction.* Am J Cardiol, 2001. **88**(2): p. 182-5, A6.
27. Xiao, H.B., Brecker, S.J., and Gibson, D.G., *Effects of abnormal activation on the time course of the left ventricular pressure pulse in dilated cardiomyopathy.* Br Heart J, 1992. **68**(4): p. 403-7.
28. Littmann, L. and Symanski, J.D., *Hemodynamic implications of left bundle branch block.* J Electrocardiol, 2000. **33 Suppl**: p. 115-21.
29. Manisty, C.H., Al-Hussaini, A., Unsworth, B.*, et al.*, *The Acute Effects of Changes to AV Delay on BP and Stroke Volume.* Circulation: Arrhythmia and Electrophysiology, 2012. **5**(1): p. 122-130.
30. Bogaard, M.D., Meine, M., Tuinenburg, A.E.*, et al.*, *Cardiac resynchronization therapy beyond nominal settings: who needs individual programming of the atrioventricular and interventricular delay?* EP Europace, 2012. **14**(12): p. 1746-1753.

31. Befeler, B., Berkovits, B.V., Aranda, J.M.*, et al.*, *Programmed simultaneous biventricular stimulation in man, with special reference to its use in the evaluation of intraventricular reentry.* Eur J Cardiol, 1979. **9**(5): p. 369-78.
32. Foster, A.H., Gold, M.R., and McLaughlin, J.S., *Acute hemodynamic effects of atrio-biventricular pacing in humans.* Ann Thorac Surg, 1995. **59**(2): p. 294-300.
33. Cazeau, S., Ritter, P., Bakdach, S.*, et al.*, *Four chamber pacing in dilated cardiomyopathy.* Pacing Clin Electrophysiol, 1994. **17**(11 Pt 2): p. 1974-9.
34. Bakker, P.F., Meijburg, H.W., de Vries, J.W.*, et al.*, *Biventricular pacing in end-stage heart failure improves functional capacity and left ventricular function.* J Interv Card Electrophysiol, 2000. **4**(2): p. 395-404.
35. Cazeau, S., Ritter, P., Lazarus, A.*, et al.*, *Multisite pacing for end-stage heart failure: early experience.* Pacing Clin Electrophysiol, 1996. **19**(11 Pt 2): p. 1748-57.
36. Blanc, J.J., Etienne, Y., Gilard, M.*, et al.*, *Evaluation of different ventricular pacing sites in patients with severe heart failure: results of an acute hemodynamic study.* Circulation, 1997. **96**(10): p. 3273-7.
37. Leclercq, C., Cazeau, S., Le Breton, H.*, et al.*, *Acute hemodynamic effects of biventricular DDD pacing in patients with end-stage heart failure.* J Am Coll Cardiol, 1998. **32**(7): p. 1825-31.
38. Auricchio, A., Klein, H., Tockman, B.*, et al.*, *Transvenous biventricular pacing for heart failure: can the obstacles be overcome?* The American Journal of Cardiology, 1999. **83**(5): p. 136-142.
39. Cazeau, S., Leclercq, C., Lavergne, T.*, et al.*, *Effects of multisite biventricular pacing in patients with heart failure and intraventricular conduction delay.* N Engl J Med, 2001. **344**(12): p. 873-80.
40. Abraham, W.T., Fisher, W.G., Smith, A.L.*, et al.*, *Cardiac resynchronization in chronic heart failure.* N Engl J Med, 2002. **346**: p. 1845-1853.
41. Bristow, M.R., Saxon, L.A., Boehmer, J.*, et al.*, *Cardiac-resynchronization therapy with or without an implantable defibrillator in advanced chronic heart failure.* N Engl J Med, 2004. **350**(21): p. 2140-50.
42. Moss, A.J., Hall, W.J., Cannom, D.S.*, et al.*, *Cardiac-resynchronization therapy for the prevention of heart-failure events.* N Engl J Med, 2009. **361**(14): p. 1329-38.
43. Tang, A.S., Wells, G.A., Talajic, M.*, et al.*, *Cardiac-resynchronization therapy for mild-to-moderate heart failure.* N Engl J Med, 2010. **363**(25): p. 2385-95.
44. Linde, C., Abraham, W.T., Gold, M.R., Daubert, C., and Group, R.S., *Cardiac resynchronization therapy in asymptomatic or mildly symptomatic heart failure patients in relation to etiology: results from the REVERSE (REsynchronization reVErses Remodeling in Systolic Left vEntricular Dysfunction) study.* J Am Coll Cardiol, 2010. **56**(22): p. 1826-31.
45. Auricchio, A., Stellbrink, C., Sack, S.*, et al.*, *Long-term clinical effect of hemodynamically optimized cardiac resynchronization therapy in patients with heart failure and ventricular conduction delay.* J Am Coll Cardiol, 2002. **39**(12): p. 2026-33.
46. Yancy, C.W., Jessup, M., Bozkurt, B.*, et al.*, *2013 ACCF/AHA guideline for the management of heart failure: a report of the American College of Cardiology Foundation/American Heart Association Task Force on Practice Guidelines.* J Am Coll Cardiol, 2013. **62**(16): p. e147-239.

47. *Implantable cardioverter defibrillators and cardiac resynchronisation therapy for arrhythmias and heart failure*. NICE Guidance, 2014.
48. Kass, D.A., Maughan, W.L., Guo, Z.M.*, et al.*, *Comparative influence of load versus inotropic states on indexes of ventricular contractility: experimental and theoretical analysis based on pressure-volume relationships.* Circulation, 1987. **76**(6): p. 1422-36.
49. Mason, D.T., *Usefulness and limitations of the rate of rise of intraventricular pressure (dp/dt) in the evaluation of myocardial contractility in man∗.* The American Journal of Cardiology, 1969. **23**(4): p. 516-527.
50. Katz, A.M., *Influence of altered inotropy and lusitropy on ventricular pressure-volume loops.* J Am Coll Cardiol, 1988. **11**(2): p. 438-45.
51. Steendijk, P., Tulner, S.A., Schreuder, J.J.*, et al.*, *Quantification of left ventricular mechanical dyssynchrony by conductance catheter in heart failure patients.* Am J Physiol Heart Circ Physiol, 2004. **286**(2): p. H723-30.
52. Bastos, M.B., Burkhoff, D., Maly, J.*, et al.*, *Invasive left ventricle pressure-volume analysis: overview and practical clinical implications.* Eur Heart J, 2020. **41**(12): p. 1286-1297.
53. Steendijk, P., Tulner, S.A.F., Wiemer, M.*, et al.*, *Pressure-volume measurements by conductance catheter during cardiac resynchronization therapy.* European Heart Journal Supplements, 2004. **6**(D): p. D35-D42.
54. Burkhoff, D., Mirsky, I., and Suga, H., *Assessment of systolic and diastolic ventricular properties via pressure-volume analysis: a guide for clinical, translational, and basic researchers.* Am J Physiol Heart Circ Physiol, 2005. **289**(2): p. H501-12.
55. Auricchio, A., Stellbrink, C., Block, M.*, et al.*, *Effect of pacing chamber and atrioventricular delay on acute systolic function of paced patients with congestive heart failure. The Pacing Therapies for Congestive Heart Failure Study Group. The Guidant Congestive Heart Failure Research Group.* Circulation, 1999. **99**(23): p. 2993-3001.
56. Kass, D.A., Chen, C.H., Curry, C.*, et al.*, *Improved left ventricular mechanics from acute VDD pacing in patients with dilated cardiomyopathy and ventricular conduction delay.* Circulation, 1999. **99**(12): p. 1567-73.
57. Sohal, M., Hamid, S., Perego, G.*, et al.*, *A multicenter prospective randomized controlled trial of cardiac resynchronization therapy guided by invasive dP/dt.* Heart Rhythm O2, 2021. **2**(1): p. 19-27.
58. Duckett, S.G., Ginks, M., Shetty, A.K.*, et al.*, *Invasive acute hemodynamic response to guide left ventricular lead implantation predicts chronic remodeling in patients undergoing cardiac resynchronization therapy.* J Am Coll Cardiol, 2011. **58**(11): p. 1128-36.
59. de Roest, G.J., Allaart, C.P., de Haan, S.*, et al.*, *Effects of QRS duration and pacing location on pressure-volume loop evaluation of cardiac resynchronization therapy in end-stage heart failure.* Am J Cardiol, 2011. **108**(11): p. 1581-8.
60. Delnoy, P.P., Ottervanger, J.P., Vos, D.H.*, et al.*, *Upgrading to biventricular pacing guided by pressure-volume loop analysis during implantation.* J Cardiovasc Electrophysiol, 2011. **22**(6): p. 677-83.
61. de Roest, G., Knaapen, P., Gotte, M.*, et al.*, *Stroke work or systolic dP/dtmax to evaluate acute response to cardiac resynchronization therapy: are they interchangeable?* Eur J Heart Fail, 2009. **11**(7): p. 706-8.

62. de Roest, G.J., Allaart, C.P., Kleijn, S.A*., et al.*, *Prediction of long-term outcome of cardiac resynchronization therapy by acute pressure-volume loop measurements.* Eur J Heart Fail, 2013. **15**(3): p. 299-307.
63. Zweerink, A., Salden, O.A.E., van Everdingen, W.M*., et al.*, *Hemodynamic Optimization in Cardiac Resynchronization Therapy: Should We Aim for dP/dtmax or Stroke Work?* JACC Clin Electrophysiol, 2019. **5**(9): p. 1013-1025.
64. Vecera, J., Penicka, M., Eriksen, M*., et al.*, *Wasted septal work in left ventricular dyssynchrony: a novel principle to predict response to cardiac resynchronization therapy.* Eur Heart J Cardiovasc Imaging, 2016. **17**(6): p. 624-32.
65. Hoke, U., Thijssen, J., van Bommel, R.J*., et al.*, *Influence of diabetes on left ventricular systolic and diastolic function and on long-term outcome after cardiac resynchronization therapy.* Diabetes Care, 2013. **36**(4): p. 985-91.
66. Kim, G.H., Uriel, N., and Burkhoff, D., *Reverse remodelling and myocardial recovery in heart failure.* Nat Rev Cardiol, 2018. **15**(2): p. 83-96.
67. Saraon, T. and Katz, S.D., *Reverse Remodeling in Systolic Heart Failure.* Cardiol Rev, 2015. **23**(4): p. 173-81.
68. Aimo, A., Gaggin, H.K., Barison, A., Emdin, M., and Januzzi, J.L., *Imaging, Biomarker, and Clinical Predictors of Cardiac Remodeling in Heart Failure With Reduced Ejection Fraction.* JACC: Heart Failure, 2019. **7**(9): p. 782-794.
69. Nicolas, J.M., Fernandez-Sola, J., Estruch, R*., et al.*, *The effect of controlled drinking in alcoholic cardiomyopathy.* Ann Intern Med, 2002. **136**(3): p. 192-200.
70. Patel, H., Madanieh, R., Kosmas, C.E., Vatti, S.K., and Vittorio, T.J., *Reversible Cardiomyopathies.* Clin Med Insights Cardiol, 2015. **9**(Suppl 2): p. 7-14.
71. Reis Filho, J.R., Cardoso, J.N., Cardoso, C.M., and Pereira-Barretto, A.C., *Reverse Cardiac Remodeling: A Marker of Better Prognosis in Heart Failure.* Arq Bras Cardiol, 2015. **104**(6): p. 502-6.
72. Tanabe, K. and Sakamoto, T., *Heart failure with recovered ejection fraction.* J Echocardiogr, 2019. **17**(1): p. 5-9.
73. Rahmouni, H.W., Kirkpatrick, J.N., and St John Sutton, M.G., *Effects of cardiac resynchronization therapy on ventricular remodeling.* Curr Heart Fail Rep, 2008. **5**(1): p. 25-30.
74. Prinzen, F.W., Cheriex, E.C., Delhaas, T*., et al.*, *Asymmetric thickness of the left ventricular wall resulting from asynchronous electric activation: a study in dogs with ventricular pacing and in patients with left bundle branch block.* Am Heart J, 1995. **130**(5): p. 1045-53.
75. van Oosterhout, M.F., Prinzen, F.W., Arts, T*., et al.*, *Asynchronous electrical activation induces asymmetrical hypertrophy of the left ventricular wall.* Circulation, 1998. **98**(6): p. 588-95.
76. Jaffe, L.M. and Morin, D.P., *Cardiac resynchronization therapy: history, present status, and future directions.* Ochsner J, 2014. **14**(4): p. 596-607.
77. Vernooy, K., Verbeek, X.A., Peschar, M*., et al.*, *Left bundle branch block induces ventricular remodelling and functional septal hypoperfusion.* Eur Heart J, 2005. **26**(1): p. 91-8.
78. Aiba, T., Hesketh, G.G., Barth, A.S*., et al.*, *Electrophysiological consequences of dyssynchronous heart failure and its restoration by resynchronization therapy.* Circulation, 2009. **119**(9): p. 1220-30.

79. Barth, A.S., Aiba, T., Halperin, V.*, et al.*, *Cardiac resynchronization therapy corrects dyssynchrony-induced regional gene expression changes on a genomic level.* Circ Cardiovasc Genet, 2009. **2**(4): p. 371-8.
80. Vernooy, K., Cornelussen, R.N., Verbeek, X.A.*, et al.*, *Cardiac resynchronization therapy cures dyssynchronopathy in canine left bundle-branch block hearts.* Eur Heart J, 2007. **28**(17): p. 2148-55.
81. Steendijk, P., Tulner, S.A., Bax, J.J.*, et al.*, *Hemodynamic effects of long-term cardiac resynchronization therapy: analysis by pressure-volume loops.* Circulation, 2006. **113**(10): p. 1295-304.
82. Sutton, M.G., Plappert, T., Hilpisch, K.E.*, et al.*, *Sustained reverse left ventricular structural remodeling with cardiac resynchronization at one year is a function of etiology: quantitative Doppler echocardiographic evidence from the Multicenter InSync Randomized Clinical Evaluation (MIRACLE).* Circulation, 2006. **113**(2): p. 266-72.
83. Prinzen, F.W. and Auricchio, A., *The "missing" link between acute hemodynamic effect and clinical response.* J Cardiovasc Transl Res, 2012. **5**(2): p. 188-95.
84. Mastenbroek, M.H., Van't Sant, J., Versteeg, H.*, et al.*, *Relationship Between Reverse Remodeling and Cardiopulmonary Exercise Capacity in Heart Failure Patients Undergoing Cardiac Resynchronization Therapy.* Journal of Cardiac Failure, 2016. **22**(5): p. 385-394.
85. Duchenne, J., Turco, A., Unlu, S.*, et al.*, *Left Ventricular Remodeling Results in Homogenization of Myocardial Work Distribution.* Circ Arrhythm Electrophysiol, 2019. **12**(5): p. e007224.
86. Cho, H., Barth, A.S., and Tomaselli, G.F., *Basic science of cardiac resynchronization therapy: molecular and electrophysiological mechanisms.* Circ Arrhythm Electrophysiol, 2012. **5**(3): p. 594-603.
87. Kirk, J.A. and Kass, D.A., *Cellular and Molecular Aspects of Dyssynchrony and Resynchronization.* Card Electrophysiol Clin, 2015. **7**(4): p. 585-97.
88. Sohaib, S.M., Chen, Z., Whinnett, Z.I.*, et al.*, *Meta-analysis of symptomatic response attributable to the pacing component of cardiac resynchronization therapy.* Eur J Heart Fail, 2013. **15**(12): p. 1419-28.
89. Daubert, C., Behar, N., Martins, R.P., Mabo, P., and Leclercq, C., *Avoiding non-responders to cardiac resynchronization therapy: a practical guide.* Eur Heart J, 2017. **38**(19): p. 1463-1472.
90. Rickard, J., Cheng, A., Spragg, D.*, et al.*, *Durability of the survival effect of cardiac resynchronization therapy by level of left ventricular functional improvement: fate of "nonresponders".* Heart Rhythm, 2014. **11**(3): p. 412-6.
91. Ypenburg, C., van Bommel, R.J., Borleffs, C.J.*, et al.*, *Long-term prognosis after cardiac resynchronization therapy is related to the extent of left ventricular reverse remodeling at midterm follow-up.* J Am Coll Cardiol, 2009. **53**(6): p. 483-90.
92. Cleland, J.G., Daubert, J.C., Erdmann, E.*, et al.*, *The effect of cardiac resynchronization on morbidity and mortality in heart failure.* N Engl J Med, 2005. **352**(15): p. 1539-49.
93. Fornwalt, B.K., Sprague, W.W., BeDell, P.*, et al.*, *Agreement Is Poor Among Current Criteria Used to Define Response to Cardiac Resynchronization Therapy.* Circulation, 2010. **121**(18): p. 1985-1991.

94. Sieniewicz, B.J., Gould, J., Porter, B.*, et al.*, *Understanding non-response to cardiac resynchronisation therapy: common problems and potential solutions.* Heart Fail Rev, 2019. **24**(1): p. 41-54.
95. Daubert, J.C., Saxon, L., P.B., A.*, et al.*, *2012 EHRA/HRS expert consensus statement on cardiac resynchronization therapy in heart failure: implant and follow-up recommendations and management.* EP Europace, 2012. **14**(9): p. 1236-1286.
96. Varma, N., Boehmer, J., Bhargava, K.*, et al.*, *Evaluation, Management, and Outcomes of Patients Poorly Responsive to Cardiac Resynchronization Device Therapy.* J Am Coll Cardiol, 2019. **74**(21): p. 2588-2603.
97. Steffel, J., Milosevic, G., Hurlimann, A.*, et al.*, *Characteristics and long-term outcome of echocardiographic super-responders to cardiac resynchronisation therapy: 'real world' experience from a single tertiary care centre.* Heart, 2011. **97**(20): p. 1668-74.
98. Steffel, J. and Ruschitzka, F., *Superresponse to cardiac resynchronization therapy.* Circulation, 2014. **130**(1): p. 87-90.
99. Oka, T., Inoue, K., Tanaka, K.*, et al.*, *Duration of reverse remodeling response to cardiac resynchronization therapy: Rates, predictors, and clinical outcomes.* Int J Cardiol, 2017. **243**(1874-1754 (Electronic)): p. 340-346.
100. Gold, M.R., Rickard, J., Daubert, J.C., Zimmerman, P., and Linde, C., *Redefining the Classifications of Response to Cardiac Resynchronization Therapy: Results From the REVERSE Study.* JACC Clin Electrophysiol, 2021. **7**(7): p. 871-880.
101. Coppola, G., Ciaramitaro, G., Stabile, G.*, et al.*, *Magnitude of QRS duration reduction after biventricular pacing identifies responders to cardiac resynchronization therapy.* Int J Cardiol, 2016. **221**(1874-1754 (Electronic)): p. 450-5.
102. Bazoukis, G., Naka, K.K., Alsheikh-Ali, A.*, et al.*, *Association of QRS narrowing with response to cardiac resynchronization therapy-a systematic review and meta-analysis of observational studies.* Heart Fail Rev, 2020. **25**(5): p. 745-756.
103. Rickard, J., Popovic, Z., Verhaert, D.*, et al.*, *The QRS narrowing index predicts reverse left ventricular remodeling following cardiac resynchronization therapy.* Pacing Clin Electrophysiol, 2011. **34**(5): p. 604-11.
104. Hsing, J.M., Selzman, K.A., Leclercq, C.*, et al.*, *Paced left ventricular QRS width and ECG parameters predict outcomes after cardiac resynchronization therapy: PROSPECT-ECG substudy.* Circ Arrhythm Electrophysiol, 2011. **4**(6): p. 851-7.
105. Lecoq, G., Leclercq, C., Leray, E.*, et al.*, *Clinical and electrocardiographic predictors of a positive response to cardiac resynchronization therapy in advanced heart failure.* Eur Heart J, 2005. **26**(11): p. 1094-100.
106. Bonakdar, H.R., Jorat, M.V., Fazelifar, A.F.*, et al.*, *Prediction of response to cardiac resynchronization therapy using simple electrocardiographic and echocardiographic tools.* Europace, 2009. **11**(10): p. 1330-7.
107. Coverstone, E., Sheehy, J., Kleiger, R.E., and Smith, T.W., *The postimplantation electrocardiogram predicts clinical response to cardiac resynchronization therapy.* Pacing Clin Electrophysiol, 2015. **38**(5): p. 572-80.
108. Bode, W.D., Bode, M.F., Gettes, L.*, et al.*, *Prominent R wave in ECG lead V1 predicts improvement of left ventricular ejection fraction after cardiac resynchronization therapy in patients with or without left bundle branch block.* Heart Rhythm, 2015. **12**(10): p. 2141-2147.

109. Zusterzeel, R., Selzman, K.A., Sanders, W.E*., et al.*, *Toward Sex-Specific Guidelines for Cardiac Resynchronization Therapy?* J Cardiovasc Transl Res, 2016. **9**(1): p. 12-22.
110. Zabarovskaja, S., Gadler, F., Braunschweig, F*., et al.*, *Women have better long-term prognosis than men after cardiac resynchronization therapy.* Europace, 2012. **14**(8): p. 1148-55.
111. Zusterzeel, R., Curtis, J.P., Canos, D.A*., et al.*, *Sex-specific mortality risk by QRS morphology and duration in patients receiving CRT: results from the NCDR.* J Am Coll Cardiol, 2014. **64**(9): p. 887-94.
112. Leyva, F., Qiu, T., Zegard, A*., et al.*, *Sex-Specific Differences in Survival and Heart Failure Hospitalization After Cardiac Resynchronization Therapy With or Without Defibrillation.* Journal of the American Heart Association, 2019. **8**(22): p. e013485-e013485.
113. Zusterzeel, R., Spatz, E.S., Curtis, J.P*., et al.*, *Cardiac resynchronization therapy in women versus men: observational comparative effectiveness study from the National Cardiovascular Data Registry.* Circ Cardiovasc Qual Outcomes, 2015. **8**(2 Suppl 1): p. S4-11.
114. Zusterzeel, R., Selzman, K.A., Sanders, W.E*., et al.*, *Cardiac resynchronization therapy in women: US Food and Drug Administration meta-analysis of patient-level data.* JAMA Intern Med, 2014. **174**(8): p. 1340-8.
115. Verbrugge, F.H., Dupont, M., Rivero-Ayerza, M*., et al.*, *Comorbidity significantly affects clinical outcome after cardiac resynchronization therapy regardless of ventricular remodeling.* J Card Fail, 2012. **18**(11): p. 845-53.
116. Bazoukis, G., Letsas, K.P., Korantzopoulos, P*., et al.*, *Impact of baseline renal function on all-cause mortality in patients who underwent cardiac resynchronization therapy: A systematic review and meta-analysis.* J Arrhythm, 2017. **33**(5): p. 417-423.
117. Ghali, J.K., Boehmer, J., Feldman, A.M*., et al.*, *Influence of diabetes on cardiac resynchronization therapy with or without defibrillator in patients with advanced heart failure.* J Card Fail, 2007. **13**(9): p. 769-73.
118. George, J., Barsheshet, A., Moss, A.J*., et al.*, *Effectiveness of cardiac resynchronization therapy in diabetic patients with ischemic and nonischemic cardiomyopathy.* Ann Noninvasive Electrocardiol, 2012. **17**(1): p. 14-21.
119. Sun, H., Guan, Y., Wang, L*., et al.*, *Influence of diabetes on cardiac resynchronization therapy in heart failure patients: a meta-analysis.* BMC Cardiovasc Disord, 2015. **15**: p. 25.
120. Echouffo-Tcheugui, J.B., Masoudi, F.A., Bao, H., Spatz, E.S., and Fonarow, G.C., *Diabetes Mellitus and Outcomes of Cardiac Resynchronization With Implantable Cardioverter-Defibrillator Therapy in Older Patients With Heart Failure.* Circ Arrhythm Electrophysiol, 2016. **9**(8).
121. Shah, R.V., Altman, R.K., Park, M.Y*., et al.*, *Usefulness of hemoglobin A(1c) to predict outcome after cardiac resynchronization therapy in patients with diabetes mellitus and heart failure.* Am J Cardiol, 2012. **110**(5): p. 683-8.
122. Mangiavacchi, M., Gasparini, M., Genovese, S*., et al.*, *Insulin-treated type 2 diabetes is associated with a decreased survival in heart failure patients after cardiac resynchronization therapy.* Pacing Clin Electrophysiol, 2008. **31**(11): p. 1425-32.

123. Martens, P., Verbrugge, F., Nijst, P.*, et al.*, *Impact of Iron Deficiency on Response to and Remodeling After Cardiac Resynchronization Therapy.* Am J Cardiol, 2017. **119**(1): p. 65-70.
124. Dauw, J., Martens, P., and Mullens, W., *CRT Optimization: What Is New? What Is Necessary?* Curr Treat Options Cardiovasc Med, 2019. **21**(9): p. 45.
125. Martens, P., Dupont, M., Dauw, J.*, et al.*, *The effect of intravenous ferric carboxymaltose on cardiac reverse remodelling following cardiac resynchronization therapy—the IRON-CRT trial.* European Heart Journal, 2021. **42**(48): p. 4905-4914.
126. Cleland, J., Freemantle, N., Ghio, S.*, et al.*, *Predicting the long-term effects of cardiac resynchronization therapy on mortality from baseline variables and the early response a report from the CARE-HF (Cardiac Resynchronization in Heart Failure) Trial.* J Am Coll Cardiol, 2008. **52**(6): p. 438-45.
127. Goldenberg, I., Moss, A.J., Hall, W.J.*, et al.*, *Predictors of response to cardiac resynchronization therapy in the Multicenter Automatic Defibrillator Implantation Trial with Cardiac Resynchronization Therapy (MADIT-CRT).* Circulation, 2011. **124**(14): p. 1527-36.
128. Adelstein, E.C. and Saba, S., *Scar burden by myocardial perfusion imaging predicts echocardiographic response to cardiac resynchronization therapy in ischemic cardiomyopathy.* American Heart Journal, 2007. **153**(1): p. 105-112.
129. White, J.A., Yee, R., Yuan, X.*, et al.*, *Delayed Enhancement Magnetic Resonance Imaging Predicts Response to Cardiac Resynchronization Therapy in Patients With Intraventricular Dyssynchrony.* Journal of the American College of Cardiology, 2006. **48**(10): p. 1953-1960.
130. Chalil, S., Foley, P.W.X., Muyhaldeen, S.A.*, et al.*, *Late gadolinium enhancement-cardiovascular magnetic resonance as a predictor of response to cardiac resynchronization therapy in patients with ischaemic cardiomyopathy.* EP Europace, 2007. **9**(11): p. 1031-1037.
131. Tian, Y., Zhang, P., Li, X.*, et al.*, *True complete left bundle branch block morphology strongly predicts good response to cardiac resynchronization therapy.* Europace, 2013. **15**(10): p. 1499-506.
132. Cunnington, C., Kwok, C.S., Satchithananda, D.K.*, et al.*, *Cardiac resynchronisation therapy is not associated with a reduction in mortality or heart failure hospitalisation in patients with non-left bundle branch block QRS morphology: meta-analysis of randomised controlled trials.* Heart, 2015. **101**(18): p. 1456-+.
133. Sipahi, I., Chou, J.C., Hyden, M.*, et al.*, *Effect of QRS morphology on clinical event reduction with cardiac resynchronization therapy: meta-analysis of randomized controlled trials.* Am Heart J, 2012. **163**(2): p. 260-7 e3.
134. Birnie, D.H., Ha, A., Higginson, L.*, et al.*, *Impact of QRS morphology and duration on outcomes after cardiac resynchronization therapy: Results from the Resynchronization-Defibrillation for Ambulatory Heart Failure Trial (RAFT).* Circ Heart Fail, 2013. **6**(6): p. 1190-8.
135. Sipahi, I., Carrigan, T.P., Rowland, D.Y., Stambler, B.S., and Fang, J.C., *Impact of QRS duration on clinical event reduction with cardiac resynchronization therapy: meta-analysis of randomized controlled trials.* Arch Intern Med, 2011. **171**(16): p. 1454-62.
136. Gasparini, M., Leclercq, C., Yu, C.M.*, et al.*, *Absolute survival after cardiac resynchronization therapy according to baseline QRS duration: a multinational 10-year*

experience: data from the Multicenter International CRT Study. Am Heart J, 2014. **167**(2): p. 203-209 e1.
137. Sundaram, V., Sahadevan, J., Waldo, A.L.*, et al.*, *Implantable Cardioverter-Defibrillators With Versus Without Resynchronization Therapy in Patients With a QRS Duration >180 ms.* J Am Coll Cardiol, 2017. **69**(16): p. 2026-2036.
138. Kutyifa, V., Kosztin, A., Klein, H.U.*, et al.*, *Left Ventricular Lead Location and Long-Term Outcomes in Cardiac Resynchronization Therapy Patients.* JACC Clin Electrophysiol, 2018. **4**(11): p. 1410-1420.
139. Thebault, C., Donal, E., Meunier, C.*, et al.*, *Sites of left and right ventricular lead implantation and response to cardiac resynchronization therapy observations from the REVERSE trial.* Eur Heart J, 2012. **33**(21): p. 2662-71.
140. Behon, A., Schwertner, W.R., Merkel, E.D.*, et al.*, *Lateral left ventricular lead position is superior to posterior position in long-term outcome of patients who underwent cardiac resynchronization therapy.* ESC Heart Fail, 2020. **7**(6): p. 3374-3382.
141. Gold, M.R., Birgersdotter-Green, U., Singh, J.P.*, et al.*, *The relationship between ventricular electrical delay and left ventricular remodelling with cardiac resynchronization therapy.* European Heart Journal, 2011. **32**(20): p. 2516-2524.
142. Roubicek, T., Wichterle, D., Kucera, P.*, et al.*, *Left Ventricular Lead Electrical Delay Is a Predictor of Mortality in Patients With Cardiac Resynchronization Therapy.* Circulation-Arrhythmia and Electrophysiology, 2015. **8**(5): p. 1113-1121.
143. Gold, M.R., Singh, J.P., Ellenbogen, K.A.*, et al.*, *Interventricular Electrical Delay Is Predictive of Response to Cardiac Resynchronization Therapy.* JACC Clin Electrophysiol, 2016. **2**(4): p. 438-447.
144. Gold, M.R., Yu, Y., Wold, N., and Day, J.D., *The role of interventricular conduction delay to predict clinical response with cardiac resynchronization therapy.* Heart Rhythm, 2017. **14**(12): p. 1748-1755.
145. Behar, J.M., Bostock, J., Li, A.P.Z.*, et al.*, *Cardiac Resynchronization Therapy Delivered Via a Multipolar Left Ventricular Lead is Associated with Reduced Mortality and Elimination of Phrenic Nerve Stimulation: Long-Term Follow-Up from a Multicenter Registry.* Journal of Cardiovascular Electrophysiology, 2015. **26**(5): p. 540-546.
146. Behar, J.M., Chin, H.M.S., Fearn, S.*, et al.*, *Cost-Effectiveness Analysis of Quadripolar Versus Bipolar Left Ventricular Leads for Cardiac Resynchronization Defibrillator Therapy in a Large, Multicenter UK Registry.* JACC: Clinical Electrophysiology, 2017. **3**(2): p. 107-116.
147. Leyva, F., Zegard, A., Qiu, T.*, et al.*, *Cardiac Resynchronization Therapy Using Quadripolar Versus Non-Quadripolar Left Ventricular Leads Programmed to Biventricular Pacing With Single-Site Left Ventricular Pacing: Impact on Survival and Heart Failure Hospitalization.* Journal of the American Heart Association, 2017. **6**(10): p. e007026.
148. Robertson, C., Duffey, O., Tang, P.-T.*, et al.*, *An active fixation quadripolar left ventricular lead for cardiac resynchronization therapy with reduced postoperative complication rates.* Journal of Cardiovascular Electrophysiology, 2021: p. 1-6.
149. Khan, F.Z., Virdee, M.S., Palmer, C.R.*, et al.*, *Targeted left ventricular lead placement to guide cardiac resynchronization therapy: the TARGET study: a randomized, controlled trial.* J Am Coll Cardiol, 2012. **59**(17): p. 1509-18.

150. Saba, S., Marek, J., Schwartzman, D.*, et al.*, *Echocardiography-guided left ventricular lead placement for cardiac resynchronization therapy: results of the Speckle Tracking Assisted Resynchronization Therapy for Electrode Region trial.* Circ Heart Fail, 2013. **6**(3): p. 427-34.
151. Taylor, R.J., Umar, F., Panting, J.R., Stegemann, B., and Leyva, F., *Left ventricular lead position, mechanical activation, and myocardial scar in relation to left ventricular reverse remodeling and clinical outcomes after cardiac resynchronization therapy: A feature-tracking and contrast-enhanced cardiovascular magnetic resonance study.* Heart Rhythm, 2016. **13**(2): p. 481-489.
152. Daoulah, A., Alsheikh-Ali, A.A., Al-Faifi, S.M.*, et al.*, *Cardiac resynchronization therapy in patients with postero-lateral scar by cardiac magnetic resonance: A systematic review and meta-analysis.* J Electrocardiol, 2015. **48**(5): p. 783-90.
153. Leyva, F., *The Role of Cardiovascular Magnetic Resonance in Cardiac Resynchronization Therapy.* Heart Failure Clinics, 2017. **13**(1): p. 63-77.
154. Sommer, A., Kronborg, M.B., Norgaard, B.L.*, et al.*, *Multimodality imaging-guided left ventricular lead placement in cardiac resynchronization therapy: a randomized controlled trial.* Eur J Heart Fail, 2016. **18**(11): p. 1365-1374.
155. Beshai, J.F., Grimm, R.A., Nagueh, S.F.*, et al.*, *Cardiac-resynchronization therapy in heart failure with narrow QRS complexes.* N Engl J Med, 2007. **357**(24): p. 2461-71.
156. Donahue, T., Niazi, I., Leon, A.*, et al.*, *Acute and chronic response to CRT in narrow QRS patients.* J Cardiovasc Transl Res, 2012. **5**(2): p. 232-41.
157. Ruschitzka, F., Abraham, W.T., Singh, J.P.*, et al.*, *Cardiac-resynchronization therapy in heart failure with a narrow QRS complex.* N Engl J Med, 2013. **369**(15): p. 1395-405.
158. Chung, E.S., Leon, A.R., Tavazzi, L.*, et al.*, *Results of the Predictors of Response to CRT (PROSPECT) trial.* Circulation, 2008. **117**(20): p. 2608-16.
159. Yu, C.M., Sanderson, J.E., and Gorcsan, J., 3rd, *Echocardiography, dyssynchrony, and the response to cardiac resynchronization therapy.* Eur Heart J, 2010. **31**(19): p. 2326-37.
160. Vijayaraman, P. and Subzposh, F.A., *His-Bundle Pacing and LV Endocardial Pacing as Alternatives to Traditional Cardiac Resynchronization Therapy.* Curr Cardiol Rep, 2018. **20**(11): p. 109.
161. Behar, J.M., Jackson, T., Hyde, E.*, et al.*, *Optimized Left Ventricular Endocardial Stimulation Is Superior to Optimized Epicardial Stimulation in Ischemic Patients With Poor Response to Cardiac Resynchronization Therapy: A Combined Magnetic Resonance Imaging, Electroanatomic Contact Mapping, and Hemodynamic Study to Target Endocardial Lead Placement.* JACC Clin Electrophysiol, 2016. **2**(7): p. 799-809.
162. Gamble, J.H.P., Herring, N., Ginks, M.*, et al.*, *Endocardial left ventricular pacing for cardiac resynchronization: systematic review and meta-analysis.* Europace, 2018. **20**(1): p. 73-81.
163. Upadhyay, G.A., Vijayaraman, P., Nayak, H.M.*, et al.*, *His Corrective Pacing or Biventricular Pacing for Cardiac Resynchronization in Heart Failure.* J Am Coll Cardiol, 2019. **74**(1): p. 157-159.
164. Huang, W., Su, L., Wu, S.*, et al.*, *A Novel Pacing Strategy With Low and Stable Output: Pacing the Left Bundle Branch Immediately Beyond the Conduction Block.* Can J Cardiol, 2017. **33**(12): p. 1736 e1-1736 e3.

165. Wu, S., Su, L., Vijayaraman, P.*, et al.*, *Left Bundle Branch Pacing for Cardiac Resynchronization Therapy: Nonrandomized On-Treatment Comparison With His Bundle Pacing and Biventricular Pacing.* Can J Cardiol, 2021. **37**(2): p. 319-328.
166. Liu, J., Sun, F., Wang, Z.*, et al.*, *Left Bundle Branch Area Pacing vs. Biventricular Pacing for Cardiac Resynchronization Therapy: A Meta-Analysis.* Front Cardiovasc Med, 2021. **8**: p. 669301.
167. Ravi, V., Hanifin, J.L., Larsen, T.*, et al.*, *Pros and Cons of Left Bundle Branch Pacing: A Single-Center Experience.* Circ Arrhythm Electrophysiol, 2020. **13**(12): p. e008874.
168. Arora, V. and Suri, P., *Physiological Pacing: A New Road to Future.* Indian Journal of Clinical Cardiology, 2021. **2**(1): p. 32-43.
169. Sidhu, B.S., Porter, B., Gould, J.*, et al.*, *Leadless left ventricular endocardial pacing in nonresponders to conventional cardiac resynchronization therapy.* Pacing Clin Electrophysiol, 2020. **43**(9): p. 966-973.
170. Brabham, W.W. and Gold, M.R., *The role of AV and VV optimization for CRT.* Journal of Arrhythmia, 2013. **29**(3): p. 153-161.
171. Delnoy, P.P., Ritter, P., Naegele, H.*, et al.*, *Association between frequent cardiac resynchronization therapy optimization and long-term clinical response: a post hoc analysis of the Clinical Evaluation on Advanced Resynchronization (CLEAR) pilot study.* Europace, 2013. **15**(8): p. 1174-1181.
172. Luceri, R.M., Brownstein, S.L., Vardeman, L., and Goldstein, S., *PR interval behavior during exercise: implications for physiological pacemakers.* Pacing Clin Electrophysiol, 1990. **13**(12 Pt 2): p. 1719-23.
173. Shanmugam, N., Prada-Delgado, O., Campos, A.G.*, et al.*, *Rate-adaptive AV delay and exercise performance following cardiac resynchronization therapy.* Heart Rhythm, 2012. **9**(11): p. 1815-21.
174. Ritter, P., Delnoy, P.P., Padeletti, L.*, et al.*, *A randomized pilot study of optimization of cardiac resynchronization therapy in sinus rhythm patients using a peak endocardial acceleration sensor vs. standard methods.* Europace, 2012. **14**(9): p. 1324-33.
175. Brugada, J., Delnoy, P.P., Brachmann, J.*, et al.*, *Contractility sensor-guided optimization of cardiac resynchronization therapy: results from the RESPOND-CRT trial.* Eur Heart J, 2017. **38**(10): p. 730-738.
176. Burri, H., Prinzen, F.W., Gasparini, M., and Leclercq, C., *Left univentricular pacing for cardiac resynchronization therapy.* Europace, 2017. **19**(6): p. 912-919.
177. Pappone, C., Calovic, Z., Vicedomini, G.*, et al.*, *Improving cardiac resynchronization therapy response with multipoint left ventricular pacing: Twelve-month follow-up study.* Heart Rhythm, 2015. **12**(6): p. 1250-8.
178. Rinaldi, C.A., Burri, H., Thibault, B.*, et al.*, *A review of multisite pacing to achieve cardiac resynchronization therapy.* Europace, 2015. **17**(1): p. 7-17.
179. Zanon, F., Marcantoni, L., Baracca, E.*, et al.*, *Optimization of left ventricular pacing site plus multipoint pacing improves remodeling and clinical response to cardiac resynchronization therapy at 1 year.* Heart Rhythm, 2016. **13**(8): p. 1644-51.
180. Forleo, G.B., Santini, L., Giammaria, M.*, et al.*, *Multipoint pacing via a quadripolar left-ventricular lead: preliminary results from the Italian registry on multipoint left-ventricular pacing in cardiac resynchronization therapy (IRON-MPP).* Europace, 2017. **19**(7): p. 1170-1177.

181. Barold, S.S. and Herweg, B., *Cardiac Resynchronization in Patients with Atrial Fibrillation.* J Atr Fibrillation, 2015. **8**(4): p. 1383.
182. Koplan, B.A., Kaplan, A.J., Weiner, S.*, et al.*, *Heart failure decompensation and all-cause mortality in relation to percent biventricular pacing in patients with heart failure: is a goal of 100% biventricular pacing necessary?* J Am Coll Cardiol, 2009. **53**(4): p. 355-360.
183. Lubitz, S.A. and Singh, J.P., *Biventricular pacing: more is better!* Eur Heart J, 2015. **36**(7): p. 407-9.
184. Hayes, D.L., Boehmer, J.P., Day, J.D.*, et al.*, *Cardiac resynchronization therapy and the relationship of percent biventricular pacing to symptoms and survival.* Heart Rhythm, 2011. **8**(9): p. 1469-75.
185. Ousdigian, K.T., Borek, P.P., Koehler, J.L.*, et al.*, *The epidemic of inadequate biventricular pacing in patients with persistent or permanent atrial fibrillation and its association with mortality.* Circ Arrhythm Electrophysiol, 2014. **7**(3): p. 370-6.
186. Kamath, G.S., Cotiga, D., Koneru, J.N.*, et al.*, *The utility of 12-lead Holter monitoring in patients with permanent atrial fibrillation for the identification of nonresponders after cardiac resynchronization therapy.* J Am Coll Cardiol, 2009. **53**(12): p. 1050-5.
187. Gasparini, M., Galimberti, P., and Ceriotti, C., *The importance of increased percentage of biventricular pacing to improve clinical outcomes in patients receiving cardiac resynchronization therapy.* Curr Opin Cardiol, 2013. **28**(1): p. 50-4.
188. Gasparini, M., Leclercq, C., Lunati, M.*, et al.*, *Cardiac resynchronization therapy in patients with atrial fibrillation: the CERTIFY study (Cardiac Resynchronization Therapy in Atrial Fibrillation Patients Multinational Registry).* JACC Heart Fail, 2013. **1**(6): p. 500-7.
189. Mullens, W., Grimm, R.A., Verga, T.*, et al.*, *Insights from a cardiac resynchronization optimization clinic as part of a heart failure disease management program.* J Am Coll Cardiol, 2009. **53**(9): p. 765-73.
190. Lakkireddy, D., Di Biase, L., Ryschon, K.*, et al.*, *Radiofrequency ablation of premature ventricular ectopy improves the efficacy of cardiac resynchronization therapy in nonresponders.* J Am Coll Cardiol, 2012. **60**(16): p. 1531-9.
191. Houthuizen, P., Bracke, F.A., and van Gelder, B.M., *Atrioventricular and interventricular delay optimization in cardiac resynchronization therapy: physiological principles and overview of available methods.* Heart Fail Rev, 2011. **16**(3): p. 263-76.
192. Raphael, C.E., Kyriacou, A., Jones, S.*, et al.*, *Multinational evaluation of the interpretability of the iterative method of optimisation of AV delay for CRT.* Int J Cardiol, 2013. **168**(1): p. 407-13.
193. Pujol-Lopez, M., San Antonio, R., Mont, L.*, et al.*, *Electrocardiographic optimization techniques in resynchronization therapy.* Europace, 2019. **21**(9): p. 1286-1296.
194. Ellenbogen, K.A., Gold, M.R., Meyer, T.E.*, et al.*, *Primary results from the SmartDelay determined AV optimization: a comparison to other AV delay methods used in cardiac resynchronization therapy (SMART-AV) trial: a randomized trial comparing empirical, echocardiography-guided, and algorithmic atrioventricular delay programming in cardiac resynchronization therapy.* Circulation, 2010. **122**(25): p. 2660-8.
195. Sun, J.P., Lee, A.P., Grimm, R.A.*, et al.*, *Optimisation of atrioventricular delay during exercise improves cardiac output in patients stabilised with cardiac resynchronisation therapy.* Heart, 2012. **98**(1): p. 54-9.

196. Lee, K.L., Burnes, J.E., Mullen, T.J.*, et al.*, *Avoidance of right ventricular pacing in cardiac resynchronization therapy improves right ventricular hemodynamics in heart failure patients.* J Cardiovasc Electrophysiol, 2007. **18**(5): p. 497-504.
197. Matusik, P.T., *Cardiac Resynchronization Therapy: Potential of Left Ventricular Pacing.* Eur Heart J, 2019. **40**(21): p. 1667-1669.
198. Gasparini, M., Bocchiardo, M., Lunati, M.*, et al.*, *Comparison of 1-year effects of left ventricular and biventricular pacing in patients with heart failure who have ventricular arrhythmias and left bundle-branch block: the Bi vs Left Ventricular Pacing: an International Pilot Evaluation on Heart Failure Patients with Ventricular Arrhythmias (BELIEVE) multicenter prospective randomized pilot study.* Am Heart J, 2006. **152**(1): p. 155 e1-7.
199. Rao, R.K., Kumar, U.N., Schafer, J.*, et al.*, *Reduced ventricular volumes and improved systolic function with cardiac resynchronization therapy: a randomized trial comparing simultaneous biventricular pacing, sequential biventricular pacing, and left ventricular pacing.* Circulation, 2007. **115**(16): p. 2136-44.
200. Boriani, G., Kranig, W., Donal, E.*, et al.*, *A randomized double-blind comparison of biventricular versus left ventricular stimulation for cardiac resynchronization therapy: the Biventricular versus Left Univentricular Pacing with ICD Back-up in Heart Failure Patients (B-LEFT HF) trial.* Am Heart J, 2010. **159**(6): p. 1052-1058 e1.
201. Sirker, A., Thomas, M., Baker, S.*, et al.*, *Cardiac resynchronization therapy: left or left-and-right for optimal symptomatic effect--the LOLA ROSE study.* Europace, 2007. **9**(10): p. 862-8.
202. Thibault, B., Ducharme, A., Harel, F.*, et al.*, *Left ventricular versus simultaneous biventricular pacing in patients with heart failure and a QRS complex >/=120 milliseconds.* Circulation, 2011. **124**(25): p. 2874-81.
203. Chen, J., Zhuang, X., Liao, L., Liao, X., and Wang, L., *Efficacy of isolated left ventricular and biventricular pacing is differentially associated with baseline QRS duration in chronic heart failure: a meta-analysis of randomized controlled trials.* Heart Fail Rev, 2015. **20**(1): p. 81-8.
204. Liang, Y., Pan, W., Su, Y., and Ge, J., *Meta-analysis of randomized controlled trials comparing isolated left ventricular and biventricular pacing in patients with chronic heart failure.* Am J Cardiol, 2011. **108**(8): p. 1160-5.
205. Waddingham, P.H., Lambiase, P., Muthumala, A., Rowland, E., and Chow, A.W., *Fusion Pacing with Biventricular, Left Ventricular-only and Multipoint Pacing in Cardiac Resynchronisation Therapy: Latest Evidence and Strategies for Use.* Arrhythm Electrophysiol Rev, 2021. **10**(2): p. 91-100.
206. Eschalier, R., Ploux, S., Lumens, J.*, et al.*, *Detailed analysis of ventricular activation sequences during right ventricular apical pacing and left bundle branch block and the potential implications for cardiac resynchronization therapy.* Heart Rhythm, 2015. **12**(1): p. 137-43.
207. Vatasescu, R., Berruezo, A., Mont, L.*, et al.*, *Midterm 'super-response' to cardiac resynchronization therapy by biventricular pacing with fusion: insights from electro-anatomical mapping.* Europace, 2009. **11**(12): p. 1675-82.
208. Arbelo, E., Tolosana, J.M., Trucco, E.*, et al.*, *Fusion-optimized intervals (FOI): a new method to achieve the narrowest QRS for optimization of the AV and VV intervals in*

patients undergoing cardiac resynchronization therapy. J Cardiovasc Electrophysiol, 2014. **25**(3): p. 283-92.
209. Strik, M., van Middendorp, L.B., Houthuizen, P.*, et al.*, *Interplay of electrical wavefronts as determinant of the response to cardiac resynchronization therapy in dyssynchronous canine hearts.* Circ Arrhythm Electrophysiol, 2013. **6**(5): p. 924-31.
210. Trucco, E., Tolosana, J.M., Arbelo, E.*, et al.*, *Improvement of Reverse Remodeling Using Electrocardiogram Fusion-Optimized Intervals in Cardiac Resynchronization Therapy: A Randomized Study.* JACC Clin Electrophysiol, 2018. **4**(2): p. 181-189.
211. Aubert, J.F., Burnier, M., Waeber, B.*, et al.*, *Effects of a nonpressor dose of neuropeptide Y on cardiac output, regional blood flow distribution and plasma renin, vasopressin and catecholamine levels.* J Pharmacol Exp Ther, 1988. **244**(3): p. 1109-15.
212. Birnie, D., Lemke, B., Aonuma, K.*, et al.*, *Clinical outcomes with synchronized left ventricular pacing: analysis of the adaptive CRT trial.* Heart Rhythm, 2013. **10**(9): p. 1368-74.
213. Filippatos, G., Birnie, D., Gold, M.R.*, et al.*, *Rationale and design of the AdaptResponse trial: a prospective randomized study of cardiac resynchronization therapy with preferential adaptive left ventricular-only pacing.* Eur J Heart Fail, 2017. **19**(7): p. 950-957.
214. Varma, N., O'Donnell, D., Bassiouny, M.*, et al.*, *Programming Cardiac Resynchronization Therapy for Electrical Synchrony: Reaching Beyond Left Bundle Branch Block and Left Ventricular Activation Delay.* J Am Heart Assoc, 2018. **7**(3): p. e007489.
215. Thibault, B., Ritter, P., Bode, K.*, et al.*, *Dynamic programming of atrioventricular delay improves electrical synchrony in a multicenter cardiac resynchronization therapy study.* Heart Rhythm, 2019. **16**(7): p. 1047-1056.
216. AlTurki, A., Lima, P.Y., Garcia, D.*, et al.*, *Cardiac resynchronization therapy reprogramming to improve electrical synchrony in patients with existing devices.* J Electrocardiol, 2019. **56**: p. 94-99.
217. Wang, J., Liang, Y., Chen, H.*, et al.*, *Patient-tailored SyncAV algorithm: A novel strategy to improve synchrony and acute hemodynamic response in heart failure patients treated by cardiac resynchronization therapy.* J Cardiovasc Electrophysiol, 2020. **31**(2): p. 512-520.
218. Wang, Z., Li, P., Zhang, B.*, et al.*, *Improvement of LV Reverse Remodeling Using Dynamic Programming of Fusion-Optimized Atrioventricular Intervals in Cardiac Resynchronization Therapy.* Front Cardiovasc Med, 2021. **8**: p. 700424.
219. Varma, N., Hu, Y., Connolly, A.T.*, et al.*, *Gain in real-world cardiac resynchronization therapy efficacy with SyncAV dynamic optimization: Heart failure hospitalizations and costs.* Heart Rhythm, 2021. **18**(9): p. 1577-1585.
220. AlTurki, A., Lima, P.Y., Bernier, M.L.*, et al.*, *Optimization of Chronic Cardiac Resynchronization Therapy Using Fusion Pacing Algorithm Improves Echocardiographic Response.* CJC Open, 2020. **2**(2): p. 62-70.
221. Mokrani, B., Lafitte, S., Deplagne, A.*, et al.*, *Echocardiographic study of the optimal atrioventricular delay at rest and during exercise in recipients of cardiac resynchronization therapy systems.* Heart Rhythm, 2009. **6**(7): p. 972-7.
222. Rider, O.J., Cox, P., Tyler, D., Clarke, K., and Neubauer, S., *Myocardial substrate metabolism in obesity.* Int J Obes (Lond), 2013. **37**(7): p. 972-9.

223. Stanley, W.C., Recchia, F.A., and Lopaschuk, G.D., *Myocardial substrate metabolism in the normal and failing heart.* Physiol Rev, 2005. **85**(3): p. 1093-129.
224. Taegtmeyer, H., Golfman, L., Sharma, S., Razeghi, P., and van Arsdall, M., *Linking gene expression to function: metabolic flexibility in the normal and diseased heart.* Ann N Y Acad Sci, 2004. **1015**(1): p. 202-13.
225. Evans, R.D. and Clarke, K., *Myocardial substrate metabolism in heart disease.* Front Biosci (Schol Ed), 2012. **4**(2): p. 556-80.
226. Fillmore, N. and Lopaschuk, G., *Impact of fatty acid oxidation on cardiac efficiency.* Heart and Metabolism, 2011. **53**: p. 33-37.
227. Stockli, J., Fazakerley, D.J., and James, D.E., *GLUT4 exocytosis.* J Cell Sci, 2011. **124**(Pt 24): p. 4147-59.
228. Greenwell, A.A., Gopal, K., and Ussher, J.R., *Myocardial Energy Metabolism in Non-ischemic Cardiomyopathy.* Front Physiol, 2020. **11**(1191): p. 570421.
229. Bergman, B.C., Tsvetkova, T., Lowes, B., and Wolfel, E.E., *Myocardial glucose and lactate metabolism during rest and atrial pacing in humans.* J Physiol, 2009. **587**(Pt 9): p. 2087-99.
230. Stanley, W.C., Lopaschuk, G.D., Hall, J.L., and McCormack, J.G., *Regulation of myocardial carbohydrate metabolism under normal and ischaemic conditions. Potential for pharmacological interventions.* Cardiovasc Res, 1997. **33**(2): p. 243-57.
231. Gertz, E.W., Wisneski, J.A., Stanley, W.C., and Neese, R.A., *Myocardial substrate utilization during exercise in humans. Dual carbon-labeled carbohydrate isotope experiments.* J Clin Invest, 1988. **82**(6): p. 2017-25.
232. Stanley, W.C., *Myocardial lactate metabolism during exercise.* Med Sci Sports Exerc, 1991. **23**(8): p. 920-4.
233. Hui, S., Ghergurovich, J.M., Morscher, R.J*., et al.*, *Glucose feeds the TCA cycle via circulating lactate.* Nature, 2017. **551**(7678): p. 115-118.
234. Lopaschuk, G.D., Ussher, J.R., Folmes, C.D., Jaswal, J.S., and Stanley, W.C., *Myocardial fatty acid metabolism in health and disease.* Physiol Rev, 2010. **90**(1): p. 207-58.
235. Wisneski, J.A., Gertz, E.W., Neese, R.A., and Mayr, M., *Myocardial metabolism of free fatty acids. Studies with 14C-labeled substrates in humans.* J Clin Invest, 1987. **79**(2): p. 359-66.
236. Ussher, J.R. and Lopaschuk, G.D., *Targeting malonyl CoA inhibition of mitochondrial fatty acid uptake as an approach to treat cardiac ischemia/reperfusion.* Basic Res Cardiol, 2009. **104**(2): p. 203-10.
237. Watson, W.D., Miller, J.J.J., Lewis, A*., et al.*, *Use of cardiac magnetic resonance to detect changes in metabolism in heart failure.* Cardiovascular Diagnosis and Therapy, 2020. **10**(3): p. 583-597.
238. Mitchell, P., *Chemiosmotic coupling in energy transduction: a logical development of biochemical knowledge.* J Bioenerg, 1972. **3**(1): p. 5-24.
239. Wesselink, E., Koekkoek, W.A.C., Grefte, S., Witkamp, R.F., and van Zanten, A.R.H., *Feeding mitochondria: Potential role of nutritional components to improve critical illness convalescence.* Clin Nutr, 2019. **38**(3): p. 982-995.
240. Bertero, E. and Maack, C., *Metabolic remodelling in heart failure.* Nat Rev Cardiol, 2018. **15**(8): p. 457-470.

241. Randle, P.J., Garland, P.B., Hales, C.N., and Newsholme, E.A., *The glucose fatty-acid cycle. Its role in insulin sensitivity and the metabolic disturbances of diabetes mellitus.* Lancet, 1963. **1**(7285): p. 785-9.
242. Hue, L. and Taegtmeyer, H., *The Randle cycle revisited: a new head for an old hat.* Am J Physiol Endocrinol Metab, 2009. **297**(3): p. E578-91.
243. Hardie, D.G. and Carling, D., *The AMP-activated protein kinase--fuel gauge of the mammalian cell?* Eur J Biochem, 1997. **246**(2): p. 259-73.
244. Guzun, R., Kaambre, T., Bagur, R.*, et al.*, *Modular organization of cardiac energy metabolism: energy conversion, transfer and feedback regulation.* Acta Physiol (Oxf), 2015. **213**(1): p. 84-106.
245. Dzeja, P.P., Vitkevicius, K.T., Redfield, M.M., Burnett, J.C., and Terzic, A., *Adenylate kinase-catalyzed phosphotransfer in the myocardium : increased contribution in heart failure.* Circ Res, 1999. **84**(10): p. 1137-43.
246. Pucar, D., Dzeja, P.P., Bast, P.*, et al.*, *Cellular energetics in the preconditioned state: protective role for phosphotransfer reactions captured by 18O-assisted 31P NMR.* J Biol Chem, 2001. **276**(48): p. 44812-9.
247. Abdurrachim, D., Luiken, J.J., Nicolay, K.*, et al.*, *Good and bad consequences of altered fatty acid metabolism in heart failure: evidence from mouse models.* Cardiovasc Res, 2015. **106**(2): p. 194-205.
248. Honka, H., Solis-Herrera, C., Triplitt, C.*, et al.*, *Therapeutic Manipulation of Myocardial Metabolism: JACC State-of-the-Art Review.* J Am Coll Cardiol, 2021. **77**(16): p. 2022-2039.
249. Karwi, Q.G., Uddin, G.M., Ho, K.L., and Lopaschuk, G.D., *Loss of Metabolic Flexibility in the Failing Heart.* Front Cardiovasc Med, 2018. **5**(68): p. 68.
250. How, O.J., Aasum, E., Kunnathu, S.*, et al.*, *Influence of substrate supply on cardiac efficiency, as measured by pressure-volume analysis in ex vivo mouse hearts.* Am J Physiol Heart Circ Physiol, 2005. **288**(6): p. H2979-85.
251. Korvald, C., Elvenes, O.P., and Myrmel, T., *Myocardial substrate metabolism influences left ventricular energetics in vivo.* Am J Physiol Heart Circ Physiol, 2000. **278**(4): p. H1345-51.
252. Simonsen, S. and Kjekshus, J.K., *The effect of free fatty acids on myocardial oxygen consumption during atrial pacing and catecholamine infusion in man.* Circulation, 1978. **58**(3 Pt 1): p. 484-91.
253. Murray, A.J., Anderson, R.E., Watson, G.C., Radda, G.K., and Clarke, K., *Uncoupling proteins in human heart.* Lancet, 2004. **364**(9447): p. 1786-8.
254. Boehm, E.A., Jones, B.E., Radda, G.K., Veech, R.L., and Clarke, K., *Increased uncoupling proteins and decreased efficiency in palmitate-perfused hyperthyroid rat heart.* Am J Physiol Heart Circ Physiol, 2001. **280**(3): p. H977-83.
255. Jaswal, J.S., Keung, W., Wang, W., Ussher, J.R., and Lopaschuk, G.D., *Targeting fatty acid and carbohydrate oxidation--a novel therapeutic intervention in the ischemic and failing heart.* Biochim Biophys Acta, 2011. **1813**(7): p. 1333-50.
256. Abdul Kadir, A., Clarke, K., and Evans, R.D., *Cardiac ketone body metabolism.* Biochim Biophys Acta Mol Basis Dis, 2020. **1866**(6): p. 165739.
257. Veech, R.L., *The therapeutic implications of ketone bodies: the effects of ketone bodies in pathological conditions: ketosis, ketogenic diet, redox states, insulin resistance, and*

mitochondrial metabolism. Prostaglandins Leukot Essent Fatty Acids, 2004. **70**(3): p. 309-19.
258. Cotter, D.G., Schugar, R.C., and Crawford, P.A., *Ketone body metabolism and cardiovascular disease.* Am J Physiol Heart Circ Physiol, 2013. **304**(8): p. H1060-76.
259. Kashiwaya, Y., King, M.T., and Veech, R.L., *Substrate signaling by insulin: a ketone bodies ratio mimics insulin action in heart.* Am J Cardiol, 1997. **80**(3A): p. 50A-64A.
260. Lopaschuk, G.D. and Ussher, J.R., *Evolving Concepts of Myocardial Energy Metabolism: More Than Just Fats and Carbohydrates.* Circ Res, 2016. **119**(11): p. 1173-1176.
261. Qureshi, W.T. and Nasir, U.B., *Principals and clinical applications of magnetic resonance cardiac spectroscopy in heart failure.* Heart Fail Rev, 2017. **22**(4): p. 491-499.
262. Ingwall, J.S. and Weiss, R.G., *Is the failing heart energy starved? On using chemical energy to support cardiac function.* Circ Res, 2004. **95**(2): p. 135-45.
263. Abdurrachim, D. and Prompers, J.J., *Evaluation of cardiac energetics by non-invasive (31)P magnetic resonance spectroscopy.* Biochim Biophys Acta Mol Basis Dis, 2018. **1864**(5 Pt B): p. 1939-1948.
264. Balaban, R.S., Kantor, H.L., Katz, L.A., and Briggs, R.W., *Relation between work and phosphate metabolite in the in vivo paced mammalian heart.* Science, 1986. **232**(4754): p. 1121-3.
265. Schaefer, S., Schwartz, G.G., Steinman, S.K*., et al.*, *Metabolic response of the human heart to inotropic stimulation: in vivo phosphorus-31 studies of normal and cardiomyopathic myocardium.* Magn Reson Med, 1992. **25**(2): p. 260-72.
266. Naumova, A.V., Weiss, R.G., and Chacko, V.P., *Regulation of murine myocardial energy metabolism during adrenergic stress studied by in vivo 31P NMR spectroscopy.* Am J Physiol Heart Circ Physiol, 2003. **285**(5): p. H1976-9.
267. Lygate, C.A. and Neubauer, S., *Metabolic flux as a predictor of heart failure prognosis.* Circ Res, 2014. **114**(8): p. 1228-30.
268. Peterzan, M.A., Lewis, A.J.M., Neubauer, S., and Rider, O.J., *Non-invasive investigation of myocardial energetics in cardiac disease using (31)P magnetic resonance spectroscopy.* Cardiovasc Diagn Ther, 2020. **10**(3): p. 625-635.
269. Befroy, D.E., Rothman, D.L., Petersen, K.F., and Shulman, G.I., *(3)(1)P-magnetization transfer magnetic resonance spectroscopy measurements of in vivo metabolism.* Diabetes, 2012. **61**(11): p. 2669-78.
270. Herrmann G, D.G., *The Chemical Nature of Heart Failure.* Annals of Internal Medicine, 1939. **12**(8): p. 1233-1244.
271. Olson, R.E., *Myocardial metabolism in congestive heart failure.* J Chronic Dis, 1959. **9**(5): p. 442-64.
272. Lopaschuk, G.D., Karwi, Q.G., Tian, R., Wende, A.R., and Abel, E.D., *Cardiac Energy Metabolism in Heart Failure.* Circ Res, 2021. **128**(10): p. 1487-1513.
273. Neubauer, S., Horn, M., Pabst, T*., et al.*, *Contributions of 31P-magnetic resonance spectroscopy to the understanding of dilated heart muscle disease.* Eur Heart J, 1995. **16**(suppl O): p. 115-8.
274. Neubauer, S., Krahe, T., Schindler, R*., et al.*, *31P magnetic resonance spectroscopy in dilated cardiomyopathy and coronary artery disease. Altered cardiac high-energy phosphate metabolism in heart failure.* Circulation, 1992. **86**(6): p. 1810-8.

275. Hardy, C.J., Weiss, R.G., Bottomley, P.A., and Gerstenblith, G., *Altered myocardial high-energy phosphate metabolites in patients with dilated cardiomyopathy.* Am Heart J, 1991. **122**(3 Pt 1): p. 795-801.
276. Conway, M.A., Allis, J., Ouwerkerk, R.*, et al.*, *Detection of low phosphocreatine to ATP ratio in failing hypertrophied human myocardium by 31P magnetic resonance spectroscopy.* The Lancet, 1991. **338**(8773): p. 973-976.
277. Neubauer, S., Horn, M., Cramer, M.*, et al.*, *Myocardial phosphocreatine-to-ATP ratio is a predictor of mortality in patients with dilated cardiomyopathy.* Circulation, 1997. **96**(7): p. 2190-6.
278. Weiss, R.G., Gerstenblith, G., and Bottomley, P.A., *ATP flux through creatine kinase in the normal, stressed, and failing human heart.* Proc Natl Acad Sci U S A, 2005. **102**(3): p. 808-13.
279. Bottomley, P.A., Panjrath, G.S., Lai, S.*, et al.*, *Metabolic rates of ATP transfer through creatine kinase (CK Flux) predict clinical heart failure events and death.* Sci Transl Med, 2013. **5**(215): p. 215re3.
280. Gabr, R.E., El-Sharkawy, A.M., Schar, M.*, et al.*, *Cardiac work is related to creatine kinase energy supply in human heart failure: a cardiovascular magnetic resonance spectroscopy study.* J Cardiovasc Magn Reson, 2018. **20**(1): p. 81.
281. Neubauer, S., *The failing heart--an engine out of fuel.* N Engl J Med, 2007. **356**(11): p. 1140-51.
282. Schirone, L., Forte, M., Palmerio, S.*, et al.*, *A Review of the Molecular Mechanisms Underlying the Development and Progression of Cardiac Remodeling.* Oxidative Medicine and Cellular Longevity, 2017. **2017**: p. 3920195.
283. Lucia, C.d., Eguchi, A., and Koch, W.J., *New Insights in Cardiac β-Adrenergic Signaling During Heart Failure and Aging.* Frontiers in Pharmacology, 2018. **9**.
284. Peterzan, M.A., Lygate, C.A., Neubauer, S., and Rider, O.J., *Metabolic remodeling in hypertrophied and failing myocardium: a review.* Am J Physiol Heart Circ Physiol, 2017. **313**(3): p. H597-H616.
285. Neglia, D., De Caterina, A., Marraccini, P.*, et al.*, *Impaired myocardial metabolic reserve and substrate selection flexibility during stress in patients with idiopathic dilated cardiomyopathy.* Am J Physiol Heart Circ Physiol, 2007. **293**(6): p. H3270-8.
286. Diakos, N.A., Navankasattusas, S., Abel, E.D.*, et al.*, *Evidence of Glycolysis Up-Regulation and Pyruvate Mitochondrial Oxidation Mismatch During Mechanical Unloading of the Failing Human Heart: Implications for Cardiac Reloading and Conditioning.* JACC Basic Transl Sci, 2016. **1**(6): p. 432-444.
287. Funada, J., Betts, T.R., Hodson, L.*, et al.*, *Substrate utilization by the failing human heart by direct quantification using arterio-venous blood sampling.* PLoS One, 2009. **4**(10): p. e7533.
288. Voros, G., Ector, J., Garweg, C.*, et al.*, *Increased Cardiac Uptake of Ketone Bodies and Free Fatty Acids in Human Heart Failure and Hypertrophic Left Ventricular Remodeling.* Circ Heart Fail, 2018. **11**(12): p. e004953.
289. Bedi, K.C., Jr., Snyder, N.W., Brandimarto, J.*, et al.*, *Evidence for Intramyocardial Disruption of Lipid Metabolism and Increased Myocardial Ketone Utilization in Advanced Human Heart Failure.* Circulation, 2016. **133**(8): p. 706-16.
290. Aubert, G., Martin, O.J., Horton, J.L.*, et al.*, *The Failing Heart Relies on Ketone Bodies as a Fuel.* Circulation, 2016. **133**(8): p. 698-705.

291. Murashige, D., Jang, C., Neinast, M.*, et al.*, *Comprehensive quantification of fuel use by the failing and nonfailing human heart.* Science, 2020. **370**(6514): p. 364-368.
292. Nielsen, R., Moller, N., Gormsen, L.C.*, et al.*, *Cardiovascular Effects of Treatment With the Ketone Body 3-Hydroxybutyrate in Chronic Heart Failure Patients.* Circulation, 2019. **139**(18): p. 2129-2141.
293. Ashrafian, H., Frenneaux, M.P., and Opie, L.H., *Metabolic mechanisms in heart failure.* Circulation, 2007. **116**(4): p. 434-48.
294. Karwi, Q.G., Jörg, A.R., and Lopaschuk, G.D., *Allosteric, transcriptional and post-translational control of mitochondrial energy metabolism.* Biochemical Journal, 2019. **476**(12): p. 1695-1712.
295. Papandreou, I., Cairns, R.A., Fontana, L., Lim, A.L., and Denko, N.C., *HIF-1 mediates adaptation to hypoxia by actively downregulating mitochondrial oxygen consumption.* Cell Metabolism, 2006. **3**(3): p. 187-197.
296. Collins-Nakai, R.L., Noseworthy, D., and Lopaschuk, G.D., *Epinephrine increases ATP production in hearts by preferentially increasing glucose metabolism.* American Journal of Physiology-Heart and Circulatory Physiology, 1994. **267**(5): p. H1862-H1871.
297. Hiraoka, T., DeBuysere, M., and Olson, M.S., *Studies of the effects of beta-adrenergic agonists on the regulation of pyruvate dehydrogenase in the perfused rat heart.* Journal of Biological Chemistry, 1980. **255**(16): p. 7604-7609.
298. Wahrenberg, H., LÖNnqvist, F., HellmÉR, J., and Arner, P., *Importance of beta-adrenoceptor function in fat cells for lipid mobilization.* European Journal of Clinical Investigation, 1992. **22**(6): p. 412-419.
299. Tricò, D., Baldi, S., Frascerra, S.*, et al.*, *Abnormal Glucose Tolerance Is Associated with a Reduced Myocardial Metabolic Flexibility in Patients with Dilated Cardiomyopathy.* Journal of Diabetes Research, 2016. **2016**: p. 3906425.
300. Gulsin, G.S., Athithan, L., and McCann, G.P., *Diabetic cardiomyopathy: prevalence, determinants and potential treatments.* Ther Adv Endocrinol Metab, 2019. **10**: p. 2042018819834869.
301. Kannel, W.B., Hjortland, M., and Castelli, W.P., *Role of diabetes in congestive heart failure: the Framingham study.* Am J Cardiol, 1974. **34**(1): p. 29-34.
302. Aronow, W.S. and Ahn, C., *Incidence of heart failure in 2,737 older persons with and without diabetes mellitus.* Chest, 1999. **115**(3): p. 867-8.
303. Bertoni, A.G., Tsai, A., Kasper, E.K., and Brancati, F.L., *Diabetes and idiopathic cardiomyopathy: a nationwide case-control study.* Diabetes Care, 2003. **26**(10): p. 2791-5.
304. Aasum, E., Hafstad, A.D., Severson, D.L., and Larsen, T.S., *Age-dependent changes in metabolism, contractile function, and ischemic sensitivity in hearts from db/db mice.* Diabetes, 2003. **52**(2): p. 434-41.
305. Ritchie, R.H. and Abel, E.D., *Basic Mechanisms of Diabetic Heart Disease.* Circulation Research, 2020. **126**(11): p. 1501-1525.
306. Scheuermann-Freestone, M., Madsen, P.L., Manners, D.*, et al.*, *Abnormal cardiac and skeletal muscle energy metabolism in patients with type 2 diabetes.* Circulation, 2003. **107**(24): p. 3040-6.
307. Levelt, E., Rodgers, C.T., Clarke, W.T.*, et al.*, *Cardiac energetics, oxygenation, and perfusion during increased workload in patients with type 2 diabetes mellitus.* Eur Heart J, 2016. **37**(46): p. 3461-3469.

308. Bashir, A., Coggan, A.R., and Gropler, R.J., *In vivo creatine kinase reaction kinetics at rest and stress in type II diabetic rat heart.* Physiol Rep, 2015. **3**(1): p. e12248.
309. Rayner, J.J., Peterzan, M.A., Watson, W.D.*, et al.*, *Myocardial Energetics in Obesity: Enhanced ATP Delivery Through Creatine Kinase With Blunted Stress Response.* Circulation, 2020. **141**(14): p. 1152-1163.
310. Labbe, S.M., Grenier-Larouche, T., Noll, C.*, et al.*, *Increased myocardial uptake of dietary fatty acids linked to cardiac dysfunction in glucose-intolerant humans.* Diabetes, 2012. **61**(11): p. 2701-10.
311. Makrecka-Kuka, M., Liepinsh, E., Murray, A.J.*, et al.*, *Altered mitochondrial metabolism in the insulin-resistant heart.* Acta Physiol (Oxf), 2020. **228**(3): p. e13430.
312. Abel, E.D., *Free fatty acid oxidation in insulin resistance and obesity.* Heart Metab, 2010. **48**: p. 5-10.
313. Buchanan, J., Mazumder, P.K., Hu, P.*, et al.*, *Reduced cardiac efficiency and altered substrate metabolism precedes the onset of hyperglycemia and contractile dysfunction in two mouse models of insulin resistance and obesity.* Endocrinology, 2005. **146**(12): p. 5341-9.
314. Peterson, L.R., Herrero, P., Schechtman, K.B.*, et al.*, *Effect of obesity and insulin resistance on myocardial substrate metabolism and efficiency in young women.* Circulation, 2004. **109**(18): p. 2191-6.
315. Korosoglou, G., Humpert, P.M., Ahrens, J.*, et al.*, *Left ventricular diastolic function in type 2 diabetes mellitus is associated with myocardial triglyceride content but not with impaired myocardial perfusion reserve.* J Magn Reson Imaging, 2012. **35**(4): p. 804-11.
316. Rijzewijk, L.J., van der Meer, R.W., Smit, J.W.*, et al.*, *Myocardial steatosis is an independent predictor of diastolic dysfunction in type 2 diabetes mellitus.* J Am Coll Cardiol, 2008. **52**(22): p. 1793-9.
317. Levelt, E., Mahmod, M., Piechnik, S.K.*, et al.*, *Relationship Between Left Ventricular Structural and Metabolic Remodeling in Type 2 Diabetes.* Diabetes, 2016. **65**(1): p. 44-52.
318. Makrecka, M., Kuka, J., Volska, K.*, et al.*, *Long-chain acylcarnitine content determines the pattern of energy metabolism in cardiac mitochondria.* Mol Cell Biochem, 2014. **395**(1-2): p. 1-10.
319. Tominaga, H., Katoh, H., Odagiri, K.*, et al.*, *Different effects of palmitoyl-L-carnitine and palmitoyl-CoA on mitochondrial function in rat ventricular myocytes.* Am J Physiol Heart Circ Physiol, 2008. **295**(1): p. H105-12.
320. Levelt, E., Gulsin, G., Neubauer, S., and McCann, G.P., *MECHANISMS IN ENDOCRINOLOGY: Diabetic cardiomyopathy: pathophysiology and potential metabolic interventions state of the art review.* Eur J Endocrinol, 2018. **178**(4): p. R127-R139.
321. Gollmer, J., Zirlik, A., and Bugger, H., *Mitochondrial Mechanisms in Diabetic Cardiomyopathy.* Diabetes Metab J, 2020. **44**(1): p. 33-53.
322. Kerr, M., Miller, J.J., Thapa, D.*, et al.*, *Rescue of myocardial energetic dysfunction in diabetes through the correction of mitochondrial hyperacetylation by honokiol.* JCI Insight, 2020. **5**(17): p. e140326.
323. Antoniou, C.K., Manolakou, P., Magkas, N.*, et al.*, *Cardiac Resynchronisation Therapy and Cellular Bioenergetics: Effects Beyond Chamber Mechanics.* Eur Cardiol, 2019. **14**(1): p. 33-44.

324. van der Wall, E.E., Schalij, M.J., van der Laarse, A., and Bax, J.J., *Cardiac resynchronization therapy; the importance of evaluating cardiac metabolism.* Int J Cardiovasc Imaging, 2010. **26**(3): p. 293-7.
325. Xu, Y.Z., Chen, C.F., Chen, B.*, et al.*, *The Modulating Effects of Cardiac Resynchronization Therapy on Myocardial Metabolism in Heart Failure.* Pacing Clin Electrophysiol, 2016. **39**(12): p. 1404-1409.
326. Mills, R.W., Cornelussen, R.N., Mulligan, L.J.*, et al.*, *Left ventricular septal and left ventricular apical pacing chronically maintain cardiac contractile coordination, pump function and efficiency.* Circ Arrhythm Electrophysiol, 2009. **2**(5): p. 571-9.
327. Zanco, P., Desideri, A., Mobilia, G.*, et al.*, *Effects of left bundle branch block on myocardial FDG PET in patients without significant coronary artery stenoses.* J Nucl Med, 2000. **41**(6): p. 973-7.
328. Ono, S., Nohara, R., Kambara, H., Okuda, K., and Kawai, C., *Regional myocardial perfusion and glucose metabolism in experimental left bundle branch block.* Circulation, 1992. **85**(3): p. 1125-31.
329. Degtiarova, G., Claus, P., Duchenne, J.*, et al.*, *Low septal to lateral wall (18)F-FDG ratio is highly associated with mechanical dyssynchrony in non-ischemic CRT candidates.* EJNMMI Res, 2019. **9**(1): p. 105.
330. Larsen, C.K., Aalen, J.M., Stokke, C.*, et al.*, *Regional myocardial work by cardiac magnetic resonance and non-invasive left ventricular pressure: a feasibility study in left bundle branch block.* Eur Heart J Cardiovasc Imaging, 2020. **21**(2): p. 143-153.
331. Masci, P.G., Marinelli, M., Piacenti, M.*, et al.*, *Myocardial structural, perfusion, and metabolic correlates of left bundle branch block mechanical derangement in patients with dilated cardiomyopathy: a tagged cardiac magnetic resonance and positron emission tomography study.* Circ Cardiovasc Imaging, 2010. **3**(4): p. 482-90.
332. Degtiarova, G., Claus, P., Duchenne, J.*, et al.*, *Impact of left bundle branch block on myocardial perfusion and metabolism: A positron emission tomography study.* journal of Nuclear Cardiology, 2021. **28**: p. 1730-1739.
333. Claridge, S., Chen, Z., Jackson, T.*, et al.*, *Current concepts relating coronary flow, myocardial perfusion and metabolism in left bundle branch block and cardiac resynchronisation therapy.* Int J Cardiol, 2015. **181**: p. 65-72.
334. Birnie, D., de Kemp, R.A., Tang, A.S.*, et al.*, *Reduced septal glucose metabolism predicts response to cardiac resynchronization therapy.* J Nucl Cardiol, 2012. **19**(1): p. 73-83.
335. Brown, M., Marshall, D.R., Sobel, B.E., and Bergmann, S.R., *Delineation of myocardial oxygen utilization with carbon-11-labeled acetate.* Circulation, 1987. **76**(3): p. 687-96.
336. Lindner, O., Vogt, J., Baller, D.*, et al.*, *Global and regional myocardial oxygen consumption and blood flow in severe cardiomyopathy with left bundle branch block.* Eur J Heart Fail, 2005. **7**(2): p. 225-30.
337. Nowak, B., Sinha, A.M., Schaefer, W.M.*, et al.*, *Cardiac resynchronization therapy homogenizes myocardial glucose metabolism and perfusion in dilated cardiomyopathy and left bundle branch block.* J Am Coll Cardiol, 2003. **41**(9): p. 1523-1528.
338. Neri, G., Zanco, P., Zanon, F., and Buchberger, R., *Effect of biventricular pacing on metabolism and perfusion in patients affected by dilated cardiomyopathy and left bundle branch block: evaluation by positron emission tomography.* Europace, 2003. **5**(1): p. 111-5.

339. van Campen, C.M., Visser, F.C., van der Weerdt, A.P.*, et al.*, *FDG PET as a predictor of response to resynchronisation therapy in patients with ischaemic cardiomyopathy.* Eur J Nucl Med Mol Imaging, 2007. **34**(3): p. 309-15.
340. Ukkonen, H., Beanlands, R.S., Burwash, I.G.*, et al.*, *Effect of cardiac resynchronization on myocardial efficiency and regional oxidative metabolism.* Circulation, 2003. **107**(1): p. 28-31.
341. Sundell, J., Engblom, E., Koistinen, J.*, et al.*, *The effects of cardiac resynchronization therapy on left ventricular function, myocardial energetics, and metabolic reserve in patients with dilated cardiomyopathy and heart failure.* J Am Coll Cardiol, 2004. **43**(6): p. 1027-33.
342. Kitaizumi, K., Yukiiri, K., Masugata, H.*, et al.*, *Acute improvement of cardiac efficiency measured by 11C-acetate PET after cardiac resynchronization therapy and clinical outcome.* Int J Cardiovasc Imaging, 2010. **26**(3): p. 285-92.
343. Christenson, S.D., Chareonthaitawee, P., Burnes, J.E.*, et al.*, *Effects of simultaneous and optimized sequential cardiac resynchronization therapy on myocardial oxidative metabolism and efficiency.* J Cardiovasc Electrophysiol, 2008. **19**(2): p. 125-32.
344. Lindner, O., Vogt, J., Kammeier, A.*, et al.*, *Effect of cardiac resynchronization therapy on global and regional oxygen consumption and myocardial blood flow in patients with non-ischaemic and ischaemic cardiomyopathy.* Eur Heart J, 2005. **26**(1): p. 70-6.
345. Brandao, S.C., Nishioka, S.A., Giorgi, M.C.*, et al.*, *Cardiac resynchronization therapy evaluated by myocardial scintigraphy with 99mTc-MIBI: changes in left ventricular uptake, dyssynchrony, and function.* Eur J Nucl Med Mol Imaging, 2009. **36**(6): p. 986-96.
346. Nelson, G.S., Berger, R.D., Fetics, B.J.*, et al.*, *Left ventricular or biventricular pacing improves cardiac function at diminished energy cost in patients with dilated cardiomyopathy and left bundle-branch block.* Circulation, 2000. **102**(25): p. 3053-9.
347. Kyriacou, A., Pabari, P.A., Mayet, J.*, et al.*, *Cardiac resynchronization therapy and AV optimization increase myocardial oxygen consumption, but increase cardiac function more than proportionally.* Int J Cardiol, 2014. **171**(2): p. 144-52.
348. Obrzut, S., Tiongson, J., Jamshidi, N.*, et al.*, *Assessment of metabolic phenotypes in patients with non-ischemic dilated cardiomyopathy undergoing cardiac resynchronization therapy.* J Cardiovasc Transl Res, 2010. **3**(6): p. 643-51.
349. Martens, P., Dupont, M., Vermeersch, P.*, et al.*, *Impact of Cardiac Resynchronization Therapy on Global and Cardiac Metabolism and Cardiac Mitochondrial Function.* J Card Fail, 2021. **27**(6): p. 706-715.
350. Lindner, O., Sorensen, J., Vogt, J.*, et al.*, *Cardiac efficiency and oxygen consumption measured with 11C-acetate PET after long-term cardiac resynchronization therapy.* J Nucl Med, 2006. **47**(3): p. 378-83.
351. Agnetti, G., Kaludercic, N., Kane, L.A.*, et al.*, *Modulation of mitochondrial proteome and improved mitochondrial function by biventricular pacing of dyssynchronous failing hearts.* Circ Cardiovasc Genet, 2010. **3**(1): p. 78-87.
352. Wang, S.B., Foster, D.B., Rucker, J.*, et al.*, *Redox regulation of mitochondrial ATP synthase: implications for cardiac resynchronization therapy.* Circ Res, 2011. **109**(7): p. 750-7.

353. Nemutlu, E., Zhang, S., Xu, Y.Z*., et al.*, *Cardiac resynchronization therapy induces adaptive metabolic transitions in the metabolomic profile of heart failure.* J Card Fail, 2015. **21**(6): p. 460-9.
354. Gong, X., Sun, Z., Huang, Z*., et al.*, *Circulating metabolite profiles to predict response to cardiac resynchronization therapy.* BMC Cardiovasc Disord, 2020. **20**(1): p. 178.
355. Zhu, M.R., Fulati, Z., Liu, Y*., et al.*, *The value of serum metabolomics analysis in predicting the response to cardiac resynchronization therapy.* J Geriatr Cardiol, 2019. **16**(7): p. 529-539.
356. Heggermont, W., Auricchio, A., and Vanderheyden, M., *Biomarkers to predict the response to cardiac resynchronization therapy.* Europace, 2019. **21**(11): p. 1609-1620.
357. Iyengar, S., Haas, G., Lamba, S*., et al.*, *Effect of cardiac resynchronization therapy on myocardial gene expression in patients with nonischemic dilated cardiomyopathy.* J Card Fail, 2007. **13**(4): p. 304-11.
358. Mullens, W., Bartunek, J., Tang, W.H*., et al.*, *Early and late effects of cardiac resynchronization therapy on force-frequency relation and contractility regulating gene expression in heart failure patients.* Heart Rhythm, 2008. **5**(1): p. 52-9.
359. Vanderheyden, M., Mullens, W., Delrue, L*., et al.*, *Myocardial gene expression in heart failure patients treated with cardiac resynchronization therapy responders versus nonresponders.* J Am Coll Cardiol, 2008. **51**(2): p. 129-36.
360. Holland, A.E., Spruit, M.A., Troosters, T*., et al.*, *An official European Respiratory Society/American Thoracic Society technical standard: field walking tests in chronic respiratory disease.* Eur Respir J, 2014. **44**(6): p. 1428-46.
361. *https://euroqol.org/publications/user-guides/*.
362. DeFronzo, R.A., Tobin, J.D., and Andres, R., *Glucose clamp technique: a method for quantifying insulin secretion and resistance.* American Journal of Physiology-Endocrinology and Metabolism, 1979. **237**(3): p. E214.
363. Olivieri, L.J., Cross, R.R., O'Brien, K.E., Ratnayaka, K., and Hansen, M.S., *Optimized protocols for cardiac magnetic resonance imaging in patients with thoracic metallic implants.* Pediatr Radiol, 2015. **45**(10): p. 1455-64.
364. Tyler, D.J., Emmanuel, Y., Cochlin, L.E*., et al.*, *Reproducibility of 31P cardiac magnetic resonance spectroscopy at 3 T.* NMR Biomed, 2009. **22**(4): p. 405-13.
365. Robson, M.D., Tyler, D.J., and Neubauer, S., *Ultrashort TE chemical shift imaging (UTE-CSI).* Magn Reson Med, 2005. **53**(2): p. 267-74.
366. Vanhamme, L., van den Boogaart, A., and Van Huffel, S., *Improved method for accurate and efficient quantification of MRS data with use of prior knowledge.* J Magn Reson, 1997. **129**(1): p. 35-43.
367. Befroy, D.E. and Shulman, G.I., *Magnetic resonance spectroscopy studies of human metabolism.* Diabetes, 2011. **60**(5): p. 1361-9.
368. Clarke, W.T., Peterzan, M.A., Rayner, J.J*., et al.*, *Localized rest and stress human cardiac creatine kinase reaction kinetics at 3 T.* NMR Biomed, 2019. **32**(6): p. e4085.
369. Schar, M., El-Sharkawy, A.M., Weiss, R.G., and Bottomley, P.A., *Triple repetition time saturation transfer (TRiST) 31P spectroscopy for measuring human creatine kinase reaction kinetics.* Magn Reson Med, 2010. **63**(6): p. 1493-501.
370. Peterzan, M.A., Clarke, W.T., Lygate, C.A*., et al.*, *Cardiac Energetics in Patients With Aortic Stenosis and Preserved Versus Reduced Ejection Fraction.* Circulation, 2020. **141**(24): p. 1971-1985.

371. Steendijk, P., van der Velde, E.T., and Baan, J., *Single and dual excitation of the conductance-volume catheter analysed in a spheroidal mathematical model of the canine left ventricle.* Eur Heart J, 1992. **13 Suppl E**(suppl_E): p. 28-34.
372. Williams, N., *The Borg Rating of Perceived Exertion (RPE) scale.* Occupational Medicine-Oxford, 2017. **67**(5): p. 404-405.
373. Borg, G.A., *Psychophysical bases of perceived exertion.* Med Sci Sports Exerc, 1982. **14**(5): p. 377-81.
374. Fillmore, N., Levasseur, J.L., Fukushima, A.*, et al.*, *Uncoupling of glycolysis from glucose oxidation accompanies the development of heart failure with preserved ejection fraction.* Molecular Medicine, 2018. **24**(1): p. 3.
375. Stojiljkovic, M.P., Zhang, D., Lopes, H.F.*, et al.*, *Hemodynamic effects of lipids in humans.* Am J Physiol Regul Integr Comp Physiol, 2001. **280**(6): p. R1674-9.
376. Paolisso, G., Manzella, D., Rizzo, M.R.*, et al.*, *Elevated plasma fatty acid concentrations stimulate the cardiac autonomic nervous system in healthy subjects.* Am J Clin Nutr, 2000. **72**(3): p. 723-30.
377. Suga, H., *Ventricular energetics.* Physiol Rev, 1990. **70**(2): p. 247-77.
378. Pitt, B. and Gregg, D.E., *Coronary hemodynamic effects of increasing ventricular rate in the unanesthetized dog.* Circ Res, 1968. **22**(6): p. 753-61.
379. Overgaard, C.B. and Džavík, V., *Inotropes and Vasopressors.* Circulation, 2008. **118**(10): p. 1047-1056.
380. Dass, S., Holloway, C.J., Cochlin, L.E.*, et al.*, *No Evidence of Myocardial Oxygen Deprivation in Nonischemic Heart Failure.* Circ Heart Fail, 2015. **8**(6): p. 1088-93.
381. Bersin, R.M., Wolfe, C., Kwasman, M.*, et al.*, *Improved hemodynamic function and mechanical efficiency in congestive heart failure with sodium dichloroacetate.* J Am Coll Cardiol, 1994. **23**(7): p. 1617-24.
382. Gao, D., Ning, N., Niu, X., Hao, G., and Meng, Z., *Trimetazidine: a meta-analysis of randomised controlled trials in heart failure.* Heart, 2011. **97**(4): p. 278-86.
383. Schmidt-Schweda, S. and Holubarsch, C., *First clinical trial with etomoxir in patients with chronic congestive heart failure.* Clinical Science, 2000. **99**(1): p. 27-35.
384. Saremi, F., Muresian, H., and Sanchez-Quintana, D., *Coronary veins: comprehensive CT-anatomic classification and review of variants and clinical implications.* Radiographics, 2012. **32**(1): p. E1-32.
385. Molhoek, S.G., Bax, J.J., van Erven, L.*, et al.*, *Comparison of benefits from cardiac resynchronization therapy in patients with ischemic cardiomyopathy versus idiopathic dilated cardiomyopathy.* The American Journal of Cardiology, 2004. **93**(7): p. 860-863.
386. St John Sutton, M.G., Plappert, T., Abraham, W.T.*, et al.*, *Effect of Cardiac Resynchronization Therapy on Left Ventricular Size and Function in Chronic Heart Failure.* Circulation, 2003. **107**(15): p. 1985-1990.
387. Linde, C., Leclercq, C., Rex, S.*, et al.*, *Long-term benefits of biventricular pacing in congestive heart failure: results from the MUltisite STimulation in cardiomyopathy (MUSTIC) study.* Journal of the American College of Cardiology, 2002. **40**(1): p. 111-118.
388. Foley, P.W.X., Chalil, S., Khadjooi, K.*, et al.*, *Left ventricular reverse remodelling, long-term clinical outcome, and mode of death after cardiac resynchronization therapy.* European Journal of Heart Failure, 2011. **13**(1): p. 43-51.

389. Grothues, F., Smith, G.C., Moon, J.C.C*., et al.*, *Comparison of interstudy reproducibility of cardiovascular magnetic resonance with two-dimensional echocardiography in normal subjects and in patients with heart failure or left ventricular hypertrophy.* The American Journal of Cardiology, 2002. **90**(1): p. 29-34.
390. Gardner, B.I., Bingham, S.E., Allen, M.R., Blatter, D.D., and Anderson, J.L., *Cardiac magnetic resonance versus transthoracic echocardiography for the assessment of cardiac volumes and regional function after myocardial infarction: an intrasubject comparison using simultaneous intrasubject recordings.* Cardiovascular ultrasound, 2009. **7**: p. 38-38.
391. Vago, H., Czimbalmos, C., Papp, R*., et al.*, *Biventricular pacing during cardiac magnetic resonance imaging.* Europace, 2020. **22**(1): p. 117-124.
392. Toner, L., Flannery, D., Sugumar, H*., et al.*, *Electrical remodelling and response following cardiac resynchronization therapy: A novel analysis of intracardiac electrogram using a quadripolar lead.* Journal of arrhythmia, 2018. **34**(3): p. 274-280.
393. Diab, O., Lotfy, H.-A.A., and Khalid, S., *Reverse electric remodeling after cardiac resynchronization therapy and relation to clinical and echocardiographic outcomes.* The Egyptian Heart Journal, 2014. **66**(4): p. 343-350.
394. Mischke, K., Knackstedt, C., Fache, K*., et al.*, *Electrical remodelling in cardiac resynchronization therapy: Decrease in intrinsic QRS duration.* Acta cardiologica, 2011. **66**: p. 175-80.
395. Knappe, D., Pouleur, A.-C., Shah, A.M*., et al.*, *Acute Effects of Withdrawal of Cardiac Resynchronization Therapy on Left and Right Ventricular Function, Dyssynchrony, and Contractile Function in Patients With New York Heart Association Functional Class I/II Heart Failure: MADIT-CRT.* Journal of Cardiac Failure, 2013. **19**(3): p. 149-155.
396. Liang, Y., Wang, Q., Zhang, M*., et al.*, *Cessation of pacing in super-responders of cardiac resynchronization therapy: A randomized controlled trial.* Journal of Cardiovascular Electrophysiology, 2018. **29**(11): p. 1548-1555.
397. Cay, S., Ozeke, O., Ozcan, F., Aras, D., and Topaloglu, S., *Mid-term clinical and echocardiographic evaluation of super responders with and without pacing: the preliminary results of a prospective, randomized, single-centre study.* EP Europace, 2016. **18**(6): p. 842-850.
398. Guazzi, M., Adams, V., Conraads, V*., et al.*, *EACPR/AHA Joint Scientific Statement. Clinical recommendations for cardiopulmonary exercise testing data assessment in specific patient populations.* Eur Heart J, 2012. **33**(23): p. 2917-27.
399. Malhotra, R., Bakken, K., D'Elia, E., and Lewis, G.D., *Cardiopulmonary Exercise Testing in Heart Failure.* JACC Heart Fail, 2016. **4**(8): p. 607-16.
400. Baldi, F. and Castriotti, M.R., *The cardiopulmonary exercise test (CPET) in the evaluation of functional capacity before and after cardiac resynchronization therapy (CRT).* European Respiratory Journal, 2018. **52**(suppl 62): p. PA3368.
401. Arora, S., Aarones, M., Aakhus, S*., et al.*, *Peak oxygen uptake during cardiopulmonary exercise testing determines response to cardiac resynchronization therapy.* Journal of Cardiology, 2012. **60**(3): p. 228-235.
402. Sidhu, B.S., Rua, T., Gould, J*., et al.*, *Economic evaluation of a dedicated cardiac resynchronisation therapy preassessment clinic.* Open Heart, 2020. **7**(2): p. e001249.
403. Pinto, R., M, S., Abreu, A*., et al.*, *Optimizing Patient Selection For Cardiac Resynchronization Therapy Trough Cardiopulmonary Exercise Testing*. 2014.

404. Sims, D.B., Mignatti, A., Colombo, P.C.*, et al.*, *Rate responsive pacing using cardiac resynchronization therapy in patients with chronotropic incompetence and chronic heart failure.* Europace, 2011. **13**(10): p. 1459-63.
405. Whinnett, Z.I., Sohaib, S.M.A., Mason, M.*, et al.*, *Multicenter Randomized Controlled Crossover Trial Comparing Hemodynamic Optimization Against Echocardiographic Optimization of AV and VV Delay of Cardiac Resynchronization Therapy: The BRAVO Trial.* JACC Cardiovasc Imaging, 2019. **12**(8 Pt 1): p. 1407-1416.
406. Cohn, J.N., Johnson, G.R., Shabetai, R.*, et al.*, *Ejection fraction, peak exercise oxygen consumption, cardiothoracic ratio, ventricular arrhythmias, and plasma norepinephrine as determinants of prognosis in heart failure. The V-HeFT VA Cooperative Studies Group.* Circulation, 1993. **87**(6 Suppl): p. VI5-16.
407. Myers, J., Gullestad, L., Vagelos, R.*, et al.*, *Cardiopulmonary exercise testing and prognosis in severe heart failure: 14 mL/kg/min revisited.* Am Heart J, 2000. **139**(1 Pt 1): p. 78-84.
408. Keteyian, S.J., Patel, M., Kraus, W.E.*, et al.*, *Variables Measured During Cardiopulmonary Exercise Testing as Predictors of Mortality in Chronic Systolic Heart Failure.* J Am Coll Cardiol, 2016. **67**(7): p. 780-9.
409. Cole, C.R., Blackstone, E.H., Pashkow, F.J., Snader, C.E., and Lauer, M.S., *Heart-rate recovery immediately after exercise as a predictor of mortality.* N Engl J Med, 1999. **341**(18): p. 1351-7.